PEOPLE'S DEMOCRATIC REPUBLIC OF ALGERIA
MINISTRY OF HIGHER EDUCATION AND SCIENTIFIC RESEARCH
ABDELHAMID IBN BADIS UNIVERSITY – MOSTAGANEM
FACULTY OF NATURAL AND LIFE SCIENCES
DEPARTEMENT FOOD SCIENCES

Field : Natural and Life Sciences

Course : Food Sciences

Speciality : Nutrition et Pathology

THESIS

For the fulfillment of the Doctorate degree (3rd cycle LMD)

Defended by :

Tarik SEBBAH

TOPIC

Exploration des activités biologiques des principes actifs de *Portulaca oleracea* L. extraits par des solvants thérapeutiques eutectiques profonds (STEP)

Defended on :**--/09/2025**

Jury :

President :	ZIAR Hasnia	Pr.	University of Mostaganem
Supervisor :	YAHLA Imene	MCA.	University of Mostaganem
Examiner :	TEFIANI Choukri	Pr.	University of Tlemcen
Examiner :	BENHAMED nadjia	Pr.	USTO-MB University of Oran
Examiner :	CHAALEL Abdelmalek	MCA.	University of Mostaganem

Laboratory of Beneficial Microorganisms, Functional Foods and Health (LMBAFS)

***Année universitaire* : 2024/2025**

Acknowledgments

First and foremost, I would like to express my sincere gratitude to the **Laboratory of Beneficial Microorganisms, Functional Foods, and Health (LMBAFS)** for welcoming me within the **University of Mostaganem** and providing me with the necessary resources to carry out this research.

I am deeply grateful to my supervisors, **Dr. Yahla** and **Professor Riazi**, for their invaluable guidance, continuous support, and insightful advice that have significantly contributed to the completion of this thesis.

I also wish to express my sincere appreciation to the **jury members** for dedicating their time and expertise to evaluating my work:

President: **Professor Ziar Hasnia** – University of Mostaganem
Examiner: **Professor Tefiani Choukri** – University of Tlemcen
Examiner: **Professor Nadjia Benhamed** – USTO-MB, University of Oran
Examiner: **Professor Chaalel Abdelmalek** – University of Mostaganem

I extend my heartfelt thanks to our laboratory engineer, **Dr. Djahira Hamedi**, for all the facilities and assistance she provided throughout my work.

This research would not have been possible without the support of international collaborations. I would like to extend my gratitude to the **Beijing Advanced Innovation Center for Food Nutrition and Human Health, Beijing Technology and Business University (China)**, where this project was initially conceived during the first two years, and to the **LAQV/REQUIMETE Laboratory at the Faculty of Pharmacy, University of Porto (Portugal)**, where it was further developed.

A special thanks goes to my supervisors in Portugal for their unwavering support:

Professor Maria Da Conceição Branco, for her warm welcome and integration into the university,

Dr. Edite Cunha, for her co-supervision and valuable guidance,

Pr. Célia, for her contribution to the revision of the article,

Pr. Pereira David, for opening the doors of his laboratory and allowing us to conduct our cancer-related tests.

To all of you, I extend my deepest appreciation and gratitude.

Dedication

*To my **beloved mother**, whose love and sacrifices continue to guide me even in her absence. This work is a tribute to her strength, kindness, and the values she instilled in me. Though she is no longer here, her presence remains in every step I take.*

*To my **best friend, Aminadiel**, for being my rock, offering unwavering support, and believing in me even when I doubted myself.*

*To my **dear friend, Diane**, for her encouragement, kindness, and companionship throughout this journey.*

This work is dedicated to you, with all my love and gratitude.

ملخص

تهدف هذه الدراسة الى تصميم وتوصيف وتقييم النشاط البيولوجي للأنظمة العميقة الطبيعية للسوائل الأيوتكتية (NADES) لاستخراج المكونات الصيدلانية النشطة (APIs) من أوراق *Portulaca oleracea L.* (POL) تم تحليل التفاعلات الجزيئية داخل NADES باستخدام منهجيات حسابية، مثل حسابات نظرية الكثافة الوظيفية (DFT) ومحاكاة الديناميكيات الجزيئية (MD) ، لتقييم قوة الروابط الهيدروجينية واستقرار البنية. أظهرت مستخلصات NADESs-POL كفاءة استخراجية أعلى بشكل ملحوظ لمجموع المركبات الفينولية (TPC) والفلافونويدات (TFC) والتانينات (CT) مقارنة بمستخلص الإيثانول التقليدي .(EtOH-POL) تم استخدام كروماتوغرافيا السائل عالية الأداء (HPLC-DAD) لعزل المركبات المضادة للأكسدة الرئيسية، مما أكد زيادة مردود الاستخلاص باستخدام NADESs مقارنة بالإيثانول.

تم تقييم النشاط المضاد للأكسدة من خلال اختبارات التقاط الجذور الحرة، حيث أظهرت مستخلصات NADESs-POL قيم EC_{50} أقل بشكل ملحوظ مقارنة بمستخلصات EtOH-POL، وقد تم تأكيد هذه النتائج باستخدام اختبار القدرة المضادة للأكسدة المكافئة للتروكس .(TEAC) كما تم تقييم النشاط المضاد للميكروبات لمستخلصات NADESs-POL ضد سلالات بكتيرية موجبة وسالبة الجرام، حيث أظهرت تأثيرات قوية مثبطة للبكتيريا، خاصة ضد *Staphylococcus aureus* و*Escherichia coli*

علاوة على ذلك، تم دراسة التأثيرات السمية الخلوية لمستخلصات NADESs-POL على خلايا سرطان المعدة من نوع AGS ، مما كشف عن انخفاض حيوية الخلايا حسب الجرعة. كما تم إجراء دراسات السمية الحادة *in vivo* على فئران ويستار لتحديد الجرعة الآمنة للـ NADESs المختارة، حيث تم تحديد جرعة 200 ميكرولتر كجرعة آمنة للإعطاء اليومي.

لتقييم التأثيرات الأنظمة العلاجية العميقة للسوائل الأيوتكتية (THEDESs) في حماية الكبد تلقت جرذان ويستار جرعة يومية من 200 ميكرولتر من مستخلص NADESs-POL لمدة خمسة أيام، تلتها حقن الميثوتركسات (MTX) بجرعة 20 ملغ/كغ لتحفيز السمية الكبدية. تم تحليل مؤشرات وظائف الكبد والفحوصات النسيجية المرضية لتقييم فعالية .THEDESs من بين التركيبات المختبرة، أظهرت G1 و G7 أقوى التأثيرات الواقية للكبد، حيث خفضت بشكل ملحوظ الإجهاد التأكسدي وعلامات الالتهاب والتلف البطاني، مع منع تطور التليف الكبدي. كما أكدت التحاليل النسيجية المرضية أن THEDESs 1 ، 3، 4، و7 كانت فعالة في منع الإصابة بالكبد الدهني، في حين كانت THEDESs 5 و6 أقل فعالية في الحد من احتقان الجيوب الكبدية.

تؤكد هذه النتائج إمكانات NADESs كمذيبات مستدامة لاستخلاص وتثبيت المركبات النشطة بيولوجيًا، مع تقديم THEDESs كاستراتيجية جديدة لحماية الكبد من الإصابة الناجمة عن الميثوتركسات. يبرز دمج المناهج الحسابية والتجريبية المزايا الهيكلية والوظيفية لـNADESs ، مما يمهد الطريق لاستخدامها في التطبيقات الصيدلانية والتدخلات العلاجية.

الكللمات المفتاحية: *Portulaca oleracea,* HPLC-DAD, NADES, HPLC-DAD, الحماية الكبدية ,

AGS.

Résumé

Cette étude porte sur la conception, la caractérisation et les interactions moléculaires présentes dans le SNEP, elles ont été analysées à l'aide de méthodologies informatiques, notamment des calculs de théorie fonctionnelle de la densité (TFD) et des simulations de dynamique moléculaire (DM), afin d'évaluer la force des liaisons hydrogène et la stabilité de la structure. L'efficacité d'extraction du contenu phénolique total (CPT), de la teneur totale en flavonoïdes (CFT) et de tannins condensés (TC) s'est révélée considérablement supérieure dans tous les extraits SNEP-POL par rapport aux extraits traditionnels à l'éthanol (EtOH-POL). La chromatographie liquide à haute performance avec détection l'évaluation biologique des solvants eutectiques profonds naturels (SNEPs) utilisés pour l'extraction des ingrédients pharmaceutiques actifs (IPA) des feuilles de *Portulaca oleracea* L. (POL). par réseau de diodes (CLHP-DRD) a été utilisée pour isoler les principaux composés antioxydants, validant ainsi les rendements d'extraction accrus du SNEP par rapport à l'EtOH. L'efficacité antioxydante a été évaluée au moyen de tests antiradicalaires, qui ont indiqué des valeurs de CE_{50} significativement plus faibles dans les extraits SNEPs-POL lorsqu'ils sont juxtaposés à des extraits d'EtOH-POL, ces résultats étant encore corroborés par le test de capacité antioxydante équivalente du Trolox (CAET). L'efficacité antimicrobienne du SNEP-POL a été évaluée contre des souches bactériennes à Gram positif et à Gram négatif, révélant des propriétés bactériostatiques prononcées, en particulier contre *Staphylococcus aureus* et *Escherichia coli*. De plus, les effets cytotoxiques du SNEPs-POL ont été examinés sur des cellules d'adénocarcinome gastrique AGS, démontrant un déclin de la viabilité cellulaire dépendant de la dose.

Des évaluations de toxicité aiguë *in vivo* ont été réalisées sur des rats Wistar afin d'établir le profil de sécurité du SNEP sélectionné, une dose de 200 µL ayant été jugée sûre pour une administration quotidienne. Pour étudier le potentiel hépatoprotecteur du STHEP, des rats Wistar ont reçu 200 µL de SNEP-POL par jour pendant cinq jours, puis du méthotrexate (MTX) (20 mg/kg) pour induire une hépatotoxicité. Des marqueurs de la fonction hépatique ainsi que des évaluations histopathologiques ont été réalisés pour déterminer l'efficacité du STHEP. Parmi les formulations évaluées, STHEPs G1 et G7 ont démontré les effets hépatoprotecteurs les plus robustes, atténuant significativement le stress oxydatif, les marqueurs inflammatoires et les dommages endothéliaux tout en inhibant la progression de la fibrose hépatique. L'évaluation histopathologique a confirmé que STHEPs 1, 3, 4 et 7 bloquaient efficacement le développement de la stéatose hépatique, tandis que STHEPs 5 et 6 démontraient une efficacité réduite pour soulager la congestion sinusoïdale.

Ces résultats soulignent les promesses du SNEPs en tant que solvants durables pour l'extraction et la stabilisation de composés bioactifs, STHEPs présentant une nouvelle stratégie d'hépatoprotection contre les lésions hépatiques induites par le MTX. La synthèse de méthodologies computationnelles et expérimentales permet d'élucider les mérites structuraux et fonctionnels des SNEPs, facilitant ainsi leur application potentielle dans des formulations pharmaceutiques et des interventions thérapeutiques.

Mots clés : *Portulaca oleracea,* HPLC-DAD, SNEP, STHEP, Hepatoprotection, AGS.

Abstract

This study explores the design, characterization, and biological evaluation of NADESs for the extraction of active pharmaceutical ingredients (APIs) from *Portulaca oleracea* leaves (POL), The molecular interactions within NADESs were explored using computational approaches such as density functional theory (DFT) calculations and molecular dynamics (MD) simulations to assess hydrogen bond strength and structural stability. Extraction efficiency of TPC, TFC and CT was significantly higher in all NADESs-POL extracts, comparing them to conventional EtOH-POL extract. HPLC-DAD was employed to isolate major antioxidant compounds, confirming enhanced extraction yields in NADESs compared to EtOH. Antioxidant activity was assessed using anti-radical scavenging assays, revealing significantly lower EC_{50} values in NADESs-POL compared to EtOH-POL extracts, these findings were further confirmed by Trolox equivalent antioxidant capacity (TEAC). The antimicrobial activity of NADESs-POL was evaluated against Gram-positive and Gram-negative bacterial strains, demonstrating potent bacteriostatic effects, particularly against *Staphylococcus aureus* and *Escherichia coli*. Furthermore, the cytotoxic effects of NADESs-POL were investigated in AGS gastric adenocarcinoma cells, indicating a dose-dependent reduction in cell viability.

In vivo acute toxicity studies were conducted in Wistar rats to determine the safety profile of selected NADESs, through which 200 µL was determined a safe dose for daily administration. To evaluate the hepatoprotective potential of THEDESs, Wistar rats received 200 µL of NADESs-POL daily for five days, followed by MTX administration (20 mg/kg) to induce hepatotoxicity. Liver function markers and histopathological examinations were performed to assess THEDES efficacy. Among the tested formulations, THEDESs G1 and G7 exhibited the most potent hepatoprotective effects, significantly reducing oxidative stress, inflammatory markers, and endothelial damage while preventing hepatic fibrosis. Histopathological analysis confirmed that THEDESs 1, 3, 4, and 7 effectively prevented hepatic steatosis, whereas THEDESs 5 and 6 were less effective in mitigating sinusoidal congestion.

These findings underscore the potential of NADESs as sustainable solvents for extracting and stabilizing bioactive compounds, with THEDESs offering a novel hepatoprotective strategy against MTX-induced liver injury. The integration of computational and experimental approaches highlights the structural and functional advantages of NADESs, paving the way for their application in pharmaceutical formulations and therapeutic interventions.

Key words: *Portulaca oleracea,* HPLC-DAD, NADES, THEDES, Hepatoprotection, AGS.

Content

Content

Results and Discussion

Conclusion and perspectives

Tables list

Figures list

Abbreviations list

ACE2: Angiotensin-converting enzyme 2

AGS: Adenocarcinoma gastric cancer cell line

ALAT: Alanine aminotransferase

ALP: Alkaline phosphatase

APIs: Active pharmaceutical ingredients

APIs: Active pharmaceutical ingredients

ASAT: Aspartate aminotransferase

C5H8: Multiple isoprene units

CAGE: Choline and geranic acid system

CPA: Cryoprotectant agent

CPAs: Cryoprotective agents

CT: Condensed tannin

DESs: Deep eutectic systems

DMEM: Dulbecco's modified Eagle's medium

DMSO: Dimethyl sulfoxide

FAO: Food and agriculture organization

FBS: Fetal bovine serum

GGT: Gamma-glutamyl transferase

GI: Gastrointestinal

HaCaT cells: Spontaneously immortalized, human keratinocyte line

HaCat: Human keratinocytes

HBA: Hydrogen-bond acceptor

HBD: Hydrogen-bond donor

HEK: Human epidermal keratinocytes

HIFs : Homoisoflavonoids

HNADES: Hydrophobic natural deep eutectic solvents

HPLC: High - performance liquid chromatography

HT29: Colorectal cancer cells.

ICH: International council for harmonisation

LD50: Median lethal dose

LIM: limonene

MD: Molecular dynamic

ME: Microemulsion

Mpro: Main protease

MTX: Methotrexate

NADESs: Natural deep eutectic systems

NSAIDs: non-steroidal anti-inflammatory drugs

PAS: Periodic acid-schiff

PCL: Polycaprolactone

PME: Particle-mesh Ewald

POL: *Portulaca oleracea* L.

PLV: polyvinylpyrrolidone K30

PPO: Polyphenol oxidase

PPAR-α: Peroxisome proliferator-activated receptor alpha

PS: Penicillin–streptomycin

PVA: Poly-vinyl alcohol

RBD: Receptor-binding domain.

SSPs: Stable states pictures

TBd: Trypan blue dye

TFC : Total flavonoid content

THEDESs : Therapeutic deep eutectic systems

TMPRSS: Transmembrane serine protease 2

TNF:Tumor necrosis factor

TPC: Total phenolic content

UAE: Ultrasound assisted extraction

VMD: Visual molecular dynamics

Introduction

Portulaca oleracea L. (commonly known as purslane) is a globally distributed plant valued for its nutritional and medicinal properties (Kumar et *al*., 2022). Traditionally consumed in various forms: fresh, cooked, or fermented. Purslane is recognized as one of the richest terrestrial sources of omega-3 and omega-6 fatty acids, ascorbic acid, tocopherols, glutathione, and β-carotene (Simopoulos et *al*., 1992). The name *Portulaca* originates from the Latin words "porto" (to carry) and "lac" (milk), referring to the characteristic milky sap found in its tissues (Kumar et *al*., 2022; Chugh et *al*., 2019)**.**

Beyond its nutritional composition, purslane is a rich source of specialized metabolites, including alkaloids, catecholamines, phenolic acids, flavonoids, lignans, terpenoids, and betalains (Kumar et *al*., 2022). These bioactive compounds are associated with various health benefits, such as antioxidant, anti-diabetic, anti-obesity, anti-cancer, and anti-atherosclerotic properties (Nemzer et *al*., 2020a). Notably, phenolic acids like caffeic, p-coumaric (Erkan, 2012), ferulic, gallic and gentisic acids, benzoic, and anisic acids (R. Silva et Carvalho, 2014a) have been identified in purslane, contributing to its pharmacological potential. Additionally, flavonoids such as quercetin (Aghababaei & Hadidi, 2023), rutin, kaempferol (Silva dos Santos et *al*., 2021), and luteolin exhibit anti-inflammatory, antitumor, antiviral, and cardioprotective effects (Chagas et *al*., 2022). A newly identified alkaloid, oleraurea, has shown anticholinesterase activity, suggesting a possible role in Alzheimer's disease treatment (Konrath et *al*., 2013). Given the increasing global interest in plant-based nutraceuticals, as highlighted by the Food and Agriculture Organization (FAO) (Klapp et *al*., 2022)**,** optimizing the extraction of these bioactive compounds is crucial for their effective utilization in pharmaceutical and functional food industries, many studies have shown improved yields of the extracted bioactive compounds, especially antioxidants after having optimized certain parameters (Bi et *al*., 2013; Chen et *al*., 2018; A. Pandey et *al*., 2018; L. Wu et *al.*, 2020; Z. Xu et *al*., 2021; G. Zhao et *al*., 2017)**.**

The extraction of phytochemicals from *P. oleracea* has been extensively studied using qualitative and quantitative analytical tools. Traditional solvent-based extraction methods commonly employ ethanol (X. F. Liu et *al*., 2015)**,** methanol (Habibian et *al*., 2020)**,** acetone (Gatea et *al*., 2017), and hexane (Dheyab et *al*., 2021) While ethanol and methanol are widely used in phytopharmacy and considered relatively safe, their large-scale use and disposal can pose environmental and health challenges including toxicity, high cost, volatility, flammability, and poor biodegradability (Log et Moi, 2018). Additionally, solvent residues necessitate

extensive purification steps before *in vivo* or clinical applications due to potential toxicity risks. The International Council for Harmonisation (ICH) has established guidelines recommending the use of less toxic solvents and defining toxicologically acceptable residual levels in pharmaceuticals (International Council for Harmonisation (ICH), 2024) highlighting the need for more sustainable alternatives for extracting bioactive compounds from plants, including toxicity, high cost, volatility, flammability, and poor biodegradability. Additionally, solvent residues necessitate extensive purification steps before *in vivo* or clinical applications due to potential toxicity risks.

Deep eutectic systems (DESs) have emerged as promising green solvents for natural product extraction (Abranches et *al*., 2019a; Florindo et *al*., 2019), offering advantages over conventional organic solvents. A subclass known as natural deep eutectic solvents (NADESs) is particularly appealing due to its biocompatibility, low volatility, biodegradability, and ease of synthesis. NADESs have demonstrated high extraction efficiency for bioactive compounds in various plant matrices, such as *Camellia oleifera* flowers (Ma, Liu, Tan, et *al*., 2018a)**,** orange peel (Viñas-Ospino, Panić, Bagović, et *al*., 2023; Viñas-Ospino, Panić, Radojčić-Redovniković, et *al*., 2023)**,** and grape skin (Cvjetko Bubalo et *al*., 2016). However, research on NADESs-based extraction of *P. oleracea* remains scarce, with only one study reporting its effectiveness in extracting dopamine (K. Liu et *al*., 2022)**.**

(UAE) using NADESs represents an innovative and eco-friendly approach to enhancing phytochemical yield (Bakirtzi et *al*., 2016; Bosiljkov et *al*., 2017; Chen et *al*., 2018; Y. Li et *al*., 2020; Meng et *al*., 2018; G. Zhao et *al*., 2017)**.** UAE facilitates the disruption of plant cell walls through acoustic cavitation, increasing the recovery of bioactive compounds while reducing solvent consumption, labor, and energy costs (Demesa et *al*., 2024)**.** While most studies on NADESs-based phenolic extraction utilize hydrophilic eutectic solvents (primarily choline chloride-based systems) (Molnar et *al*., 2018; Weng et Toner, 2018; B.Y. Zhao et *al*., 2015), even the only study highlighted the use of eutectic solvents for extraction of dopamine from *P. oleracea* was with hydrophilic choline chloride-based NADES (K. Liu et *al*., 2022)**,** the potential of hydrophobic terpene-based NADESs in combination with UAE remains unexplored for *P. oleracea*.

Despite the extraction of bioactive compounds such as bioactive compounds from *Portulaca oleracea*, their in vivo bioavailability often remains low, limiting therapeutic efficacy. Factors such as poor solubility, rapid metabolism, and limited absorption contribute

to this challenge. For instance, a study identified six new alkaloids from *P. oleracea*, but their pharmacokinetic profiles were not extensively explored, leaving their bioavailability uncertain (Su et *al*., 2023)**.** Similarly, while *P. oleracea* contains various bioactive compounds like flavonoids and alkaloids, comprehensive studies on their *in-vivo* bioavailability are limited, hindering the understanding of their therapeutic potential (Y. X. Zhou et *al*., 2015a)**.** Addressing these bioavailability issues is crucial for developing effective therapeutic applications of *P. oleracea* bioactives.

This study aims to (i) identify the most efficient NADESs for extracting phenolic antioxidants from *P. oleracea* and compare it with ethanol-based extraction, (ii) optimize key extraction parameters, including hydrogen bond donor/acceptor molar ratio, sonication duration, and acid incorporation in NADESs, to maximize recovery of total phenolics, flavonoids, condensed tannins, and separate specific bioactive compounds (caffeic acid, syringic acid, p-coumaric acid, ferulic acid, gallic acid, rutin, and quercetin), (iii) assess the antioxidant potential of the extracts using multiple assays (DPPH, Trolox), (iv) evaluate antimicrobial activity against selected Gram-positive, Gram-negative bacteria, and yeast to determine the impact of NADESs and NADESs-enriched *P. oleracea* extracts, (v) investigate the in vitro anticancer potential of therapeutic deep eutectic systems (THEDESs) incorporating *P. oleracea* bioactive compounds, (vi) conduct in vivo acute toxicity studies to establish the toxicological profile of NADESs before any potential *in-vivo* or clinical use, and (vii) examine the hepatoprotective effects of THEDESs in mitigating methotrexate-induced liver injury. By addressing these objectives, this research contributes to the growing interest in green extraction technologies and their potential applications in nutraceutical and pharmaceutical formulations.

Bibliographic Review

PART I

Eutectic mixtures and therapeutic deep eutectic systems (THEDESs)

1 Eutectic mixtures

A eutectic mixture refers to a specific composition of at least two solid components that undergoes a phase transition to a liquid state at a distinct temperature, known as the eutectic point. This temperature represents the lowest melting point achievable among all possible compositions of the components (Alonso et *al*., 2016). As illustrated in Figure 1, the melting points of the individual pure components (A or B) are invariably higher than that of the eutectic mixture. This characteristic highlights the unique thermodynamic properties of eutectic systems, which are widely studied for their applications in various scientific and industrial fields.

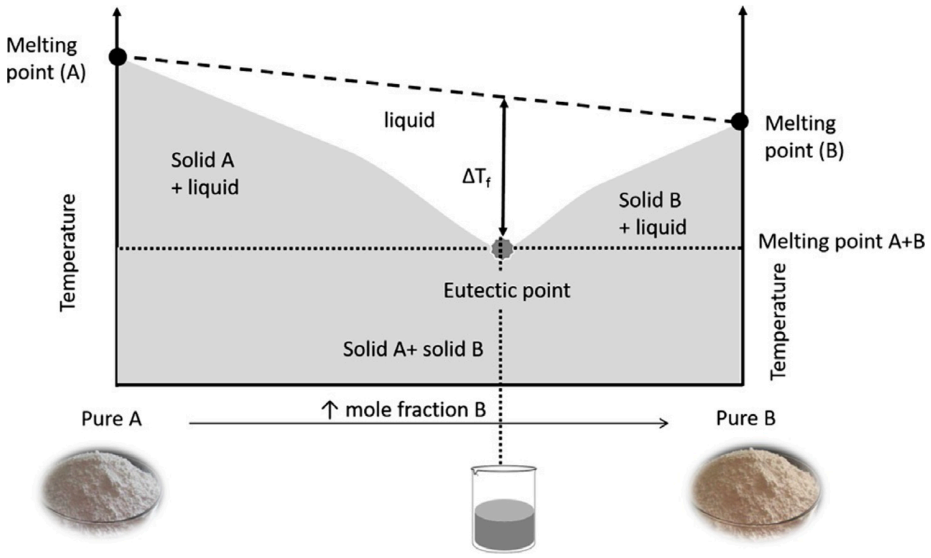

Figure 01: Scheme of the diagram of phases of two components (Francisco Pena-Pereira and Inmaculada de la Calle. 2018)

1.1 Deep eutectic systems (DESs)

Deep eutectic systems (DESs) are a class of innovative solvents composed of eutectic mixtures involving Lewis or Brønsted acids and bases. These mixtures can incorporate a diverse range of anionic, cationic, or even neutral species. Lewis acids and bases are defined by their ability to accept or donate electron pairs, respectively, while Brønsted acids and bases are characterized by their capacity to donate or accept protons (Tomé et *al.*, 2018). The interactions between the components of DESs "typically a halide salt or hydrogen-bond acceptor (HBA) and a hydrogen-bond donor (HBD)" are primarily governed by hydrogen bonding, although electrostatic forces and van der Waals interactions may also play a role. The properties of DESs, such as their solubility and stability, are influenced by the purity of their individual constituents.

DESs are generally hydrophilic due to their ability to form extensive hydrogen bonds, making them highly soluble in aqueous solutions. However, recent studies have also reported the development of hydrophobic DESs, expanding their potential applications (van Osch et *al.*, 2015; Ribeiro et *al*., 2015).

1.2 Natural deep eutectic systems (NADESs)

NADES are a specific type of DESs formed by natural products, such as organic acids, amino acids, sugars, choline halides or urea (Dai et *al.*, 2013a). These natural products commonly offer chemical diversity, renewability, biodegradability and reduced toxicity. Some examples of NADES include mixtures formed by fructose/glucose/sucrose, malic acid/citric acid, glucose/sorbitol/malic acid or choline chloride/proline/malic acid.

1.3 Therapeutic deep eutectic systems (THEDESs)

Therapeutic deep eutectic systems (THEDESs) represent a specialized category of deep eutectic systems (DESs) designed for pharmaceutical and therapeutic applications. In THEDESs, an active pharmaceutical ingredient (API) serves as one of the constituents of the eutectic mixture (Tomé et *al*., 2018). These systems are particularly advantageous for enhancing the solubility and permeability of drugs, thereby improving their bioavailability and therapeutic efficacy.

Several examples of THEDESs have been documented, including combinations such as menthol/ibuprofen, lidocaine/ibuprofen, and choline chloride/menthol complexed with APIs like acetylsalicylic acid, benzoic acid, and phenylacetic acid. Additionally, mixtures of choline chloride/urea and choline chloride/malonic acid have been explored with APIs such as benzoic acid, danazol, griseofulvin, and itraconazole (Tomé et *al.*, 2018). These examples illustrate the versatility of THEDESs in addressing challenges related to drug formulation and delivery.

2 Routes of THEDESs delivery

Therapeutic deep eutectic systems (THEDESs) can be administered through various routes, including oral, transdermal, intravenous, vaginal, and buccal delivery. Among these, the transdermal route has garnered significant attention due to the unique ability of DESs to facilitate the transport of larger molecules across the skin. This property makes THEDESs particularly promising for transdermal drug delivery, offering a non-invasive and efficient method for administering medications as reported by (Javed et *al*., 2024).

2.1 Transdermal delivery

Transdermal drug delivery offers a safer and more convenient alternative to oral administration. However, challenges such as poor water solubility of drugs complicate their incorporation into hydrophilic biopolymer systems. One promising solution is the use of therapeutic deep eutectic systems (THEDESs) for transdermal delivery. Several DESs have shown potential in enhancing the delivery of both small and large molecules. Notably, choline-based systems, such as the choline and geranic acid system, have been widely explored for this purpose. Additionally, a eutectic mixture of lidocaine and thymol incorporated into a microemulsion (ME) demonstrated extended anesthetic activity and skin compatibility, offering a promising approach for topical anesthesia (Y. Wang, Wang, et *al*., 2019). Another study highlighted the combination of skin needling with a lidocaine and prilocaine THEDES, which significantly improved pain management compared to THEDES alone (Fabbrocini et *al*., 2014). Furthermore, THEDESs of menthol and flurbiprofen stabilized within mesoporous silica hosts have been developed. This approach stabilizes amorphous menthol and controls the drug's release profile, showcasing the versatility of THEDESs in drug delivery (Cordeiro et *al*., 2017).

2.2 Oral delivery

A novel approach utilizing a natural deep eutectic system (NADES) was developed to enhance the oral delivery of RA-XII, a unique natural cyclopeptide with anti-tumor properties. This amorphous solid dispersion demonstrated significant advantages for oral cancer therapy, offering a non-invasive and patient-friendly alternative. The strategy effectively improved the solubility, permeability, and bioavailability of RA-XII, highlighting its potential in pharmaceutical applications (M. Liu et *al.*, 2021).

Similarly, therapeutic deep eutectic systems (THEDESs) of celecoxib were formulated using a supercritical CO_2 technique to enhance its oral bioavailability. Various processing methods, including evaporation crystallization, spray drying, and supercritical fluid techniques, were employed. Among these, the supercritical CO_2 method resulted in superior dissolution rates, underscoring its effectiveness in improving drug solubility and absorption (Hong et *al*., 2022).

2.3 Buccal delivery

Buccal drug delivery represents a promising non-invasive strategy for therapeutic administration. However, the effective systemic delivery of proteins and peptides via this route

remains challenging. To address this, chitosan was employed as a mucoadhesive polymer, while deep eutectic solvents (DESs) functioned as transport enhancers in the formulation of a biodegradable polymeric patch for insulin buccal delivery. Notably, a viscoelastic CAGE-insulin gel, structured with two layers of biodegradable polymer, achieved a sevenfold increase in insulin transport across porcine buccal mucosa in an ex vivo model (Vaidya et Mitragotri, 2020).

2.4 Intravenous delivery

A deep eutectic solvent (DES)-based formulation was developed for the intravenous administration of verteporfin, utilizing a lipoidal DES composed of choline and oleate to enhance its solubility in stable nanocomplexes. This approach significantly improved cellular uptake, retention, penetration, and in vivo tumor accumulation of the drug. These findings suggest the potential of DES-based systems for optimizing intravenous chemotherapy delivery (Kim et *al.*, 2021).

2.5 Percutaneous delivery

A study developed a menthol/camphor-based eutectic system of tacrolimus for percutaneous delivery to treat atopic dermatitis. This nanoscale system demonstrated enhanced drug delivery and treatment efficacy, effectively addressing atopic dermatitis while minimizing skin irritation (Yixuan Wang et *al*., 2019).

2.6 Vaginal delivery

A THEDES containing metronidazole was developed for intravaginal application to treat bacterial vaginosis. The system utilized a polycaprolactone (PCL) matrix, processed using a bench-scale twin-screw hot melt extruder, to achieve extended drug release. The THEDES-PCL matrix demonstrated a faster onset of action and controlled drug release over seven days, proving to be more effective than oral therapy (Li et *al*., 2021)

3 Medical applications of NADES and THEDESs

3.1 Pharmaceutical applications of natural deep eutectic systems (NADESs)

A key characteristic of NADESs is their ability to form eutectic mixtures with lower melting points than their individual components. This phenomenon is attributed to strong molecular interactions, including hydrogen bonding and π-π stacking, which disrupt the

crystalline structure and promote the formation of a stable liquid phase (Liu et *al*., 2021). The versatility of NADES allows for fine-tuning their physicochemical properties; such as viscosity, polarity, and melting point by adjusting the composition and ratio of their constituents, making them adaptable for various applications, including drug delivery, extraction, biocatalysis, and chemical synthesis (Figure 02).

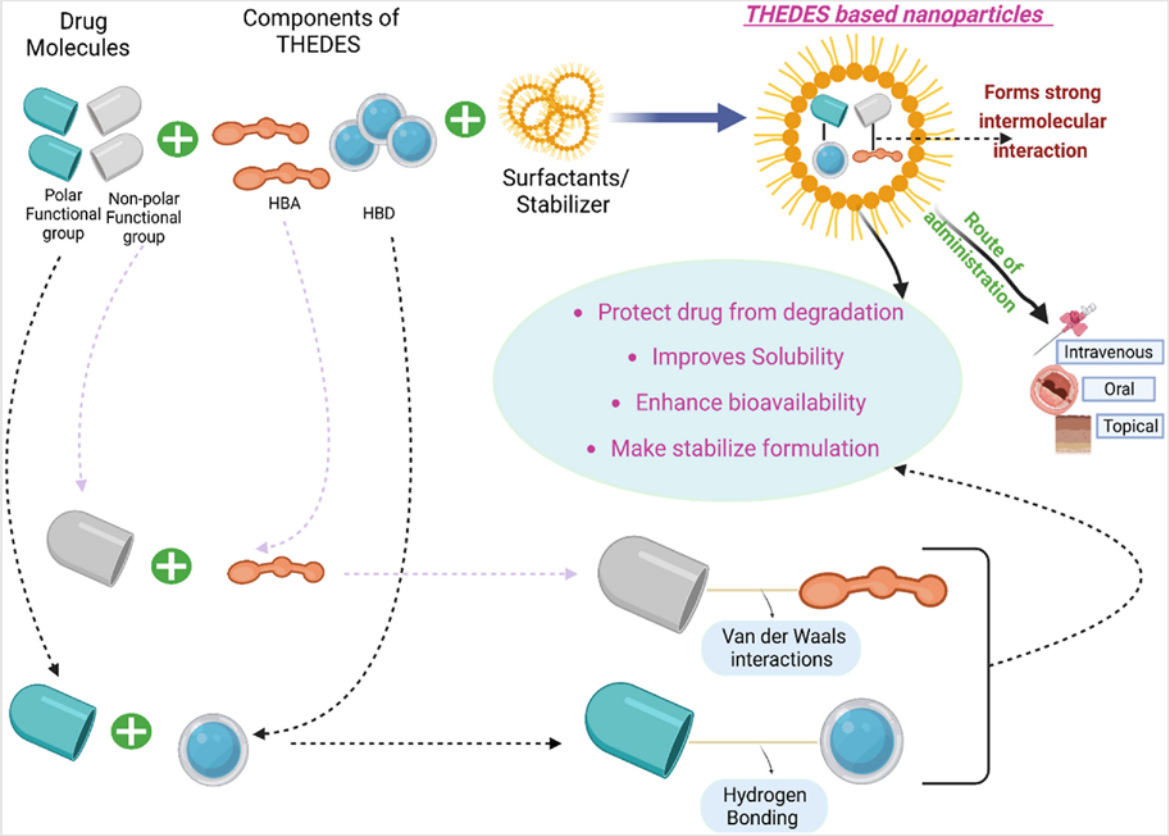

Figure 02: Various pharmaceutical applications of THEDES (Shamama Javed et *al*., 2024)

3.1.1 NADESs in drug delivery

The biocompatibility, biodegradability, and ability of NADESs to solubilize hydrophobic or poorly water-soluble drugs have positioned them as promising candidates for pharmaceutical applications. As alternative solvents or carriers in drug formulations, NADES offer several advantages, including improved drug solubility, enhanced bioavailability, and controlled release properties (Liu et *al.*, 2021)

Another notable advantage of NADESs is their natural origin, aligning with the increasing demand for sustainable and eco-friendly alternatives in various industries. By utilizing renewable resources, NADESs reduce dependence on synthetic solvents, thereby minimizing environmental impact.

3.1.2 Cryoprotective properties of NADESs

Additionally, NADESs exhibit cryoprotective effects, which can be beneficial for preserving biological materials during freezing and thawing processes. Cryopreservation techniques often rely on synthetic cryoprotectants such as dimethyl sulfoxide (DMSO) and glycerol. However, their toxicity limits their use in clinical applications. NADES, on the other hand, function as natural cryoprotective agents (CPAs), mimicking the protective mechanisms of antifreeze proteins and sugars by preserving cellular integrity during freezing and thawing (Marcantonini et *al*., 2022)

Recent studies have evaluated NADESs as CPAs in mammalian cell lines, including L929 and HaCaT cells, using the vitrification method. The results demonstrated their effectiveness in cryopreservation, highlighting their potential as a safer alternative to traditional CPAs (Jesus et *al*., 2021; Jesus, Duarte et Paiva, 2022). Additionally, a deep eutectic solvent composed of proline and glycerol was found to be an efficient cryoprotectant with lower toxicity than its individual components (Bryant et *al*., 2022).

3.2 Therapeutic applications of therapeutic deep eutectic systems (THEDESs)

3.2.1 THEDESs in cancer treatment

Cancer remains a major global health challenge, necessitating alternative therapies with enhanced efficacy and fewer side effects. Therapeutic deep eutectic systems (THEDESs) have emerged as promising carriers for anticancer drugs due to their simple preparation, stability, and cost-effectiveness. Several studies have explored the potential of THEDESs in cancer treatment by incorporating anticancer drugs into these systems, for cancer prevention as shown in (Figure 03).

One study developed temperature-responsive eutectic formulations for doxorubicin using fatty acids (stearic and myristic acid) combined with liquid lipids like oleic acid. These formulations, prepared via hot melt encapsulation and sonication, demonstrated enhanced permeability. Toxicity assessments, including acute toxicity studies and hemolysis assays, confirmed their safety compared to free doxorubicin (Parveen et *al*., 2022).

In another approach, THEDESs were formulated by combining natural terpenes with anticancer properties (safranal, menthol, and linalool) with non-steroidal anti-inflammatory drugs (NSAIDs) such as flurbiprofen, ibuprofen, and ketoprofen. Among these, a menthol-

ibuprofen (3:1) mixture significantly improved drug solubility and bioavailability (Pereira et *al.*, 2022). Additionally, in vitro studies on colorectal cancer models suggested that an ibuprofen-perillyl alcohol-based THEDESs could serve as a promising alternative to conventional therapies (Silva et *al.*, 2020).

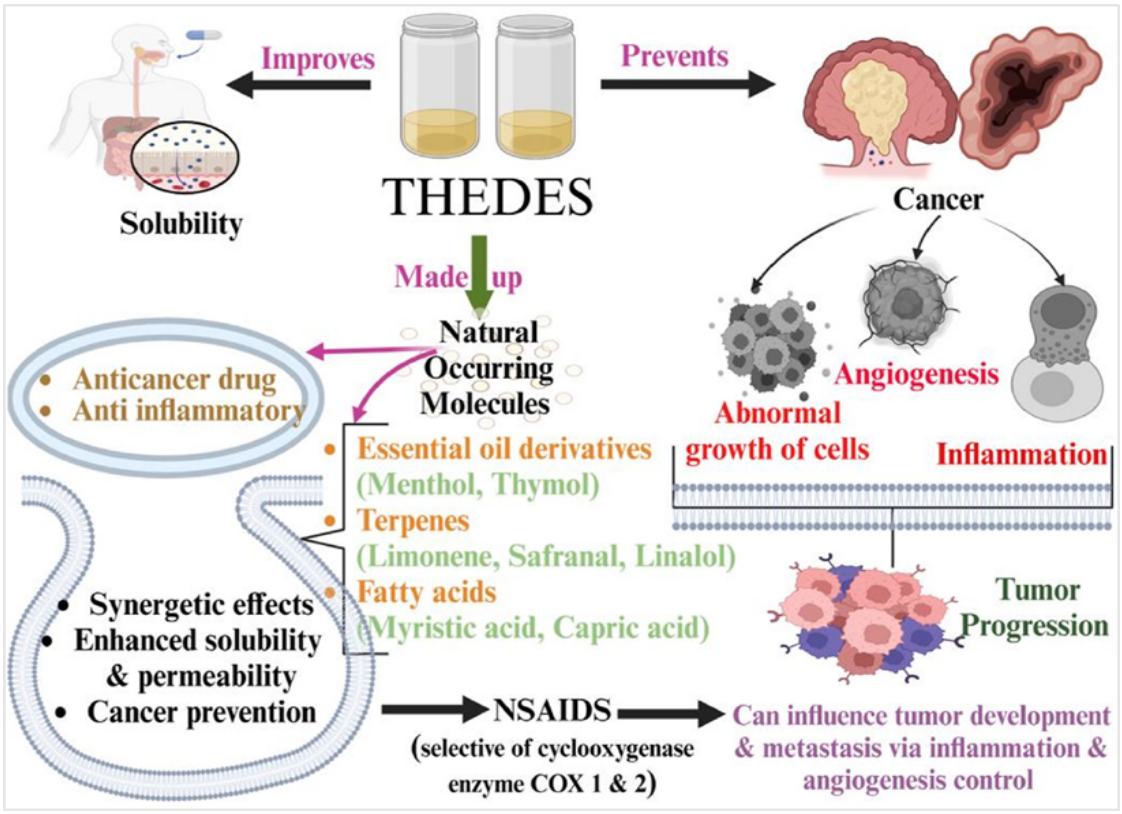

Figure 03: Pharmacological mechanism of cancer prevention by THEDESs (Shamama Javed et *al.*, 2024)

Furthermore, a limonene (LIM)-based THEDES was developed for cancer treatment due to LIM's known anticancer activity. Various formulations, including IBU:LIM (1:4), IBU:LIM (1:8), and menthol:LIM (1:1), were tested for their antiproliferative effects against HT29 colorectal cancer cells. The LIM:IBU (1:4) combination exhibited synergistic effects, highlighting its potential application in anticancer therapies (Pereira et *al.*, 2019).

3.2.2 THEDESs and wound healing

Recent studies have highlighted the wound healing potential of hydrophobic THEDESs formulated with menthol and saturated fatty acids such as stearic, myristic, and lauric acids (Figure 04). The menthol-stearic acid THEDES was evaluated for cytotoxicity on HACaT cells

and was found to be non-cytotoxic while exhibiting significant wound healing properties (J. M. Silva, Pereira, et *al*., 2019).

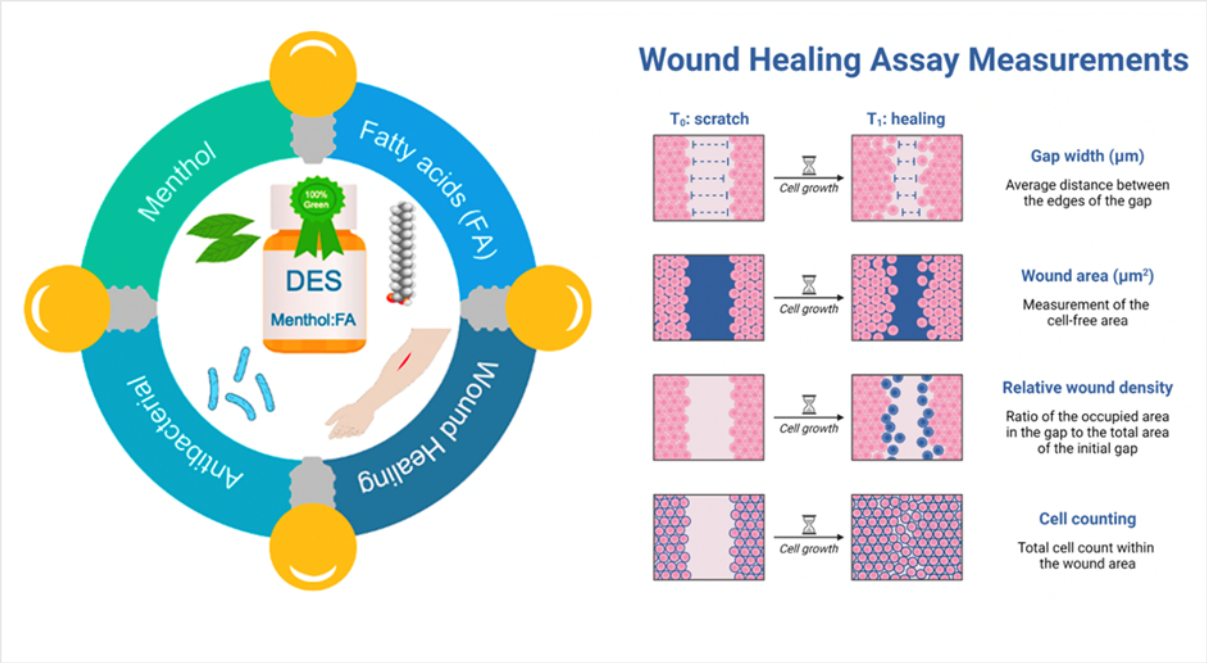

Figure 04: Wound healing potential of hydrophobic THEDESs (J. M. Silva, Pereira, et *al*., 2019).

Another study explored the development of green poly (vinyl alcohol) (PVA) nanofibers using NADES for the rapid dissolution and delivery of acetylsalicylic acid (aspirin) and honey. These nanofibers demonstrated biocompatibility, non-cytotoxicity, and benefits such as targeted drug delivery, improved solubility, and controlled drug release. In vivo experiments revealed an accelerated wound healing process, with an impressive 85.2% improvement in wound closure observed six days post-surgery using PVA-DES-honey nanofibers (Zhang et *al*., 2021).

3.2.3 Hepatoprotective effects of THEDESs

Eutectic mixtures incorporating silymarin and polyvinylpyrrolidone K30 (PVP K30) in different ratios were formulated and assessed for their hepatoprotective and anti-inflammatory properties. The resulting solid dispersion of silymarin with PVP K30 significantly enhanced solubility by five times compared to pure silymarin. This improved solubility contributed to superior hepatoprotective and anti-inflammatory effects observed in the developed formulation (Sherikar et *al*., 2021).

3.2.4 Fortification of bioactive molecules with THEDESs

Therapeutic deep eutectic solvents (THEDESs) provide an effective strategy for stabilizing bioactive compounds, ensuring their preservation and efficacy across various applications. These systems play a crucial role in protecting sensitive bioactive molecules, such as drugs, natural extracts, enzymes, and proteins, thereby enhancing their stability, shelf life, and therapeutic potential.

One notable advantage of THEDESs lies in drug stabilization. By encapsulating drugs, THEDESs shield them from degradation caused by external factors such as light, heat, oxygen, and pH fluctuations. This protective environment helps maintain drug potency and prolongs efficacy, leading to improved therapeutic outcomes. Additionally, THEDES contribute to preserving natural extracts, which often contain fragile bioactive compounds susceptible to degradation. Acting as solvents or carriers, THEDESs help prevent oxidation and extend the shelf life of these extracts, ensuring their integrity for applications in nutraceuticals and cosmeceuticals (Javed et *al*., 2024).

4 Mechanisms of action of NADESs and THEDESs

Natural deep eutectic systems (NADESs) and therapeutic deep eutectic systems (THEDES) exhibit unique mechanisms of action that make them promising for various pharmaceutical and biotechnological applications.

4.1 Interaction with cell membranes and enhancement of bioavailability

NADES can interact with cell membranes, altering their permeability and facilitating the transport of bioactive molecules across biological barriers. This interaction primarily occurs due to NADES's ability to form hydrogen bonds with membrane components, which can disrupt lipid structure and increase membrane fluidity (Cajnko et *al*., 2023). Recent studies have indicated that hydrophobic natural deep eutectic solvents (HNADES) exhibit antimicrobial properties, primarily through interactions with bacterial cell membranes. These solvents can integrate into the lipid bilayer of bacterial membranes, enhancing membrane permeability and leading to cellular lysis (Bedair, Samir and Mansour, 2024; Gidado M. J. et *al*., 2025)

4.2 Modulation of oxidative stress and inflammation

Some NADES components possess intrinsic antioxidant properties. When used as solvents or co-solvents, they can reduce oxidative stress by scavenging free radicals,

contributing to anti-inflammatory effects (Figure 3). This modulation of oxidative stress is crucial in the treatment of various inflammatory conditions (Cajnko et *al*., 2023), Recent studies have demonstrated that terpene-based NADESs and THEDESs exhibit inherent antiradical (antioxidant) activity (Rodrigues et *al*., 2020 ; Sebbah et *al*., 2025).

4.3 Enzymatic interactions and metabolic pathways

NADESs can influence enzymatic activity by stabilizing enzymes or modifying their conformation. For instance, certain NADESs have been shown to stabilize thermolabile enzymes, enhancing their activity at high temperatures. Additionally, by modulating enzyme-substrate interactions, NADESs can affect metabolic pathways, opening new opportunities for the development of innovative therapeutic strategies (Cajnko et *al*., 2023). additionally, it was recently suggested that acidic eutectic mixtures stabilize phenolic extracts by inhibiting the action of polyphenol oxidase (PPO) (Sebbah et *al*., 2025). While specific studies on acidic eutectic mixtures, acidulants like citric acid and ascorbic acid are commonly used to lower pH, thereby inhibiting PPO and reducing enzymatic browning in foods (Liang et *al*., 2024).

4.4 Solubility enhancement of APIs

Solubility is a critical factor influencing the efficacy of active pharmaceutical ingredients (APIs), particularly those with poor water solubility. natural deep eutectic solvents (NADESs) and therapeutic deep eutectic systems (THEDESs) have emerged as effective solubilizers, improving drug dissolution and stability (Figure 05).

NADES, composed of naturally derived hydrogen bond donors (HBDs) and acceptors (HBAs), create a solubilizing microenvironment by forming extensive hydrogen bonding networks. This interaction disrupts the crystalline structure of APIs, enhancing their solubility. Studies have demonstrated that NADES-based formulations significantly improve the solubility of hydrophobic bioactives like curcumin, quercetin, and rutin (Jeliński, Przybyłek and Cysewski, 2019).

THEDESs, an advanced subclass of NADESs incorporating bioactive pharmaceutical compounds, further enhance solubility by acting as both a solvent and a stabilizer. For example, THEDESs incorporating non-volatile terpenoids have shown superior dissolution properties for hydrophobic compounds, making them promising carriers for poorly water-soluble drugs (Faggian et *al*., 2016).

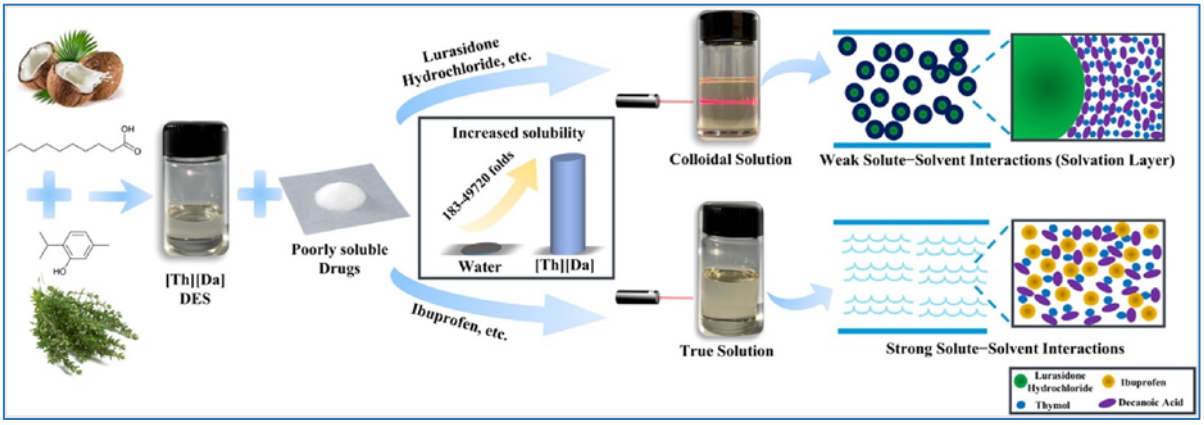

Figure 05: Increased solubility of most insoluble APIs (Junxiao Zhu et *al*., 2023)

Additionally, NADESs have been explored in various drug delivery systems, including oral and dermal applications. Their tunable viscosity and polarity enable the dissolution of both hydrophilic and lipophilic APIs, making them ideal candidates for solubility enhancement strategies (Lomba et *al*., 2021).

4.5. Bioavailability enhancement of delivered APIs

Beyond solubility enhancement, NADESs and THEDESs significantly impact the bioavailability of delivered APIs by improving absorption, distribution, and systemic uptake. Bioavailability refers to the proportion of an administered drug that reaches systemic circulation in an active form, and NADESs-based formulations have been shown to improve this parameter through multiple mechanisms. NADESs enhance gastrointestinal absorption by increasing API solubility in gastric and intestinal fluids. They also modulate intestinal permeability, potentially interacting with efflux transporters to reduce drug elimination. In a study on rutin, its oral bioavailability in mice was significantly improved when formulated in NADESs compared to conventional solvents (Faggian et *al*., 2016). In transdermal applications, NADESs and THEDESs serve as permeation enhancers, facilitating drug transport across the stratum corneum. Their ability to solubilize both lipophilic and hydrophilic molecules makes them effective carriers for topical formulations, potentially replacing traditional penetration enhancers (Lomba et *al.*, 2021).

PART II

Portulaca oleracea (Purslane) and its bioactive compounds

1 General presentation of *Portulaca oleracea* L.

Portulaca oleracea, commonly known as purslane, is a succulent annual herb that thrives in various climates across the globe. Historically, it has been utilized in traditional medicine and as a nutritious food source in many cultures. Purslane is recognized for its high content of omega-3 fatty acids, vitamins, and minerals, contributing to its reputation as a health-promoting plant (Zhou et *al*., 2015b).

Figure 06: Natural habitat and parts of purslane plant. (a) Purslane plant in natural habitat; (b) young stem with leaves; (c) harvested plant showing roots; and (d) young fruits, known as pyxidia with black-colored seeds (Kumar et *al*., 2022b)

2 Taxonomy and botanical characteristics

2.1 Taxonomy and distribution

The exact origin of *Portulaca oleracea* remains uncertain, though it is often linked to arid regions such as North Africa. Archaeological pollen analysis suggests its presence in the New World before Columbian times. Its succulent stems and fleshy leaves indicate adaptation to desert climates, particularly in the Middle East and India. Today, purslane is widely distributed across Europe, Africa, North America, Australia, and Asia (Vishal Chugh et *al*., 2019). The taxonomy of Purselane is here reported as classified by The National Resources Conservation Service, USDA (United States Department of Agriculture) 2012 :

- **Kingdom:** Plantae
- **Clade:** Angiosperms
- **Clade:** Eudicots

- **Order:** Caryophyllales
- **Family:** Portulacaceae
- **Genus:** *Portulaca*
- **Species:** *P. oleracea*

2.2 Botanical characteristics

P. oleracea is characterized by its smooth, reddish, and mostly prostrate stems. The leaves are fleshy, oval-shaped, and tend to cluster at stem joints and ends. The plant produces small yellow flowers with five heart-shaped petals, which can appear throughout the year, depending on environmental conditions. Following flowering, seed capsules form, which split open upon maturation to release numerous tiny seeds (Kumar et *al*., 2022b).

3. Diverse metabolites of *P. oleracea* and their bioactivities

3.1 Phenolic acids and their biological effects

Phenolic acids are essential specialized metabolites found in plants, derived from benzoic and cinnamic acids (Vincente et *al*., 2014; Chandrasekara, 2019). They are characterized by carboxylic acid groups associated with phenolic compounds (Kumar and Goel, 2019). Several phenolic acids, such as caffeic acid, p-coumaric acid, ferulic acid, gallic acid, gentisic acid, benzoic acid, and anisic acid, have been identified in purslane (Silva and Carvalho, 2014b; V. Sicari, 2018). Additionally, Santiago-Saenz et *al*. detected the presence of caffeic, gallic, vanillic, ferulic, and syringic acids in this plant (Santiago-Saenz et *al*., 2018)

These bioactive compounds exhibit potent antioxidant, anti-inflammatory, and antimicrobial properties, contributing to various health benefits. Caffeic acid and ferulic acid, for instance, play a crucial role in reducing oxidative stress and protecting cells from damage linked to chronic diseases such as cardiovascular disorders and neurodegenerative conditions. Gallic acid has been reported for its anticancer potential, while p-coumaric acid and syringic acid contribute to metabolic health by regulating glucose levels and lipid metabolism. The presence of these phenolic acids in purslane underscores its potential as a functional food with therapeutic applications.

3.2 Flavonoids and their pharmacological properties

Plant flavonoids are a large group of naturally occurring phenyl chromones found in various parts of plants, including the roots, stems, flowers, and fruits (Middleton, 1996). These

bioactive compounds are well known for their antioxidant, anti-inflammatory, antitumor, antiviral, and antibacterial activities (Cushnie and Lamb, 2011). Flavonoids also play a crucial protective role against coronary diseases by improving vascular function and reducing oxidative stress in blood vessels (Cazarolli et *al*., 2008).

Several flavonoids, such as apigenin, kaempferol, luteolin, quercetin, isorhamnetin, kaempferol-3-O-glucoside, and rutin, have been isolated from purslane (V. Sicari, 2018 ; Xu et *al.,* 2006) identified five flavonoids—kaempferol, apigenin, myricetin, quercetin, and luteolin-using capillary electrophoresis with electrochemical detection. Among these, quercetin has demonstrated neuroprotective effects by significantly improving learning and memory in mice, suggesting its potential role in preventing neurodegenerative diseases such as Alzheimer's (Lu et *al.*, 2006). As lately in 2018 Santiago-Saenz et *al.* have quantified myricetin in purslane, further supporting its role as a flavonoid-rich plant. Additionally, three newly identified flavonoids, oleracone C, D, and E, were reported for the first time in purslane (Yang et *al.*, 2018).

Apigenin, another major flavonoid found in purslane, has demonstrated antibacterial properties against pathogenic bacteria, including *Pseudomonas aeruginosa, Salmonella typhimurium, Proteus mirabilis, Klebsiella pneumoniae,* and *Enterobacter aerogenes* (Nayaka et *al.*, 2014). The presence of these bioactive compounds highlights purslane's potential as a functional food with cardiovascular, neuroprotective, and antimicrobial benefits.

3.3 Homoisoflavonoids and their potential applications

Homoisoflavonoids (HIFs) are a distinct class of plant compounds that differ from flavonoids by an additional carbon atom (Castelli et López, 2017). To date, over 300 HIFs have been identified in various plant species (Lin, Liu and Ye, 2014). These bioactive molecules exhibit antimicrobial, antimutagenic, anti-inflammatory, antidiabetic, and antioxidant properties (Siddaiah et *al*., 2006; Abegaz, Mutanyatta-Comar et Nindi, 2007; Melilli et *al*., 2020).

Purslane is a notable source of HIFs, with several significant compounds synthesized by the plant. Duan et *al.* (2009) recently isolated two novel HIFs, oleracone J and oleracone K, while Nemzer (Nemzer, Al-Taher and Abshiru, 2020b) recently identified four others, portulacanones A–D, from its aerial parts. Additionally, Yang et *al*. (2018) discovered oleracone C as a unique HIF in purslane. Another key compound, (E)-5-hydroxy-7-methoxy-

3-(2'-hydroxybenzyl)-4-chromanone (HM-Chromanone), demonstrated a protective effect against glucose-induced apoptosis in pancreatic β-cells, highlighting its antidiabetic potential (Park et *al.*, 2019). Moreover, HIFs have been shown to inhibit 5-lipoxygenase, an enzyme linked to inflammatory conditions such as asthma, allergic rhinitis, and osteoarthritis (Siddaiah et *al*., 2006). These findings underscore purslane's richness in HIFs and their potential therapeutic applications.

3.4. Terpenoids from *P. oleracea*

Terpenoids, also known as isoprenoids, are organic compounds derived from isoprene units and are widely synthesized in plants and other organisms (Tholl, 2015). Purslane has been identified as a rich source of terpenoids, with Elkhayat, Ibrahim, and Aziz (2008) reporting portulene as a newly discovered diterpene. In addition, several other terpenoids, including portuloside A, portuloside B, lupeol, friedelane, taraxerol, portaraxeroic acid A, and portaeaxeroic acid B, have been isolated from this plant (Wang et Yang, 2010; Mir et Ali, 2016).

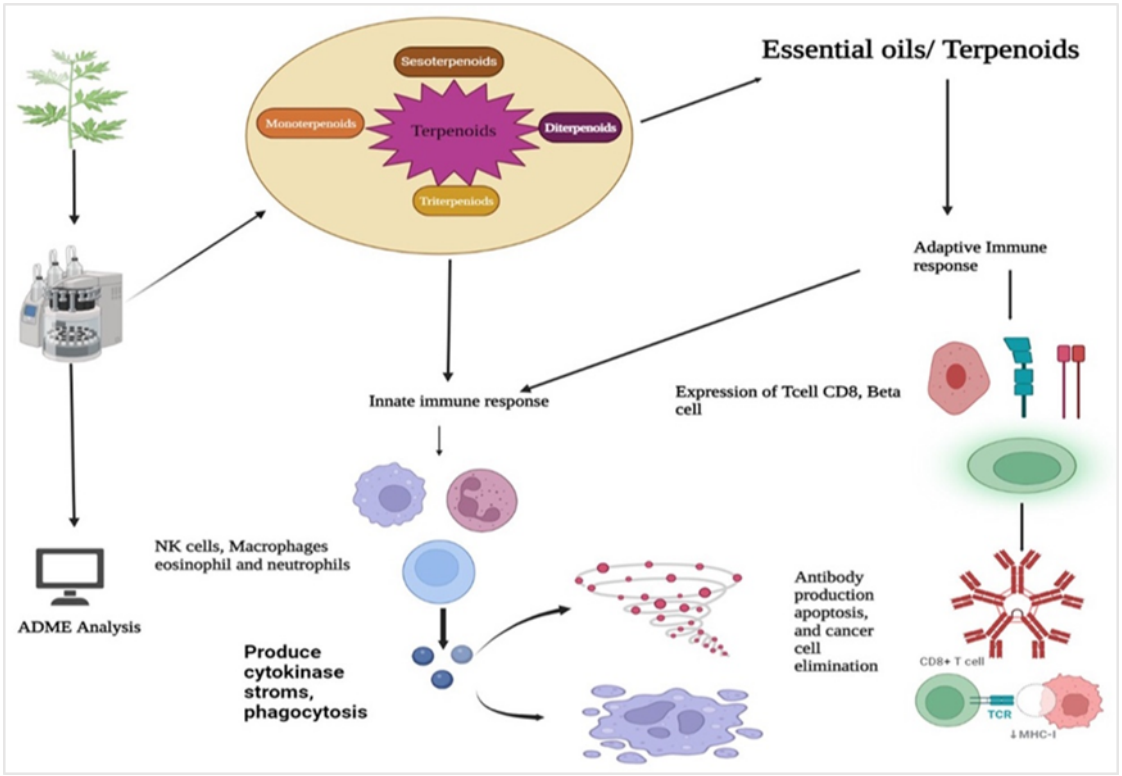

Figure 07: Terpenoids in EOs diverse and sustainable antimicrobial, anti-inflammatory, antioxidants (Tohfa Siddiqui et *al*., 2024).

These bioactive terpenoids contribute to various health benefits. Lupeol and taraxerol exhibit strong anti-inflammatory and antioxidant properties, which may help combat oxidative stress-related diseases (Figure 07). Additionally, some terpenoids have been linked to anticancer, hepatoprotective, and antimicrobial effects, making purslane a promising source of natural therapeutic agents.

3.5. Other phytochemicals and their bioactivities

Purslane is a rich source of diverse phytochemicals, including various organic acids, phenolic compounds, and sterols. Research has identified numerous organic acids in different parts of *P. oleracea*, such as oxalic acid, butanedioic acid, phenylpropionic acid, *p*-hydroxybenzoic acid, lauric acid, vanillic acid, myristic acid, pentadecanoic acid, palmitoleic acid, palmitic acid, heptadecanoic acid, oleic acid, stearic acid, arachidic acid, behenic acid, quinolinecarboxylic acid, indole-carboxylic acid, catechol, lonchocarpic acid, fumaric acid, aconitic acid, citric acid, and malic acid (Oliveira et *al*., 2009; Wang and Yang, 2010; Wang, Zhang and Wang, 2017; Chugh Vishal et *al*., 2019). Among these, oxalic and citric acids are the most abundant (Oliveira et *al*., 2009; Petropoulos et *al*., 2015).

Additionally, phenolic compounds like 3-caffeoylquinic acid and 5-caffeoylquinic acid have been identified, contributing to the plant's strong antioxidant properties. Purslane also contains allantoin, a byproduct of purine metabolism with wound-healing and skin-protective effects (Selamoglu, 2018). Other notable phytoconstituents include *N,N′*-dicyclohexylurea, β-sitosterol, and β-sitosteryl glucoside, which have been associated with anti-inflammatory and cholesterol-lowering benefits (Asia N Rashed et *al*., 2004).

These phytochemicals collectively contribute to purslane's potential in promoting health, offering antioxidant, anti-inflammatory, and lipid-lowering effects, making it a valuable dietary component.

PART III

Terpenes and terpenoids in therapeutics

1 Classification of terpenes and terpenoids

Terpenes are volatile hydrocarbons naturally produced by numerous plants and some animals, primarily as secondary metabolites in response to stress. In plants, they serve as infochemicals, attractants, or repellents, and at higher concentrations, act as potent defenses against pathogens due to their high toxicity (Paduch et *al.*, 2007). Structurally, terpenes are composed of multiple isoprene units (C5H8), linked head to tail to form linear chains or arranged into rings (Aqil et *al*., 2007a). Terpenoids, a subclass of terpenes, contain oxygen molecules and are formed through biochemical modifications such as the removal or addition of methyl groups (Pandey et *al*., 2017). These oxygenated derivatives include alcohols, aldehydes, esters, ethers, epoxides, ketones, and phenols, with notable examples being carvacrol, citronellal, geraniol, linalool, linalyl acetate, piperitone, menthol, and thymol. Both terpenes and terpenoids exhibit diverse biological activities, including anticancer, anti-allergic, antibacterial, and antioxidant properties (Masyita et *al.*, 2022). The main terpenes and terpenoids used in this study are all shown in (Figure 08).

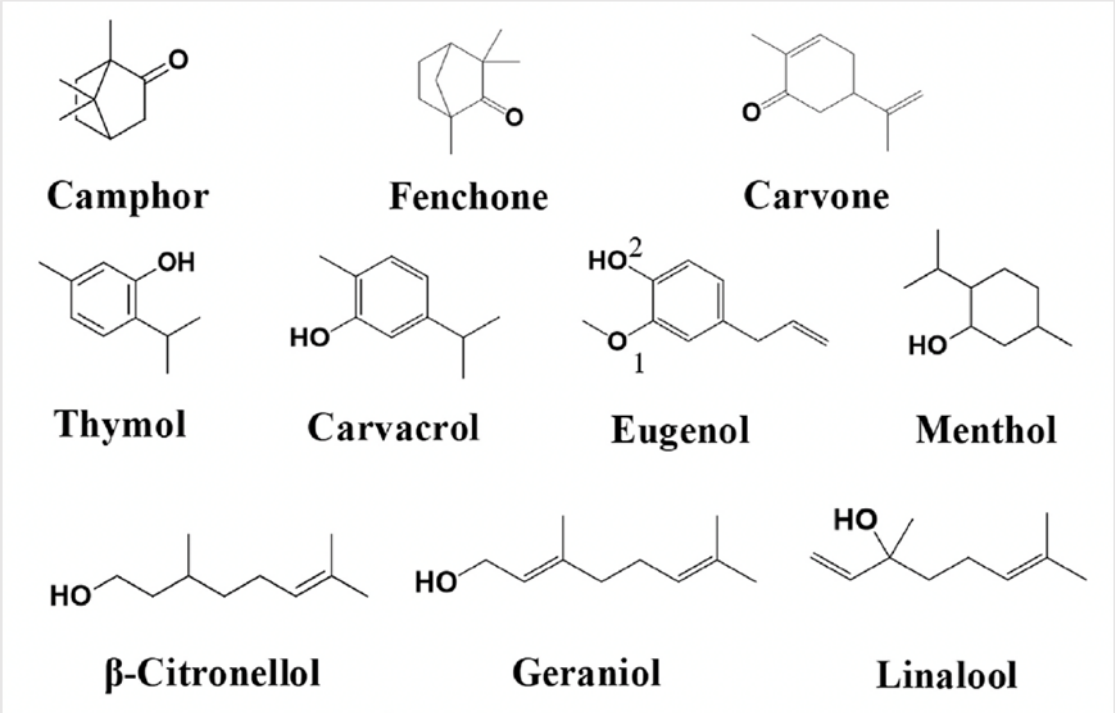

Figure 08: Monoterpens classified into 3 subclasses: Cyclic monoterpenes (Fenchone, Carvone, Menthol), Phenolic monoterpenes (Carvacrol, Thymol, Eugenol), Acyclic monoterpenes (Linalool, Geraniol, Citronellol) (Fan, Sebbah, et *al*., 2021)

1.1 Monoterpenes

They are dimers of isoprene and can be divided into acyclic, monocyclic, bicyclic, and tricyclic compounds. Monoterpene derivatives typically containing oxygen or nitrogen atoms are known as *monoterpenoids*.

1.1.1 Cyclic monoterpene *(Fenchone, Carvone, Menthol)*

Fenchone ($C_{10}H_{16}O$) is a bicyclic monoterpene ketone naturally present in essential oils derived from *Foeniculum vulgare* (fennel) and *Artemisia absinthium* (wormwood). It has a camphoraceous aroma and is widely used in the fragrance and flavor industries, particularly in herbal and minty compositions.

Biologically, fenchone exhibits antimicrobial, antifungal, antioxidant, and anti-inflammatory activities. It has also been explored for its potential as a natural preservative in food and cosmetic formulations. Fenchone's low toxicity and versatility make it a valuable compound in both traditional and modern applications (Ahmad et *al*., 2022).

Carvone ($C_{10}H_{14}O$) is a monoterpene ketone found predominantly in the essential oils of *Mentha spicata* (spearmint) and *Carum carvi* (caraway). It exists as two enantiomers:

1. **(R)-Carvone** (commonly found in caraway seeds) with a spicy, earthy aroma.
2. **(S)-Carvone** (commonly found in spearmint leaves) with a sweet, minty aroma.

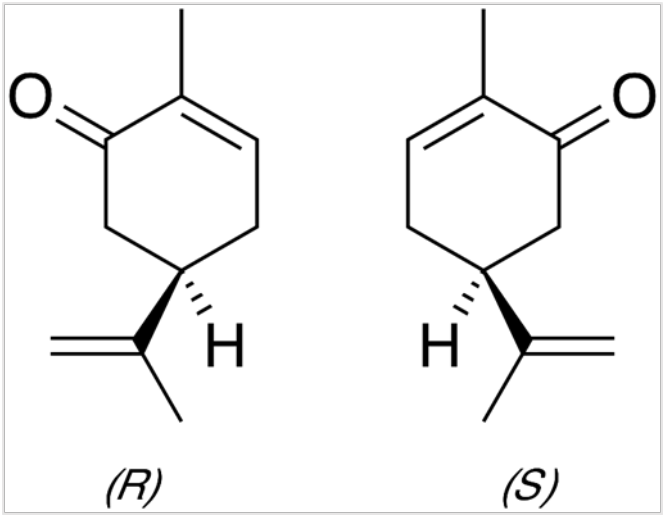

Figure 09: Two different configurations of carvone, (R)-Carvone and (S)-Carvone (Bouyahya et *al*., 2021).

Carvone is extensively utilized in the food and flavor industries to impart characteristic flavors in chewing gums, toothpastes, and baked goods. It also demonstrates various biological properties, including antimicrobial, antifungal, antioxidant, anti-inflammatory, and insecticidal activities (Bouyahya et *al.*, 2021). Furthermore, carvone has shown potential in agriculture as a natural herbicide and in pharmacology for its therapeutic effects, including anticancer and analgesic properties. Indeed, has an antiproliferative potential by induction of apoptosis and the G2/Mcell cycle arrest as shown in Figure 10. Carvone can induce anticancer effects by two main mechanisms: (1) intrinsic apoptotic action via decreasing Bcl2 and decreasing Bax, as well the release of cytochrome C which induce caspases expression and PARP cleavage; (2) cell cycle arrest at G2/M via its action on cyclin-dependent kinase 1.)

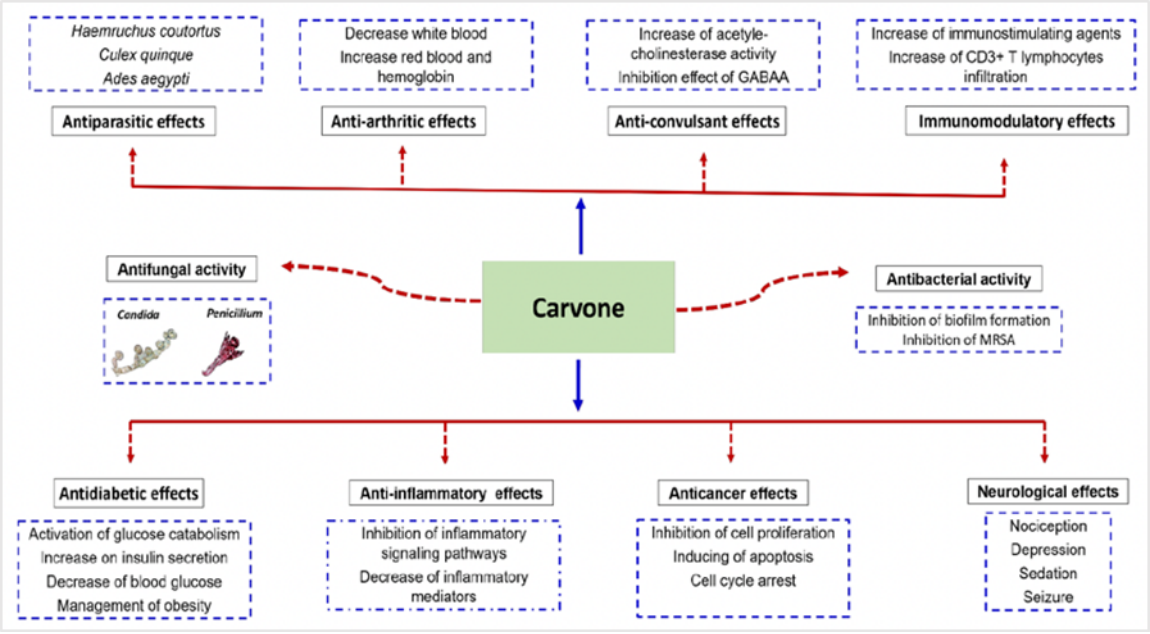

Figure 10: Pharmacological applications of carvone (Bouyahya et *al*., 2021)

Menthol ($C_{10}H_{20}O$) is a cyclic monoterpene alcohol obtained from essential oils of *Mentha canadensis* L. (cornmint) and *Mentha* x *piperita* L. (peppermint) (Aqil et *al*., 2007a; Kamatou et *al*., 2013). It is known for its upper respiratory tract decongestant properties and its multiple biological properties, such as analgesic, antimicrobial, antifungal, antipruritic, penetration-enhancing, chemopreventive, anticancer and anti-inflammatory activities (Aqil et *al.*, 2007a; Kamatou et *al.*, 2013). Moreover, menthol is an agonist of the transient receptor potential melastatin 8 (TRPM8) thus, it can chemically activate this cold-sensitive receptor and elicit a cooling effect or sensation and an analgesic effect (Kamatou et *al*., 2013; Liu et *al.*, 2016).

1.1.2 Phenolic monoterpenes *(Carvacrol, Thymol, Eugenol)*

Carvacrol ($C_{10}H_{14}O$) as it appears in figure 07, is a monoterpene phenol primarily obtained from the essential oils of *Origanum vulgare* L. (oregano) and *Thymus capitatus* L. (thyme). It is well recognized for its potent antimicrobial, antifungal, and antioxidant properties, as well as additional biological activities, including anti-inflammatory, anticancer, and antiparasitic effects. Carvacrol is widely used in the pharmaceutical, food, and agricultural industries due to its bioactivity and natural origin. Furthermore, carvacrol interacts with bacterial membranes and disrupts their integrity, which underlies its strong antimicrobial action. It also exhibits modulatory effects on ion channels and cellular signaling pathways, supporting its therapeutic potential (Can Baser, 2008).

Thymol ($C_{10}H_{14}O$) is a monoterpene phenol obtained from essential oils of *Thymus vulgaris* L. (thyme) and other plants from the Lamiaceae family. It is well known for its antimicrobial and antifungal properties, as well as its multiple biological activities, such as antioxidant, anti-inflammatory, antiviral, and antiparasitic effects (Nagoor Meeran et *al*., 2017). Thymol is widely used in pharmaceuticals, food preservatives, and cosmetics due to its bioactivity and safety profile. Moreover, thymol interacts with biological membranes and proteins, leading to its antimicrobial mechanisms and modulation of ion channel activity, which contributes to its therapeutic applications (Nagoor Meeran et *al*., 2017; Li et *al*., 2022).

Eugenol ($C_{10}H_{12}O_2$) is a monoterpene phenol derived from the essential oils of *Syzygium aromaticum* (clove), *Ocimum basilicum* (basil), and *Cinnamomum verum* (cinnamon). It is widely known for its analgesic, antimicrobial, antifungal, anti-inflammatory, antioxidant, and anticancer properties. Eugenol is commonly used in dentistry as a local anesthetic and antiseptic, as well as in food and cosmetic industries as a flavoring agent and preservative. Additionally, eugenol acts by disrupting microbial cell membranes, scavenging free radicals, and modulating inflammatory pathways, which contribute to its therapeutic efficacy and broad spectrum of biological activity (Ulanowska et Olas, 2021).

1.1.3. Acyclic monoterpenes *(Linalool, Geraniol, Citronellol)*

Linalool ($C_{10}H_{18}O$) a naturally occurring acyclic monoterpene alcohol obtain from *Coriandrum sativum* fruits that has a variety of commercial applications in cosmetics, soaps, perfumes and detergents due to their fragrance and odour, but it is also used in traditional medicine to alleviate pain, relax, sedate or eliminate certain Bacteria (Carson et Riley, 1995;

Aqil et *al*., 2007b; Lapczynski, Letizia and Api, 2008; Peana and Moretti, 2008) It is a cheap and well-known chemical with no irritation and sensitization reactions on the human body (Peana et *al*., 2002; Lapczynski, Letizia and Api, 2008) that present antimicrobial, anti-inflammatory, analgesic, anticancer and antihypertensive activities (Peana et *al*., 2002; Peana and Moretti, 2008; Anjos et *al.*, 2013; Chang and Shen, 2014) Its anticancer properties have been already studied and three mechanisms of action have been described: induction of apoptosis (CHERNG et *al*., 2007; Gu et *al*., 2010), induction of oxidative stress (Usta et *al*., 2009) and immunomodulation (Chang and Shen, 2014).

Geraniol ($C_{10}H_{18}O$) is a naturally occurring acyclic monoterpene alcohol found in the essential oils of plants such as *Cymbopogon martinii* (palmarosa), *Pelargonium graveolens* (geranium), and *Rosa damascena* (rose). It is widely utilized in perfumes, cosmetics, and flavoring agents due to its sweet, floral fragrance. Geraniol also serves as a precursor in the synthesis of various terpenoid derivatives.

In addition to its commercial applications, geraniol exhibits significant biological activities, including antimicrobial, antioxidant, anti-inflammatory, antifungal, and insect-repellent properties. It has shown promise in anticancer research through mechanisms such as the induction of apoptosis, inhibition of cell proliferation, and modulation of signaling pathways. Geraniol's safety and low toxicity make it suitable for applications in pharmaceuticals, traditional medicine, and functional products (Mączka, Wińska and Grabarczyk, 2020).

Citronellol ($C_{10}H_{20}O$) is a monoterpene alcohol monoterpene found in the essential oil of plants of the genus Cymbopogon and has several pharmacological activities already described in the literature, such as anticonvulsant, antihyperalgesic and orofacial antinociceptive properties (Brito et *al.*, 2015a,b, 2013a; Sousa et *al*., 2006). is a naturally occurring acyclic monoterpene alcohol found in essential oils of plants such as *Cymbopogon citratus* (lemongrass), *Rosa damascena* (rose), and *Pelargonium graveolens* (geranium). It exists in two stereoisomeric forms (shown in figure 10): (+)-citronellol and (–)-citronellol which differ in their optical activity and biological properties. Citronellol is widely used in perfumes, cosmetics, soaps, and insect repellents due to its pleasant floral fragrance.

Beyond its commercial applications, citronellol exhibits significant biological activities, including antimicrobial, antioxidant, anti-inflammatory, analgesic, and insecticidal properties.

It is known for its safety profile, as it is non-irritating and non-sensitizing to human skin. Recent studies have also highlighted its potential anticancer effects, primarily mediated through the induction of oxidative stress, apoptosis, and inhibition of cancer cell proliferation.

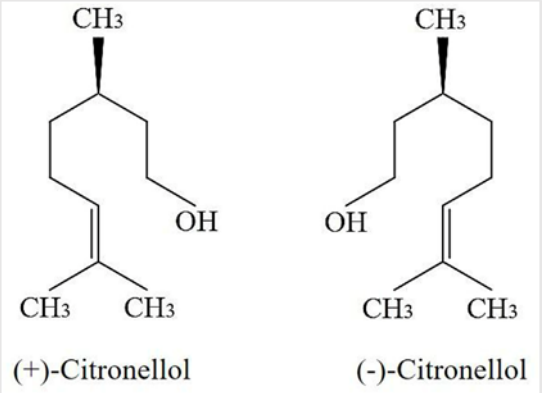

Figure 11: Two stereoisomeric forms of citronellol: (+)-citronellol and (–)-citronellol (Bouyahya et *al*., 2021)

1.2 Other terpenoid classes (sesquiterpenes, diterpenes)

Terpenoids, a diverse class of natural compounds derived from isoprene units, exhibit a broad range of therapeutic properties. Beyond monoterpenes, sesquiterpenes and diterpenes represent significant subgroups with potent pharmacological activities, making them valuable in drug discovery and therapeutic applications.

1.2.1 Sesquiterpenes,

Composed of three isoprene units (C15), are widely distributed in plants and essential oils. Many sesquiterpenes, such as β-caryophyllene, artemisinin, and farnesol, demonstrate anti-inflammatory, anticancer, antimicrobial, and neuroprotective effects. Artemisinin, a sesquiterpene lactone derived from *Artemisia annua*, is one of the most well-known antimalarial agents (Tu, 2011). β-Caryophyllene, found in various essential oils, interacts with cannabinoid receptors (CB2), offering potential applications in pain management and neuroprotection (Russo, 2011). Farnesol, a natural sesquiterpene alcohol, has shown anticancer effects through apoptosis induction and cell cycle arrest in various cancer models (Yilmaz Öztürk et *al.*, 2022).

1.2.2 Diterpenes

Consisting of four isoprene units (C20), are another crucial class with notable biological activities. Examples include taxanes**,** retinoids**,** and clerodane diterpenes, all of which contribute to therapeutic advancements. Taxol (paclitaxel)**,** a diterpene from *Taxus* species, is a widely used chemotherapeutic agent that stabilizes microtubules, inhibiting cancer cell division (Kingston, 2011) Retinoids, derived from vitamin A (all-trans retinoic acid), play essential roles in cell differentiation and are used in dermatology and oncology (Tang et Gudas, 2011). Clerodane diterpenes, found in medicinal plants, exhibit antimicrobial and cytotoxic effects, making them promising candidates for new drug development (Ghisalberti, 1998).

These sesquiterpenes and diterpenes contribute significantly to modern pharmacology, providing both direct therapeutic applications and scaffolds for semi-synthetic drug development. Their diverse bioactivities underline the importance of terpenoid research in advancing new treatments for infectious diseases, cancer, neurodegenerative disorders, and inflammatory conditions.

2 Main recent therapeutic applications of terpenes and terpenoids

2.1 Terpenoids and antiviral effects against SARS-CoV-2

Terpenoids have gained attention for their potential role in combating SARS-CoV-2 by interfering with viral replication and targeting key proteins essential for viral attachment and entry. Given the severity and rapid spread of the disease as shown in (Figure 12), researchers have explored the antiviral properties of various terpenoids, demonstrating their promising effects against SARS-CoV-2 infection (Das et *al*., 2021).

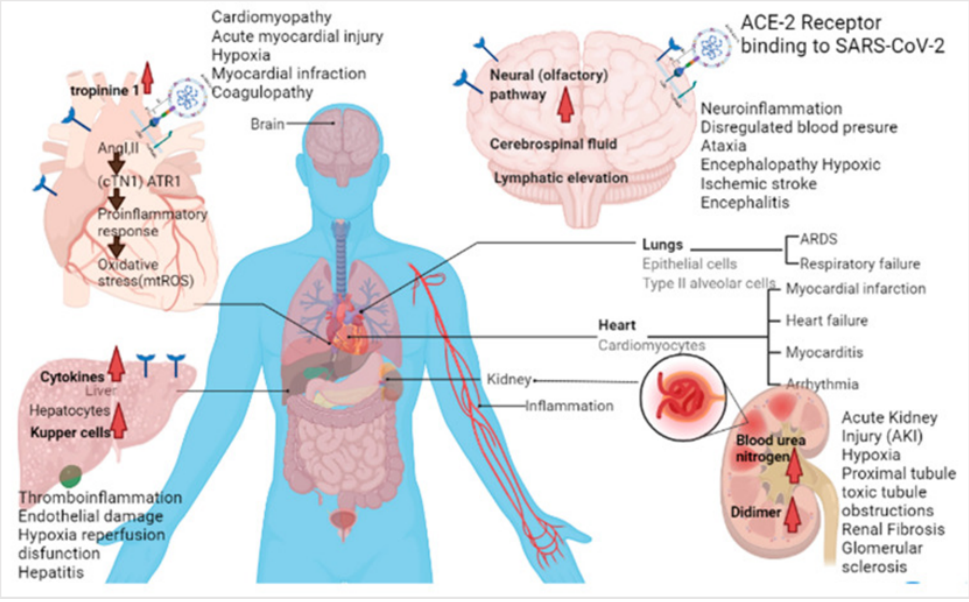

Figure 12. Pathophysiological spread mechanism of SARS-CoV-2 (Das et *al.*, 2021)

Several studies have investigated the inhibitory activity of terpenoids on viral glycoproteins, such as the main protease (Mpro) and the receptor-binding domain (RBD) of the spike protein, both of which are associated with ACE2 inhibition, the primary receptor facilitating viral entry (Figure 13). Notably, terpenoids have shown the ability to regulate viral protease activity, particularly through interactions with 3CLpro, also known as 3-chymotrypsin-like protease or C30 endopeptidase, a crucial enzyme required for coronavirus replication (Udugama et *al*. 2020).

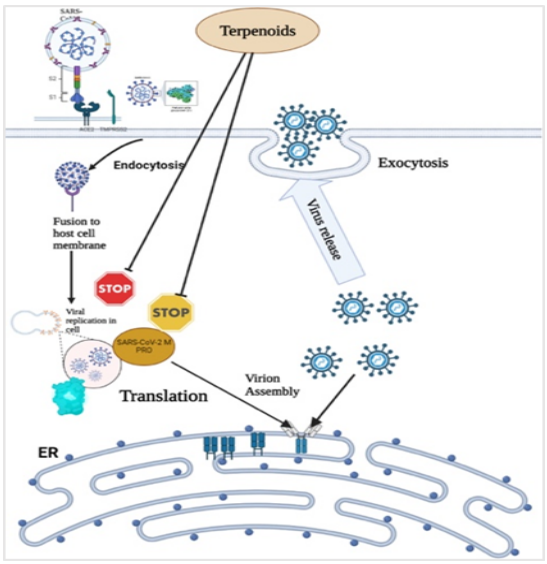

Figure 13. inhibitory activity of terpenoids on viral glycoproteins, such as the main protease (Mpro) and the receptor-binding domain (RBD) of the spike protein (Das et *al.*, 2021)

Among the terpenoids with notable antiviral potential, citronellol has emerged as a promising natural agent against SARS-CoV-2. Similarly, a diterpenoid extracted from *Andrographis paniculata* has been identified through in silico studies as a potential inhibitor of Mpro, the virus's main protease (Saha et *al*., 2021). Additionally, molecular docking analyses have highlighted the strong binding affinity of compounds such as thymol and carvacrol, both of which exhibit significant inhibitory activity against SARS-CoV-2 proteases, particularly 3CLpro and PLpro, with pronounced potency against PLpro.

Another noteworthy compound is eucalyptol (1,8-cineole), a major component of eucalyptus essential oil, which has demonstrated inhibitory potential against SARS-CoV-2 based on computational modeling (Astani and Schnitzler, 2014). Furthermore, linalool, a

monoterpene predominantly found in lavender, has shown promising inhibitory effects on SARS-CoV-2 infection.

In addition to these findings, various in silico studies have been conducted on FDA-approved antiviral drugs to identify novel phytochemicals with anti-SARS-CoV-2 properties. Several terpenoids, including limonene, oleanolic acid, β-amyrin, betulinic acid, and β-sitosterol, have been predicted to inhibit viral entry by blocking ACE2 and TMPRSS receptors. Beyond their role in preventing viral attachment, these terpenoids may also enhance immune response by activating CD4 and CD8 T-lymphocytes. Computational models suggest that terpenoids could effectively inhibit viral proteins essential for replication, further highlighting their therapeutic potential in managing SARS-CoV-2 infections.

2.2 Immunomodulatory effects

Terpenoids, naturally occurring in various fruits, vegetables, and spices, exhibit diverse pharmacological properties, particularly in anticancer activity. Different classes of terpenoids—including monoterpenoids, sesquiterpenoids, diterpenoids, sesterterpenoids, triterpenoids, tetraterpenoids, and polyterpenoids have been shown to inhibit the NF-κB signaling pathway. This inhibition occurs through multiple mechanisms, including IκB phosphorylation, DNA interactions, and the translocation of the p65 subunit (Figure 6) (Yang and Dou, 2010).

Tumor necrosis factor (TNF) plays a key role in activating NF-κB by stimulating the IKK complex subunits. This activation leads to the phosphorylation and subsequent degradation of IκB inhibitors, thereby initiating the classical NF-κB signaling pathway (Li and Verma, 2002).

Further downstream, NF-κB-inducing kinase (NIK) phosphorylates and activates the IκB kinase (IKK) cascade, which in turn modifies p100. The phosphorylation of p100 facilitates NF-κB translocation to the nucleus, where it binds to primary target genes, promoting their activation (Liu et *al*., 2017).

Materials and Methods

1 Materials

1.1 Chemicals and reagents

The reagents used for the preparation and characterization of natural deep eutectic systems (NADESs) were carefully selected based on their purity and physicochemical properties. These included camphor (95% purity, melting point 179 °C, CAS: 76-22-2), menthol (99% purity, 41–43 °C, CAS: 2216-51-5), thymol (97% purity, 52 °C, CAS: 89-83-8), β-citronellol (92% purity, <25 °C, CAS: 106-22-9), lactic acid (92% purity, 16.8 °C, CAS: 50-21-5), acetic acid (99% purity, 16.6 °C, CAS: 64-19-7), and formic acid (98% purity, 8.4 °C, CAS: 64-18-6), all of which were purchased from Heowens Biochemical Technology Co., Ltd. (Tianjin, China). Other essential terpenoid-based and organic acid-based reagents such as fenchone (CAS: 1195-79-5), carvone (CAS: 99-49-0), carvacrol (CAS: 499-75-2), eugenol (CAS: 97-53-0), geraniol (CAS: 106-24-1), linalool (CAS: 78-70-6), capric acid (CAS: 334-48-5), and lauric acid (CAS: 143-07-7) were procured from Macklin Biochemical Co., Ltd. (Shanghai, China).

For the extraction process and biological activity assessments, additional chemical standards and solvents were sourced from Sigma-Aldrich. These included menthol, β-citronellol (95%, CAS: 106-22-9), and capric acid (99-100%, CAS: 334-48-5), along with key antioxidant and phenolic compounds such as: DPPH (≥95%, CAS: 1898-66-4), gallic acid (≥98%, CAS: 149-91-7), quercetin (≥95%, CAS: 117-39-5), and catechin (CAS: 154-23-4). Furthermore, Folin–Ciocalteu's reagent (CAS: 9005-32-7), sodium carbonate (99.5%, CAS: 497-19-8), and Trolox (97%, CAS: 53188-07-1) were included in the experimental workflow and were also obtained from Sigma-Aldrich (Madrid, Spain).

Other essential reagents were acquired from various suppliers to ensure the accuracy and reproducibility of the experiments. Lactic acid (90%) was supplied by Biochim, while absolute ethanol (>99.8%) was purchased from Honeywell. Additionally, glacial acetic acid was obtained from Biochem Chemopharma, and HPLC-grade acetonitrile and acetic acid were sourced from Fisher Scientific (Lisbon, Portugal). Phenolic standards used in high-performance liquid chromatography (HPLC) analyses, including gallic acid (≥99%, CAS: 149-91-7), L-ascorbic acid (99%, CAS: 50-81-7), caffeic acid (≥98%, CAS: 331-39-5), syringic acid (≥95%, CAS: 530-57-4), p-coumaric acid (≥98%, CAS: 501-98-4), ferulic acid (≥99%, CAS: 537-98-4), rutin (≥94%, CAS: 207671-50-9), and quercetin (≥95%, CAS: 117-39-5), were obtained

from Sigma-Aldrich (Madrid, Spain). The water used for all experiments was purified using a Milli-Q water purification system (TGI Pure Water Systems, USA).

The cytotoxicity assessment of NADESs and NADESs-based extracts (THEDESs) was conducted using AGS human gastric adenocarcinoma cells (CRL-1739), obtained from ATCC (Manassas, VA, USA). The cells were cultured in RPMI-1640 medium supplemented with heat-inactivated fetal bovine serum (FBS), penicillin–streptomycin (PS) solution (1%), and phosphate-buffered saline (PBS, pH 7.4), all of which were supplied by Gibco, Thermo Fisher Scientific (Waltham, MA, USA). The cytotoxicity assay employed MTT reagent (3-[4,5-dimethylthiazol-2-yl]-2,5-diphenyltetrazolium bromide, 5 mg/mL in PBS) from Sigma-Aldrich, St. Louis, MO, USA, with dimethyl sulfoxide (DMSO) serving as the solvent for formazan dissolution.

All experiments were conducted in 96-well culture plates (Corning, Corning, NY, USA) and incubated under controlled conditions (37°C, 5% CO_2, humidified atmosphere) using a CO_2 incubator. The absorbance readings of MTT assays were recorded using a microplate reader (VICTOR Nivo™) from PerkinElmer, Waltham, MA, USA. These experimental conditions were optimized to ensure the reliability of the cytotoxicity results and facilitate accurate interpretation of the NADES-extract effects on AGS cell viability.

Regarding the *in vivo* study, methotrexate (MTX) that was administered was supplied by Ebewe laboratories to the university hospital center of Mostaganem, as injection of (20 mg syringe, 10 mg/mL concentration). Tween 80 was used as a vehicle for the oral administration of THEDESs.

1.2 Animal models

The study was conducted on Wistar rats (*Rattus norvegicus*) obtained from the Pasteur Institute of Algiers, a commonly used model in toxicological studies due to their genetic similarity to humans, rapid growth, ease of handling, and affordability. Experiments were carried out at the Laboratory of Beneficial Microorganisms, Functional Food and Health (LMBAFS).

Three-month-old rats (175± 25 g) were housed in plastic cages under controlled conditions (22 ± 2°C, 12/12h light/dark cycle) with free access to water and a corn-based pellet diet (ONAB, Annex). They were acclimatized for two weeks before treatment began.

1.3 Equipment and apparatus

UAE was conducted using a sonicator from J-P Selecta with a 5L capacity, a frequency of 40 kHz, a power of 120 W, a heating power of 90 W, and powered by AC 220V/240V at 50/60 Hz. The sonicator was employed for specific extractions requiring ultrasound treatment.

Furthermore, various parameters were measured using a DLAB spectrophotometer, model SP-UV 1100. This spectrophotometer features a spectral bandwidth of 2.0 nm, a wavelength accuracy of ±0.5 nm, wavelength repeatability ≤0.3 nm, and a photometric range of -0.3 to 3.0A and 0-200%T. Photometric accuracy is ±0.002A at 0.5A. These characteristics were crucial for the photometric analyses of the samples, ensuring precise and reliable measurement of the studied components.

The method was carried out using HPLC equipment, model LC-4000, an integrated system from Jasco, Japan, equipped with an AS-4050 autosampler, a PU-4180 pump, and an MD-4010 multiwavelength diode array detector (DAD) of the same brand.

1.4 Plant samples

The plant *Portulaca oleracea* L. (POL), as show in figure 13, was initially identified and sourced from the Mostaganem region in Algeria (35°55.869′ Nord 0°5.3508′ Est) between May and July 2022. The plant was thoroughly washed, its leaves separated, air-dried in the dark for a week, and then subjected to a 24-hour dry at 45°C. After drying, the leaves were ground into powder, which was subsequently stored at -20°C.

2 Prepartion and characterization of NADESs

2.1 NADESs Formulation and Screening

The synthesis of natural deep eutectic solvents (NADESs) was carried out employing molar ratios between hydrogen donors and acceptors of 1:1, 1:2, 2:1. This was achieved using a heating and magnetic stirring method at 50°C or 80 °C for 30 to 45 minutes until the formation of a homogeneous transparent liquid, as described in our previous studies (Fan, Liu, et *al*., 2021; Fan, Sebbah, et *al*., 2021). Over 150 combinations were tested, only stable eutectic mixtures were retained for further exploration. Clear eutectic combinations that remained as transparent liquids at room temperature were screened to deeply study the intermolecular interactions.

2.2 Physicochemical properties

2.2.1 Density and viscosity measurements

The viscosities and densities of the NADESs were measured at 25 °C and atmospheric pressure using a NDJ-8S digital rotational viscometer and MDJ-600G densitometer (density 0.0001 $g \cdot cm^{-3}$; viscosity 2%), respectively. The properties of menthol/acetic acid, menthol/lactic acid, and camphor/formic acid systems have been studied (Ribeiro et *al*., 2015b; Ramon and Guillena, 2020) Their viscosities at different temperatures were also evaluated. Equimolar ratio was chosen according to the reported eutectic mixture, H-bond interaction sites, and same conditions for MD simulations.

2.2.2 Fourier transform infrared characterization

The Fourier transform infrared characterization of menthol/β-citronellol and thymol/β-citronellol systems were conducted to prove the presence of hydrogen-bond network (Annex 3)

3 Extraction and characterization of bioactive compounds

3.1 Extraction using NADESs and EtOH

The ethanolic extract was prepared using the classical method, where 10 g of *Portulaca oleracea* L. (POL) were macerated in 100 ml of absolute ethanol under magnetic stirring for 24 hours in hermetically sealed bottles and protected from light. As for the eutectic extracts, the blends were prepared following the same m/v ratio; 10 g of dry matter were added to 100 ml of NADES in opaque test tubes. Subsequently, the extraction was carried out using the ultrasound treatment method coupled with vortex, at temperatures ranging from 45°C to 51°C, with a deviation interval of +/- 2°C controlled using a thermometer, for 1 hour and 30 minutes, with cyclic intervals of 30 minutes UAE alternated with vortex agitation for 2 to 3 minutes at the end of each cycle. The mixtures were recovered and centrifuged at 30,000 RPM for 15 minutes, the supernatant was collected, and stored at -20°C.

3.2 Spectrophotometric analysis

3.2.1 Total phenolic content (TPC)

Total polyphenols were determined using the Folin-Ciocalteu method, as described by (Talbi et *al*., 2015). In summary, 5 mL of 1:10 diluted Folin-Ciocalteu's reagent was added to 1 mL of sample or standard. After 4 minutes, the reaction was neutralized with 4 mL of sodium

carbonate solution (75 g/L). The absorbance was measured at 760 nm after 2 hours of incubation at room temperature against a reagent blank. Gallic acid was used as the standard for the calibration curve at increasing concentrations of 15.525, 31.25, 63.5, 125, and 250 mg/ml. The results were expressed in milligrams of gallic acid equivalent (GAEq) per gram of extract (mg GAEq / g extract).

3.2.2 Total flavonoids content (TFC)

Quercetin was used as the standard for the calibration curve with dilutions ranging from 200 to 1000 microliters. For each sample or standard, 1 ml of extract was added to 1 ml of 2% $AlCl_3$ solution. The mixture was incubated for 10 minutes in the dark at room temperature, and the absorbance was measured at 430 nm. Flavonoid concentrations were deduced from the calibration range curve established with quercetin. Three repetitions were performed for each tube, and the results are expressed in milligrams of quercetin equivalent per gram of extract (mg QEq/g extract) (Alsaud et *al*., 2021)**.**

3.2.3 Condensed tannins (CT)

Fifty microliters (50 µL) of the extract or standard were added to 1500 µL of vanillin solution. Subsequently, a volume of 750 µL of concentrated hydrochloric acid (HCl) was added. Absorbance was measured at 550 nm after a 20-minute incubation at room temperature. The concentration of condensed tannins was calculated using the regression equation derived from the calibration range established with catechin (at concentrations of 0 and 2000 µg/ml), and it is expressed in milligrams of catechin equivalent per gram of extract (mg CEq/g extract), following the methodology described by (Ali-Rachedi et *al*., 2018)**.**

3.3 High - performance liquid chromatography (HPLC) separation

High-Performance Liquid Chromatography (HPLC) method was developed and validated to directly determine several phenols from the extracts. The following fused-core stationary-phase chemistries were used: a Thermo Scientific Hypersil Gold C18 (150 mm × 2.1 mm, 3µm) column. All analyses were conducted at room temperature. Detection was performed in the near-UV region, from 200 to 400 nm, and absorbances at the wavelength of 320 nm were used for phenol quantification. The sample injection volume was 10 µL. A gradient solvent system of 0.5% acetic acid (A) and acetonitrile (B) was used. The gradient program started with 65% A and remained at this concentration for the first 10 minutes; 15 minutes at 100% (B); 16

minutes at 100% (A); at a constant flow of 1 mL/min. Detection was carried out in a DAD, using 320 nm as the preferred wavelength. Before analysis, samples were diluted with acetonitrile at a dilution factor of 3, thoroughly mixed, and filtered using a 0.22 mm PTFE microfilter. Each sample was analyzed using HPLC with triplicate measurements.

4 *In-silico* studies

4.1 Molecular dynamic simulation method

A same method of molecular dynamic (MD) simulations was applied for both Terpenes-Bases NADESs and Capric acid-based NADESs. They were conducted with GROMACS, version disparities are observed (GROMACS 2019 in Method 1 and in Method 2) (Van Der Spoel et *al.*, 2005). Molecular descriptions utilized the General Amber Force Field (GAFF) for both methods (J. Wang et *al*., 2004)**.** Cubic simulation boxes of approximately 5 × 5 × 5 nm were constructed with specified quantities of hydrogen bond acceptor (HBA) and hydrogen bond donor (HBD) molecules, generated using the Packmol package (L. Martínez et *al.*, 2009)**.** Energy minimization at 400 K and subsequent annealing from 400 K to 298 K for 5 ns were common steps in both methods (Abedin et *al*., 2020). However, differences arise in the simulation runs, with Method 1 employing a 10 ns duration and Method 2 extending to 50 ns.

Temperature control methods also diverge, Isothermal-isobaric (NPT) and canonical (NVT) ensemble steps were used to further relax these systems, with Method 1 utilizing the Berendsen thermostat and Method 2 employing the Nosé−Hoover thermostats. Pressure control, performed using the Parrinello–Rahman approach, remains consistent between the methods, The MD simulations runs of 10 ns were conducted for all systems at 1 bar and at 298 K with a non-bonded interactions cutoff of 1.2 nm, and long-range interactions are calculated using the particle-mesh Ewald (PME) procedure with a grid spacing of 0.16 nm and interpolation order of 4 (Jiang et *al*., 2019). Hydrogen bond analyses, initiated after ≈1 ns of equilibration, and visualization using Multiwfn package 3.7 (Lu et Chen, 2012a) and Visual Molecular Dynamics (VMD) (Humphrey et *al*., 1996). are shared practices. Periodic boundary conditions with a tolerance of 2.0 Å are applied in both simulations.

4.2 Quantum chemistry calculations

Geometries of camphor, fenchone, carvone, thymol, carvacrol, eugenol, menthol, β-citronellol, geraniol and linalool were fully optimized at the B3LYP/6–311++g (d,p) level with

Grimme's DFT-D3(BJ) empirical dispersion correction by using ORCA 4.2.1 package (Neese, 2018)**.** Quantitative analysis of molecular surface was conducted with Multiwfn (T. Lu & Chen, 2012b)**.** Molecular surfaces of terpenoids coloured by electrostatic potential surfaces were plotted via VMD program.

5 *In-vitro* studies

5.1 Antioxidant activity assessment

5.1.1 DPPH free radical scavenging

To assess antioxidant activity using the DPPH test, solutions were prepared, including ~~a~~ 0.004% DPPH solution (0.004 g DPPH in 100 ml ethanol), an extract (10 mg extract in 100 ml ethanol/DES), and a 200 µg/ml ascorbic acid solution (stock solution: 1 mg ascorbic acid in 1 ml ethanol, then a working solution: 400 µL of stock solution + 1600 µL ethanol).

In the protocol, 2500 µL of DPPH were mixed with 100 µL of the sample or standards at various concentrations. The mixtures were incubated in the dark at room temperature for 30 minutes, and absorbance was measured at 517 nm. The percentage of DPPH radical scavenging activity was calculated using the following equation:

DPPH radical scavenging activity: DPPH (%) = (A0 – A1) /A0 × 100

where *A*0 is the absorbance of the control (DPPH solution) and *A*1 is the absorbance of the sample/standard, following the methodology of (Nasri et *al*., 2017)**,** curve in Annex 2.

5.1.2 Trolox equivalent antioxidant capacity (TEAC)

The Trolox [6-hydroxy-2,5,7,8-tetramethylchromano-2-carboxylic acid] calibration curve was established by measuring the absorbance of a 100 µM DPPH ethanolic solution after the addition of Trolox at various concentrations (0–40 µM). Absorbance was recorded at 517 nm after a 20 min reaction between Trolox and the DPPH radical, as was described by Lingfeng et *al*. (2021) with some modifications (curve in Annex 2).

The equation for the calibration curve is:

$$Y = -0.0237\,x + 1.3513$$

Where Y is the absorbance at 517 nm and x is the Trolox concentration in µM.

5.2 Antimicrobial activity assessment

This study used 9 microbial strains: 3 Gram-positive: *Staphylococcus aureus* (ATCC 33862)*, Bacillus subtilis (*ATCC 6633), and *Bacillus cereus (*ATCC 10876); 5 Gram-negative: *Escherichia coli (*ATCC 25922)*, Salmonella typhi* (ATCC 6539), *Klebsiella pneumoniae* (ATCC 13883), *Proteus mirabilis* (ATCC 12453), and *Pseudomonas aeruginosa* (ATCC 27853); and *Candida albicans* (ATCC10231). The methodology follows the principles of the disk diffusion method in Mueller–Hinton (MH) agar as described by the European Committee on Antimicrobial Susceptibility Testing (EUCAST, 2009). Sterile Wattman paper disks, with a diameter of 6 mm, soaked in tubes containing the sample under testing, were carefully placed on the surface of a suitable agar medium for each strain, such as Milan Hinton medium. This medium was previously inoculated with 100 µL of microbial suspension, with turbidity adjusted to 10^8 CFU/mL for bacteria and 10^6 CFU/mL for yeast (Haddouchi, Chaouche and Halla, 2016). Negative controls were used as a reference. Petri dishes were sealed and left to diffuse at room temperature for 1 h, then incubated at 37 °C for 24 h for all microbial agents. Trials were conducted in triplicate. The antimicrobial activity of NADESs and POL extracts was determined by measuring the diameter of the inhibition zone around each disk. The size of these zones indicates the effectiveness of NADESs and POL extracts on the tested microbial strains.

5.3 Cytotoxic and cell viability assessment

The anticancer potential of THEDESs and NADESs was evaluated simultaneously in terms of their cytotoxic and antiproliferative effects on human gastric adenocarcinoma (AGS) cells. The AGS cell line (CRL-1739, ATCC, Manassas, VA, USA) was cultured in RPMI-1640 medium (Gibco, Thermo Fisher Scientific, Waltham, MA, USA), supplemented with 10% heat-inactivated fetal bovine serum (FBS) and 1% penicillin–streptomycin (PS) solution. Cells were maintained at 37°C in a humidified atmosphere with 5% CO_2.

For the cytotoxicity assay, AGS cells were seeded into 96-well plates at a density of 2 × 10^4 cells/well and allowed to adhere for 24 hours. Cells were then incubated with either culture medium (control), pure mixture (NADESs), or THEDESs diluted in culture medium. After 24 hours, cells were washed twice with PBS, and cell viability was assessed using the MTT assay. Briefly, 100 µL of MTT reagent (5 mg/mL in PBS) was added to each well and incubated for 3 hours. The formazan crystals formed were solubilized using dimethyl sulfoxide (DMSO), and absorbance was measured at 570 nm using a microplate reader (VICTOR

NivoTM, PerkinElmer, Waltham, MA, USA). Cell viability was expressed as a percentage of living cells relative to the control. Three independent experiments were performed in triplicate.

The antiproliferative effect of THEDESs on AGS cells was assessed using the same methodology. Cells were seeded at 1×10^5 cells/well in 96-well plates, incubated with culture media (control), pure compounds, or THEDESs for 24 hours, and proliferation was measured using the MTT assay as described above. Three independent experiments were performed in triplicate.

5.3.1 Cell culture and maintenanace

In this study, the AGS cell line (Adenocarcinoma Gastric Cancer) is used as the cellular model.

- **Cell aintenance**

AGS cells are maintained in Dulbecco's Modified Eagle's Medium (DMEM) with phenol red, supplemented with 10% (v/v) fetal bovine serum (FBS) and 1% (v/v) penicillin-streptomycin (PS). The cells are routinely cultured as a monolayer in 75 cm^2 culture flasks until reaching 80–90% confluence in a humidified atmosphere (~112%), at 37°C with 5% CO_2.

- **Sub-culturing procedure**

- Cells are detached from the T-flask by adding 2–3 mL of trypsin-EDTA and incubating at 37°C for 3–5 minutes.
- To neutralize trypsin activity, sub-culturing medium (culture medium with 10% FBS and 1% PS) is added.
- The cell suspension is centrifuged at 1300 RPM for 3 minutes, the supernatant is discarded by tube inversion, and cells are resuspended in 3 mL of sub-culturing medium.
- Cell Counting

Cells are counted using a Neubauer hemocytometer with Trypan Blue dye (TBd) to differentiate viable cells from dead cells. The dye is diluted 1:20 by mixing 25 µL of cell suspension with 475 µL of TBd, and the cell concentration is calculated using the appropriate equation.

$$[\text{Cells}] = (\text{number of cells counted}) \times DF \times 1000$$

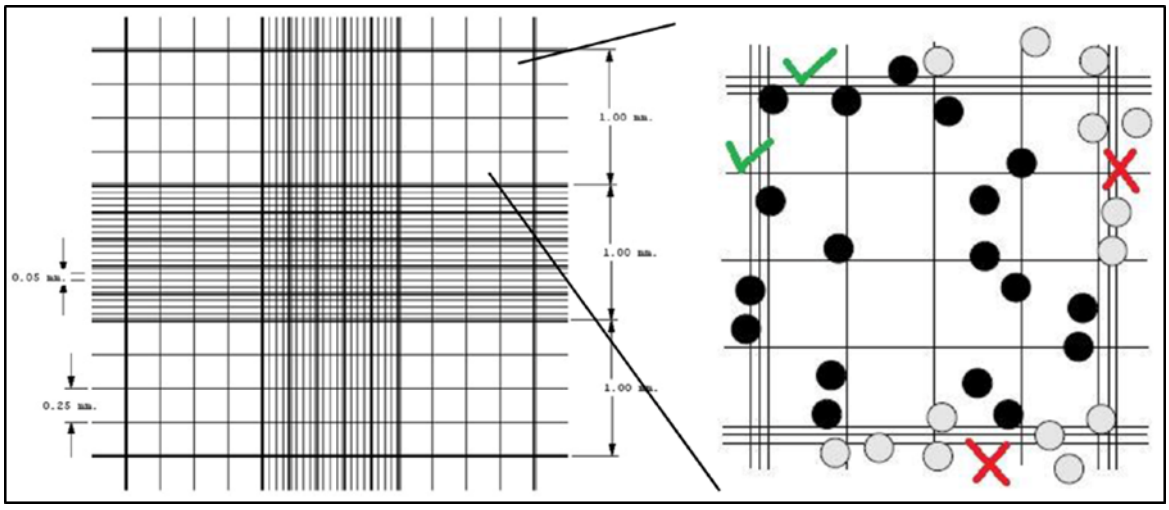

Figure 14: Improved Neubauer hemocytometer grid for trypan blue–based cell counting

5.3.2 Cell thawing

The cells are gently thawed in a water bath at 37 °C, followed by the addition of 9 mL of the appropriate sub-culturing medium. The number of viable and non-viable cells is then determined as described previously (section I.1), and cell viability is calculated using the formula outlined in section I.2. Only cultures with a viability of at least 60% are used. The recovered cells are subsequently transferred to a 25 cm² T-flask to facilitate optimal culture recovery.

Cell viability= ([live cells]/([live cells]+[dead cells])) ×1

5.3.3 Cell freezing

AGS cell cultures are cryopreserved once they reach 80–90% confluence as a monolayer in a 150 cm² T-flask. The cells are detached following the same procedure outlined in the sub-culturing protocol. The resulting cell suspensions are then resuspended in a freezing medium, prepared according to the specifications provided in the table within this section. Cell counting is performed as previously described, and the concentration is determined using the corresponding equation. Based on the calculated concentration, the required volumes of freezing medium and DMSO cryoprotectant are adjusted to obtain a final suspension of 2×10^6 cells/mL in 1 mL per cryovi*al.* The mixture of cells, freezing medium, and DMSO is kept on ice during the transfer into cryovials. The cryovials are then placed in a CoolCell freezing container and stored at -80°C for 24 hours, ensuring a gradual cooling rate of 1°C per minute to reduce the risk of osmotic stress and intracellular ice formation. Once the cultures exhibit stable behavior and optimal confluence, they are frozen according to this protocol.

Table 01: Freezing culture and medium cryoprotectant agent volume to freeze AGS cell line.

Cell lines	Freezing culture medium	Cryoprotectant agent (CPA) - DMSO	Freezing temperature
AGS	DMEM + 20% FBS	10 %	-80°C for short to middle-term storage or -196°C for long-term storage

5.3.4 Cell viability assessment

Selecting an appropriate cellular model is crucial for accurately evaluating the anticancer potential of a drug. AGS cells, derived from human gastric adenocarcinoma, are widely utilized for studying gastric cancer as they offer a relevant in vitro model to explore tumorigenesis mechanisms and assess the efficacy of gastric cancer-specific treatments.

To determine cell viability, the MTT (3-(4,5-dimethylthiazol-2-yl)-2,5-diphenyltetrazolium bromide) assay is employed. This in vitro cytotoxicity test is widely used due to its simplicity, cost-effectiveness, precision, speed, sensitivity, and high reproducibility. The assay relies on the enzymatic conversion of the tetrazolium salt into a purple formazan product by mitochondrial dehydrogenase enzymes present in viable cells. The intensity of the formazan colour is directly proportional to the number of living cells and is quantified spectrophotometrically at 560 nm.

By utilizing AGS cells in conjunction with the MTT assay, researchers can effectively evaluate the cytotoxic impact of anticancer compounds on gastric cancer cells, providing valuable data on their potential therapeutic efficacy.

Table 02: Dilutions applied to NADESs and THEDESs in the medium before cytotoxic assay

Final concentration aimed	First dilution (50:50 éthanol)	Second dilution (1:100)	Third dilution
0,025%	50 µL NADES + 50 µL éthanol	5 µL of solution 50% + 495 µL DMEM	25 µL of solution à 0,5% + 475 µL d'eau (1:20)
0,05%	50 µL NADES + 50 µL ethanol	5 µL of solution 50% + 495 µL DMEM	50 µL of solution à 0,5% + 450 µL DMEM (1:10)
0,075%	50 µL NADES + 50 µL ethanol	5 µL of solution 50% + 495 µL DMEM	75 µL of solution à 0,5% + 425 µL DMEM (1:6.66)

0,1%	50 µL NADES + 50 µL ethanol	5 µL of solution 50% + 495 µL DMEM	100 µL of solution à 0,5% + 400 µL DMEM (1:5)
0,125%	50 µL NADES + 50 µL ethanol	5 µL of solution 50% + 495 µL DMEM	125 µL of solution à 0,5% + 375 µL DMEM (1:4)

6 *In-vitro* studies

6.1 Acute dose escalation toxicity study of NADESs

An acute dose escalation toxicity study was designed to evaluate the oral toxicity of seven distinct NADES formulations, as defined by (Federal Register, 1996). Each NADES was administered orally to separate groups of rats (n=5 per group). The NADESs were delivered with an initial volume of 50 µL, which was doubled daily over a period of five days, culminating in a maximum dose of 1000 µL. Tween 80 served as the vehicle to facilitate the oral delivery of the NADESs.

6.1.1 Experimental animals and housing

a. Selection of animals

Male Wistar rats (6–8 weeks old) were selected, ensuring homogeneity in body weight. They were housed in controlled conditions: 22 ± 2°C, 50–60% humidity, and a 12-hour light/dark cycle, with ad libitum access to food and water.

b. Animal grouping

A total of 35 rats (5 per group) were assigned as follows:

- Control Group: Received the vehicle (Tween 80).
- Treatment Groups (NADES1–NADES7, n=5 per group): Evaluated for acute toxicity.

c. Dose Administration

Rats received escalating oral doses of NADESs over 5 days. Doses were adjusted daily based on body weight

- **Day 1**: 50 µL
- **Day 2**: 100 µL
- **Day 3**: 200 µL
- **Day 4**: 500 µL
- **Day 5**: 1000 µL

6.1.2 Clinical observations and measurements

Throughout the acute dose escalation toxicity study, all animals were closely monitored for signs of systemic toxicity, behavioral alterations, and mortality. Among the parameters typically assessed in such studies: such as changes in body weight, food and water intake, fur condition, posture, respiratory patterns, and autonomic responses were crucial to determine the subacute toxic effects of NADESs. Only mortality and a single case of convulsion were observed, the mortality of the rats was carefully recorded and conducted twice daily.

The number of dead rats in each group was noted daily. Each individual death was monitored and represents a case of acute toxicity at the dose administered. The convulsion, indicative of a potential nervous system reaction, was transient and did not recur in other test groups, Convulsions have been reported as an acute toxicological response in studies assessing neurotoxic effects of chemical compounds (Dieter, 2007). Given the absence of additional observable toxicological signs, we opted to focus solely on mortality and neurological-related manifestations, particularly convulsive activity and potential shock states, as the primary indicators of acute toxicity in this study. This approach aligns with refined toxicity assessment practices that prioritize relevant endpoints while reducing unnecessary observations (Bassan et *al*., 2021). This strategic decision was made to refine the assessment criteria while ensuring the most relevant toxicological endpoints were considered.

6.1.3 Ethical considerations and animal welfare

- **Animal monitoring**
    - Ensure vigilant monitoring to minimize animal suffering.
    - Consider humane euthanasia for rats showing severe distress.

- **Ethical compliance**
    - Follow ethical and regulatory guidelines for animal experimentation.
    - Obtain approval from the institutional ethics committee before starting the study.

- **Analysis of results**

    - Calculate the percentage mortality for each dose group.
    - Analyse the data to determine the median lethal dose (LD_{50}).

6.2 Hepatotoxicity and hepatoprotective study

6.2.1 Study design and animal grouping

Male Wistar rats, aged 6-8 weeks weighing approximately 150 to 200 g, were divided into 10 groups, each consisting of 5 rats, with a closer wight of rats in each group. The toxic dose of MTX was determined at 20mg/Kg according to previous studies (Ebrahimi et *al*., 2019; Elsawy et *al*., 2020)

- **Group 1**: Received 200 micrograms of *P. oleracea* L. extract in THEDES 01 composed of Me/La 1:1 at 10% in Tween 80, followed by an intraperitoneal injection of 20 mg/kg MTX on the 5th day of treatment.
- **Group 2**: Received 200 micrograms of *P. oleracea* L. extract in THEDES 02 composed of Me/La 1:2 at 10% in Tween 80, followed by an intraperitoneal injection of 20 mg/kg MTX on the 5th day of treatment.
- **Group 3**: Received 200 micrograms of *P. oleracea* L. extract in THEDES 03 composed of Me/β-C 1:1 at 10% in Tween 80, followed by an intraperitoneal injection of 20 mg/kg MTX on the 5th day of treatment.
- **Group 4**: Received 200 micrograms of *P. oleracea* L. extract in THEDES 04 composed of Me/β-C 1:2 at 10% in Tween 80, followed by an intraperitoneal injection of 20 mg/kg MTX on the 5th day of treatment.
- **Group 5**: Received 200 micrograms of *P. oleracea* L. extract in THEDES 05 composed of β-C/Ca 1:1 at 10% in Tween 80, followed by an intraperitoneal injection of 20 mg/kg MTX on the 5th day of treatment.
- **Group 6**: Received 200 micrograms of *P. oleracea* L. extract in THEDES 06 composed of β-C/Ca 2:1 at 10% in Tween 80, followed by an intraperitoneal injection of 20 mg/kg MTX on the 5th day of treatment.
- **Group 7**: Received 200 micrograms of *P. oleracea* L. extract in THEDES 07 composed of Me/Aa 1:2 at 10% in Tween 80, followed by an intraperitoneal injection of 20 mg/kg MTX on the 5th day of treatment.
- **Group 8 (EtOH-POL)**: (EtOH-POL extract + tween 80) Received ethanolic extract diluted in distilled water, followed by an intraperitoneal injection of 20 mg/kg MTX on the 5th day of treatment.
- **Group 9 (Conrol)**: Received physiological water orally and tween 80.

- **Group 10 (MTX)**: Received physiological water orally and tween 80 plus an intraperitoneal injection of 20 mg/kg MTX.

At the end of experiment, all animals were sacrificed after a fasting for 12 hours by intramuscular injection of ketamine at a dose of 150 mg/kg body weight. Blood samples were collected in heparinized tubes from the retro-orbital sinus for biochemical analysis. Tubes were centrifuged at 30000 rpm/10 min; plasma was stored at -20°C until analysis. Liver was then removed, weighed, rinsed with physiological water and fixed in 10% formalin for histological study.

6.2.2 Histopathological analysis

6.2.2.1 Tissue fixation and processing

a. Fixation

Fixation is essential for deactivating mitotic and enzymatic activities to prevent tissue degradation (autolysis) and to preserve the tissue as close to its living state as possible. Hepatic tissue samples from Wistar rats were immediately rinsed with 0.9% NaCl solution and then fixed in 10% formalin. The tissues were fully immersed in the fixative, with the volume of the fixative being at least 20 times the volume of the tissue sample. Large organs were cut into small pieces to ensure thorough fixation. After 24 to 48 hours of fixation, the samples were placed into cassettes for dehydration.

b. Dehydration, clearing, and paraffin infiltration

The purpose of dehydration is to remove intracellular and interstitial water, replacing it with paraffin to maintain cellular structure during sectioning. This process involves immersing the tissues in a series of alcohol (ethanol or acetone) baths of increasing concentration: 50%, 70%, 90%, and 100%. Paraffin, an inclusion medium insoluble in alcohols, is a solid hydrocarbon mixture with a high molecular weight. For paraffin infiltration, the dehydrated tissues need to be cleared using a solvent such as toluene or xylene, since paraffin is not soluble in alcohol.

Histological samples were dehydrated in an automated system with 12 baths as follows:

1. **First bath:** Fixation in 10% formalin to ensure proper fixation (1 hour).

2. **2^{d} to 5th baths**: Dehydration in ethanol at concentrations of 50%, 70%, 90%, and 96%, respectively (1 hour each).
3. **6th to 9th baths**: Clearing in toluene (1 hour each) to replace ethanol with toluene.
4. **10th to 12th baths**: Paraffin infiltration at 56°C (1 hour in the first two baths and 10 hours in the final bath).

c. Paraffin embedding

Paraffin embedding involves encasing the infiltrated tissue fragments in paraffin blocks to prepare them for sectioning. Histological samples were placed into metal embedding molds, and molten paraffin was poured over the tissue fragments. The molds were then placed in a freezer to solidify the paraffin.

d. **Sectioning and mounting**

Sectioning allows for obtaining thin slices of tissue, typically 2 to 5 µm thick, for optical microscopic examination. Paraffin blocks were sectioned using a microtome, producing ribbons of 3 µm thick sections. These ribbons (2 to 3 sections each) were mounted onto glass slides with a few drops of an albumin solution (2g albumin + 50 ml glycerin + 1000 ml distilled water). The sections were then flattened on a warming plate set at 40°C. The slides were drained and dried at room temperature or in an incubator overnight at 45°C or 37°C.

e. Staining and slide preparation

Since the stains used are hydrophilic, the sections must undergo deparaffinization and rehydration. Slides were first immersed in solvent baths (xylene or toluene) to remove the paraffin, followed by rehydration in alcohol baths of decreasing concentrations: 96%, 70%, and 50%. The final rehydration step involved rinsing with running water.

Hematoxylin and eosin (H&E) staining is the standard topographic staining method. Hematoxylin is a basic dye that stains acidic components (nuclei) blue-violet, while eosin is an acidic dye that stains basic structures (cytoplasm) pink.

Before mounting the sections, an inverse dehydration and clearing process is required, involving immersion of the stained slides in alcohol baths of increasing concentration, followed by solvent baths.

The automated staining system used 21 baths arranged as follows:

1. **1st to 3d baths**: Toluene baths for deparaffinization (10 min each).
2. **4th to 6th baths**: Ethanol baths of decreasing concentrations (10 min each).
3. **7th bath**: Running water rinse for final rehydration (1 min).
4. **8th to 9th baths**: Harris hematoxylin staining (2 min each) for nuclei.
5. **10th bath**: Water rinse (2 min).
6. **11th bath**: Acid water rinse to remove excess stain (1 min).
7. **12th bath**: Ammonia water to fix the blue-violet colour on acidic components (1 min).
8. **13th to 14th baths**: 2% alcoholic eosin staining (2 min each) for cytoplasm.
9. **15th bath**: Water rinse to remove excess eosin (2 min).
10. **16th to 18th baths**: Ethanol baths of increasing concentrations (2 min each).
11. **19th to 21st baths**: Toluene baths for clearing (10 min each).

Finally, a drop of Eukitt mounting medium was placed on the section, and a coverslip was applied, ensuring no air bubbles were trapped. The slides were left to dry at room temperature before microscopic examination.

6.2.2.2 Staining and microscopic examination

Liver tissue samples were collected, fixed in 10% formalin, and embedded in paraffin. Sections of 4-5 µm thickness were obtained and stained with hematoxylin and eosin (H&E) to assess general histopathological changes.

For specific hepatocellular damage and fibrosis evaluation, additional staining methods such as Masson's trichrome (for collagen deposition) and periodic acid-Schiff (PAS) (for glycogen storage) were performed.

Stained sections were examined under a light microscope at various magnifications to assess morphological alterations, including hepatocyte integrity, inflammatory infiltration, vacuolization, and necrosis.

Histological scoring was conducted based on predefined criteria to quantify liver damage and evaluate the hepatoprotective effects of the tested compounds.

6.2.3 Hepatic-biomarkers evaluation

Serum biomarkers were analyzed to assess liver function and hepatocellular integrity. Blood samples were collected, centrifuged, and sent to the University Hospital Center Biochemistry Lab for biochemical analysis.

- **Alanine aminotransferase (ALAT):** A key enzyme released during hepatocyte damage, used to assess liver injury.
- **Aspartate aminotransferase (ASAT):** An enzyme indicating hepatocellular damage, often evaluated alongside ALAT for liver function assessment.
- **Gamma-glutamyl transferase (GGT):** A marker of hepatobiliary dysfunction and oxidative stress, useful for detecting cholestasis.
- **Alkaline phosphatase (ALP):** An enzyme associated with bile duct function, often elevated in liver diseases involving bile flow obstruction.
- **Bilirubin:** A byproduct of hemoglobin breakdown, used to assess hepatic clearance and bile excretion capacity**.**

7. Statistical analysis

All statistical analyses were performed using GraphPad Prism, SPSS, and R. Data were expressed as mean ± standard deviation (SD). The normality of data distribution was assessed using the Shapiro-Wilk test.

For comparisons between multiple groups, one-way analysis of variance (ANOVA) was conducted, followed by Tukey's post hoc test to identify significant differences between specific groups. In cases where data were not normally distributed, the Kruskal-Wallis test was used, followed by Dunn's multiple comparisons test.

To evaluate correlations between variables, Pearson's correlation coefficient was applied for normally distributed data, whereas Spearman's correlation coefficient was used for non-parametric data.

Statistical significance was set at $p < 0.05$. Graphs and figures were generated using Office Excel and all experiments were conducted in triplicate unless otherwise specified.

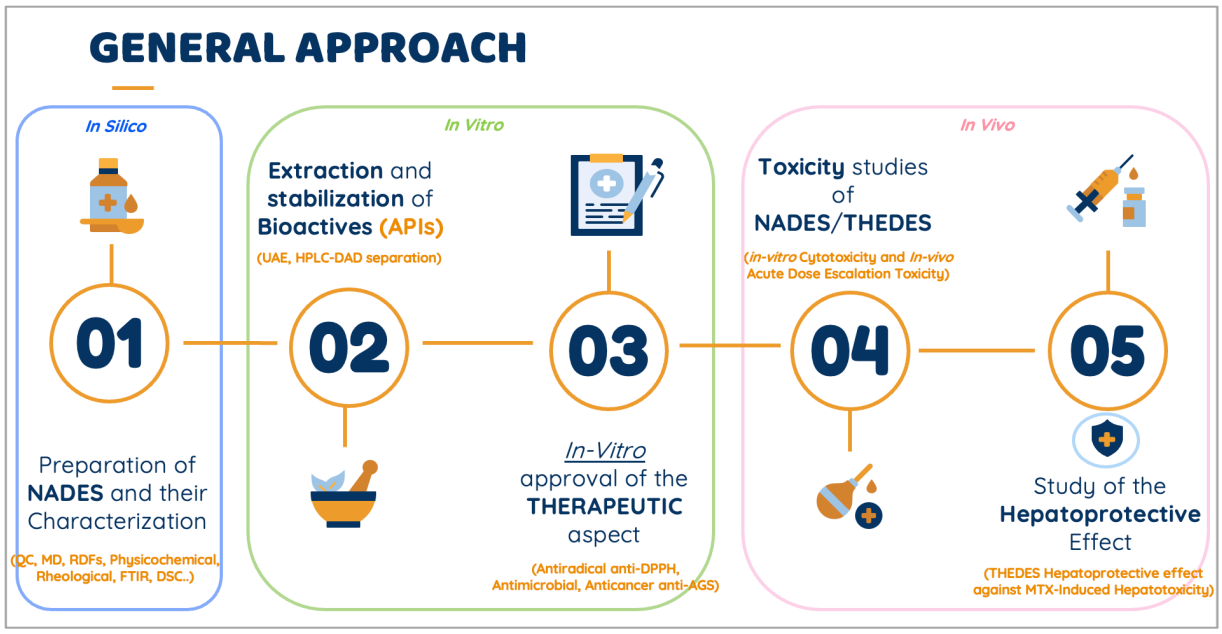

Figure 15: Holistic presentation of the study plan of this thesis

Results and Discussion

1 *In-silico* studies of NADESs

1.1 Characterization of screened natural deep eutectic systems properties (NADESs)

1.1.1 Capric-based NADESs

- **Structural properties of capric-based NADESs**

The densities and viscosities of ten capric acid-based NADESs systems were first calculated to test the accuracy of the used force field. As shown in Table 1, all calculated results are consistent with the experimental density (error less than 2%). This indicates that the employed all atom force field (GAFF) is suitable for the NADES systems. The NADES systems were investigated in terms of atom-atom radial distribution functions (RDFs). They provided an insight into the structural properties of different eutectic solvents and the functions of different constituents in entire systems. Term g (Γ) is a measure of the probability that an atom will be located a distance from another atom. The interactions around 2 Å presumably refer to intra- or intermolecular hydrogen-bonding forces in the relatively simple systems (Perkins et *al*., 2014). In Figure 16, all investigated peaks for RDFs between the oxygen and hydrogen atoms of target part are located at less than 0.3 nm. This suggests the existence of hydrogen-bond interactions. Peaks at or greater than 0.3 nm are probably non-hydrogen bonded intermolecular interactions and do not contribute to the hydrogen-bonding network (Perkins et *al*., 2014). The intensity of some peaks is weak, suggesting that these atom-atom interactions do not play significant roles in the solvation of target systems (Abedin et *al*., 2020).

Table 03: Comparison between experimental and simulated density (ρ) data at 1 bar and 298 K, and viscosity (μ) values of different NADESs at 298.15 K and 313.15 K.

NADES	Molar ratio	ρ^{exp} (g/ cm^3)	ρ^{sim} (g/ cm^3)	Deviation (%)	$\mu^{298.15\ K}$ (mPa.s)	$\mu^{313.15\ K}$ (mPa.s)
Capric acid-based NADESs						
Capric acid/ Carvacrol	1 :1	0.933	0.933	0.05	18.3	16.90
Capric acid/ Carvone	1 :1	0.926	0.922	0.43	09.70	07.80
Capric acid/ Thymol	1 :1	0.931	0.940	0.97	17.50	13.00
Capric acid/ Eugenol	1 :1	0.962	0.979	1.77	07.25	09.40
Capric acid/ Menthol	1 :1	0.909	0.909	0.00	12.60	15.50

Capric acid/ Fenchon	1 :1	0.914	0.929	1.64	17.90	11.60
Capric acid/ Camphor	1 :1	0.925	0.933	0.86	11.90	09.70
Capric acid/ β-citronellol	1 :1	0.867	0.883	1.85	11.90	10.20
Capric acid/ Geraniol	1 :1	0.886	0.890	0.45	/	12.40
Capric acid/ Linalool	1 :1	0.883	0.887	0.45	/	12.40
Terpenoids-based NADESs						
Menthol/ Lactic acid	1 :1	0.988	0.984	0.41	17.30	32.20
Menthol/ Acetic acid	1 :1	0.931	0.954	2.47	/	/
Camphor/ Formid acid	1 :1	1.000	1.009	0.90	11.60	10.90
Menthol/ β-citronellol	1 :1	0.873	0.880	0.80	23.30	14.70
Thymol/ β-citronellol	1 :1	0.911	0.913	0.22	17.00	14.90

The densities of ten capric acid-based NADESs systems were first calculated to test the accuracy of the used force field. As shown in Table 1, all calculated results are consistent with the experimental density (error less than 2%). This indicates that the employed all atom force field (GAFF) is suitable for the NADESs. The NADESs systems were investigated in terms of atom-atom radial distribution functions (RDFs). They provided an insight into the structural properties of different eutectic solvents and the functions of different constituents in entire systems. Term g (Γ) is a measure of the probability that an atom will be located a distance from another atom. The interactions around 2 Å presumably refer to intra- or intermolecular hydrogen-bonding forces in the relatively simple systems (Perkins et *al*., 2014). In Fig. 1, all investigated peaks for RDFs between the oxygen and hydrogen atoms of target part are located at less than 0.3 nm. This suggests the existence of hydrogen-bond interactions. Peaks at or greater than 0.3 nm are probably non-hydrogen bonded intermolecular interactions and do not contribute to the hydrogen-bonding network (Perkins et *al*., 2014). The intensity of some peaks is weak, suggesting that these atom-atom interactions do not play significant roles in the solvation of target systems (Abedin et *al*., 2020).

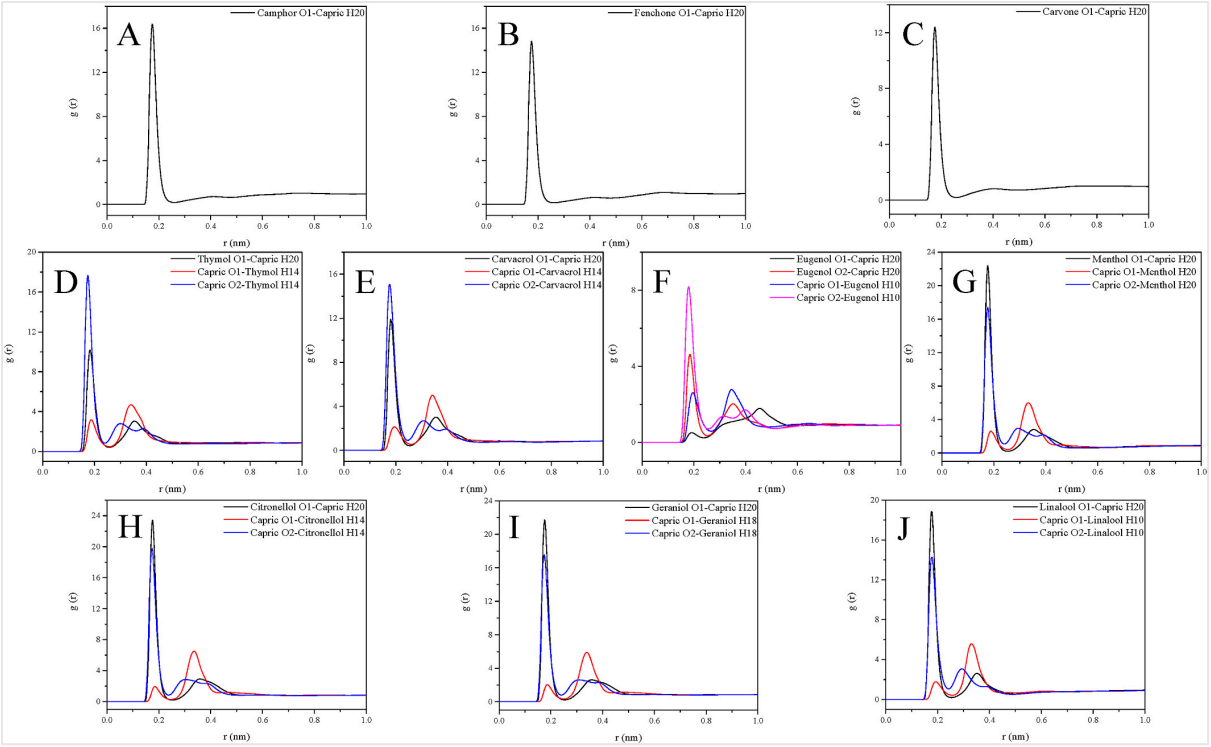

Figure 16: Atom-atom radial distribution functions (RDFs) of different Capric acid-based natural deep eutectic solvent at 1 bar and 298 K. (A) Camphor/capric acid; (B) Fenchone/capric acid; (C) Carvone/capric acid; (D) Thymol/capric acid; (E) Carvacrol/capric acid; (F) Eugenol/capric acid; (G) Menthol/capric acid; (H) β-Citronellol/capric acid; (I) Geraniol/capric acid; (J) Linalool/capric acid.

A series of terpenoids was used to form NADES systems, and they can be classified into three groups: ketones, phenols and alkenyl alcohols. For ketone-based NADES systems (including camphor, fenchone and carvone), only one peak (ketone O1-capric H20) demonstrates that the proton hydrogen of the acid shows strong interactions (Figure 1(A)–(C)). Ketones from terpenoids manifest strong hydrogen-bond accepting capability in the formation of NADES. For phenol-capric acid NADES systems (including thymol, carvacrol and eugenol; menthol for comparison), the formation probability of capric O2-phenolic hydroxyl H is larger than phenol O1-capric H20 (Figure 1(D)–(F)). This indicates that phenol is prone to act as HBD in terpenoid-capric acid-based NADES system. Inversely, the RDF intensity of menthol O1-capric H20 is slightly larger than that of capric O2-menthol H20 (Figure 1(G)). The constituents of DES were not clearly categorized as “HBA” or “HBD” _because of the dual nature of many molecules (especially for terpenoids), where most of them could be categorized both as HBAs in some systems and as HBDs in other types of mixtures (Lemaoui et *al*., 2020). Menthol was proven to interact with other constituents in eutectic mixtures as both HBA and HBD (Fan et

al., 2019). In the case of menthol-capric acid NADES, it shows the stronger hydrogen-bond accepting ability.

Versus the above single-site eutectic mixtures, the eugenol-based system should have multiple interaction sites due to methoxy. It is interesting to find that methoxyl oxygen atom connecting carboxyl hydrogen atom is the most unnoticeable interaction. In contrast with the aforementioned phenol-capric acid NADES systems, the formation probability of hydroxy O1-capric H20 is a bit larger than that of capric O2-hydroxy H for alkenyl alcohols-based NADES systems (including β-citronellol, geraniol and linalool), indicating that alkenyl alcohols mainly function as HBA (Figure 1(H)–(J)). Moreover, increasing the number of double bonds and changing the position of hydroxyl groups cannot bring substantive transform in the microstructure of studied NADES systems. Overall, the alkenyl alcohols act as HBA in terpenoid-capric acid-based NADES systems, the same as ketones, and phenols are apt to be HBD. The underlying reasons and in-depth discussions would be proposed in the following sections.

- **Theorical characterization of capric based NADESs**

For the purpose of deeply investigating the connection between viscosity and non-bonded interactions in terpenoid-capric acid-based NADESs, H-bond number and lifetime were studied. The calculated lifetime based on Stable States Pictures (SSP) includes unsuccessful hydrogen-bond exchanges, which can describe the hydrogen-bonding network more realistically. The hydrogen bond relaxation is considered as a hydrogen bond exchanging process, which means that the labeled hydrogen switches its HBA from oxygen a to oxygen b (Laage et Hynes, 2008). Calculation processes were used according to previously published works (Z. Xia et *al.*, 2011a). As shown in Figure 17, the viscosity of capric acid-based NADES systems ranges from as low as 7.25 mPa s to 21.6 mPa s at ambient conditions. In comparison with widely studied ChCl-based NADES, the terpenoid-capric acid-based systems obviously have lower viscosity (Elhamarnah et *al*., 2019). It can be seen from Figure 17 (A).

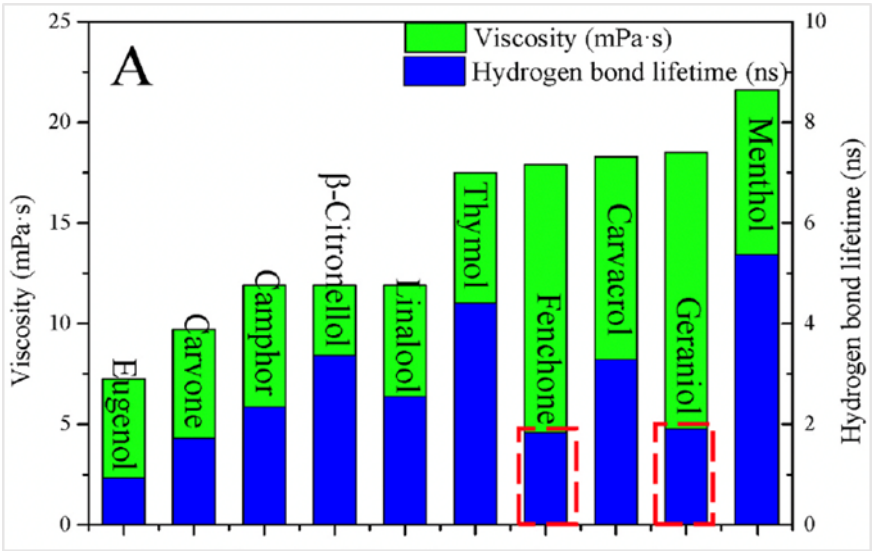

Figure 17.A: Hydrogen-bond lifetime of capric acid-based NADESs at 298°K

Hydrogen-bond lifetime decreases in the order of menthol > thymol > β-citronellol > carvacrol > linalool > camphor > geraniol > fenchone > carvone > eugenol. The relationship between the lifetime of hydrogen bonds and viscosity of NADESs nearly follows a linear correlation when fenchone and geraniol-based systems are not included. This suggests that the viscosity of the two eutectic mixtures is affected by complex items (Figure 17 (B)).

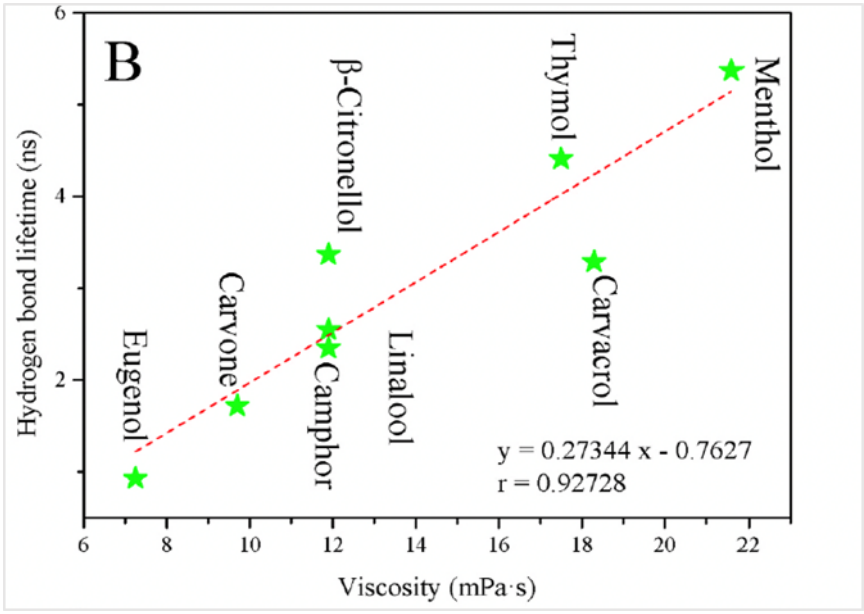

Figure 17. B: Correlation between experimental viscosity and hydrogen-bond lifetime of capric acid-based NADESs at 298°K

Meanwhile, the lifetime is usually considered an important factor to evaluate the strength of the hydrogen bond (Z. Xia et *al*., 2011a). Additionally, the average hydrogen-bond number increases in the order of carvone < fenchone < camphor < eugenol < thymol <

carvacrol < linalool < menthol < geraniol < β-citronellol, which is inconsistent with the viscosity of investigated systems (Figure 17 (C)).

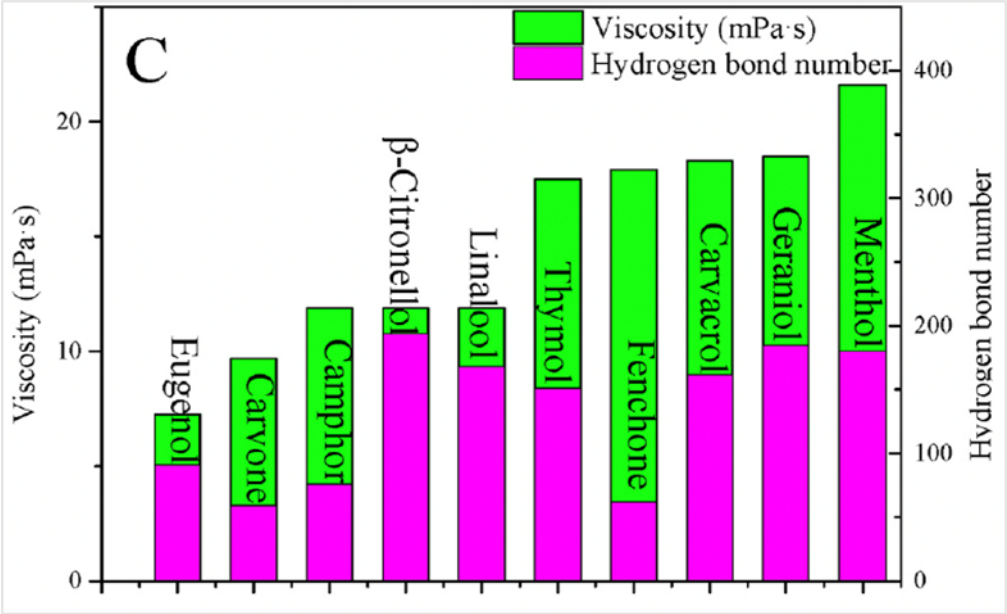

Figure 17 .C: Hydrogen-bond number of capric acid-based NADESs at 298°K

The NADES systems with ketones possess the smallest hydrogen-bond number and lifetime. This probably results in their relatively lowest viscosity among the three groups. Generally, the lifetime and number synthetically influence the viscosity of capric acid based NADES. The former has a greater effect.

- **Hydrogen-bonds number and lifetime**

Figure 4 presents the non-bonded interactions energy of studied terpenoid-based NADES systems. The energy is divided into van der Waals and electrostatic force in the layout of stacked columns. In Figure 18 (A)–(B), there is an identical trend between viscosity and weak interactions energy. The larger the viscosity is, the higher the non-bonded interactions energy is.

This is the same as the trend of subdivided energy derived from van der Waals and electrostatic force. Furthermore, it can be observed that the van der Waals interactions between terpenoid and fatty acid are more dominant than the electrostatic interactions. ChCl-based NADES is a kind of ionic DES, whose high viscosity is mainly due to strong electrostatic interactions (Ramon & Guillena, 2020). However, the used HBA and HBD of this work were all non-ionic compounds, and electrostatics is less likely to dominate their binding energy (Paul et *al.*, 2020). That is part of the reason for their low viscosity. In order to further understand the

inner nature of their unique properties, lauric acid (higher carboxylic acids with C12) was used to prepare a series of eutectic mixtures. As can be seen from Figure 18 (C), it is interesting to find that lauric acid-based NADES systems have relatively high viscosity compared with capric acid-based systems. For alkenyl alcohols, their viscosity values are even up to 300 times higher than that of corresponding capric acid-based mixtures. To some extent, this is attributed to relatively higher non-bonded interactions energy in the NADESs network (Figure 18 (D)).

Additionally, the increase of weak interactions energy mainly stems from the enhancement of van der Waals force. Taken together, these results suggest that there is a connection between viscosity and non-bonded interactions energy in the NADES network. The van der Waals interaction plays an important role affecting the certain property of NADES systems.

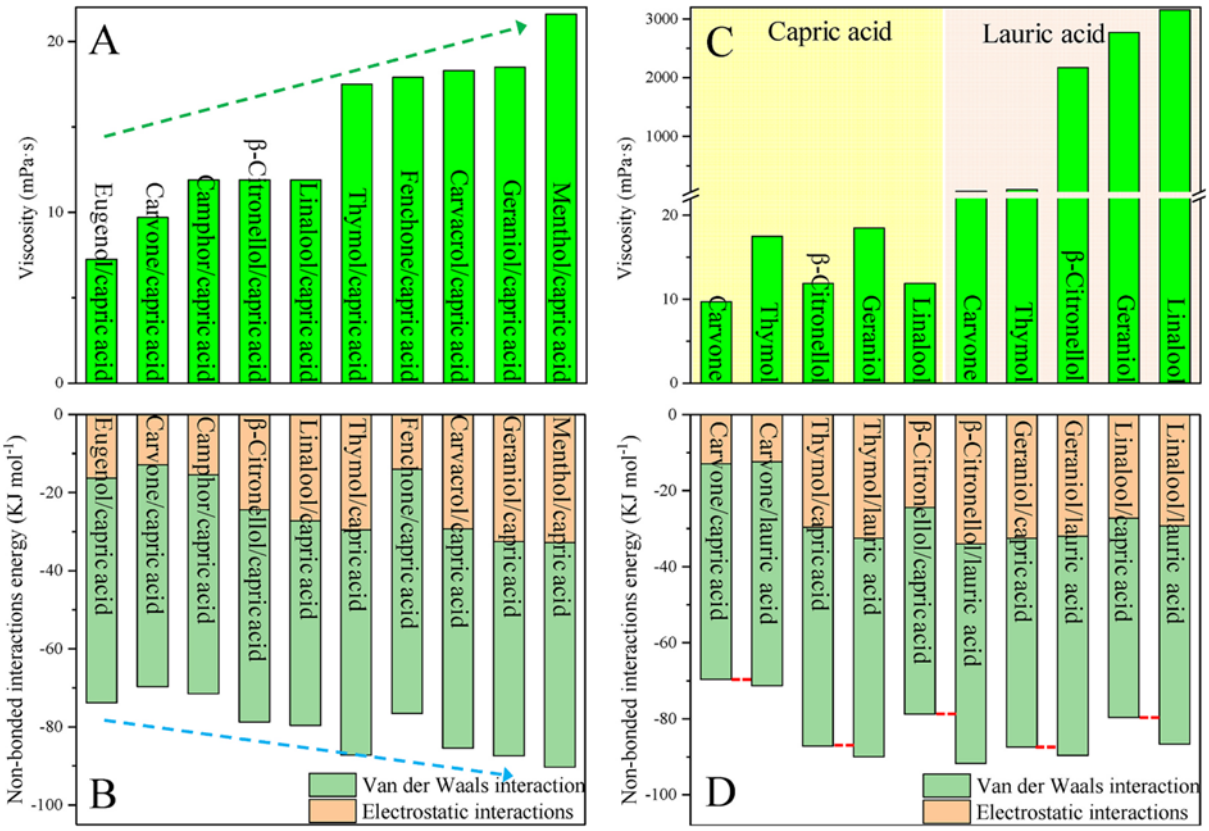

Figure 18: (A) Viscosities of capric acid based natural deep eutectic solvent (NADESs); (B) Non-bonded interactions energy of capric acid based NADESs; (C) Viscosities of corresponding capric acid and terpenoid-lauric acid based NADESs; (D) Non-bonded interactions energy of corresponding capric acid and terpenoid-lauric acid based NADESs.

1.1.2 Terpenoids-based NADESs

- **Structural properties of terpenoids-based NADESs**

The densities of all NADESs were first calculated to test the accuracy of the used force field. As shown in Table 1, all calculated results are consistent with the experimental densities (error less than 3%). This indicates that the employed all-atom general AMBER force field (GAFF) is suitable for the five NADESs systems. All systems were investigated in terms of atom–atom radial distribution functions (RDFs) and spatial distribution functions (SDFs) (Figure 19). Term g(r) is a measure of the probability that an atom will be located a distance from another atom. In Figure 16 A, all investigated peaks for RDF between the oxygen and hydrogen atoms of target part are located at near 2 Å, which presumably refer to the intermolecular hydrogenbonding forces for the relatively simple systems(Perkins, Painter and Colina, 2014). Peaks at or greater than 0.3 nm are probably non-hydrogen bond intermolecular interactions and do not contribute to the hydrogen-bonding network (Perkins, Painter et et *al*., 2014). The intensity of some peaks is weak, suggesting that these atom–atom interactions do not play significant roles in the solvation of target systems (Abranches et *al.*, 2019b) For camphor/formic acid system, only one peak for camphor O1-formic H2 at around 0.2 nm demonstrates that the proton hydrogen of the acid shows strong interactions.

For the menthol/acetic acid system, the probability of menthol O1-acetic H4 is slightly larger than that of menthol H20-acetic O2. This indicates that menthol is prone to act as HBA in this system. Menthol O1-citronellol H14 and menthol H20-citronellol O1 have almost the same chance to form hydrogen bonds in the menthol/β-citronellol system. In our previously published work, menthol or thymol was proven to interact with other constituents in eutectic mixtures as both HBA and HBD (Fan et *al*., 2019). Menthol, thymol, and β-citronellol (all natural small molecules and terpenoids) can undoubtedly act as mutual HBAs and HBDs in terpene-terpene based NADES systems. For thymol/β-citronellol system, the intensity of the RDF in thymol H14-citronellol O1 is slightly stronger than that of thymol O1-citronellol H14 due to the strong electrophilic effect of the benzene ring. Versus the above single-site eutectic mixtures, the menthol/lactic acid system has multiple sites. The hydroxyl oxygen atom of menthol connecting carboxyl hydrogen atom is the most noticeable interaction, and it presents similar features as the menthol/acetic acid system. However, menthol O1-lactic H5 and menthol H20-lactic O1 have almost the same probability, suggesting that there is typical dual-site phenomenon in this kind of eutectic mixture.

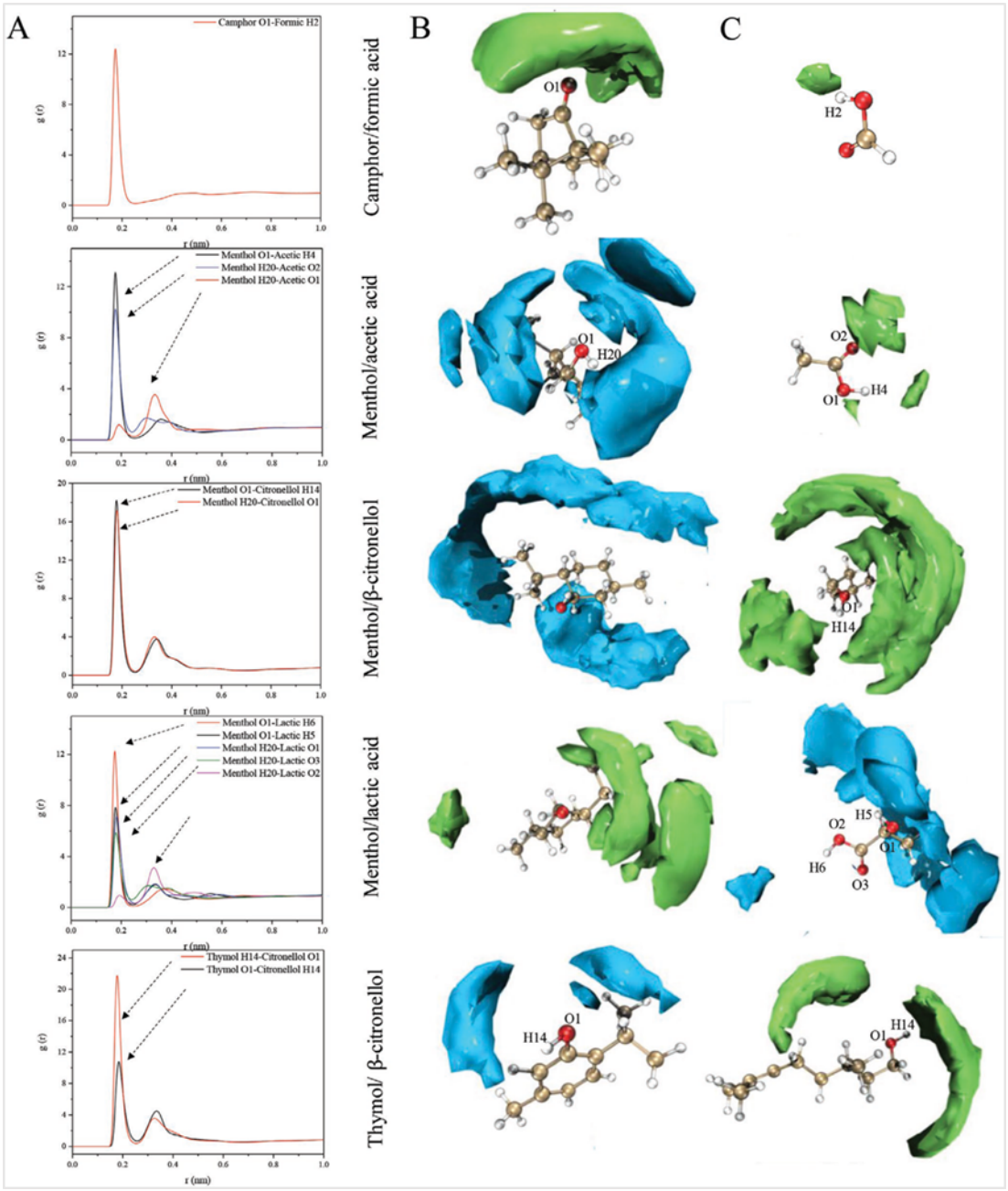

Figure 19: Radial and spatial distribution functions (RDF and SDF) of different terpenoides-based natural deep eutectic solvent at 1 bar and 298 K. A) Atom–atom radial distribution functions; B,C) Hydrogen bond donor (HBD)-hydrogen bond acceptor (HBA) spatial distribution functions. The surfaces represent isosurfaces of normalized concentration for mass center of different components (blue or green).

As a result of complex hydrogen-bonding interactions, it has the largest viscosity of the five systems. The coordination numbers of the NADESs systems were calculated based on RDF: 0.42 for menthol/lactic acid, 0.34 for menthol/acetic acid, 0.24 for camphor/formic acid, 0.27 for menthol/β-citronellol, and 0.33 for thymol/β-citronellol. These mixtures are not only

formed at a given stoichiometric proportion (usually connected to complex formation) but in a mole fraction range for individual system(Martins et *al*., 2019) To visualize the distribution of HBA or HBD around the other component in NADES system, the SDF results are also plotted in Figure 19 B,C. They are almost consistent with the above-mentioned RDF results and intuitively show the types and distributions of interaction sites in the entire NADES systems.

- **Hydrogen-bonds number and lifetime of terpenoids-based NADESs**

The hydrogen-bond number and lifetime were studied to further investigate the relationship between viscosity and hydrogen-bonding interactions in terpene-based NADES. The calculated lifetime based on stable states pictures (SSPs) includes unsuccessful H-bond exchanges, which can describe the hydrogen-bonding network more realistically. The hydrogen bond relaxation is a hydrogen bond exchanging process, which means that the labeled hydrogen switches its HBA from Oa to Ob (oxygen atom a and b). (Laage & Hynes, 2008) Calculation procedures were used according to previously published works. (Laage et Hynes, 2008; Z. Xia et *al*., 2011a).

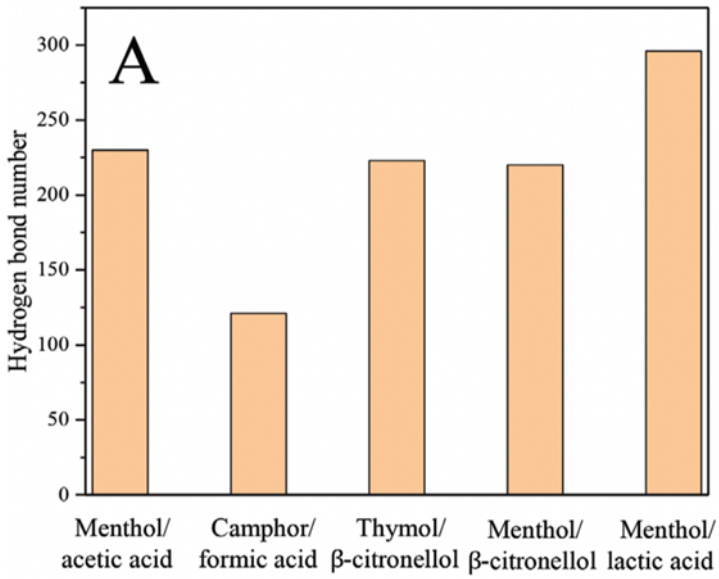

Figure 20. A: Hydrogen-bond number of terpenoids-based NADESs at 298°K

Figure 20 A shows that the average hydrogen bond number decreases on the order of menthol/lactic acid > menthol/acetic acid > thymol/β-citronellol > menthol/β- citronellol > camphor/formic acid, suggesting that lactic acid-based system has multiple interaction sites. Additionally, hydrogen-bond lifetime increases on the order of camphor/formic acid< menthol/acetic acid < thymol/β-citronellol < menthol/lactic acid < menthol/β-citronellol, which is inconsistent with the viscosity of investigated systems (Figure 20 B). According to the

literature, the relationship between lifetime of hydrogen bonds and viscosity of ILs nearly followed a linear correlation. (Ma, Liu, Su, et *al*., 2018) Therefore, they are quite different at this point. Moreover, the average numbers of H-bond per DES molecule were obtained: 1.21 for menthol/lactic acid, 0.94 for menthol/ acetic acid, 0.49 for camphor/formic acid, 0.88 for menthol/β-citronellol, and 0.89 for thymol/β-citronellol. The viscosity of terpene-based NADES increases with the product of the number and lifetime of H-bonds (Figure 20 C).

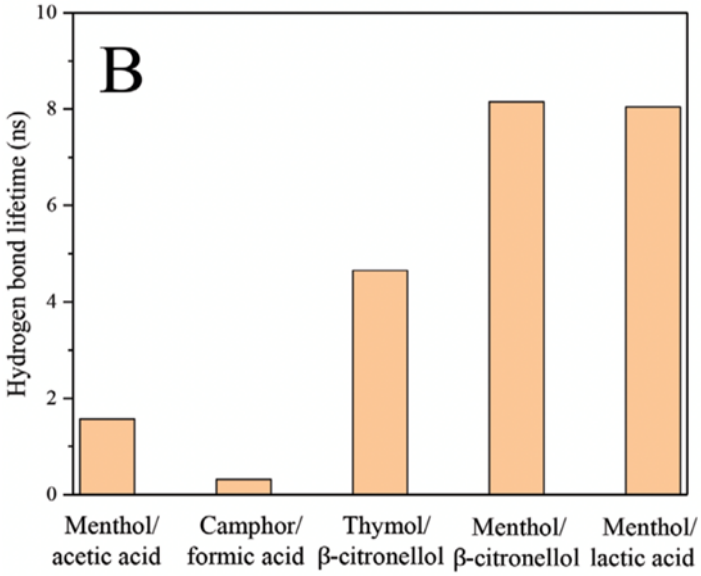

Figure 20. B: Hydrogen-bond lifetime of terpenoids-based NADESs at 298°K

Furthermore, for single-site eutectic mixtures, the relationship between viscosity and product of two factors has an excellent linear correlation. This means that the number and lifetime synthetically influence the viscosity of NADES. The types of systems (single or multiple sites) decide the number of hydrogen bonds. Meanwhile, the lifetime is traditionally considered an important element to evaluate the strength of the H bond (Xia, Qiang and Dong-Xia, 2011a).

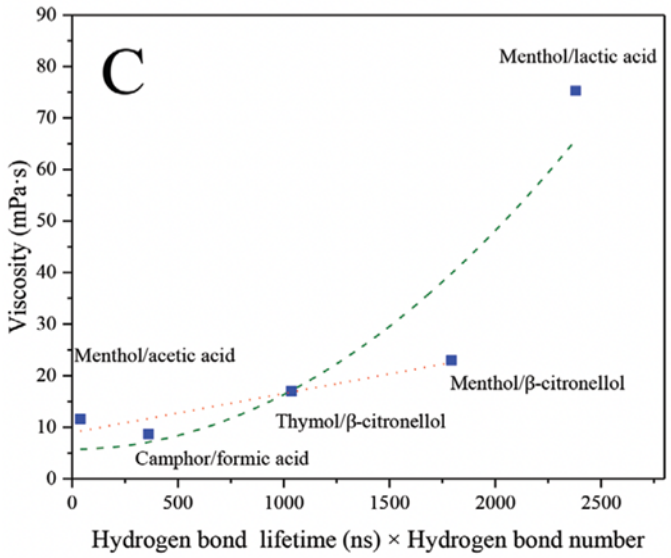

Figure 20. C: Correlation between experimental viscosity of terpenoids-based NADES at 298°K with their corresponding product of hydrogen-bond lifetime × hydrogen-bond number

- **Molecular surface analysis of terpenoids-based NADESs**

Quantum chemistry calculations were carried out to further probe the formation of terpenoid-capric acid-based NADES with low viscosity. Quantitative analysis of molecular surface is a powerful tool, which has considerable practical applications such as investigation of intermolecular weak interactions, calculation of molecular properties and prediction of reactive sites (T. Lu et Chen, 2012b). More useful information can be obtained through the quantification of the electrostatic potential on van der Waals surface. The analysis of magnitude and positions of vertices on the surface is apt to study the strength and orientation of weak interaction. The global minimum of electrostatic potential exactly locates at the oxygen atom in ketone-based terpenoids (as shown in figure 21), and there is almost only one minimum. This indicates that they are prone to be HBA in NADES systems.

For phenol-based terpenoids, the absolute value of the maximum point is larger than that of the minimum point, which illustrates that they have stronger hydrogen-donors capability and prefer to act as HBD. Thymol, carvacrol and eugenol possess resonance effects due to hydroxyl groups directly attaching to aromatic rings. These make their hydroxyl groups more positive than usual (Abranches et *al*., 2019b). Inversely, menthol retains a normal hydroxyl group owing to the absence of aromaticity. According to the analysis of the eugenol surface, methoxy is a site for hydrogen bond acceptor, whereas its negative charge is highly shielded by

methyl group. This limits interactions between the precursors (Abranches et *al*., 2019b). It is proven by the results of RDF and aNCI.

For alkenyl alcohol-based terpenoids, the gap between the absolute value of maximum and minimum point is small. This suggests that they have same hydrogen accepting and donning ability, which is consistent with RDF analysis. The alkenyl alcohols together with menthol can be both HBDs and HBAs (their roles depend on another component in DES), while phenols are a regular HBD but a weak HBA. The ketones have strong hydrogen-bond accepting capability. What is more interestingly, global minimum decreases in the order of fenchone > camphor > carvone for ketone group, and the viscosity of corresponding NADES systems also decreases in the same order. Their viscosity and global minimum almost followed the linear correlation (Fig. S1). However, this trend does not be found in the phenol- and alkenyl alcohol-based NADES systems as a result of their more complex microstructure.

Furthermore, the mixture with smallest viscosity possesses a relatively large extreme value of electrostatic potential (global maxima for phenols, global minima for alkenyl alcohols) in the two groups. Many studies tried to put forward the rules correlating structural characteristics of molecules and viscosity of liquids (Prezhdo et *al*., 2013). On the other hand, given a large number of possible combinations in starting materials of NADES, it is difficult to relate one certain micro-structural item to viscosity in a direct way owing to considerable complex factors (Martins et *al*., 2019).

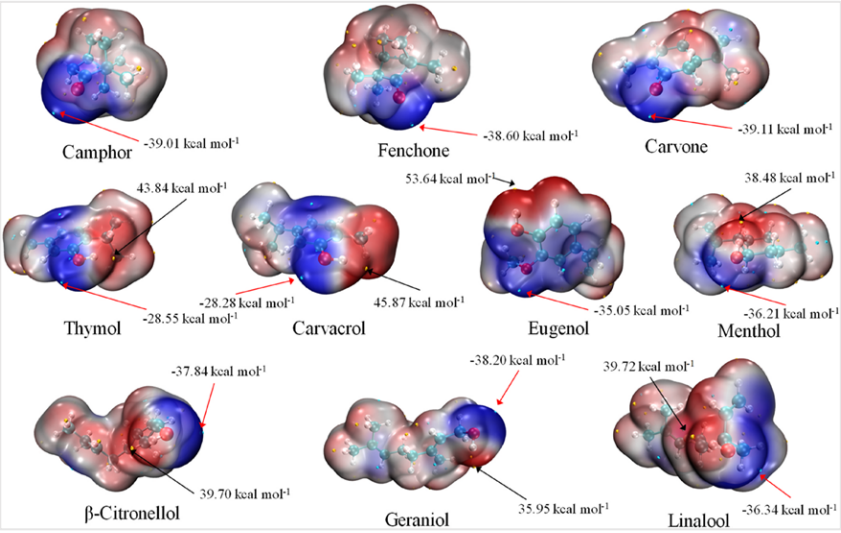

Figure 21: Molecular surface colored by electrostatic potential surface. The surfaces represent isosurfaces with high electron density regions (potential HBA sites) in blue and low electron density regions (potential HBD sites) in red. The ESP surface minima and maxima are represented as the green and yellow spheres, respectively.

2 Extraction and characterization of bioactive compounds with NADESs

2.1 Spectrophotometric analysis of TPC, TFC and CT

In the study of the phytocompounds extracts, evaluating the presence and concentration of total polyphenols, flavonoids, and condensed tannins is of vital importance. Polyphenols, a diverse group of naturally occurring compounds, are crucial in preventing oxidative stress and related diseases. Flavonoids, a subclass of polyphenols, have been linked to various therapeutic effects, such as cardiovascular protection and neuroprotection and their derivatives have shown promising anti-inflammatory properties (Ysrafil et *al*., 2023) and some antimicrobial activities against *Candida Albicans*.(Al Aboody et Mickymaray, 2020) Condensed tannins, another important group of polyphenols, are recognized for their ability to bind and precipitate proteins, which can be beneficial in reducing the risk of chronic diseases. They are increasingly of major interest to the scientific community due to their potential anticarcinogenic therapeutic properties.(Kleszcz et *al*., 2023) Tannic acid, in particular, has been studied for its potential anti-inflammatory and antioxidant activities, as well as its inhibition of carcinogen activation (Baer-Dubowska et *al*., 2020).

Concurrently, the determination of condensed tannin (CT) levels is also often studied to assess bioactive molecule content (Kouamé et *al*., 2021) Therefore, by comprehensively analyzing these compounds, researchers can better understand the medicinal potential of phytoextracts, paving the way for the development of effective natural medicines and health supplements. The yield of extracting bioactive compounds from plants may depend on several factors, including the nature of the solvent, its physicochemical and rheological intrinsic parameters, and even the extraction technique. Regarding the use of NADES as an extractor, the UAE technique proved to be the most efficient for the extraction of TPC and TFC enhancing the antioxidant activity of the extracts because the ultrasounds disrupt the cellulose in the outer cell barrier of the plant matrix, leading to subsequent hydrolysis (Y. Li et *al*., 2020).

Several scientific studies have demonstrated a positive correlation between the biological activity of the extracts and the yield of extraction of the bioactive molecules, particularly the antioxidant activity of TPC and TFC (L. Wu et *al*., 2020). Numerous studies have explored the extraction effectiveness of NADES by correlating it with its lipophilic properties in order to optimize the extraction process (Cao et *al*., 2018) The chemical composition of those NADES in terms of HBA and HBD significantly impacts the eutectic

systems formed (Kyriakoudi et *al*., 2022). Indeed, according to the "like-solvent-like" theory, the efficiency of extracting bioactive substances from natural sources using NADESs is significantly influenced by the polarity of these solvents (L. Wu et *al*., 2021). NADESs based on terpenes and carboxylic acids may exhibit some hydrophobicity (Martins et *al*., 2018) Terpenes, due to their chemical structure, have hydrophobic characteristics (Florindo et *al*., 2019; Křížek et *al*., 2018).

The apolar nature of terpenes and the addition of polar functional groups from organic acids, provides these NADES with a broad spectrum of polarity to extract polyphenols, flavonoids, and tannins from a plant matrix.(L. Wu et *al*., 2020) Therefore, NADES can offer increased solubility compared to more polar solvents, like water. The degree of hydrophobicity of NADES, for example, seems to improve the yields of TFC and TPC extraction.(Bajkacz & Adamek, 2017; Ma, Liu, Tan, et *al.*, 2018b) Along with other physicochemical parameters such as difusibility, solubility, density, viscosity, and surface tension (Bi et *al*., 2013; Fan, Liu, et *al*., 2021; Fan, Sebbah, et *al.*, 2021; G.-H. Xia et *al*., 2021). For example, NADES with more hydrophobic characteristics are less viscous compared to more hydrophilic ones, making them more suitable for use as extracting solvents (Kyriakoudi et *al*., 2022)

In this study, 7 NADESs were used to extract total phenolic compounds, flavonoids, and tannins, in comparison with ethanolic extract. These NADES combine two different terpenoids or terpenoids with organic acids (Table 01). Menthol, a key component in many of these NADES, has been shown to enhance bioactive compound yields in several studies.(Kyriakoudi et *al*., 2022; Manurung, 2020; Y. P. A. Silva et *al*., 2019) Which is why it plays a major role in most of the combinations we tested. The bioactive molecules from *Portulaca oleracea* leaves were extracted using the UAE method, as previously described, and the results were compared to those obtained through conventional ethanol extraction (Figures 22, 23 and 24).

Figure 22: Total phenolic content in µg Eq GA/mg in different eutectic extracts and ethanol extract

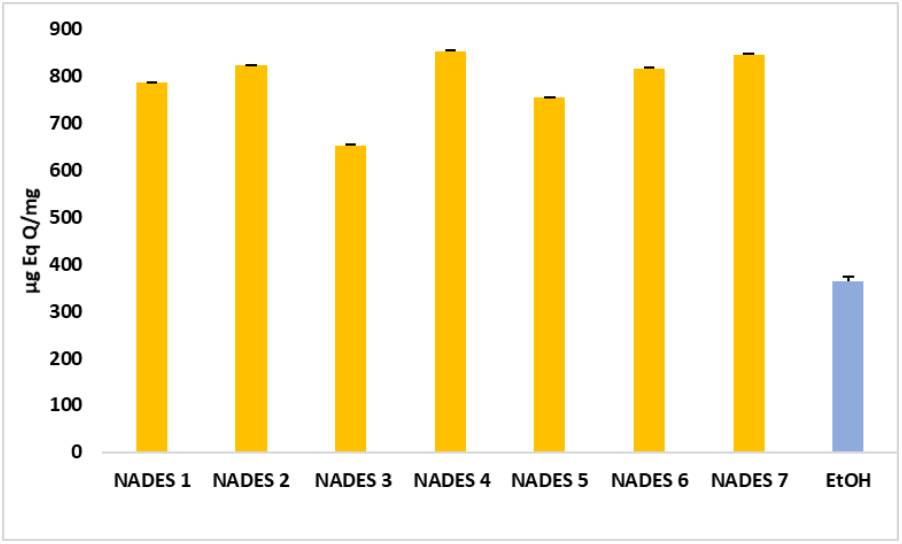

Figure 23: Total flavonoids content in µg Eq QA/mg in eutectic extracts and ethanol extract

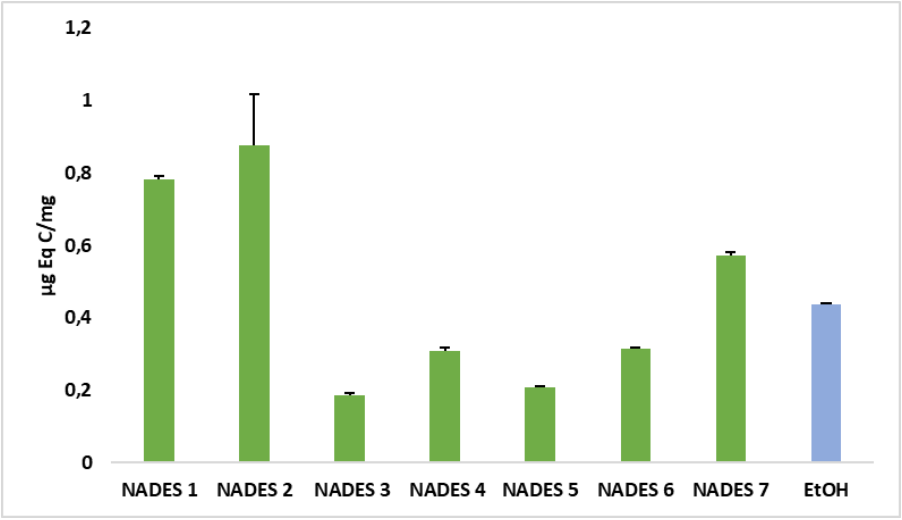

Figure 24: Condensed tannins content in µg Eq C/mg in eutectic extracts and ethanol extract

- **Total flavonoid content (TFC)**

It was found that the yield of bioactive compounds extracted was different depending on the combinations used. In particular, all NADESs combinations (1-7) extracted much more flavonoids than the traditional extraction process using ethanol.
The yield for flavonoids (Figure 23) is not specifically affected by the extractant composition, but rather by the molar ratio of each compound in the mixtures, especially for NADESs 3 and 4. These results are corroborated by previous studies in which the authors report a higher yield when using organic-acid based NADESs for extraction of phenolic compounds (L. Wu et *al.*, 2020; Yu et *al*., 2021) or flavonoids(G.-H. Xia et *al*., 2021). The pH of the medium has been reported as a crucial condition for the extraction of active molecules (Bosiljkov et *al*., 2017; Y. Li et *al*., 2020; Nadia et *al*., 2018).

Therefore, in this study, mixtures whose pH varied between approximately 1 and 4 were used. (see Table 1). However, in this pH range, the extraction of flavonoids was not significantly influenced. When the molar ratio of HBD and HBA was manipulated, and consequently the viscosity and surface tension of the mixtures, there was an increase in the extraction yield for flavonoids, whenever the viscosity decreased (Wei et *al*., 2015; G.-H. Xia et *al*., 2021). Although in previously published work by Xia et *al.,* (G.-H. Xia et *al*., 2021) it was demonstrated that varying the molar ratio of lactic acid in the mixture improved the extraction yield of flavonoids to an optimal value, with this study only a minor variation was recorded, whenever menthol was combined in different proportions.

- **Total phenolic content (TPC)**

Regarding the TPC extraction, the yields were comparable to or higher than those obtained using ethanol, with notably high yields observed for NADESs 2 and 7, where the ratio of terpenoids to organic acids (acetic acid and lactic acid) was 1:2. Nevertheless, in terms of polyphenol yields, NADES containing β-citronellol achieved a similar extraction yield to ethanol but was less effective than NADES formulations based on lactic or acetic acid, such as NADESs 1, 2, and 7 (Figure 22). Flavonoids and phenolic compounds contain hydrophobic groups, and the use of a hydrophobic solvent can facilitate their dissolution. This explains the significant yields of these compounds achieved with hydrophobic NADESs (see Figures 1 and 2).

In contrast Xia et *al.,*(G.-H. Xia et *al*., 2021) found that hydrophilic NADESs composed of choline chloride and betaine, as hydrogen bond donors (HBD), produced lower flavonoid yields compared to those composed of menthol (NADESs 1, 2, 3, 4, and 7). This is because menthol can act as either a hydrogen bond donor (HBD) or acceptor (HBA), depending on the composition.(Fan, Liu, et *al*., 2021).

- **Condensed tannins (CT)**

The extraction yields of condensed tannins showed varied widely but surpassed those obtained with ethanol particularly when terpenoids were combined with organic acids, regardless of the proportion used in the mixture (Figure 24).

Comparing the extractions obtained with NADES 1 and 2 (based on lactic acid) relatively higher extractions were obtained at lower pH. Although NADES 7 has the same pH as NADES 1 (table 1), the inclusion of acetic acid in its formulation reduced the extraction efficiency. For NADESs 3 and 4 composed of menthol and β-citronellol, the extraction efficiency for tannins ranged between 40% and 72% of the yield achieved with ethanol extraction. This may be due to the weaker binding forces between menthol O1 and citronellol H14, and menthol H20 and citronellol O1, with enthalpy values of -4.80 kcal/mol and -5.90 kcal/mol, respectively.(Fan, Liu, et *al*., 2021) On the other hand, NADESs 5 and 6, the only formulations containing a fatty acid (C=10) combined with a terpenoid, showed limited extractive capacities, probably due to their low densities (Fan, Sebbah, et *al.*, 2021; Kyriakoudi et *al.,* 2022; Lalikoglu, 2022; Martins et *al*., 2018).

In conclusion, these results demonstrate that certain bioactive compounds, such as phenolic compounds and tannins, are more effectively extracted by NADES containing organic acids, which serve as hydrogen bond donors (HBD), like lactic and acetic acid. Furthermore, the extraction yield appears to depend on the molar ratio, with higher yields observed when larger amounts of organic acid-based HBDs are used, as seen with NADESs 2 and 7.

2.2 HPLC-DAD separation and quantification of bioactive compounds

Different deep eutectic systems were employed for the extraction of bioactive molecules from *Portulaca oleracea* leaves. These eutectic systems comprise a combination of carboxylic acids (Lactic acid, Acetic acid, and Capric acid) and terpenes (Menthol and β-citronellol). Our natural deep eutectic solvents (NADESs) were classified from 1 to 7 based on their

compositions and the molar ratio of their hydrogen bond acceptors (HBA) and hydrogen bond donors (HBD): NADES1 (Menthol/Lactic acid 1:1), NADES2 (Menthol/Lactic acid 1:2), NADES3 (menthol/β-citronellol 1:1), NADES4 (menthol/β-citronellol 1:2), NADES5 (β-citronellol/capric acid 1:1), NADES 6 (β-citronellol/capric acid 2:1), and NADES 7 (menthol/acetic acid 1:2).

These NADES were employed to extract some specific bioactive molecules from *Portulaca oleracea*, and then the separation was made following HPLC-DAD method, the targeted molecules in our study include 5 phenolic acids, namely ferulic acid, gallic acid, coumaric acid, caffeic acid, and syringic acid, along with two flavonoids, rutin and quercetin. The chromatogram in Annex 4 shows different pics representing each of the previous bioactives.

NADES 4 exhibited the highest yield for ferulic, coumaric, and gallic acids. Ferulic acid was extracted efficiently by nearly all seven NADES, particularly NADES 4 at 17.1 mg/g and NADES 2 at 16.1 mg/g. Gallic acid showed higher yields in NADES 4 at 13.1 mg/g and NADES 1 at 12.7 mg/g, with similar yields in NADES 3 and 7 at 10.8 mg/g and 10.4 mg/g, respectively, and in NADES 5 and 6 at 8.0 mg/g and 8.1 mg/g, respectively (Figure 25). This suggests that the specific combination and ratio of terpenes and carboxylic acids in NADES 4 are particularly favorable for these compounds.

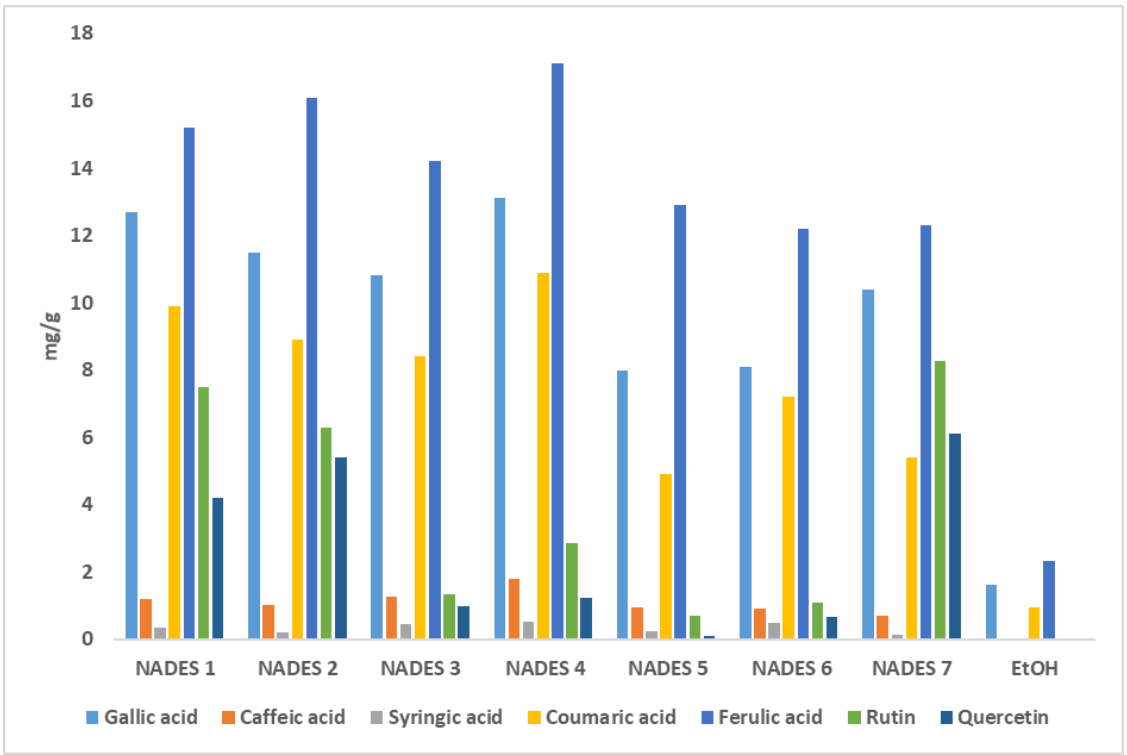

Figure 25: Separated bioactive compounds with HPLC in different extracts

Ferulic acid was successfully extracted by most of the seven NADESs, with NADES 4 and NADES 2 yielding particularly high amounts at 17.1 mg/g and 16.1 mg/g, respectively. This indicates that the presence of both terpenes and carboxylic acids in these NADESs enhances the solubility and extraction efficiency of ferulic acid.

Gallic acid exhibited similar yields in NADES 3 and NADES 7 (10.8 mg/g and 10.4 mg/g) and in NADES 5 and NADES 6 (8.0 mg/g and 8.1 mg/g), respectively. It also showed higher yields in NADES 4 (13.1 mg/g) and NADES 1 (12.7 mg/gsuggesting that the ratio and combination of components are key factors for gallic acid extraction.

Coumaric acid appeared to have an affinity for NADESs with a higher molar ratio of terpenes, notably NADES 4 (10.9 mg/g), followed by NADES 1 (9.9 mg/g). A slight decrease in coumaric acid concentration was observed when the molar ratio of acid was higher than that of the terpene, as in NADES 2 (8.9 mg/g), followed by NADES 3 (8.4 mg/g). Once again, yields in NADESs 5 and 6, with ratios favouring terpenes (4.9 mg/g and 5.2 mg/g), showed a positive correlation. Coumaric acid appeared to favor NADES with higher molar ratios of terpenes, particularly NADES 4 (10.9 mg/g), and NADES 6 (7,2 mg/g).). A decrease in concentration was observed when the molar ratio of acid was higher than that of the terpen, notably in NADES 2 (8.9 mg/g). indicating that a higher proportion of terpenes in the eutectic system may facilitate the extraction of coumaric acid.

Caffeic acid exhibited an affinity for NADESs where the HBD was a terpene, especially menthol. NADES 3 and NADES 4, both terpene-based NADES, yielded the highest amounts of caffeic acid at 1.25 mg/g and 1.8 mg/g, respectively. NADES 1 and NADES 2, with menthol as the HBD, also showed substantial yields (15.2 mg/g and 16.1 mg/g), while NADES 5 and NADES 6 had approximately similar yields (0.93 mg/g and 0.9 mg/g). NADES 7 had the lowest yield for caffeic acid at 0.7 mg/g. This highlights the importance of the specific HBD in the eutectic system for efficient extraction.

Syringic acid exhibited the lowest concentration in all our solvents, with a particular affinity for NADESs where β-citronellol was the HBD. Higher concentrations were observed in those where the molar ratio of β-citronellol was doubled compared to the other HBA Significant yields in NADES 4 and NADES 6 at 0.5 mg/g was obtained . This suggests that certain compounds may have a stronger affinity for specific components within the eutectic system.

Regarding the two flavonoids, rutin and quercetin, we have noticed the highest yields were reported in NADESs 1, 2 and 7. And the highest yield of both flavonoids simultaneously was in NADES 7. It is noteworthy that rutin yields were significantly higher than those of quercetin in all NADESs.

The yield of quercetin increased with an increase in the molar ratio in each combination, with the highest yield observed in NADES 7 at 6.12 mg/g. The lowest yields were in NADES 5 and NADES 6 at 0.11 mg/g and 0.67 mg/g, followed by NADES 3 and NADES 4 at 0.98 mg/g and 1.22 mg/g, and NADES 1 and NADES 2 at 4.2 mg/g and 5.4 mg/g, respectively. Additionally, the presence of carboxylic acids or organic acids with significant proportions in each DES enhanced the extraction yield of quercetin. Rutin concentration appeared to follow the same trend as quercetin, except NADES 1 and NADES 2, where the concentration was higher in NADES 1 (7.5 mg/g) and experienced a slight decrease in NADES 2 (6.3 mg/g). This flavonoid also seemed to have an affinity for the mixtures containing lactic acid and acetic acid as HBA, likely due to their high acidity.

Rutin concentration followed a similar trend as quercetin, except in NADESs 1 and 2, where the concentration was higher in the first (7.5 mg/g) and slightly lower in in the second (6.3 mg/g).

In summary, these results emphasize the importance of tailoring the composition of eutectic systems to the specific of interest. The choice of components, their ratios, and the nature of hydrogen bond donors and acceptors all have a significant impact on the efficiency of extraction. This study provides valuable insights into optimizing eutectic systems for the extraction of bioactive compounds from natural sources.

Based on our analysis of the efficiency of our Natural Deep Eutectic Solvents (NADESs) in extracting bioactive molecules, we observed that many factors influencing NADES efficiency in bioactive molecule extraction are primarily related to their physicochemical characteristics and the polarity of the bioactives. In this regard, the various bioactives targeted in our study can be categorized into polar molecules such as syringic, caffeic, and gallic acids, in addition to the two flavonoids, rutin and quercetin. Moreover, there are amphiphilic molecules like ferulic and coumaric acids. Consequently, all our NADES are classified, based on their composition and molar ratio, into primary NADES, such as NADES

1, 3, and 5, with a molar ratio of 1:1, and NADES 7, which was the subject of our study on viscosity and the intramolecular interactions forming them.

NADESs 2, 4, and 6 resulted from adjustments made to the molar ratio, which involved both the hydrogen bond acceptors (HBA) and hydrogen bond donors (HBD). This change in the molar ratio can indeed have a crucial impact on DES selectivity for the targeted bioactive molecules and consequently their yields. This represents one aspect of the physicochemical characteristics influenced by the molar ratio (Jin et *al.*, 2020).The significance of yield in our study also extends to the suitability of the extraction technique used. Ultrasounds, in the context of Ultrasound-Assisted Extraction (UAE), are known for their cellulose disruption effects in the outer cell barrier of plant matrix and subsequent hydrolysis (Y. Li et *al*., 2020).

Among the physicochemical characteristics of NADES, viscosity plays a crucial role in their effectiveness in extracting bioactive molecules. This is not only due to the ease of molecule transfer (G. Zhao et al., 2017) but also because of the strength of intramolecular bonds connecting NADES components. Among the NADES we worked with in this research, those with good extraction yields, NADES 3 and NADES 5, exhibited lower viscosity (Fan, Liu, et *al*., 2021; Fan, Sebbah, et *al*., 2021).

It has been demonstrated in our previous studies that viscosity correlates with hydrogen bond stability and strength. Other factors may also be considered in terms of viscosity variation. The product of the number of hydrogen bonds and their lifetime is an important ratio in evaluating viscosity, as the bond duration reflects their strength (Z. Xia et *al*., 2011b). This depends on the nature of the HBAs and HBDs in the DES composition, tending to be lower in terpene-based NADESs where less stable bonds exist. The NADESs becomes more viscous when composed of terpenes only, forming more stable bonds (Fan, Liu, et *al*., 2021).

The issue of viscosity poses a major challenge in using DESs in extraction processes. To address this, some authors have resorted to adding a certain volume of water to reduce DES viscosity and enhance material transfer. However, this technique may not be suitable for all DES. Excessive water addition to certain DESs can disrupt intermolecular bonds, reducing their efficiency (A. Pandey et Pandey, 2014; Weng et Toner, 2018)**.** This technique may even be problematic in the case of hydrophobic DES, as it forms a biphasic system when in contact with water molecules.

In our study, we increased the extraction temperature to reduce solvent viscosity upon contact with dry material, facilitating the transfer of bioactive molecules. The effect of viscosity was evident in this study, given the importance of yields in all our NADES extracts, especially those with lower viscosity like NADES 3 and NADES 5. Their experimental viscosities were 0.873 g/cm³ and 0.867 g/cm³, respectively (table 1), while simulated viscosities were estimated at 0.880 g/cm³ and 0.883 g/cm³, respectively (Fan, Liu, et *al*., 2021; Fan, Sebbah, et *al*., 2021)**.** The low viscosity of these two NADESs compared to others likely contributed to the high extraction yield of bioactives, aided by the high temperature, which impacts the arrangement of molecules and positively affects extraction efficiency (Alkhatib et *al*., 2020; Chen et *al*., 2018)**.** However, uncontrolled or excessive temperature increases could potentially destroy thermolabile molecules (K. Liu et *al*., 2022).

The yields we obtained in our study result from a combination of conditions, including the solvent/solute ratio, which in our case was 10 mg/100 mL. The solvent-to-dry material ratio was also a subject of previous studies in some research aiming to optimize dopamine extraction from *Portulaca oleracea* leaves, and it was estimated at 40 mg/mL (K. Liu et *al*., 2022)**.** This ratio is much lower in our study, intentionally reduced to decrease solute concentration in the solvent and facilitate mass transfer during extraction. Indeed, increasing the solvent-to-solute ratio significantly improved the extraction of bioactives from *Baphicantus cusia* leaves using hydrophobic deep eutectic solvents (Z. Xu et *al*., 2021).

In the context of our study, lactic acid, as an HBA, proves to be crucial for the extraction of polar phenolic compounds when present in an equimolar ratio with the HBD. However, its effectiveness decreases as the molar ratio of HBA increases. Additionally, NADESs containing acetic acid may potentially exhibit an affinity for flavonoids. Within NADESs, intermolecular interactions between HBA and HBD can demonstrate significant efficiency in the extraction process.

In a related study involving Hydrophobic Deep Eutectic Solvents (HDESs), a range of fatty acids was tested in combination with a terpenoid at various molar ratios for bioactive compound extraction. This investigation shed light on the substantial benefits of forming effective associations between different components of a NADESs. Notably, the terpenoid alone exhibited negligible extraction efficiency, but when combined with C=8 fatty acids to form a eutectic system, a marked improvement in yield was observed (H. Zhang et *al*., 2022).

This observation underscores the potential for achieving favorable results through well-designed combinations of terpenes in the extraction of phenolic compounds. This is exemplified by the performance of NADES 3. Furthermore, eutectic mixtures with optimized molar ratios have demonstrated enhanced efficacy, a point substantiated by the extraction yield obtained with NADES 4.

In DESs based on saturated C=10 fatty acids as HBA and β-citronellol as HBD, a notable improvement in the extraction yield of three phenolic acids and the entire spectrum of flavonoids was observed. However, it's important to note that the yields of ferulic and caffeic acids experienced a slight reduction in the extract produced using NADES 4. This suggests a potential enhancement in the solubility of the DES when the molar ratio of β-citronellol increased from 1 in NADESs 3 to 2 in NADES 4.

These findings emphasize the significance of tailored NADESs compositions and optimized molar ratios in optimizing the extraction of, particularly phenolic compounds and flavonoids. Such insights have the potential to inform future studies and applications in the field of green and sustainable extraction processes.

3 *In-vitro* studies

3.1 Antioxidant activity

- **DPPH free radical scavenging**

The antioxidant potential of the described NADESs was assessed using the DPPH method. The inhibition concentration (IC_{50}) values of the NADES extracts, which represent the concentration required to achieve 50% scavenging activity, were compared with the IC_{50} value for ascorbic acid. Ascorbic acid was used as a strong benchmark due to its potent antioxidant properties, as reflected by its very low IC_{50} value.

Two key factors influence the antioxidant effectiveness of the extracts. First, the extraction yield significantly determines the concentration of antioxidant compounds in the *Portulaca oleracea* extracts, directly impacting their antioxidant potential, as highlighted by (Samira et *al*., 2017) Secondly, the extractant's ability to stabilize bioactive molecules is dependent on various intermolecular interactions within the extract (Choi et Verpoorte, 2019; Paiva et *al*., 2014) as demonstrated in Figures 22, 24, and 34. This stabilizing capacity, crucial

for preserving the efficacy of the extract, is additionally influenced by intrinsic factors including the characteristics of the components within the eutectic system, particularly the hydrogen bond acceptors (HBA) and donors (HBD). Furthermore, extrinsic factors like extraction time, temperature, and the method used also play significant roles in determining the overall antioxidant efficacy of extracts (He et *al*., 2019; Oliveira et *al*., 2021). Our results indicate that most of the studied NADESs-POL extracts (3-7) exhibit higher IC_{50} values compared to ascorbic acid, suggesting they are less effective as antioxidants than the reference compound. However, the NADES with the highest extraction capacities (NADESs 1 and 2) demonstrate antioxidant activity that is comparable to that of ascorbic acid (Figure 26).

The lowest IC_{50} values of NADESs extracts were observed for 1 and 2 (Me/LA) suggesting that the combination of menthol and lactic acid may synergistically stabilize antioxidant compounds(Dai et *al*., 2013b; Zeng et *al*., 2018), by inhibiting the polyphenol oxidase (PPO) enzyme which degrades phenolic compounds after extraction.(L. Zhou et al., 2020) This may be attributed to the higher viscosity of lactic acid-based NADES, their chelating effect, and the enhanced solubility of the extracted compounds. (He et *al*., 2019; G. Oliveira et *al*., 2021) NADES 3 and 4 extracts (Me/βC) show intermediate IC_{50} values, indicating moderate antioxidant activity. The presence of β-citronellol contributes to the observed activity; however, its full potential may be constrained by the absence of stronger acids, such as lactic acid or acetic acid.

NADESs extracts 5 and 6 (βC/CA) have higher IC_{50} values, suggesting lower antioxidant activity. This may be attributed to capric acid's higher susceptibility to oxidation compared to lactic or acetic acids. In addition to the previously reported high yields of polyphenols and flavonoids, NADES-POL extract 7 exhibited a higher IC_{50} value compared to NADESs extracts 1 and 2. While the presence of acetic acid in NADES 7 (M/AA) may enhance antioxidant activity through mechanisms similar to those of lactic acid, such as solubilization and metal chelation, it appears to be less effective than lactic acid in this role, as indicated by the IC_{50} values.

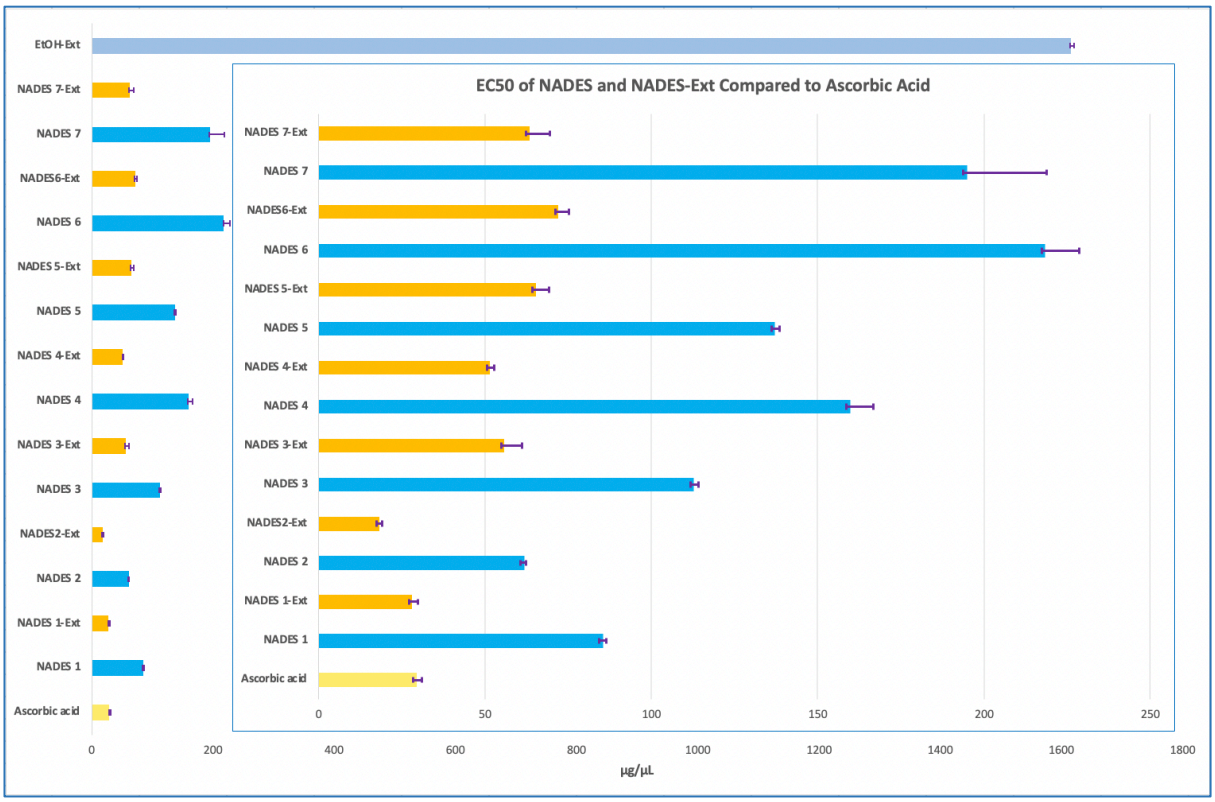

Figure 26: Antioxidant potential expressed as IC_{50} in µg/µL of different extracts and eutectic systems

The variability of IC_{50} values recorded for the different NADES indicates that their composition significantly affects the antioxidant activity. The presence of lactic acid (in NADES 1 and 2) and acetic acid (in NADES 7) appears to contribute more evidently to the antioxidant activity, by stabilization of the extract, compared to the combinations of β-citronellol and capric acid.

Ethanol extract, commonly used as a solvent in plant extractions, exhibited the highest IC_{50} value among all tested samples, indicating the lowest antioxidant activity. In contrast, the significantly lower IC_{50} values of NADESs suggest that they are more effective at stabilizing and enhancing the antioxidant properties of their constituents. The study demonstrates that the type of NADESs can significantly influence both the extraction yield and the antioxidant activity of their components through mechanisms such as increased solubility, metal ion chelation, and the creation of a stable microenvironment. The combination of specific NADESs components, such as menthol and lactic acid, demonstrates promising potential for stabilizing antioxidants, making these solvents valuable for various applications in food, cosmetics, and pharmaceuticals where antioxidant stability is essential. Further exploration of the specific

molecular interactions would be beneficial for fully understanding and optimizing these eutectic systems.

- **Trolox equivalent antioxidant capacity ($TEAC_{DPPH}$)**

A strong linear correlation was observed for the Trolox calibration curve (Annex n°2), with a determination coefficient (r = 0.9997) across the concentration range of 0 to 40 µM, with absorbance values ranging from 1.36 to 0.40 nm. The involvement of this extensive method to present the antiradical activity in this study has a major advantage that allows it to be comparable to other studies. Results obtained through this experiment are expressed in Trolox equivalent antioxidant capacity ($TEAC_{DPPH}$) for all NADESs, expressed as a vehicle, and all extracts, which represent different solvents (NADES or EtOH) with active pharmaceutical ingredients (APIs) of POL. The results are shown in (Figure 27).

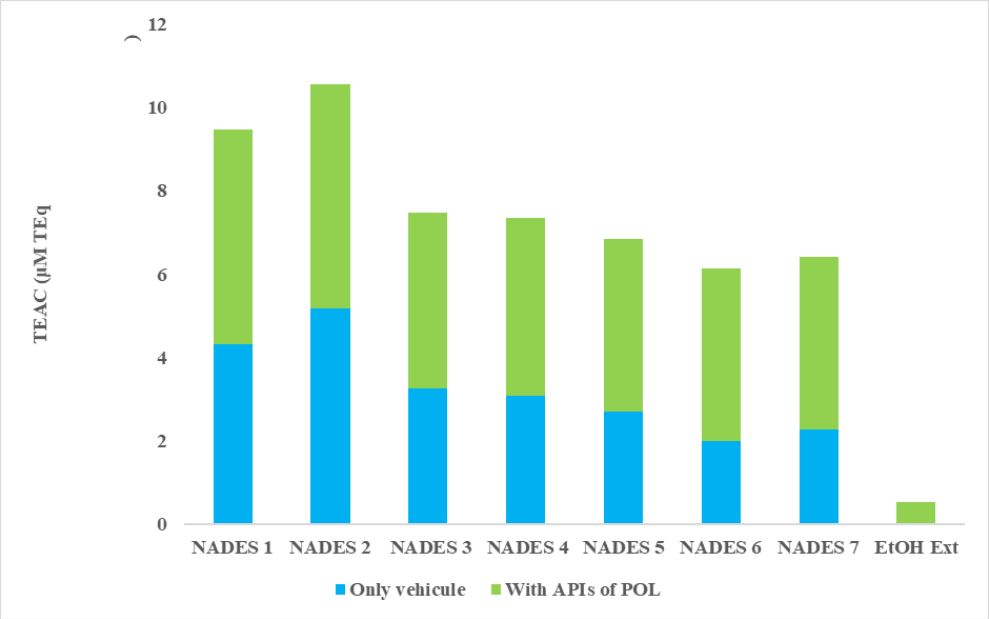

Figure 27: Trolox equivalent antioxidant capacities ($TEAC_{DPPH}$) of NADESs, NADESs-Enriched Extracts, and Ethanolic Extract expressed in (µM TEq) measured at the absorbance of each sample at 50% of its concentration.

The TEAC values obtained confirm the trends previously observed in the antioxidant activity of the samples. Specifically, Trolox equivalents follow a decreasing order among the pure NADES: NADES2 > NADES1 > NADES3 NADES4 > NADES5 > NADES7 > NADES6, reflecting a gradual decline in intrinsic antioxidant capacity from NADES1 to NADES6 as it was previously discussed through the IC_{50} values, and highlighting the moderate antioxidant activity of the vehicles alone. Furthermore, NADESs enriched with POL exhibit significantly

enhanced antioxidant capacities, following almost the same trends same trend: NADES2-Ext > NADES1-Ext > NADES4-Ext> NADES3-Ext > NADES7-Ext > NADES7-Ext > NADES6-Ext > EtOH-Ext. These results highlight once again the synergistic effect between NADES and POL bioactive compounds, enhancing their radical scavenging potential.

Conversely, the ethanolic extract (EtOH-Ext) showed extremely low antioxidant capacity, with a TEAC of just 0.11 µM TEq These findings underline the superior performance of NADES, particularly those enriched with POL, as efficient matrices for the extraction and stabilization of antioxidant compounds.

3.2 Antimicrobial activity

The obtained results outline the antimicrobial activity of various NADESs alone and in combination with *Portulaca oleracea* L. (POL) extracts. The results are quantified in terms of inhibition zones (measured in mm), reflecting these substances effectiveness in inhibiting microbial growth (Figure 28).

Generally, the inhibitory effect of the studied NADESs is more pronounced against Gram-negative bacteria than against Gram-positive bacteria. Analysis of the results indicates that NADES 1 and 2 show the most significant effectiveness. NADES 2, composed of menthol and lactic acid, in a molar ratio of 1:2, generally manifested a more pronounced effect on Gram-negative bacteria, in strong contrast to NADES 1. However, this enhanced effect did not extend to *Escherichia coli* and *Proteus mirabilis*. Although NADES 1 and NADES 2 are composed of the same HBA and HBD components, NADES 2 contains a higher proportion of HBD due to differing molar ratios, resulting in a unique antimicrobial property.

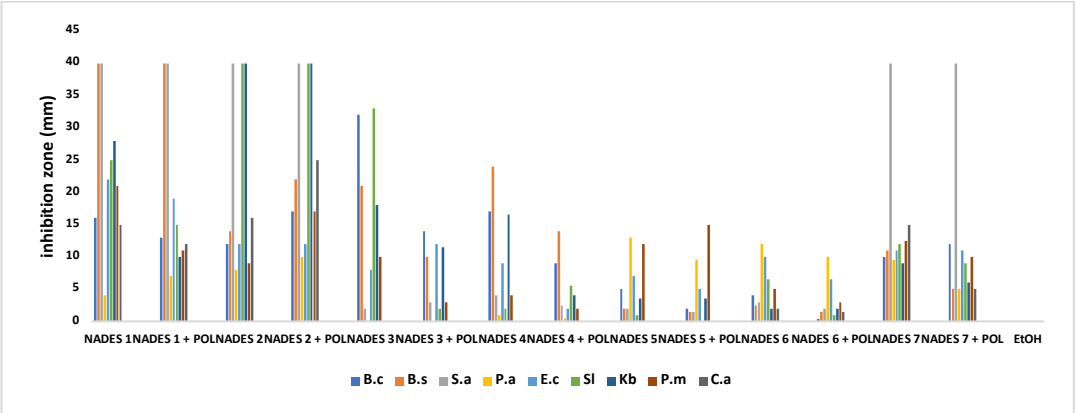

Figure 28: Inhibition zones of different NADES and NADES with POL extract on microbial stains, expressed in (mm)

The acid characteristics due to the carboxylic group content in NADES are responsible for the bactericidal effects. Although the outer membrane of bacteria is generally more resistant to acidic conditions, destabilization of inner membrane proteins resulting from changes in pH can contribute to increased permeability of the outer membrane. This makes bacteria more susceptible to acidic environment (NADES 2 vs NADES 1), creating an inhospitable condition for many microorganisms and enhancing the antimicrobial efficacy of the formulations (Wikene et *al*., 2017; B.-Y. Zhao et *al*., 2015). Previous studies suggest a possible synergistic intramolecular reaction within the structure of NADESs, involving its HBD and HBA components. It has been reported that NADESs exhibit greater toxicity compared to their individual components due to delocalized charges resulting from hydrogen bonding, particularly in deep eutectic acid-based systems (Radošević et *al.*, 2018; Silva et *al*., 2021).

Staphylococcus aureus showed the highest sensitivity to multiple NADESs containing organic acids (Lactic acid and acetic acids) and their POL extracts, consistently exhibiting large inhibition zones. On the other hand, NADESs based on terpenes or combined with fatty acids have reduced effects against this pathogen. A synergistic effect between NADES 2 and the active components of POL was observed across all the studied strains, making it a promising candidate for further exploration as natural antimicrobial agent. In contrast, for NADES 1 and 7, the presence of POL bioactive compounds exhibited negative effects on all the studied microorganisms, except for *Pseudomonas aeruginosa* (NADES 1) and *Bacillus cereus* (NADES 7), respectively. *Pseudomonas aeruginosa* are known from the literature to possess a terpenoid catabolism (García-Salinas et *al*., 2018; E. Silva et *al*., 2021). This is particularly evident with NADES 3 and 4 (composed of terpene/terpene), where no/low inhibition was observed, as shown in Figure 5. This phenomenon can be attributed to the inherent resistance of Gram-negative bacteria to natural substances, including terpenoids (Aguilar et *al*., 2006; Cox et Markham, 2007; Vaara et Nurminen, 1999; Wiener et Horanyi, 2011).

According to the literature, β-citronellol is a terpenoid known for its high solubility and lipophilicity, as well as limonene (C. V. Pereira et *al*., 2019; E. Silva et *al*., 2021). Its association with capric acid (NADES 5 and 6) significantly reduces the overall viscosity of the eutectic system(Fan, Sebbah, et *al*., 2021), thereby increasing the diffusion coefficient across the bacterial cell barrier (E. Silva et *al*., 2021). However, this increase is not sufficient to produce a significant inhibitory effect against all microorganisms studied (Figure 5). The effect is more pronounced for *Pseudomonas aeruginosa* when using eutectic mixtures containing fatty acids compared to those containing acetic or lactic acids. However, reducing the fatty acid content in

NADES 6 produced a negative effect on *Proteus mirabilis* inhibition, but exhibited a diffuse effect on *Salmonella typhi* and a relatively substantial impact on *E. coli*, particularly when tested together with POL extract. In general, the difference between NADES containing organic acids and those with fatty acids against Gram-negative bacteria are in accordance with literature (Al-Akayleh et *al*., 2022; J. M. Silva, Silva, et *al*., 2019). Gram-negative bacteria are often more resistant to fatty acid-based antibacterial agents due to their complex cell membrane structure, which includes lipopolysaccharides that repel fatty acids and block their antimicrobial action (J. M. Silva, Silva, et *al*., 2019).

Candida albicans showed the least sensitivity, with generally lower inhibition zones against all NADESs and NADESs-POL extracts. It is well-documented in the literature that *Candida albicans* displays a remarkable ability to modulate the hydrophobicity of its membrane surface during various stages of its growth and development. Fatty acids, particularly those of medium and long chain lengths, have been documented to possess inhibitory activity against *Candida albicans* (Huang et *al*., 2011) it has been suggested that physicochemical characteristics, such as solubility, may not be the sole determinant of antimicrobial activity. However, our study did not show this inhibitory effect, possibly because capric acid loses its efficacy on cell lipopolysaccharides when combined with terpenes like β-citronellol. Furthermore, eutectic systems are often reported to exhibit novel physicochemical properties and biological activities that differ from those of their components.

In conclusion, this data highlights the importance of selecting the appropriate combinations of NADESs and plant extracts based on the specific microbial target. Utilizing NADESs as solvents has the potential to enhance the extraction efficiency of bioactive compounds from plant materials, thereby improving their antimicrobial efficacy. However, the effectiveness of these combinations can vary significantly depending on the type of microorganism being targeted.

3.3 Cytotoxic and cell viability assessment

To evaluate the safety and toxicity, determine the anticancer potential, and identify the optimal dosage of THEDESs and NADESs as potential therapeutic or delivery agents, *in vitro* cell models were utilized. This required assessing the effects of THEDESs and NADESs separately on cell viability in three distinct cell lines: HEK (Human Epidermal Keratinocytes), HaCat (Human Adult Low Calcium High Temperature Keratinocytes), and AGS (gastric adenocarcinoma cells). This approach helps to examine the selectivity of THEDESs toward cancer cells and anticipate potential side effects on non-target cells (Constant et *al.*, 2013; Hayyan et *al.*, 2015).

In order to have a number of 15K/well of AGS cells after seeding, 10 µl of cell suspension was incubated for 48-72h, (Figure 29) shows cells in division phase and ready to differentiate. After 24h incubation cell will be fully differentiated and ready for their first passage (Figure 30)

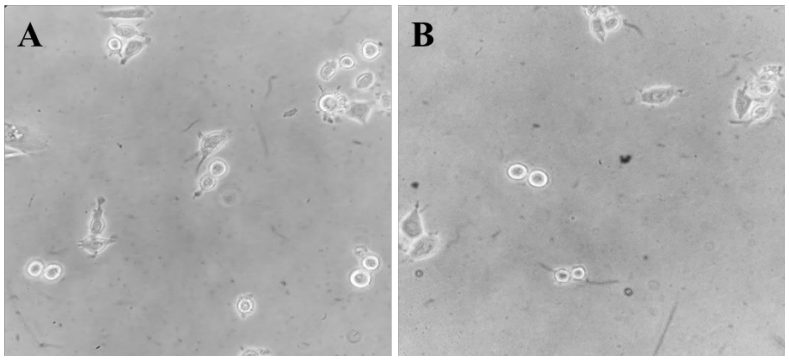

Figure 29: Representative images of AGS cells during the first hours of culture before the first passage. (A) Actively dividing cells, indicating proliferation. (B) Cells showing early signs of differentiation in T-flask.

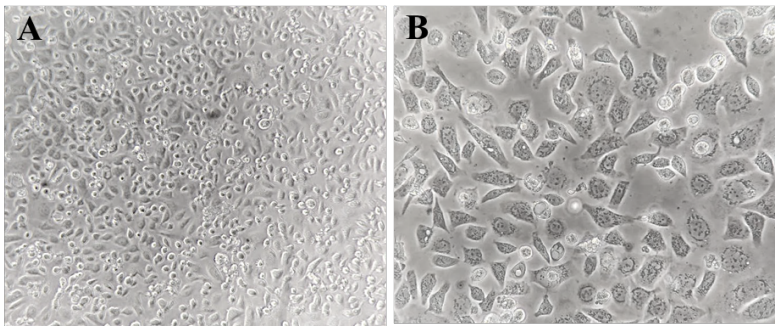

Figure 30: Morphological characterization of AGS cells at 70-80% confluence after 48-72 hours of incubation under standard conditions (37°C, 5% CO_2, DMEM with 10% FBS) at two different magnifications (A: resolution X10/0.25) (B: resolution X20/0.40).

In this study, the MTT cell viability assay was employed as an approach. Due to the observed dose-dependent cytotoxic effect, only the AGS cell line was retained for further analysis, as it allowed for assessing the impact of THEDESs and NADESs on the viability of gastric adenocarcinoma cells. This assay evaluates these cells as a confluent monolayer in the stationary phase of the growth curve, providing insight into the safety and toxicity of THEDESs. (Figure 31) shows viable and dead AGS cells after adding different treatments. Meanwhile, the HEK and HaCat cell lines were excluded from subsequent tests due to inconclusive results.

AGS cells, derived from human gastric adenocarcinoma, exhibit characteristics of differentiated epithelial cells with an adherent growth pattern. As shown in the image, differentiated cell cultures consist of cells that have lost their ability to further differentiate,

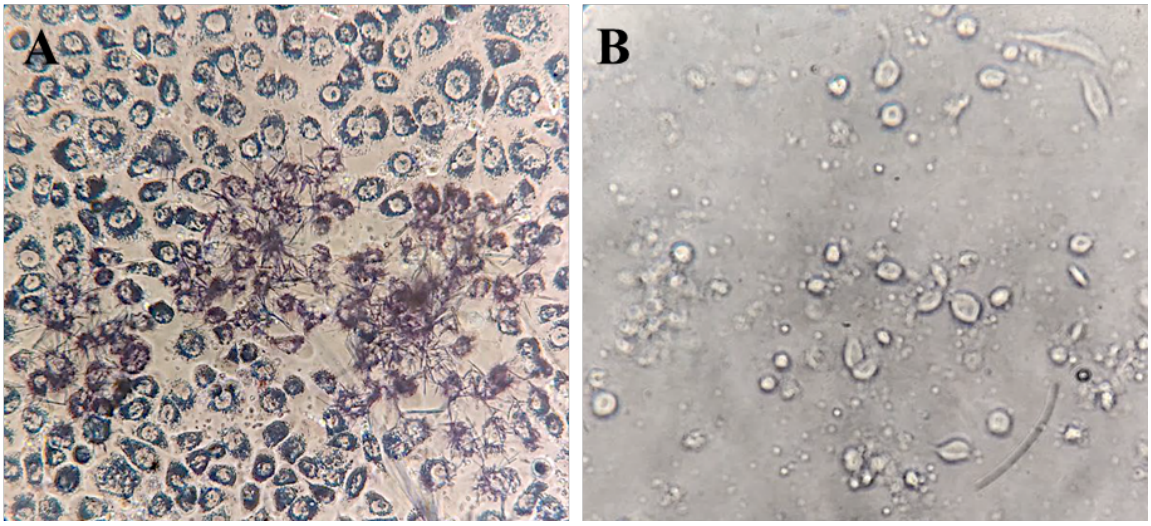

Figure 31: Representative microscopic images of AGS cells after MTT treatment. (A) Viable cells with purple formazan crystals, indicating metabolic activity. (B) Cell fragments without coloration, demonstrating loss of viability due to THEDES/NADES treatment-induced cytotoxicity.

which aligns with the nature of AGS cells. These cells adhere to a solid surface, forming monolayers typical of adherent cell cultures**.** Their epithelial morphology, characterized by squamous, columnar, or cuboidal shapes, influences their interactions with the extracellular environment, affecting nutrient uptake, signaling pathways, and response to therapeutic agents.

This adhesion-dependent growth is essential for their proliferation and experimental manipulation *in vitro*.

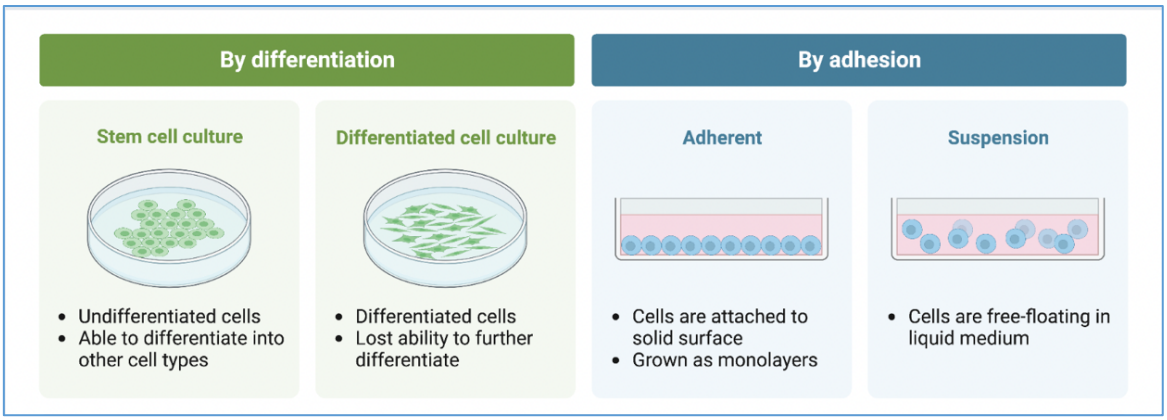

Figure 32: Classification of cell cultures based on differentiation or adhesion

Although 3D cell culture models offer a more physiologically relevant environment by better mimicking in vivo tumor conditions, they were not utilized in this study due to their increased complexity, longer incubation times, and the need for specialized infrastructure and expertise. Given that the primary aim was to screen the cytotoxicity and selectivity of THEDESs and NADESs at 5 different concentrations **(**0.025%, 0.05%, 0.075%, 0.1%, and 0.125%) results represented in Annex 4**,** a 2D monolayer approach using the MTT assay provided a rapid and cost-effective method to obtain preliminary insights before considering more complex models, the method is shown in (Figure 33).

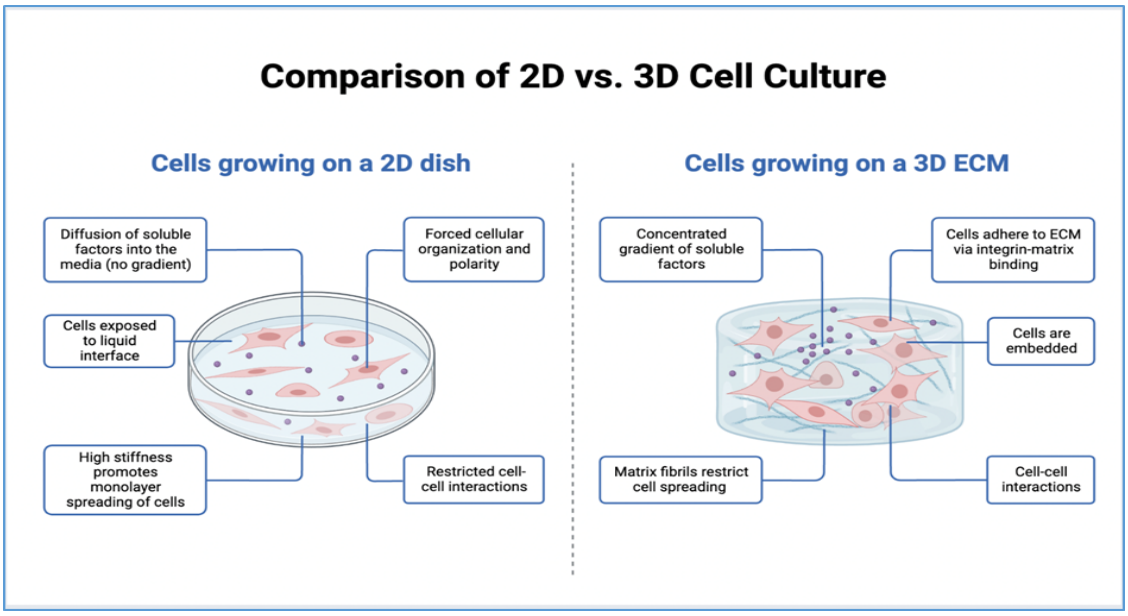

Figure 33: Comparison of 2D monolayer and 3D cell cultures of AGS cell line.

The results for the 0.025% and 0.05% concentrations were excluded from the analysis due to their lack of relevance. At these concentrations, AGS cell inhibition remained minimal,

and no synergistic effect was observed when the active compound was combined with eutectic formulations in THEDESs. Therefore, it was deemed more appropriate and meaningful to focus the discussion on the 0.075%, 0.1%, and 0.125% concentrations, where more pronounced effects were evident.

Cell cytotoxicity has been reported to depend on various factors, including the viscosity, concentration, and pH of eutectic mixtures, as well as its composition and the specific interactions between its individual components and the functional groups present on the cell surface. Additionally, the sensitivity of different cell lines to these interactions plays a crucial role in determining cytotoxic effects (Hayyan et *al*., 2013, 2015, 2016; J. M. Silva et *al*., 2018a). (Figure 34) shows different cytotoxic mechanism observed under microscope.

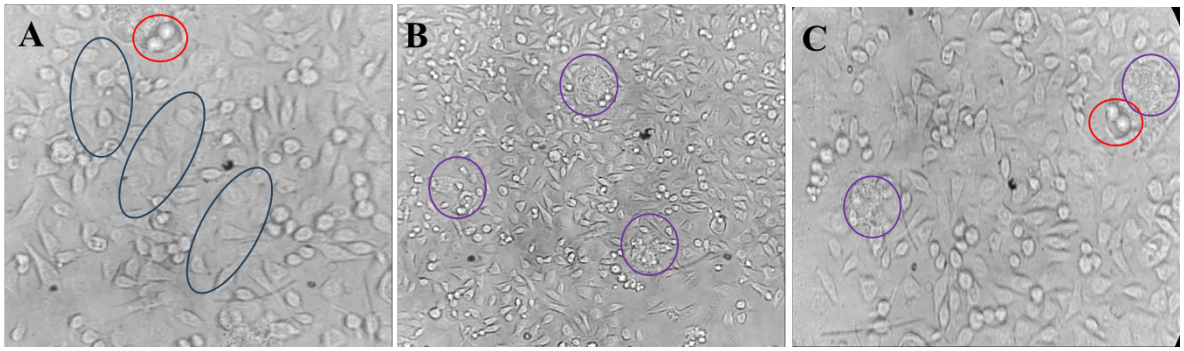

Figure 34: Major Mechanisms of AGS cell death induced by NADES/THEDES: Viscosity-induced damage (Blue ovals), Mitotic Arrest (Red circles), and Cytoplasmic leakage with cell lysis (Purple arrows and circles).

- ✓ **Cytotoxic effects at 0.075%, 0.1%, and 0.125% concentrations of NADESs and THEDESs**

The evaluation of cell viability across 0.075%, 0.1%, and 0.125% concentrations of NADESs- and THEDESs-based formulations reveals a dose-dependent cytotoxic effect, with distinct trends observed between the two formulations (see results in Annex 5). Given the fact that Menthol was a key component of all NADESs and THEDESs used in this study, The antiproliferative effect appears to be primarily linked to the presence of Menthol, aligning with the notion that the HBD plays a crucial role in the cytotoxic profile of NADESs and THEDESs, possibly due to its stronger influence on the system's acidity (Hayyan et *al*., 2013, 2016).

Menthol can function as an anticancer agent either dependently or independently of TRPM8. In cancer cells, the loss of expression of TRPM Ca^{2+} channels have been observed

(Pérez-Riesgo et *al*., 2017), suggesting that menthol likely exerts its effects through a TRPM8-independent mechanism. In contrast, studies on Caco-2 cells indicate that menthol's action is dose-dependent, as these cells express TRPM8, and its activation by menthol has been linked to increased proliferation (Yee, 2015). One proposed mechanism for menthol-induced cell death, as described by Cornmell et al., involves the accumulation of hydrophobic ionic liquids in cell membranes through interactions with negatively charged groups. This interaction may lead to the penetration of these groups into the cytoplasm, ultimately disrupting membrane integrity by increasing permeability and fluidity, which results in cell death (Cornmell et *al.*, 2008).

At 0.075%**,** NADESs-treated cells maintained a high viability, ranging from 60.97% to 70.37%**,** while THEDES treatment resulted in slightly lower values **(**59.10% to 66.43%**).** The minor reduction in viability in the THEDES group suggests an early onset of cytotoxic effects, potentially due to an enhanced bioavailability of active compounds, this can be explained by a synergetic or addictive effect between the compounds, as previous reported (Hayyan et *al*., 2013, 2015; J. M. Silva et *al*., 2018b), However, at this concentration, both formulations exhibited relatively mild cytotoxicity, indicating that cells were still capable of maintaining homeostasis despite treatment.

When the concentration was increased to 0.1%**,** a moderate decline in cell viability was observed in both groups. NADESs-treated samples displayed viability values within the range of 55-65%**,** whereas THEDESs-treated samples showed a more pronounced decrease, suggesting a stronger inhibitory effect. This may be attributed to the improved solubilization properties of THEDESs, which could enhance cellular uptake and bioactivity of the active compounds, leading to increased stress responses or apoptotic signaling. The standard deviations remained low, reinforcing the reproducibility of these effects.

At the highest concentration**,** 0.125%**,** a significant cytotoxic effect was evident, particularly in samples 4, 5, and 6, where cell viability dropped below 10% in both NADESs- and THEDESs-treated cells. The cytotoxicity was more pronounced in the THEDESs group, with viability values as low as 3.73%**.** This suggests that at this threshold, the bioactive compounds, when formulated in THEDESs, exhibit potent inhibitory effects, potentially through mechanisms involving membrane permeability alteration, oxidative stress induction, or apoptosis activation. Besides, an increased concentration of THEDESs leads to higher media viscosity, which can impact cell viability by altering intracellular processes such as protein-

protein interactions, solute and macromolecule transport, and signal transduction (Hayyan et *al*., 2016; J. M. Silva et *al*., 2018b). The stark contrast between mild cytotoxicity at 0.075% and severe toxicity at 0.125% highlights the crucial role of concentration in determining cellular response to these formulations. Furthermore, the hydrogen bonding interactions between the hydrogen bond donor (HBD) and hydrogen bond acceptor (HBA) influence both the physical properties and chemical structure of the system. As a result, this may explain why cytotoxicity is not solely determined by the concentration of individual compounds (F. S. N. de Oliveira et Duarte, 2021).

The enhanced action of Menthol/Lactic acid (1:1, 1:2) (NADESs 1, 2; THEDESs 1, 2), Beta-citronellol/Capric acid (1:1, 2:1) (NADESs 5, 6; THEDESs 5, 6), and Menthol/Acetic acid (1:2) (NADES 7; THEDES 7) on cancer cells, despite the high bioactive yield in these THEDES, may be attributed to differences in membrane phospholipid composition. Since cell membranes have distinct ratios of functional groups (carboxyl, phosphate, amino), their structure influences the permeability and uptake of THEDESs into the cytoplasm, affecting their role in delivering APIs-POL (Hayyan et *al.*, 2016). Additionally, factors such as cell surface receptors, intracellular transport, drug uptake mechanisms, and the rapid division of cancer cells may further modulate THEDESs effectiveness (Abdullaev 2002; Naghshineh et *al*. 2015).

- ✓ **Comparative analysis of cell viability and implications**

Across all tested concentrations, THEDESs exhibited stronger cytotoxic effects than NADESs, particularly at 0.1% and 0.125%**,** suggesting that the eutectic mixture enhances the bioactivity of the encapsulated compounds**.** While 0.075% and 0.1% maintained moderate levels of cell viability, the 0.125% concentration exceeded a critical threshold, leading to extensive cytotoxicity. The increased cytotoxicity observed with THEDESs formulations may be attributed to their improved solubility**,** stability, and intracellular uptake of active compounds, which could enhance their bioactivity and induce apoptotic effects.

These findings suggest that 0.075% and 0.1% may be suitable concentrations for controlled bioactivity with minimal toxicity, while 0.125% exerts a potent cytotoxic effect that warrants further investigation. Future research should focus on the underlying molecular mechanisms, including ROS generation, mitochondrial dysfunction, and apoptosis pathways, to better understand the therapeutic potential and limitations of these formulations.

✓ **Statistical analysis of the cytotoxicity by tukey's test**

The statistical analysis using Tukey's test highlights significant differences between certain tested concentrations. Specifically, comparisons between 0.075% and 0.10% as well as 0.075% and 0.125% show statistically significant differences **(**$p < 0.05$**)** across all samples, indicating a notable effect of increasing concentration on the measured response.

However, the comparison between 0.10% and 0.125% yields variable results depending on the samples. For some, such as Sample 4 and Sample 5**,** this difference is not significant **(**$p > 0.05$**),** suggesting that increasing the concentration to 0.125% does not have a significant impact compared to 0.10%. Nevertheless, for other samples, this difference remains significant **(**$p < 0.05$**),** indicating a variable response depending on the experimental conditions.

✓ **Conclusion of cytotoxic analysis against AGS cell line**

The effect of concentration is generally significant, particularly between 0.075% and higher concentrations. However, the lack of a marked difference between 0.10% and 0.125% for certain samples suggests that increasing the concentration beyond 0.10% does not necessarily provide additional benefits in all cases. A graphical visualization of the results could help in better interpreting the observed trends.

4 *In-vivo* studies

4.1 Toxicological profile of NADESs

Prior to evaluating the therapeutic efficacy of the synthesized Natural Deep Eutectic Systems (NADESs) extracts against methotrexate (MTX)-induced liver injury, it is imperative to assess their oral toxicity profiles. This ensures the safety of subsequent *in vivo* applications. This method helps identify the maximum tolerated dose and potential toxic effects, providing essential data for assessing the risk associated with new compounds (Federal Register, 1996). Same protocol was previously followed in MTX context (Fuskevåg et *al*., 2000)

The dose escalation approach is a standard method in toxicological assessments, allowing for the identification of dose-related adverse effects and the determination of the maximum tolerated dose (MTD) (Le Tourneau et *al*., 2009). This systematic increment in

dosing provides a comprehensive understanding of the toxicological profile of the substances under investigation.

While NADESs are often regarded as environmentally benign, emerging studies have presented varying toxicity outcomes, emphasizing the necessity for empirical toxicity evaluations prior to their biomedical application (G. M. Martínez et *al*., 2022). Given the apolar nature of NADESs in our study, the integration of Tween 80 as a solubilizing agent is a common practice in oral administration studies, enhancing the bioavailability of hydrophobic compounds.

The data derived from this acute dose escalation study will be instrumental in determining the safety margins of the NADESs formulations. This foundational knowledge is crucial before proceeding to efficacy studies involving NADESs-based extracts as potential therapeutic agents against MTX-induced liver injury.

In summary, conducting a rigorous acute dose escalation toxicity study is a critical step in the preclinical evaluation of novel therapeutic candidates, ensuring both their safety and efficacy in subsequent applications.

4.1.1 Acute dose escalation toxicity study of NADESs

The study assessed the acute oral toxicity of seven different NADESs formulations in rats, with doses progressively increasing from 50 µL to 1000 µL. The findings revealed a clear dose-dependent toxicity profile, with NADES 1 being the safest and NADESs 2, 3, and 7 showing significant toxicity at higher doses, as shown in (Figure 35).

At 200 µL, all NADESs formulations were well tolerated, indicating that this dose does not induce immediate or observable toxic effects. This suggests that, at low concentrations, these NADES do not pose acute risks to physiological functions. However, increasing the dose to 500 µL resulted in variable effects depending on the formulation. NADESs 4, 5, and 7 were still safe at this dose, while NADES 2 caused signs of toxicity, including respiratory distress and shock, though it was not immediately lethal. The presence of digestive tract burns and organ damage in rats exposed to 500 µL of NADES 2 suggests a corrosive or irritant effect, potentially due to the acidic nature of lactic acid in this formulation, the rate was then scarified and the internal orangs were observed. Moreover, NADESs 3 and 7 were lethal at 500 µL, indicating

that these formulations have a narrow margin of safety and may induce systemic toxicity beyond a critical threshold.

Figure 35: Toxicological profile through acute dose escalation toxicity of tested NADESs showing a dose-dependent toxicity with significant effects at higher concentrations

At the highest dose of 1000 µL, all tested NADESs except NADES 1 proved lethal. This indicates that most NADESs formulations, when administered in high volumes, can lead to severe toxicity, likely due to metabolic overload, systemic organ failure, or chemical irritation of vital tissues. The rapid onset of symptoms and mortality at this dose level suggests that exceeding a certain concentration disrupts homeostasis, overwhelming detoxification pathways and causing irreversible damage.

❖ ***In-vivo* toxicity mechanisms of NADESs**

The varying toxicity profiles among the different NADESs formulations can be explained by their individual chemical compositions and physicochemical properties. NADESs containing menthol and lactic acid (NADESs 1 and 2) exhibited different toxicity behaviors, with NADES 1 being completely safe and NADES 2 showing toxicity at 500 µL. This suggests that the molar ratio of lactic acid to menthol influences biocompatibility, potentially altering solubility, bioavailability, or metabolic processing.

Similarly, NADESs formulations containing beta-citronellol (NADESs 3, 4, 5, and 6) demonstrated varying levels of toxicity. While NADESs 4 and 5 remained safe at 500 µL, NADESs 3 and 7 were lethal at this dose. The increased toxicity of NADES 3 (menthol/beta-

citronellol 1:1) suggests that the combination of these two compounds, in equal proportion, may have synergistic toxic effects, possibly by enhancing membrane permeability or interfering with enzymatic detoxification pathways. On the other hand, NADES 5 (beta-citronellol/capric acid 1:1) was safe at 500 µL, implying that capric acid might counteract some of the potential toxic effects of beta-citronellol.

The lethal effects observed at 1000 µL in most NADESs-treated groups indicate that high doses may induce systemic toxicity through multiple mechanisms. These could include oxidative stress, enzyme inhibition, hepatotoxicity, or gastrointestinal damage leading to metabolic disturbances. The presence of organ burns in NADES 2-treated rats suggests that direct mucosal irritation played a significant role in toxicity, which may be exacerbated by the acidic nature of certain NADESs components.

❖ **Implications and future considerations**

These findings provide valuable insights into the dose-dependent toxicity of NADESs and their potential limitations as solvent systems for biomedical applications. While some formulations, such as NADES 1, show promising safety profiles, others exhibit significant toxicity at relatively moderate doses. This highlights the need for careful selection of NADESs compositions, particularly for pharmaceutical or nutraceutical applications, where safety is a critical concern.

Future studies should focus on identifying the specific toxicological mechanisms at play, including histopathological analysis, biochemical markers of organ damage, and pharmacokinetic studies to determine absorption, metabolism, and excretion profiles. Additionally, long-term toxicity studies could help assess chronic effects, as some NADESs may accumulate or exert delayed toxic effects.

Overall, while NADESs present a novel approach to green solvent systems, their safety profile varies significantly depending on composition and dosage. Understanding these differences is crucial for optimizing their applications in drug delivery and other biomedical fields.

5 Results of hepatotoxicity activity

5.1 Body weight evolution

The variations in weight ($F = 17.469$, $p = 0.000$) observed among the different groups were statistically significant. For interest, group G7 exhibited a significantly lower mean weight (149.11 g) compared to all other groups. Conversely, groups G6, G5, G10 (MTX), and G3 formed a homogeneous subset, indicating no significant differences among them. The mean weight of these groups ranged from 167.11 g to 180.48 g, demonstrating a relative uniformity in their initial weight distribution.

In addition, the control group (185.40 g), along with groups G2 (185.49 g), G8 (187.91 g), and G4 (188.77 g), constituted a third subset, indicating no significant weight differences among them. Finally, group G1 (205.35 g) displayed the highest mean weight and was only grouped with G4 in the last subset, suggesting that these two groups share characteristics favouring a greater weight gain.

It is important to note that the observed weight variations are primarily due to the initial weights of the rats, which were obtained from the Pasteur Institute. These weight differences were taken into account when calculating the doses of treatments administered in the subsequent phases of the experiment. In particular, the toxic doses of methotrexate (MTX) were individually adjusted based on the body weight of each rat to ensure accurate and standardized administration.

Although the ANOVA results revealed certain weight distribution trends, the significance values obtained ($p = 0.232$, $p = 0.079$, $p = 0.059$) indicate that some observed differences remain close to the statistical significance threshold ($p < 0.05$). These findings suggest that the experimental conditions applied to the different groups induced moderate weight variations.

5.2 Hepatic biomarker levels in groups treated with THEDESs

To assess the impact of the experimental conditions on hepatic function, an ANOVA analysis was performed on key biochemical markers, including alanine aminotransferase (ALAT), aspartate aminotransferase (ASAT), alkaline phosphatase (PAL), gamma-glutamyl transferase (GGT), and bilirubin levels. The weight parameter was also included to examine potential correlations with hepatic function.

The analysis revealed distinct trends across the different biomarkers. In general, groups exposed to methotrexate (MTX) exhibited significantly higher hepatic enzyme levels compared

to the control group, confirming MTX-induced hepatotoxicity. However, treatment groups receiving therapeutic deep eutectic systems (THDESs) (G1-G7) or EtOH-POL Extract (G8) demonstrated varying degrees of hepatoprotection, as reflected in the reduction of enzyme levels. The extent of hepatoprotection depended on the type of NADESs/THEDESs used, with some formulations showing a statistically significant improvement in groups treated with THEDESs compared to the MTX-only group.

- **ALAT (F = 33.388, p = 0.000)**

The elevated F-value indicates significant variations in ALAT levels across groups. ALAT is a key biomarker for hepatocellular damage, with increased levels indicating potential liver injury. Control Group (57.80 U/L) has the lowest ALAT levels, suggesting no liver injury, it is significantly different from all other groups, indicating that treatments or MTX administration had an impact on ALAT levels; It is significantly different from all other groups, indicating that treatments or MTX administration had an impact on ALAT levels. Indeed, there is a gradual increase in ALAT levels among these Intermediate groups (G1, G7, G6, G5, G8, G2, G4, G3), whereas Some groups (G1 to G6) share overlapping subsets, meaning their ALAT values are not statistically different from each other. When G8 and G2 show a further increase, moving towards more significant liver damage.

In MTX-Treated Group (G10 - 132.20 U/L) we observed the highest ALAT levels, indicating severe hepatocellular damage caused by methotrexate (MTX) toxicity and it is significantly different from most groups, except for G3 (109.90 U/L), which also shows a high level of liver injury.

Table 04: Tukey's post hoc test for alanine aminotransferase (ALAT)

Subset	Groups in the subset	p-value	Interpretation
1	Control vs G1, G7, G6, G5, G8, G2, G4, G3, G10 (MTX)	**1.000**	Not significant (NS) between control and G1. However, control is significantly different from higher groups like G4, G3, and G10.
2	G1 vs G7, G6, G5, G8, G2, G4, G3, G10 (MTX)	**0.660**	G1 and G7 are not significantly different.
3	G6 vs G5, G8, G2, G4, G3, G10 (MTX)	**0.062**	Close to significance ($p \approx 0.06$), meaning there is a trend but no strong statistical difference.

4	G5 vs G8, G2, G4, G3, G10 (MTX)	**0.482**	Not significantly different.
5	G8 vs G2, G4, G3, G10 (MTX)	**0.211**	Not significantly different.
Highest Values	G3 vs G10 (MTX)	**1.000**	No significant difference between G3 and G10, meaning both groups exhibit severe liver damage.

- **ASAT (F = 8.234, p = 0.000)**

The significant variation in ASAT levels suggests hepatic or muscular alterations in certain groups, reinforcing the hypothesis of MTX-induced toxicity and the potential protective effects of pre-treatments. The analysis of ASAT (U/L) levels reveals a progressive increase across experimental groups, with significant differences assessed using Tukey's test ($p < 0.05$).

The control group shows the lowest ASAT level (83.07 U/L), representing the physiological baseline. G7 (113.00 U/L) exhibits a significant increase compared to the control, indicating an initial hepatic impact. Groups G1 to G3 display progressively higher values (134.70 - 162.50 U/L), while G4, G5, G8, and G2 show comparable levels (138.50 – 152.30 U/L), suggesting similar effects on hepatic function. The MTX group (G10) exhibits the highest ASAT level (179.70 U/L), confirming marked hepatocellular damage. Tukey's analysis groups the samples into three homogeneous subsets: (1) control and G7 with the lowest values, (2) G1 to G8 with moderate increases, and (3) G3, G6, and G10 (MTX) with the highest ASAT levels. The lowest significance value (0.067) suggests a trend toward statistical differences between the most affected groups and others. Overall, ASAT elevation follows a dose-dependent pattern, with severe hepatotoxicity in the MTX group, while intermediate groups exhibit variable increases, possibly reflecting either protective or exacerbating effects of different treatments.

Table 05: Tukey's post hoc test for aspartate aminotransferase (ASAT)

Subset	Groups in the subset	p-value	Interpretation
1	Control (290.00)	**1.000**	Control group has significantly lower PAL than all others
2	G1 (513.70), G7 (567.00)	**0.301**	PAL is moderately increased in these groups.
3	G5 (622.00), G10 (650.30), G3 (661.80)	**0.128**	Further increase in PAL, suggesting higher hepatocellular activity.

4	G2 (730.60), G6 (737.90), G4 (741.50), G8 (806.70)	**0.087**	Highest PAL levels, potentially indicating greater liver dysfunction or cholestasis.

- **ALP (F = 12.625, p = 0.000)**

PAL is an indicator of cholestatic injury and hepatobiliary function. The control group exhibited the lowest PAL levels (290.00 U/L) and formed a distinct subset, indicating a baseline level of enzyme activity under normal physiological conditions. This suggests that hepatic function remained stable without significant stress or damage. In the second subset, G1 (513.70 U/L) and G7 (567.00 U/L) demonstrated moderately elevated PAL levels compared to the control. Although this increase was not statistically significant, it may reflect early signs of hepatic stress or metabolic alterations. The third subset included G5 (622.00 U/L), G10 (MTX) (650.30 U/L), and G3 (661.80 U/L), showing a further increase in PAL activity. This suggests more pronounced hepatic effects, possibly due to oxidative stress, cholestasis, or enzyme leakage from damaged liver cells. Notably, the MTX-treated group (G10) falls within this subset, reinforcing methotrexate's known hepatotoxic effects. The fourth and highest subset consisted of G2 (730.60 U/L), G6 (737.90 U/L), G4 (741.50 U/L), and G8 (806.70 U/L). The substantial elevation in PAL levels in these groups suggests significant hepatobiliary dysfunction or bone metabolism alterations, with G8 showing the highest PAL activity.

While these differences did not reach statistical significance ($p = 0.087$), they exhibit a clear trend toward meaningful biological effects. In conclusion, the progressive increase in PAL activity across groups suggests varying degrees of hepatic or metabolic stress, with the highest levels observed in G8, G4, G6, and G2. While the lack of statistical significance ($p > 0.05$) means these differences cannot be definitively confirmed, the biological trend aligns with known markers of hepatic dysfunction. Further investigation is necessary to determine the exact mechanisms driving these changes.

Table 06: Tukey's post hoc test for alkaline phosphatase (ALP)

Subset	Groups in the subset	p-value	Interpretation
1	Control (290.00 U/L)	**1.000**	Baseline PAL levels, indicating normal hepatic function
2	G1 (513.70 U/L), G7 (567.00 U/L)	**0.301**	Moderate increase in PAL levels, possibly indicating early hepatic stress.

3	G5 (622.00 U/L), G10 (MTX) (650.30 U/L), G3 (661.80 U/L)	**0.128**	Further increase in PAL activity, likely reflecting hepatocellular damage.
4	G2 (730.60 U/L), G6 (737.90 U/L), G4 (741.50 U/L), G8 (806.70 U/L)	**0.087**	Highest PAL levels, suggesting significant hepatobiliary dysfunction or metabolic alterations.

- **Bilirubin (F = 31.654, p = 0.000)**

The substantial variation in bilirubin levels among groups suggests an impact on hepatic clearance, with potential impairment in bilirubin metabolism due to MTX administration. The control group had the lowest bilirubin level (3.26 mg/L) and was distinctly separate from all treated groups (p = 1.000), confirming that treatments induced a significant increase in bilirubin. This sharp contrast suggests that the applied interventions, particularly MTX treatment (G10), led to hepatic disturbances, which are commonly associated with bilirubin accumulation.

Statistical Significance is grouped as follow; the first subset (p = 1.000) includes only the control group (3.26 mg/L), indicating that its bilirubin level is significantly lower than all treated groups. The second subset (p = 0.061) includes G1 (18.15 mg/L) and G7 (18.58 mg/L), suggesting a moderate but non-significant increase in bilirubin compared to each other. However, the elevation from the control group is pronounced, confirming that the treatment applied to these groups has altered bilirubin metabolism. The third subset (p = 0.050) introduces G5 (21.28 mg/L) and G3 (23.61 mg/L), marking a significant increase from the previous subset. This shift suggests that the treatments applied to these groups led to further hepatic stress, increasing bilirubin accumulation. The fourth subset (p = 0.297) consists of G6 (23.81 mg/L), G2 (24.07 mg/L), and G4 (24.18 mg/L).

These values indicate that bilirubin levels are still rising, but the differences between these groups are not statistically significant. The lack of significance suggests that treatments affecting these groups induced similar degrees of hepatic impairment.The highest bilirubin levels are observed in G10 (MTX) (25.01 mg/L) and G8 (25.46 mg/L), with a p-value of 0.297, indicating that although these groups exhibit the most elevated bilirubin concentrations, they are not significantly different from each other. However, their distinction from lower subsets highlights their severe hepatic dysfunction, likely due to MTX-induced hepatotoxicity.

Table 07: Tukey's post hoc test for bilirubin

Subset	Groups in the subset	p-value	Interpretation
1	Control (3.26 mg/L)	**1.000**	Significantly lower bilirubin levels compared to all treated groups.
2	G1 (18.15 mg/L), G7 (18.58 mg/L)	**0.061**	Moderate bilirubin increase, not significantly different from each other but distinct from the control.
3	G5 (21.28 mg/L), G3 (23.61 mg/L)	**0.297**	Further increase in bilirubin levels, statistically significant from subset 2.
4	G6 (23.81 mg/L), G2 (24.07 mg/L), G4 (24.18 mg/L)	**0.050**	Elevated bilirubin levels, but no significant difference between them.
5	G10 (MTX) (25.01 mg/L), G8 (25.46 mg/L)	**0.297**	Highest bilirubin levels, indicating severe hepatic dysfunction.
Highest Values	G10 (MTX) (25.01 mg/L), G8 (25.46 mg/L)	**0.297**	Highest bilirubin levels, indicating severe hepatic dysfunction.

- **GGT (F = 32.534, p = 0.000)**

GGT elevation is often associated with hepatic oxidative stress and cholestatic disorders. The control group exhibited the lowest GGT level (9.39 U/L), significantly lower than all treated groups, confirming that physiological GGT activity remains low in the absence of hepatotoxic stress. Conversely, the MTX-treated group (G10) displayed the highest GGT level (70.32 U/L), indicating a marked increase in hepatocellular injury or cholestatic damage due to methotrexate exposure.

The statistical analysis categorized the groups into three subsets ($\alpha = 0.05$), providing insights into the significance of the observed differences: Subset 1 ($p = 1.000$): Only the control group belongs to this subset, indicating that its GGT levels are significantly lower than all other groups. Subset 2 ($p = 0.051$): This group includes G1 (50.66 U/L) and G7 (51.20 U/L), with GGT levels considerably higher than the control but not significantly different from one another. The marginal p-value (0.051) suggests a near-significant trend toward GGT elevation compared to the control, warranting further investigation. Subset 3 ($p = 0.316$): This cluster consists of groups with the highest GGT levels, including G5 (59.12 U/L), G6 (65.75 U/L), G3 (65.82 U/L), G2 (66.42 U/L), G4 (66.50 U/L), G8 (69.83 U/L), and G10 (70.32 U/L). The non-

significant p-value (p = 0.316) within this subset indicates that the variations in GGT levels among these groups are not statistically distinguishable.

The progressive increase in GGT across the treated groups suggests a dose-dependent or exposure-related hepatotoxic effect. The significant elevation of GGT in G10 (MTX), compared to all other groups, highlights the hepatotoxic potential of methotrexate, which is known to induce oxidative stress, bile duct damage, and impaired glutathione metabolism, leading to increased GGT synthesis. Interestingly, the near-significant difference between G1/G7 and the control (p = 0.051) suggests an early-stage hepatic response that might not yet be severe enough to reach full statistical significance. However, as GGT levels continue to rise across subsequent groups, the consistent increase without statistical differentiation in subset 3 (p = 0.316) suggests that beyond a certain threshold, GGT elevation reaches a plateau, possibly due to enzyme saturation or a ceiling effect in hepatic enzyme induction.

Table 08: Tukey's post hoc test for GGT (U/L)

subsets	Groups in the subst	p-value	Interpretations
1	Control	**1.000**	aseline GGT activity, indicating normal liver function
2	G1, G7	**0.051**	Moderate increase in GGT, suggesting early hepatic response but no severe damage
3	G5,G6, G8 and G10	**0.316**	Significant elevation in GGT, indicative of marked hepatotoxicity, particularly in the MTX-treated group (G10)

5.3 Hepatic biomarker levels in groups treated with POL extracts

The aerial parts of *Portulaca oleracea* (POL) are well known for their strong antioxidant properties, which have been shown to mitigate oxidative stress associated with liver diseases. (Gheflati et *al*., 2019) reported that bioactive compounds from POL exhibit hepatoprotective effects, particularly in non-alcoholic fatty liver disease (NAFLD), by reducing oxidative stress markers. Similarly, a recent study by (Milkarizi et *al*., 2024) demonstrated that hydroalcoholic POL extract significantly reduced the levels of AST, ALT, GGT, total bilirubin, and direct bilirubin in a treated group, while ALP levels remained unchanged.

In our study, we hypothesize that the extraction solvent and the delivery system of bioactive compounds (APIs) play a crucial role in ensuring their efficacy. Instead of conventional extraction methods, we utilized natural deep eutectic solvents (NADESs) to extract POL-APIs and administered them together as a therapeutic agent. This approach enhances the bioavailability of POL bioactives by improving solubility and stability, potentially leading to a more effective hepatoprotective outcome.

Most studies investigating the hepatoprotective effects of POL extracts require prolonged administration periods and relatively high doses to achieve significant biochemical improvements. For instance, Ali, Said, and Mohammed Hassan (2011) found that supplementing rats with liver fibrosis with POL extract at a dose of 400 mg/kg/day resulted in a significant decrease in AST, ALT, ALP, GGT, and total bilirubin levels. Similarly, (Darvish Damavandi et *al*., 2021) reported that administering 300 mg of POL extract daily for 12 weeks significantly reduced AST, ALT, and GGT levels. The delayed onset of therapeutic effects observed in these studies may be attributed to the limited bioavailability of POL bioactives in conventional extraction and administration forms.

The bioavailability issue of POL-derived compounds has been highlighted in pharmacokinetic studies (C. Zhao, Zhang, et *al.*, 2019) demonstrated that the absorption of alkaloids from POL was relatively low in oral administration due to poor solubility and rapid metabolism. Another study by Zhao, Ying, et *al.* (2019) further confirmed the challenges in delivering POL bioactives effectively. Our approach using NADES as an extractant and carrier aims to overcome these limitations, ensuring a more efficient delivery of POL bioactives and potentially enhancing hepatoprotective effects.

Here comes up novel strategies to enhance bioavailability of APIs od POL, using small amounts of administrated doses, besides, the APIs is incorporated withing a NADES to insure the stability of bioactive compounds until their delivery. The result mixtures are called “therapeutic deep eutectic systems”

The analysis of hepatic biomarkers in our study, including ALAT, ASAT, alkaline phosphatase (PAL), bilirubin, and GGT, provides crucial insights into liver function and hepatocellular integrity across the different treatment groups. Specifically, comparing G8 (ethanolic extract of POL) with G1-G7 (THEDESs-treated groups) allows us to assess which approach exhibited superior hepatoprotective effects against MTX-induced toxicity**.**

- **ALAT (U/L) and its clinical significance**

The analysis of ALAT (ALT) levels provides critical insight into the hepatoprotective effects of the tested formulations. The control group exhibited the lowest ALAT level (57.8 ±1.92 U/L), confirming normal liver function. In contrast, the methotrexate (MTX)-treated group (G10) displayed the highest ALAT level (132.2 ±13.79 U/L), indicating severe hepatotoxicity. All treatment groups (G1-G8) showed intermediate ALAT levels, reflecting varying degrees of hepatoprotection (Figure 36).

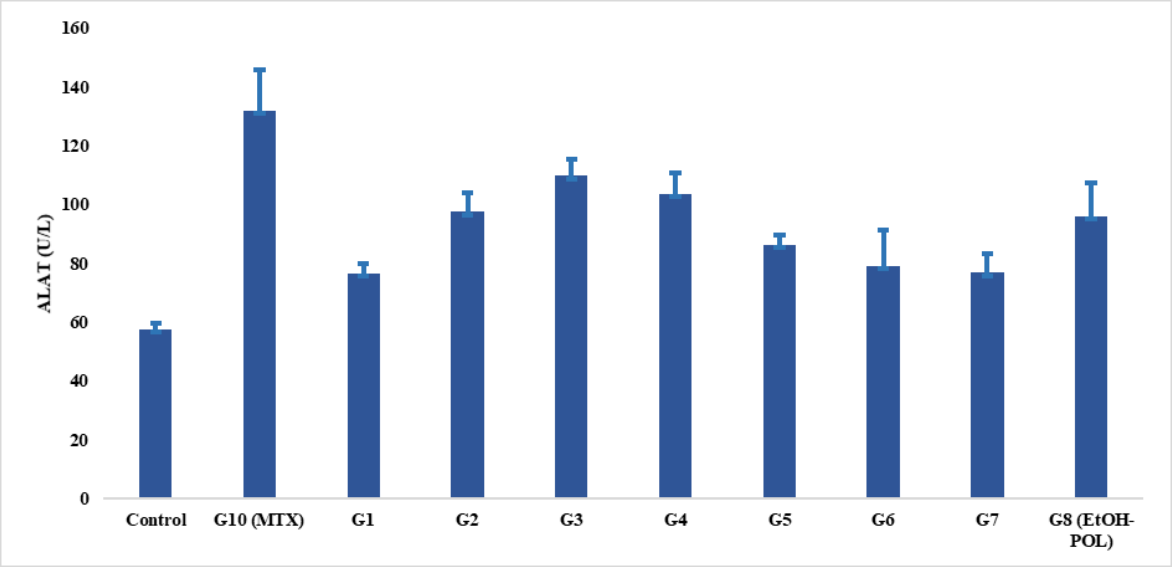

Figure 36: ALAT (U/L) levels in different experimental groups: Evaluating MTX-induced hepatic injury and THEDESs protective effects

Among the groups treated with THEDESs-based formulations (G1-G7), G1 (76.7 ±3.34 U/L) and G7 (77.0 ±6.32 U/L) exhibited the lowest ALAT levels, closely approaching those of the control group. These values were significantly lower than those observed in G8 (96.1 ±11.49 U/L), which received the ethanolic extract of *Portulaca oleracea* (POL). Other THEDES-treated groups, including G6 (79.4 ±11.98 U/L) and G5 (86.5 ±3.16 U/L), also demonstrated lower ALAT levels than G8, though to a lesser extent. This suggests that THEDESs formulations may enhance the hepatoprotective properties of POL's bioactive compounds more effectively than direct ethanolic extraction.

Statistical analysis supports these findings. ANOVA results ($p = 0.062$) indicate a borderline significant difference among groups, while Tukey's post-hoc test highlights specific intergroup variations. Notably, the ALAT levels in G1 and G7 were significantly lower than

those in G8 (96.1 ±11.4 U/L), G2 (97.7 ±6.49 U/L), and G4 (103.8 ±7.15 U/L), demonstrating the superior efficacy of THEDESs-based treatments. Furthermore, while G8 exhibited a degree of hepatoprotection compared to G10, it did not achieve the same extent of ALAT reduction as G1 and G7, further emphasizing the potential advantage of THEDESs in improving bioavailability and efficacy of POL bioactives.

Overall, these findings suggest that THEDESs-based formulations provide a more pronounced hepatoprotective effect than ethanolic extracts of POL. The significant reduction in ALAT levels observed in G1 and G7, approaching control values, indicates that THEDES may enhance the stability and delivery of bioactive compounds, ultimately leading to improved hepatoprotection.

- **ASAT (U/L) and its role in liver function**

The ASAT (AST) levels provide further insight into the extent of hepatocellular damage and the protective effects of different treatment groups. The control group exhibited the lowest ASAT level **(**83.07 U/L**),** indicating normal liver function. In contrast, the methotrexate (MTX)-treated group (G10) had the highest ASAT level **(**179.7 ±2.77 U/L**)**, reflecting significant liver injury.

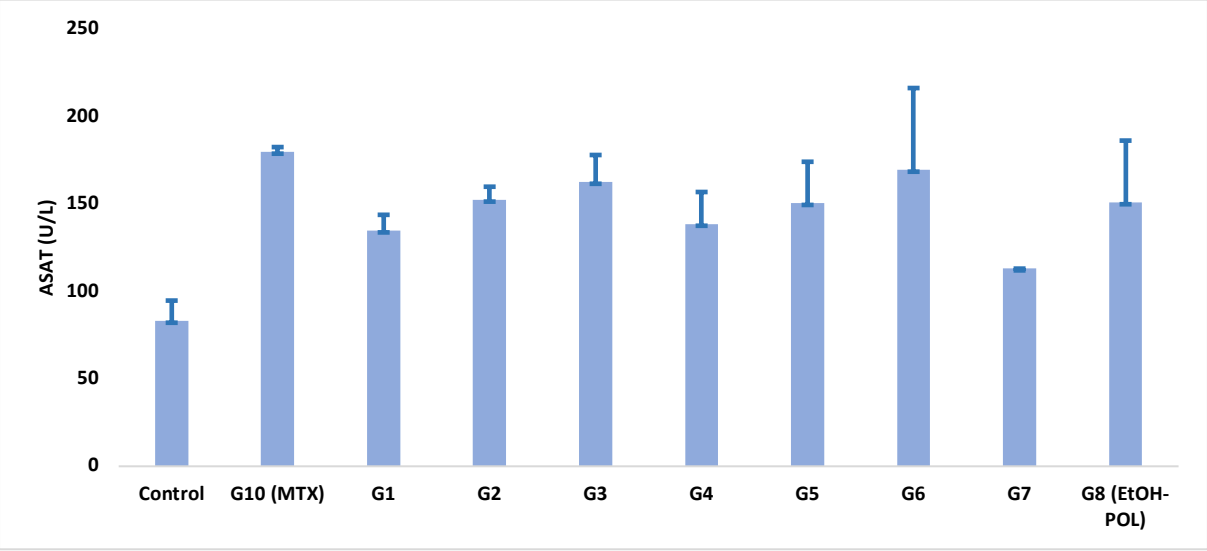

Figure 37: ASAT (U/L) activity in response to treatment: Assessing liver damage of MTX and potential hepatoprotection of THEDESs

Among the THEDESs-treated groups (G1-G7), G7 (113.0 U/L) and G1 (134.7 ±9.05 U/L) demonstrated the lowest ASAT levels, suggesting a stronger hepatoprotective effect.

These values were significantly lower than those in G8 (150.8 ±35.38 U/L), which received the ethanolic extract of *Portulaca oleracea* (POL). Other THEDESs-based groups, such as G4 (138.5 ±18.30 U/L) and G5 (150.4 ±23.68 U/L), also showed lower ASAT levels compared to G8, further reinforcing the advantage of THEDESs formulations.

Statistical analysis reveals that while ANOVA results ($p = 0.067$) suggest a borderline significant difference, Tukey's post-hoc test distinguishes multiple clusters of significance. G7 (113.0 U/L) and G1 (134.7 ±9.05 U/L) were grouped separately from G8 (150.8 ±35.38 U/L), indicating a significantly better hepatoprotective effect of THEDESs formulations. Additionally, G8, G2 (152.3 ±7.51 U/L), and G5 exhibited similar ASAT levels, suggesting that the ethanolic extract provided only moderate protection compared to THEDESs.

In summary, THEDESs-based formulations (particularly in G7 and G1) resulted in a more pronounced reduction in ASAT levels compared to the ethanolic extract (G8), demonstrating enhanced hepatoprotective potential. The ability of THEDESs to stabilize and improve the bioavailability of POL bioactive compounds may contribute to their superior efficacy in mitigating liver damage.

- **Alkaline phosphatase (PAL) and hepatic health**

Alkaline phosphatase (ALP) is a crucial biomarker of hepatobiliary function and can indicate cholestasis or hepatic injury. In this study, ALP levels varied significantly across groups, with the control group exhibiting the lowest level **(**290.00 ±7.90 U/L**),** indicating normal hepatic function. The methotrexate (MTX)-treated group (G10) showed a considerable increase **(**650.30 ±39.76 U/L**),** reflecting significant hepatic dysfunction.`

Among the THEDESs-treated groups (G1-G7), G1 (513.7 ±37.46 U/L) and G7 (567.0 ±36.36 U/L) had the lowest ALP levels, suggesting a strong hepatoprotective effect. These values were significantly lower than those of G8 (806.7 ±172.07 U/L), which received the ethanolic extract of *Portulaca oleracea* (POL), reinforcing the superior efficacy of THEDES formulations. Other THEDESs-based groups, such as G5 (622.0 ±89.74 U/L) and G3 (661.8 ±68.30 U/L), also exhibited reduced ALP levels compared to G8 but remained elevated relative to the control.

Statistical analysis shows that the ANOVA significance level ($p = 0.087$) indicates a trend toward significance, suggesting that treatment effects are substantial but with some variability.

Tukey's post-hoc test reveals distinct subgroupings, with G1 and G7 forming a separate cluster from G8 and other high-ALP groups such as G2 (730.6 ±122.10 U/L), G6 (737.9 ±160.46 U/L), and G4 (741.5 ±25.14 U/L).

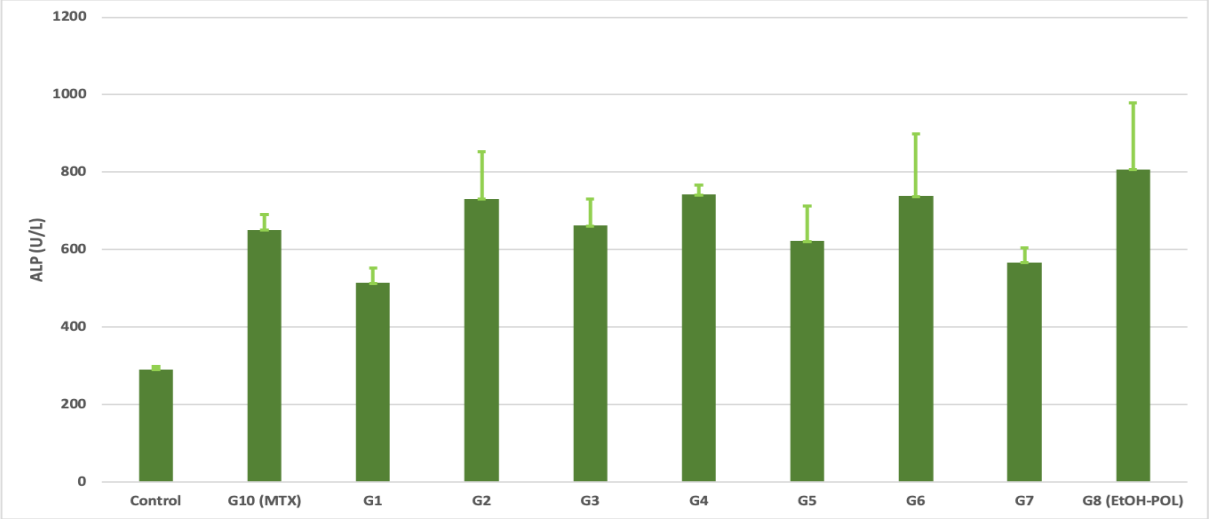

Figure 38: ALP (U/L) variations across treatment groups (THEDESs or EtOH-POL): Insights into liver and biliary function

In summary, THEDESs-based formulations (particularly G1 and G7) resulted in a notable reduction in ALP levels compared to the ethanolic extract (G8), demonstrating improved hepatoprotective potential. These findings suggest that THEDESs may enhance the bioavailability and efficacy of *Portulaca oleracea* bioactive compounds, offering better protection against MTX-induced hepatotoxicity.

- **Gamma-glutamyl transferase GGT (U/L) and its diagnostic relevance**

Gamma-glutamyl transferase (GGT) is a key biomarker for liver damage and oxidative stress. In this study, the control group exhibited the lowest GGT level (9.39 ±1.58 U/L), reflecting normal hepatic function. In contrast, the MTX-treated group (G10) had the highest GGT level (70.32 ±2.20 U/L), indicating significant hepatocellular damage.

Among the THEDESs-treated groups (G1-G7), G1 (50.66 ±2.20 U/L) and G7 (51.20 ±0.68 U/L) had the lowest GGT levels, suggesting a strong hepatoprotective effect. These values were significantly lower than G8 (69.83 ±13.68 U/L), which received the ethanolic extract of *Portulaca oleracea* (POL), reinforcing the superior efficacy of THEDESs formulations. Other THEDESs groups, such as G5 (59.12 ±6.01 U/L), G6 (65.75 ±14.29 U/L),

and G3 (65.83 ±4.28 U/L), exhibited moderate reductions in GGT levels, though they remained elevated compared to G1 and G7.

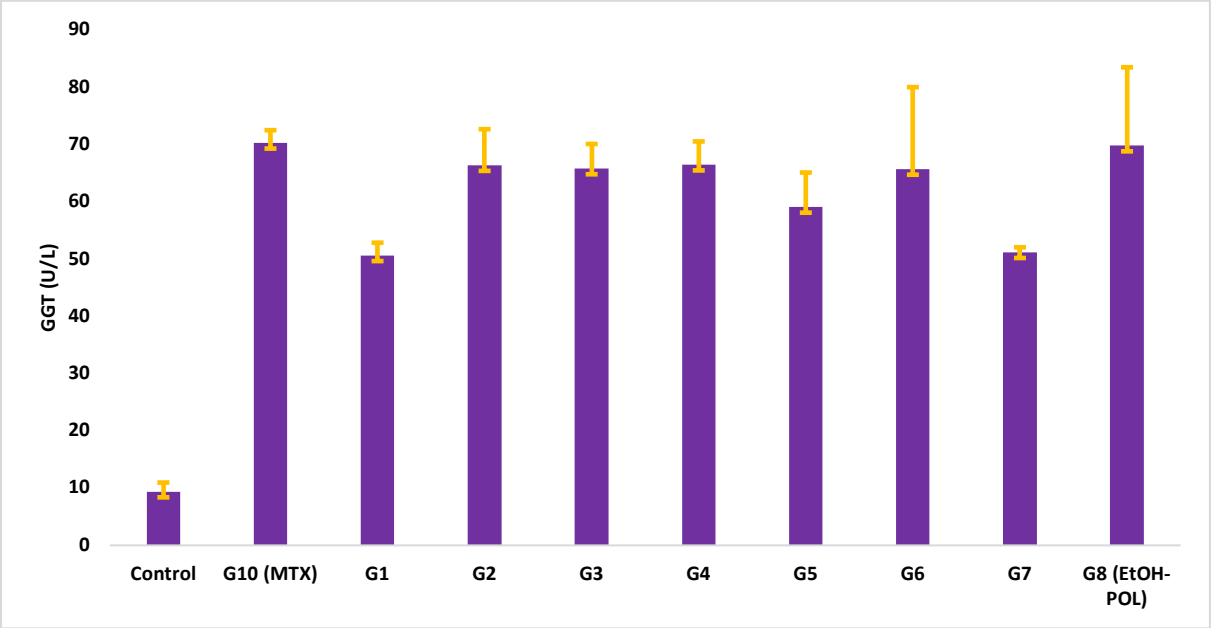

Figure 39: GGT (U/L) levels as a marker of hepatobiliary dysfunction: Protective impact of THEDESs and MTX toxicity

Statistical analysis shows a near-significant ANOVA p-value (0.051) in the second subset, indicating that treatment effects are substantial, though additional replicates may strengthen the statistical power. Tukey's post-hoc test reveals distinct subgroupings:

- G1 and G7 form a separate cluster with the lowest GGT levels, demonstrating strong hepatoprotection.
- G8 and G10 (MTX) exhibit the highest GGT levels, confirming severe hepatic injury.
- Intermediate groups (G5, G6, G3, G2, and G4) show partial protection, but not as effectively as G1 and G7.

In conclusion, THEDESs-based formulations, particularly G1 and G7, significantly reduced GGT levels compared to the ethanolic extract (G8), indicating enhanced hepatoprotection. These findings support the hypothesis that THEDESs improve the bioavailability and efficacy of Portulaca oleracea bioactive compounds, offering superior protection against MTX-induced hepatotoxicity.

- **Bilirubin (mg/L) as an indicator of liver dysfunction**

Bilirubin levels, a key indicator of liver function, were significantly elevated in the MTX-treated group (G10, 25.01 ±0.80 mg/L) compared to the control (3.26 ±0.94 mg/L), confirming severe hepatotoxicity. Among the THEDES-treated groups, G1 (18.15 ±0.82 mg/L) and G7 (18.58 ±0.41 mg/L) exhibited the lowest bilirubin levels, suggesting the strongest hepatoprotective effects. Other THEDESs groups (G5, G3, G6, G2, and G4) showed moderate reductions in bilirubin levels, while the ethanolic extract group (G8, 25.46 ±5.02 mg/L) exhibited bilirubin levels close to those of the MTX-treated group, indicating minimal protection.

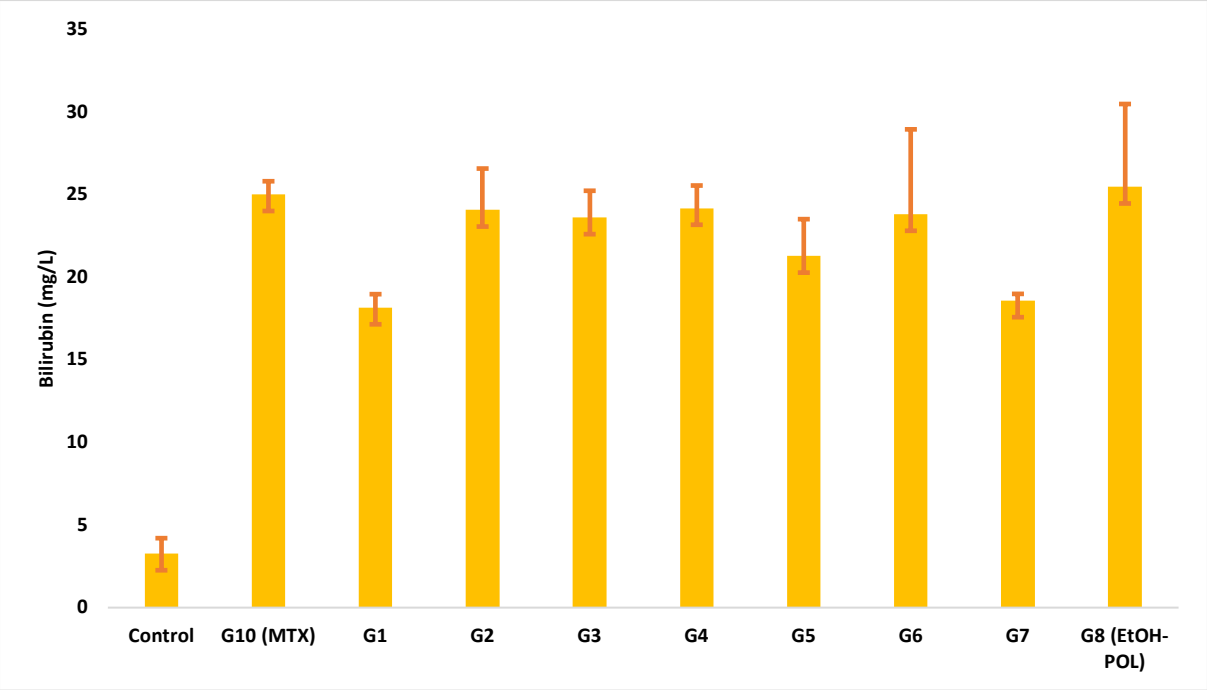

Figure 40: Bilirubin (mg/L) concentration as a liver dysfunction indicator: Protective effects of THEDESs against MTX-Induced toxicity

Statistical analysis revealed distinct subsets, with the control group significantly different from all others. G1 and G7 formed a separate cluster, indicating superior efficacy, while G10 and G8 were grouped at the highest bilirubin levels. These results highlight THEDES, particularly G1 and G7, as promising hepatoprotective formulations against MTX-induced liver damage**.**

Statistical analysis using Tukey's test ($\alpha = 0.05$) identified significant differences between the experimental groups:

The control group (3.26 ±0.94 mg/L) was significantly different from all other groups, forming an isolated subset.

- G1 and G7, which had the lowest bilirubin levels among the treated groups, formed a distinct subset, indicating superior hepatoprotective effects.
- G5, G3, G6, G2, and G4 exhibited intermediate bilirubin levels and shared overlapping subsets, suggesting moderate hepatoprotection.
- G10 (MTX-treated) and G8 (ethanolic extract) had the highest bilirubin levels and were grouped together, indicating that the ethanolic extract did not significantly mitigate MTX-induced hepatotoxicity.

These findings suggest that THEDESs, particularly G1 and G7, offer significant hepatoprotective effects by lowering bilirubin levels in MTX-induced hepatotoxicity. The moderate effects observed in other THEDESs groups indicate varying degrees of protection, while the ethanolic extract (G8) showed little to no benefit. These results highlight the potential of THEDESs as a promising strategy for mitigating liver damage induced by MTX toxicity, with certain formulations (G1 and G7) demonstrating the most protective effects.

- **General conclusion of the study on THEDESs hepatoprotective effects**

This study assessed the hepatoprotective potential of therapeutic deep eutectic systems (THEDESs) against MTX-induced hepatotoxicity, focusing on key hepatic biomarkers: ALAT, ASAT, ALP, GGT, and bilirubin. The findings indicate that THEDESs formulations, particularly G1 and G7, effectively mitigate liver damage, whereas the MTX group (G10) exhibited severe hepatotoxicity.

The analysis of ASAT and ALAT levels, which reflect hepatocellular injury, revealed that MTX administration (G10) caused a significant increase in both enzymes, confirming extensive liver damage. In contrast, THEDESs-treated groups, especially G1 and G7, showed significantly lower ASAT and ALAT levels, suggesting a protective effect on liver cells. Other THEDESs groups (G5, G3, G6, G2, and G4) exhibited moderate hepatoprotection, while the ethanolic extract (G8) failed to prevent the enzymatic elevation, indicating limited efficacy compared to THEDESs formulations.

Similarly, ALP and GGT levels, which are markers of cholestasis and bile duct dysfunction, were markedly elevated in the MTX group (G10), reinforcing the extent of hepatic injury. However, THEDESs-treated groups, particularly G1 and G7, significantly reduced ALP

and GGT levels, indicating preserved bile flow and reduced hepatic stress. Other formulations showed varying degrees of hepatoprotection, whereas G8 failed to counteract the cholestatic effects of MTX.

Regarding bilirubin levels, a marker of liver detoxification capacity, the results showed a significant increase in the MTX group, confirming impaired liver function. THEDESs formulations, mainly G1 and G7, effectively reduced bilirubin levels, suggesting their role in maintaining hepatic clearance mechanisms. In contrast, G8 (ethanolic extract) showed limited efficacy in bilirubin regulation, reinforcing the superiority of THEDESs in stabilizing and delivering bioactive compounds.

- **Overall conclusion**

These findings collectively confirm that THEDESs-based formulations provide substantial hepatoprotection against MTX-induced toxicity, with G1 and G7 emerging as the most effective formulations. Other THEDESs groups exhibited partial protective effects, while the ethanolic extract (G8) failed to prevent liver damage, emphasizing the enhanced bioavailability and stability of THEDESs-formulated bioactive molecules.

These results strongly support THEDESs as a promising hepatoprotective strategy, potentially offering a novel approach for reducing liver toxicity associated with chemotherapeutic agents like MTX. Further studies should explore the mechanistic pathways, long-term efficacy, and potential clinical applications of THEDESs-based hepatoprotective therapies.

5.4 Histological analaysis of liver tissue

5.4.1 Histology observation in control group

The examination of liver tissue architecture in control group typically reveals a normal histological structure, characterized by well-organized hepatocytes and intact sinusoidal spaces. The portal space, in liver tissue refers to the anatomical regions surrounding the portal triads, which include the portal vein, hepatic artery, and bile duct. This area plays a crucial role in liver function and structure, particularly in the context of lymph formation and cellular interactions.

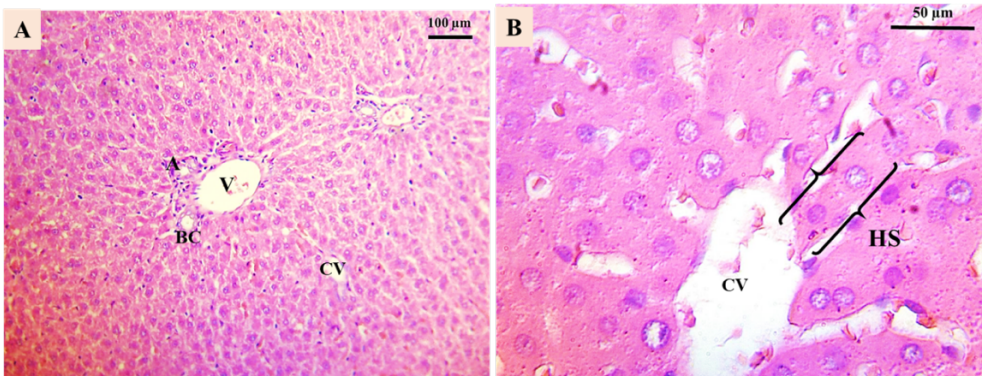

Figure 41: Histological section in control group, CV: central vein V: vein, A: arterial, BC: bile capillary, and HS: hepatocyte slides. Stained with hematoxylin-eosin (HE).

Methotrexate (MTX), an antineoplastic and immunosuppressive drug (Hasan Khudhair et al., 2022), is widely known for its hepatotoxic effects, which manifest through both biochemical and histopathological alterations (Parthasarathy et Prince, 2023). In this study, the impact of MTX-induced liver injury was assessed by evaluating changes in hepatic enzyme levels (ALT, AST, ALP, GGT, and bilirubin) alongside histological observations. A comparative analysis was conducted between the effects of therapeutic deep eutectic solvent-formulated active pharmaceutical ingredients (THEDESs-APIs) and ethanol-based *Portulaca oleracea* leaf extract (EtOH-POL) to determine their hepatoprotective potential.

5.4.2. Histopathological alterations in the MTX-treated group

Administration of MTX at a single dose of 20 mg/kg led to profound structural and functional impairments in liver tissue, as evidenced by multiple histopathological markers of hepatotoxicity:

- **Hepatocyte degeneration and cell death**

Degeneration of hepatocytes was observed, indicating compromised liver function. This was accompanied by cellular shrinkage, nuclear condensation (pyknosis), and apoptotic features, signifying programmed cell death in response to toxic stress (Parthasarathy et Prince, 2023).

- **Periportal inflammation and inflammatory infiltration**

A pronounced inflammatory response was detected, particularly around the portal tracts, as a first spot of drug arrival to the liver, characterized by immune cell infiltration, this same phenomena is observed in all studies related to liver toxicity with MTX (Al Kury et *al*. 2020; Khudhair et *al*. 2022; Parthasarathy and Prince 2023). This suggests an immune-mediated injury following MTX exposure, which can exacerbate hepatic damage as it was once again proved by our study.

- **Sinusoidal congestion and portal vein engorgement**

The liver exhibited significant vascular congestion, particularly within the sinusoids and portal veins (Al Kury et *al*., 2020). This congestion contributes to altered hepatic circulation, impairing oxygen and nutrient supply to hepatocytes, thereby promoting ischemic damage.

- **Kupffer cell activation**

Kupffer cells, the resident liver macrophages, were markedly increased, signifying an active immune response. Their proliferation is indicative of an ongoing detoxification effort against MTX-induced oxidative stress and apoptotic cell debris clearance (Parthasarathy et Prince, 2023).

- **Necrosis and apoptosis**

Necrotic zones were identified within liver lobules, signifying irreversible cell death due to severe mitochondrial and oxidative stress, same alteration was observed in previous studies (Khudhair et *al*., 2022; Parthasarathy et Prince, 2023). Additionally, the presence of apoptotic hepatocytes, as evidenced by nuclear fragmentation and formation of apoptotic bodies as it was also observed in study conducted by (García et *al*., 2019), underscores the cytotoxicity of MTX.

- **Fat droplet accumulation and steatosis**

Some hepatocytes displayed lipid accumulation, it was well known since 2001 throught study conducted by Langman et *al*. (2001), that some metabolic issues, like NAFLD and steatohepatitis could be aggravated by MTX. indicative of MTX-induced steatosis. This metabolic disturbance suggests impaired lipid metabolism. Indeed, inhibition of fatty acid β-oxidation and triglyceride secretion from the liver was identified as mechanism responsible for the MTX-induced steatogenic hepatotoxicity (Lee et *al*., 2008) which can progress into more

severe fatty liver disease if sustained. In results from the MTX-treated group show a real impairment of lipid metabolic in the liver which caused a Grade 3 steatosis with a visible macrovascular fat droplets accumulation and an impairment of about 34 - 66% of the visible hepatocytes.

We have also noted some further signs of hepatotoxicity induced by MTX single dose injection, related to severe liver injury caused and advanced grade of MTX-indiced steatosis.

- **Perinuclear vacuolization:**
  A noticeable presence of cytoplasmic vacuoles surrounding nuclei suggests early degenerative changes, possibly linked to mitochondrial dysfunction and intracellular stress responses.
- **Fibrosis and connective tissue deposition:**
  Prolonged hepatotoxic stress can lead to extracellular matrix deposition, a precursor to fibrosis. While significant fibrotic bands were not the primary observation in this acute setting, early fibrotic changes may indicate the progression toward chronic liver damage.
- **Signet ring cells and binucleation:**
  Some hepatocytes exhibited signet ring morphology, indicative of cytoplasmic lipid accumulation and metabolic stress. Additionally, binucleated hepatocytes were identified, a possible sign of regenerative response following MTX-induced injury.
- **Presence of councilman bodies:**
  The presence of Councilman bodies (eosinophilic apoptotic hepatocytes) confirms extensive hepatocyte apoptosis, reflecting severe hepatocellular stress and dysfunction.

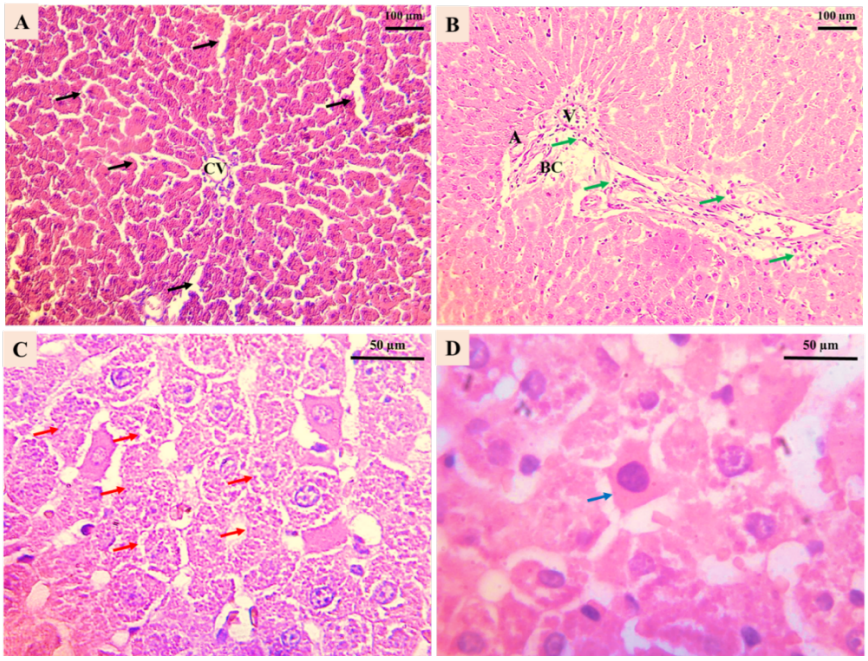

Figure 42: Histopathological section in MTX-treated group, A: Sinusoidal congestion (Black arrow) and CV: central vein, B: Inflammatory infiltration (Green arrow), V: vein, A: Arterial, and BC: Bile capillary, C: Necrosis cells (red arrow), D: Councilman body (Blue arrow). Stained with hematoxylin-eosin (HE).

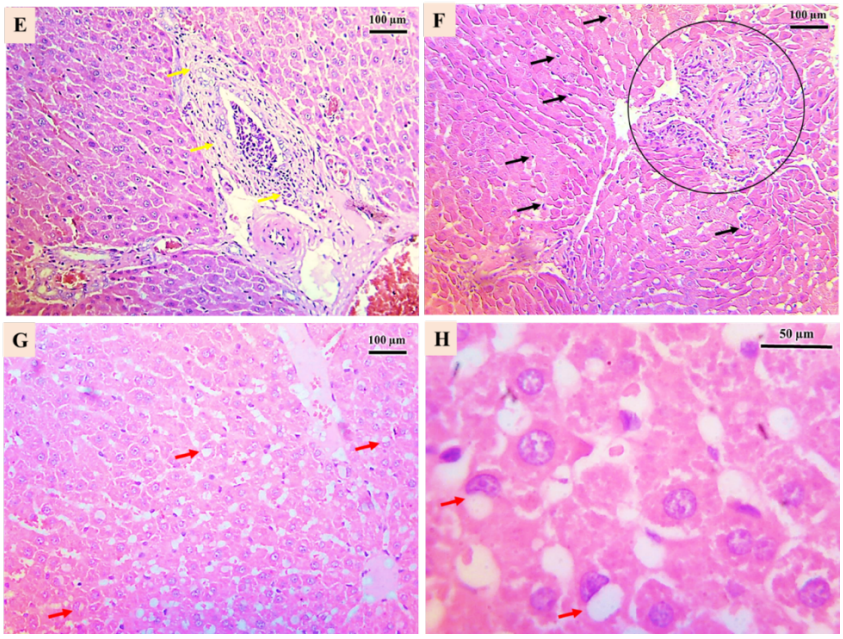

Figure 43: Histopathological section in MTX-treated group, E: Fibrosis around portal space (Yelow arrow), F: Neutralization of necrosis (Cycle), and Kupffer cell activation (Black arrow), G and H: Fat droplet accumulation, steatosis and formation of signet ring cell (Red arrow). Stained with hematoxylin-eosin (HE).

Conclusion

The histopathological findings confirm the severe hepatotoxic potential of MTX, as evidenced by widespread inflammation, vascular congestion, apoptosis, necrosis, and early signs of metabolic dysregulation (steatosis and vacuolization). These results highlight the urgency of hepatoprotective strategies to mitigate MTX-induced liver damage. The comparative evaluation of THEDESs-APIs and EtOH-POL in protecting against these alterations will provide further insights into the therapeutic potential of Portulaca oleracea-based formulations.

5.4.3 Protective effects of experimental treatments on liver tissue

The study also explores the protective effects of POL extracts (Conventional with EtOH and with different NADESs), which showed significant improvements in the evaluated histopathological parameters. Pre-treatment with this herbal extract helped restore normal liver structure and reduce inflammation, indicating its potential as a therapeutic agent against MTX-induced liver damage. Furthermore, we have noticed an evolutive steatosis induced by MTX in G10 (as an MTX-induced toxicity) which was differentiated and visible around a hepatic portal vein. However, this impairment in metabolic function of the liver were less developed in some THDESs treated groups and in some others were definitely inexistant. This, supports more the hypothesis of THEDESs being a great delivery of POL's APIs. As for future perspectives we would test the effect of NADESs on their own (without POL's APIs) to assess their own hepatoprotective effect.

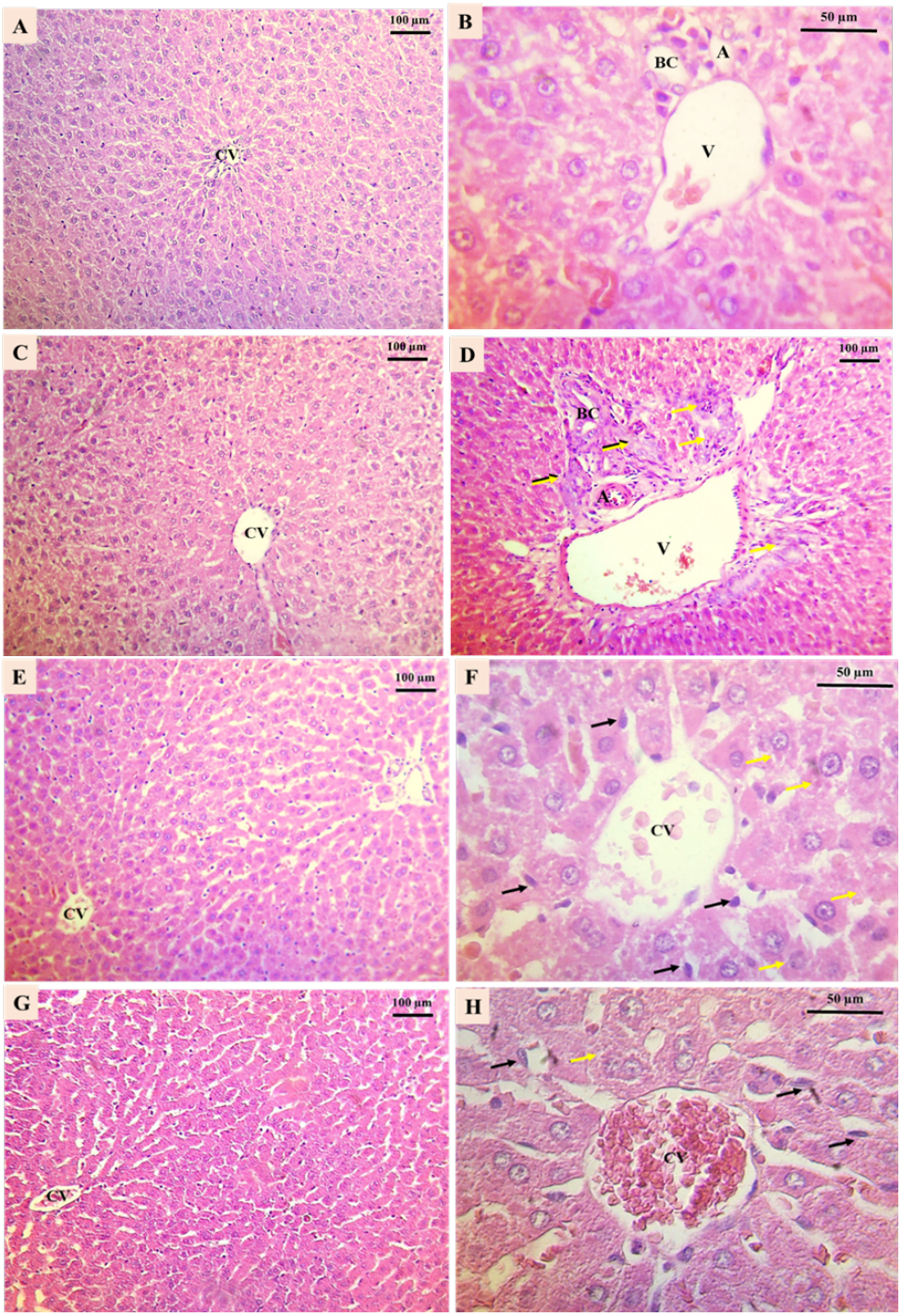

Figure 44: Histopathological section in experimental groups, A and B: Absence of sinusoidal congestion and inflammatory infiltration in G1, C and D: Fibrosis (Yellow arrow) and absence of sinusoidal congestion in G2, E and F: Moderate sinusoidal congestions, Kupffer cell activation (Black arrow) and hepatocytes degeneration (Yellow arrow) in G3, G and H: Moderate sinusoidal congestions, Kupffer cell activation (Black arrow) and hepatocyte degeneration (Yellow arrow) in G4. Stained with hematoxylin-eosin (HE).

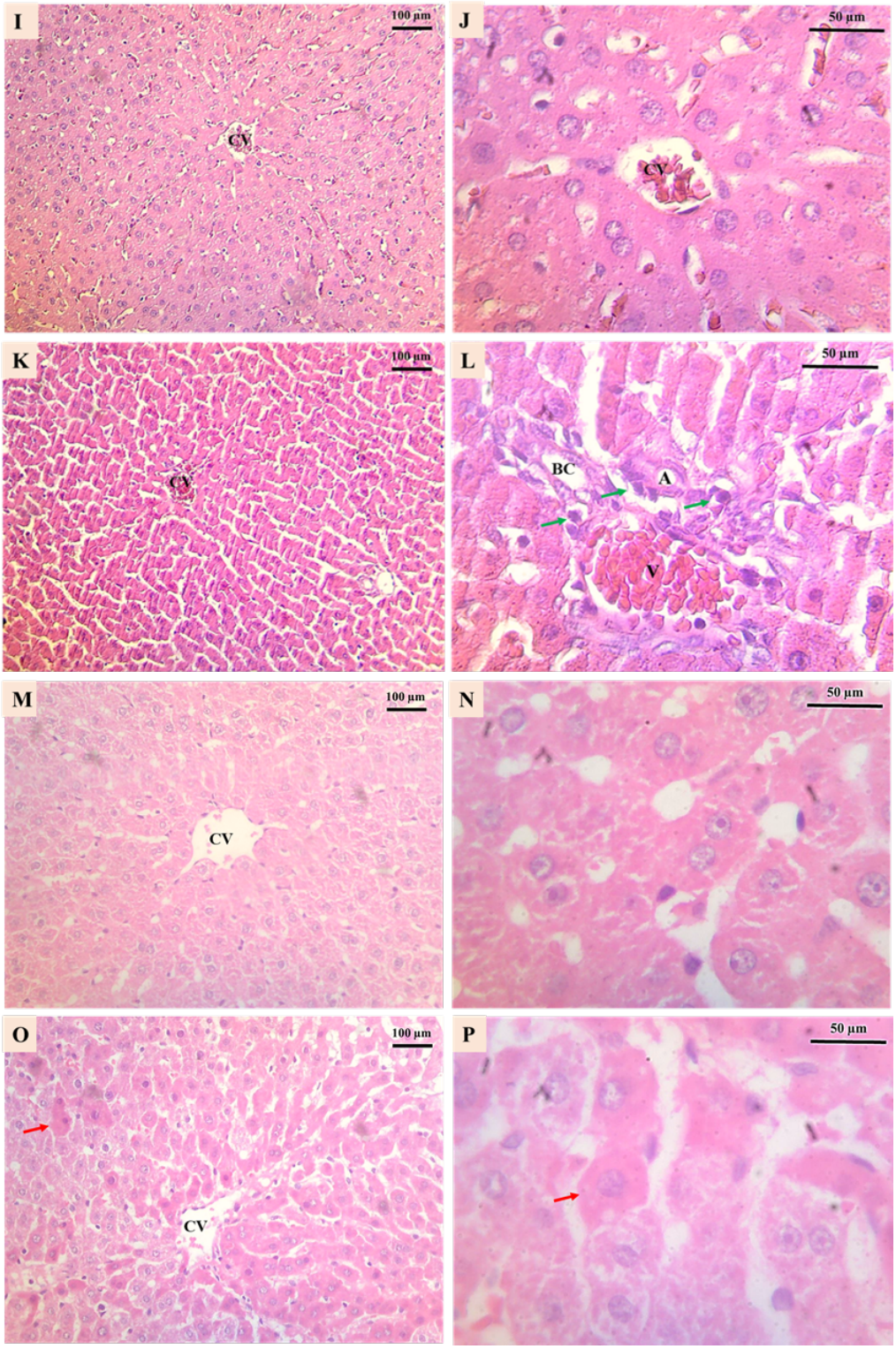

Figure 45: Histopathological section in experimental groups, I and J: Absence of sinusoidal congestion and inflammatory infiltration in G5, K and L: Sever Sinusoidal congestions, and inflammatory infiltration (Green arrow) in G6, M and N: No sinusoidal congestions and no inflammatory infiltration in G7, O and P: Moderate sinusoidal congestions and appearance of councilman body (Red arrow) in G8. Stained with hematoxylin-eosin (HE).

❖ **Possible mechanisms underlying the hepatoprotective effect of THEDESs against MTX-induced hepatotoxicity**

Methotrexate (MTX) is well known for its hepatotoxic effects, primarily through oxidative stress, mitochondrial dysfunction, and inflammation, leading to steatosis, apoptosis, sinusoidal congestion, and fibrosis. The findings suggest that certain THEDESs formulations, particularly THEDESs 1, 3, 4, and 7, exhibit strong hepatoprotective effects, while others (THEDESs 2, 5, and 6) display varying degrees of residual toxicity. The potential mechanisms underlying these protective effects are discussed below.

- **Reduction of steatosis: Modulation of lipid metabolism**

MTX disrupts lipid metabolism, leading to macro-vesicular steatosis due to impaired mitochondrial β-oxidation (Ezhilarasan, 2021). THEDESs formulations, particularly THEDESs 1, 3, 4 and 7, which completely prevented steatosis, likely achieved this by enhancing fatty acid oxidation via PPAR-α activation. The presence of terpenoids and flavonoids in the POL extracts within THEDESs may contribute to this effect by regulating lipid metabolism and reducing lipid accumulation, the enhancement of lipid profile by POL extracts was mentioned previously (Mohamed et *al*., 2019), besides some bioactive compounds detected in THEDESs studied here, like coumaric acid, were shown in a recent study ti have role in modulating lipid metabolism. It can decrease lipid accumulation in the liver (Yuan et *al.* 2023).

- **Prevention of apoptosis and necrosis: Antioxidant and mitochondrial protection**

MTX-induced oxidative stress triggers mitochondrial damage, leading to hepatocyte apoptosis and necrosis (Khudhair et *al*., 2022; Parthasarathy et Prince, 2023). The THEDESs formulations exhibited strong antioxidant effects, preventing apoptosis and necrosis by neutralizing reactive oxygen species (ROS). Flavonoids and betalains in POL extracts likely contributed to mitochondrial stabilization, with THEDESs 1, 3, 4, and 7 completely preventing apoptosis and necrosis, suggesting potent mitochondrial protection. Those THEDESs are characterized with their highest yields with coumaric and feruls acids. Coumaric acid has been shown to enhance the antioxidant capacity of liver tissues (Parvizi et *al*., 2020) while has been shown to protect liver cells by inhibiting oxidative stress and inflammation (J. Wu et *al*., 2021) and mitigate liver damage induced by various drugs (Shi et *al.*, 2023). In contrast, THEDES 2

displayed some residual necrosis, indicating a slightly lower antioxidant potency *in-vivo,* most probably due to its higher ratio of lactic acid incorporated in the formulation of the vehicle.

- **Reduction of sinusoidal congestion: Endothelial and anti-inflammatory effects**

MTX-induced sinusoidal endothelial dysfunction leads to congestion and vascular stress. The complete prevention of congestion by THEDESs 1, 4, and 7 suggests that these formulations may enhance endothelial function, possibly through nitric oxide (NO) modulation, Purslane extract has been shown to inhibit NO production by reducing the expression of inducible nitric oxide synthase (iNOS) (Ullah et *al.* 2021). POL extract exhibits anti-inflammatory properties by reducing the production of pro-inflammatory cytokines such as tumor necrosis factor-alpha (TNF-α) and interleukins (IL-1β, IL-6) (Baradaran Rahimi et al., 2019). Flavonoids extracted from *Portulaca oleracea* (POL-F) have been found to suppress NO secretion by modulating specific signaling pathways (Milkarizi et *al*., 2024) . Conversely, THEDESs 5 and 6 exhibited residual congestion, suggesting that while effective in lipid metabolism regulation, they may be less potent in vascular protection.

- **Prevention of fibrosis and portal inflammation: Anti-inflammatory and antifibrotic effects**

MTX promotes fibrosis through hepatic stellate cell (HSC) activation and TGF-β1 signaling (Ezhilarasan, 2021). The THEDESs formulations showed significant antifibrotic activity, with THEDESs 1, 4, 5, 6, and 7 completely preventing fibrosis, urslane has demonstrated antifibrotic properties in the liver by reducing the expression of profibrogenic cytokines and decreasing collagen deposition (Milkarizi et *al*., 2024). However, THEDESs 2 and 3 exhibited mild residual fibrosis, indicating a relatively lower antifibrotic effect. The suppression of portal inflammation further suggests a strong immunomodulatory role of THEDESs, The extract of POL also decreases the expression of cyclooxygenase-2 (COX-2), an enzyme linked to inflammation, as mentioned in literature (Ullah et *al*., 2021), possibly mediated by flavonoid-driven inhibition of pro-inflammatory cytokines, for the fact the THEDESs in our study have shown the highest yield of quercetine and rutin.

Quercetin has been shown to modulate inflammation by inhibiting the activation of inflammasomes, such as NLRP3 and AIM2, in macrophages. This inhibition leads to a

reduction in the release of pro-inflammatory cytokines, thereby attenuating inflammatory responses (Xiong et *al*., 2024). Additionally, quercetin has been reported to suppress the production of tumor necrosis factor-alpha (TNF-α) and interleukins (IL-1α, IL-6), which are key mediators in the inflammatory process (Aghababaei and Hadidi 2023).

As for Rutin, a glycoside of quercetin, has demonstrated potential preventive effects against drug-induced hepatotoxicity. In studies involving doxorubicin-induced liver injury in rats, rutin administration resulted in significant improvements in liver enzyme levels and histological architecture. These protective effects are attributed to rutin's ability to inhibit oxidative stress, inflammation, and apoptosis in hepatic tissues (Ahmed et *al.,* 2022).

Conclusion

The hepatoprotective efficacy of THEDESs formulations appears to be linked to their ability to stabilize and deliver POL bioactive compounds effectively. As showed in figure 46, the most protective formulations (THEDESs 1, 3, 4, and 7) exhibited robust antioxidant, anti-inflammatory, endothelial-protective, and antifibrotic properties and showed and excellent preventive effect against steatosis. Conversely, THEDESs 5 and 6 failed in preventing steatosis and were less effective against sinusoidal congestion. THEDES 2, which showed residual fibrosis and necrosis, displayed the weakest protective profile. These findings highlight the importance of optimizing NADESs composition to maximize hepatoprotection, particularly in vascular, antifibrotic responses and prevention of drug-induced hepatic steatosis.

	MTX	THEDES 1	THEDES 2	THEDES 3	THEDES 4	THEDES 5	THEDES 6	THEDES 7
Steatosis	Grade 2 34 - 66%	O	Grade 1 5 - 33%	O	O	Grade 0 < 5%	Grade 0 < 5%	O
Apoptosis	X	O	O	O	O	O	O	O
Sinusooidal Congestion	X	O	X	X	O	Moderate	Acute	X
Portal inflammation	Sever	O	X	O	X	X	O	O
Necrosis	X	O	X	O	O	O	O	O
Perinuclear vacuolization	X	O	O	O	O	X	X	O
Fibrosis	X	O	X	O	O	O	O	O

Figure 46 : Comparative analysis of MTX-induced hepatotoxicity and the hepatoprotective effect of THEDESs

Conclusion and perspectives

This thesis explored the relationship between viscosity and hydrogen bonding interactions in terpene-based NADESs using molecular dynamics (MD) simulations and quantum chemistry (QC). Our findings provide fundamental insights into the structural organization and rheological behavior of these eutectic systems, with direct implications for their application in the extraction, stabilization, and therapeutic delivery of bioactive compounds.

The structural analysis revealed that NADESs can be classified into single-site and multisite systems, with single-site systems further divided into terpene-acid-based and terpene-terpene-based NADESs. The viscosity of these systems was found to be closely correlated with the product of hydrogen bond number and lifetime, indicating that both the quantity and stability of hydrogen bonding interactions influence the overall viscosity of the eutectic mixtures. Notably, terpene-acid-based NADESs exhibited lower viscosity due to weak and transient hydrogen bonding, whereas terpene-terpene-based systems displayed more stable interactions, leading to higher viscosity.

Further investigation into the hydrogen bond donor (HBD) and hydrogen bond acceptor (HBA) behavior of different terpenoids demonstrated that alkenyl alcohol- and ketone-based terpenoids primarily act as HBAs, whereas phenol-based terpenoids function predominantly as HBDs. Viscosity trends were also influenced by the molecular composition of NADESs, as evidenced by the significantly higher viscosity of lauric acid-based mixtures compared to their capric acid counterparts. This difference, up to 300-fold, was attributed to enhanced van der Waals forces and non-bonded interaction energy.

Beyond rheological properties, this study underscored the critical role of hydrogen bonding interactions in determining the extraction efficiency and stabilization of bioactive compounds. The selection of optimal NADESs compositions and molar ratios significantly influenced the extraction yield, particularly for phenolic compounds and flavonoids in comparison to conventional solvents like ethanol. Such findings offer valuable guidance for the rational design of NADES to enhance green and sustainable extraction processes. In particular, the combination of menthol and lactic acid in NADES1 and NADES2 showed remarkable potential for stabilizing antioxidants, making these solvents promising candidates for applications in food, cosmetics, and pharmaceuticals.

Additionally, NADESs demonstrated antimicrobial potential, with extraction efficiency and efficacy varying depending on the type of microorganism targeted. These results emphasize the need for precise selection of NADESs-plant extract combinations to optimize antimicrobial activity.

A key aspect of this research was the evaluation of the anticancer potential of NADESs and THEDESs. *In vitro* studies against gastric cancer cell lines at varying concentrations revealed a significant dose-dependent effect, particularly between 0.075% and higher concentrations. However, beyond 0.10%, no additional cytotoxic benefit was observed, suggesting a saturation effect in some cases. These results highlight the therapeutic potential of THEDESs as an effective drug delivery system, although further mechanistic studies such as apoptosis assays, caspase activation analysis, and oxidative stress markers are required to elucidate the precise pathways underlying the observed cytotoxic effects.

To ensure the safe pharmaceutical application of NADESs as a vehicle of active pharmaceutical ingredients (APIs), a toxicological assessment was conducted through acute dose escalation toxicity. The results demonstrated that while certain NADESs formulations exhibited promising safety profiles, others displayed dose-dependent toxicity, highlighting the necessity for careful selection based on intended biomedical applications. Future research should focus on understanding the specific toxicological mechanisms involved, including histopathological analyses, biochemical markers of organ damage, and pharmacokinetic profiling. Long-term toxicity studies will also be crucial for assessing potential accumulation or delayed adverse effects.

Building upon these insights, we developed and tested a THEDESs-based formulation incorporating bioactive compounds from *Portulaca oleracea* leaves (POL) for hepatoprotection against methotrexate (MTX)-induced liver injury. The results were highly promising, confirming that THEDESs significantly mitigated MTX-induced hepatotoxicity, with certain formulations (G1 and G7) providing the most effective protection. Other THEDESs formulations exhibited partial protective effects, while the ethanolic extract (G8) failed to prevent liver damage, highlighting the enhanced bioavailability and stability conferred by THEDESs-based delivery, besides most THEDESs succeeded in preventing hepatic steatosis. These findings support the potential of THEDESs as a novel hepatoprotective strategy, offering a promising approach for reducing liver toxicity associated with chemotherapy. Future studies

should focus on elucidating the precise mechanistic pathways, evaluating long-term efficacy, and exploring potential clinical applications of THEDES-based hepatoprotective therapies.

Overall, this research contributes to the growing body of knowledge on NADESs and THEDESs, providing a fundamental understanding of their physicochemical properties, biological applications, and safety profiles. The insights gained from this study not only advance the development of low-viscosity NADESs for efficient bioactive extraction but also highlight the therapeutic potential of THEDESs in drug delivery and hepatoprotection. Future work should continue refining these systems to enhance their applicability in pharmaceutical, nutraceutical, and biomedical fields, ensuring both efficacy and safety in their use.

References

Bibliographies References

Abdullaev, F. I. (2002). Cancer Chemopreventive and Tumoricidal Properties of Saffron (Crocus sativus L.). *Experimental Biology and Medicine*, *227*(1), 20–25. https://doi.org/10.1177/153537020222700104

Abedin, R., Shen, Y., Flake, J. C., & Hung, F. R. (2020). Deep Eutectic Solvents Mixed with Fluorinated Refrigerants for Absorption Refrigeration: A Molecular Simulation Study. *The Journal of Physical Chemistry B*, *124*(22), 4536–4550. https://doi.org/10.1021/acs.jpcb.0c01860

Abegaz, B. M., Mutanyatta-Comar, J., & Nindi, M. (2007). Naturally Occurring Homoisoflavonoids: Phytochemistry, Biological Activities and Synthesis. *Natural Product Communications*, *2*(4). https://doi.org/10.1177/1934578X0700200418

Abranches, D. O., Martins, M. A. R., Silva, L. P., Schaeffer, N., Pinho, S. P., & Coutinho, J. A. P. (2019). Phenolic hydrogen bond donors in the formation of non-ionic deep eutectic solvents: the quest for type V DES. *Chemical Communications*, *55*(69), 10253–10256. https://doi.org/10.1039/C9CC04846D

Aghababaei, F., & Hadidi, M. (2023). Recent Advances in Potential Health Benefits of Quercetin. *Pharmaceuticals*, *16*(7), 1020. https://doi.org/10.3390/ph16071020

Aguilar, J. A., Zavala, A. N., Díaz-Pérez, C., Cervantes, C., Díaz-Pérez, A. L., & Campos-García, J. (2006). The *atu* and *liu* Clusters Are Involved in the Catabolic Pathways for Acyclic Monoterpenes and Leucine in *Pseudomonas aeruginosa*. *Applied and Environmental Microbiology*, *72*(3), 2070–2079. https://doi.org/10.1128/AEM.72.3.2070-2079.2006

Ahmad, W., Ansari, M. A., Yusuf, M., Amir, M., Wahab, S., Alam, P., Alomary, M. N., Alhuwayri, A. A., Khan, M., Ali, A., Warsi, M. H., Ashraf, K., & Ali, M. (2022). Antibacterial, Anticandidal, and Antibiofilm Potential of Fenchone: In Vitro, Molecular Docking and In Silico/ADMET Study. *Plants*, *11*(18), 2395. https://doi.org/10.3390/plants11182395

Ahmed, O. M., Elkomy, M. H., Fahim, H. I., Ashour, M. B., Naguib, I. A., Alghamdi, B. S., Mahmoud, H. U. R., & Ahmed, N. A. (2022). Rutin and Quercetin Counter Doxorubicin-Induced Liver Toxicity in Wistar Rats via Their Modulatory Effects on Inflammation, Oxidative Stress, Apoptosis, and Nrf2. *Oxidative Medicine and Cellular Longevity*, *2022*, 2710607. https://doi.org/10.1155/2022/2710607

Al Aboody, M. S., & Mickymaray, S. (2020). Anti-Fungal Efficacy and Mechanisms of Flavonoids. *Antibiotics*, *9*(2), 45. https://doi.org/10.3390/antibiotics9020045

Al Kury, L. T., Dayyan, F., Ali Shah, F., Malik, Z., Khalil, A. A. K., Alattar, A., Alshaman, R., Ali, A., & Khan, Z. (2020). Ginkgo biloba Extract Protects against Methotrexate-Induced Hepatotoxicity: A Computational and Pharmacological Approach. *Molecules*, *25*(11), 2540. https://doi.org/10.3390/molecules25112540

Al-Akayleh, F., Khalid, R. M., Hawash, D., Al-Kaissi, E., Al-Adham, I. S. I., Al-Muhtaseb, N., Jaber, N., Al-Remawi, M., & Collier, P. J. (2022). Antimicrobial potential of natural deep eutectic solvents. *Letters in Applied Microbiology*, *75*(3), 607–615. https://doi.org/10.1111/lam.13699

Ali, S. I., Said, M. M., & Mohammed Hassan, E. K. (2011). Prophylactic and curative effects of purslane on bile duct ligation-induced hepatic fibrosis in albino rats. *Annals of Hepatology*, *10*(3), 340–346. https://doi.org/10.1016/S1665-2681(19)31547-9

Ali-Rachedi, F., Meraghni, S., Touaibia, N., & Mesbah, S. (2018). Analyse quantitative des composés phénoliques d'une endémique algérienne Scabiosa Atropurpurea sub. Maritima L. *Bulletin de La Société Royale Des Sciences de Liège*, 13 – 21. https://doi.org/10.25518/0037-9565.7398

Alkhatib, I. I. I., Bahamon, D., Llovell, F., Abu-Zahra, M. R. M., & Vega, L. F. (2020). Perspectives and guidelines on thermodynamic modelling of deep eutectic solvents. *Journal of Molecular Liquids*, *298*, 112183. https://doi.org/10.1016/j.molliq.2019.112183

Alonso, D. A., Baeza, A., Chinchilla, R., Guillena, G., Pastor, I. M., & Ramón, D. J. (2016). Deep Eutectic Solvents: The Organic Reaction Medium of the Century. *European Journal of Organic Chemistry*, *2016*(4), 612–632. https://doi.org/10.1002/ejoc.201501197

Alsaud, N., Shahbaz, K., & Farid, M. (2021). Antioxidant and antibacterial evaluation of Manuka leaves (Leptospermum scoparium) extracted by hydrophobic deep eutectic solvent. *Chemical Engineering Research and Design*, *174*, 96–106. https://doi.org/10.1016/j.cherd.2021.08.004

Anjos, P. J. C., Lima, A. O., Cunha, P. S., De Sousa, D. P., Onofre, A. S. C., Ribeiro, T. P., Medeiros, I. A., Antoniolli, Â. R., Quintans-Júnior, L. J., & Santos, M. R. V. (2013). Cardiovascular Effects Induced by Linalool in Normotensive and Hypertensive Rats. *Zeitschrift Für Naturforschung C*, *68*(5–6), 181–190. https://doi.org/10.1515/znc-2013-5-603

Aqil, M., Ahad, A., Sultana, Y., & Ali, A. (2007a). Status of terpenes as skin penetration enhancers. *Drug Discovery Today*, *12*(23–24), 1061–1067. https://doi.org/10.1016/j.drudis.2007.09.001

Aqil, M., Ahad, A., Sultana, Y., & Ali, A. (2007b). Status of terpenes as skin penetration enhancers. *Drug Discovery Today*, *12*(23–24), 1061–1067. https://doi.org/10.1016/j.drudis.2007.09.001

Asia N Rashed, Fatma Afifi, Mayadah Shehadeh, & Mutasem Omar Taha. (2004). Investigation of the active constituents of Portulaca oleraceae L. (Portulacaceae) growing in Jordan. *Pakistan Journal of Pharmaceutical Sciences*, *17*(1), 37–45.

Astani, A., & Schnitzler, P. (2014). Antiviral activity of monoterpenes beta-pinene and limonene against herpes simplex virus in vitro. *Iranian Journal of Microbiology*, *6*(3), 149–155.

Baer-Dubowska, W., Szaefer, H., Majchrzak-Celińska, A., & Krajka-Kuźniak, V. (2020). Tannic Acid: Specific Form of Tannins in Cancer Chemoprevention and Therapy-Old and New Applications. *Current Pharmacology Reports*, *6*(2), 28–37. https://doi.org/10.1007/s40495-020-00211-y

Bajkacz, S., & Adamek, J. (2017). Evaluation of new natural deep eutectic solvents for the extraction of isoflavones from soy products. *Talanta*, *168*, 329–335. https://doi.org/10.1016/j.talanta.2017.02.065

Bakirtzi, C., Triantafyllidou, K., & Makris, D. P. (2016). Novel lactic acid-based natural deep eutectic solvents: Efficiency in the ultrasound-assisted extraction of antioxidant polyphenols from common native Greek medicinal plants. *Journal of Applied Research on Medicinal and Aromatic Plants*, *3*(3), 120–127. https://doi.org/10.1016/j.jarmap.2016.03.003

Baradaran Rahimi, V., Rakhshandeh, H., Raucci, F., Buono, B., Shirazinia, R., Samzadeh Kermani, A., Maione, F., Mascolo, N., & Askari, V. (2019). Anti-Inflammatory and Anti-Oxidant Activity of Portulaca oleracea Extract on LPS-Induced Rat Lung Injury. *Molecules*, *24*(1), 139. https://doi.org/10.3390/molecules24010139

Bassan, A., Alves, V. M., Amberg, A., Anger, L. T., Beilke, L., Bender, A., Bernal, A., Cronin, M. T. D., Hsieh, J.-H., Johnson, C., Kemper, R., Mumtaz, M., Neilson, L., Pavan, M., Pointon, A., Pletz, J., Ruiz, P., Russo, D. P., Sabnis, Y., … Myatt, G. J. (2021). In silico approaches in organ toxicity hazard assessment: Current status and future needs for predicting heart, kidney and lung toxicities. *Computational Toxicology (Amsterdam, Netherlands)*, *20*. https://doi.org/10.1016/j.comtox.2021.100188

Bedair, H. M., Samir, T. M., & Mansour, F. R. (2024). Antibacterial and antifungal activities of natural deep eutectic solvents. *Applied Microbiology and Biotechnology*, *108*(1), 198. https://doi.org/10.1007/s00253-024-13044-2

Bi, W., Tian, M., & Row, K. H. (2013). Evaluation of alcohol-based deep eutectic solvent in extraction and determination of flavonoids with response surface methodology optimization. *Journal of Chromatography A*, *1285*, 22–30. https://doi.org/10.1016/j.chroma.2013.02.041

Bosiljkov, T., Dujmić, F., Cvjetko Bubalo, M., Hribar, J., Vidrih, R., Brnčić, M., Zlatic, E., Radojčić Redovniković, I., & Jokić, S. (2017). Natural deep eutectic solvents and ultrasound-assisted extraction: Green approaches for extraction of wine lees anthocyanins. *Food and Bioproducts Processing*, *102*, 195–203. https://doi.org/10.1016/j.fbp.2016.12.005

Bouyahya, A., Mechchate, H., Benali, T., Ghchime, R., Charfi, S., Balahbib, A., Burkov, P., Shariati, M. A., Lorenzo, J. M., & Omari, N. El. (2021). Health Benefits and Pharmacological Properties of Carvone. *Biomolecules*, *11*(12), 1803. https://doi.org/10.3390/biom11121803

Bryant, S. J., Awad, M. N., Elbourne, A., Christofferson, A. J., Martin, A. V., Meftahi, N., Drummond, C. J., Greaves, T. L., & Bryant, G. (2022). Deep eutectic solvents as cryoprotective agents for mammalian cells. *Journal of Materials Chemistry B*, *10*(24), 4546–4560. https://doi.org/10.1039/D2TB00573E

Cajnko, M. M., Vicente, F. A., Novak, U., & Likozar, B. (2023). Natural deep eutectic solvents (NaDES): translating cell biology to processing. *Green Chemistry*, *25*(22), 9045–9062. https://doi.org/10.1039/D3GC01913F

Can Baser, K. (2008). Biological and Pharmacological Activities of Carvacrol and Carvacrol Bearing Essential Oils. *Current Pharmaceutical Design*, *14*(29), 3106–3119. https://doi.org/10.2174/138161208786404227

Cao, J., Chen, L., Li, M., Cao, F., Zhao, L., & Su, E. (2018). Two-phase systems developed with hydrophilic and hydrophobic deep eutectic solvents for simultaneously extracting various bioactive compounds with different polarities. *Green Chemistry*, *20*(8), 1879–1886. https://doi.org/10.1039/C7GC03820H

Carson, C. F., & Riley, T. V. (1995). Antimicrobial activity of the major components of the essential oil of *Melaleuca alternifolia*. *Journal of Applied Bacteriology*, *78*(3), 264–269. https://doi.org/10.1111/j.1365-2672.1995.tb05025.x

Castelli, M. V., & López, S. N. (2017). *Homoisoflavonoids: Occurrence, Biosynthesis, and Biological Activity* (pp. 315–354). https://doi.org/10.1016/B978-0-444-63929-5.00009-7

Cazarolli, L., Zanatta, L., Alberton, E., Bonorino Figueiredo, M. S., Folador, P., Damazio, R., Pizzolatti, M., & Barreto Silva, F. R. (2008). Flavonoids: Prospective Drug Candidates. *Mini-Reviews in Medicinal Chemistry*, *8*(13), 1429–1440. https://doi.org/10.2174/138955708786369564

Chagas, M. do S. S., Behrens, M. D., Moragas-Tellis, C. J., Penedo, G. X. M., Silva, A. R., & Gonçalves-de-Albuquerque, C. F. (2022). Flavonols and Flavones as Potential anti-Inflammatory, Antioxidant, and Antibacterial Compounds. *Oxidative Medicine and Cellular Longevity*, *2022*, 9966750. https://doi.org/10.1155/2022/9966750

Chandrasekara, A. (2019). Phenolic Acids. In *Encyclopedia of Food Chemistry* (pp. 535–545). Elsevier. https://doi.org/10.1016/B978-0-08-100596-5.22395-0

Chang, M.-Y., & Shen, Y.-L. (2014). Linalool Exhibits Cytotoxic Effects by Activating Antitumor Immunity. *Molecules*, *19*(5), 6694–6706. https://doi.org/10.3390/molecules19056694

Chen, S., Zeng, Z., Hu, N., Bai, B., Wang, H., & Suo, Y. (2018). Simultaneous optimization of the ultrasound-assisted extraction for phenolic compounds content and antioxidant activity of Lycium ruthenicum Murr. fruit using response surface methodology. *Food Chemistry*, *242*, 1–8. https://doi.org/10.1016/j.foodchem.2017.08.105

CHEN, W., XUE, Z., WANG, J., JIANG, J., ZHAO, X., & MU, T. (2018). Investigation on the Thermal Stability of Deep Eutectic Solvents. *Acta Physico-Chimica Sinica*, *34*(8), 904–911. https://doi.org/10.3866/PKU.WHXB201712281

CHERNG, J.-M., SHIEH, D.-E., CHIANG, W., CHANG, M.-Y., & CHIANG, L.-C. (2007). Chemopreventive Effects of Minor Dietary Constituents in Common Foods on Human Cancer Cells. *Bioscience, Biotechnology, and Biochemistry*, *71*(6), 1500–1504. https://doi.org/10.1271/bbb.70008

Choi, Y. H., & Verpoorte, R. (2019). Green solvents for the extraction of bioactive compounds from natural products using ionic liquids and deep eutectic solvents. *Current Opinion in Food Science*, *26*, 87–93. https://doi.org/10.1016/j.cofs.2019.04.003

Constant, S., Huang, S., Wiszniewski, L., & Mas, C. (2013). Colon Cancer: Current Treatments and Preclinical Models for the Discovery and Development of New Therapies. In *Drug Discovery*. InTech. https://doi.org/10.5772/53391

Cordeiro, T., Castiñeira, C., Mendes, D., Danède, F., Sotomayor, J., Fonseca, I. M., Gomes da Silva, M., Paiva, A., Barreiros, S., Cardoso, M. M., Viciosa, M. T., Correia, N. T., &

Dionisio, M. (2017). Stabilizing Unstable Amorphous Menthol through Inclusion in Mesoporous Silica Hosts. *Molecular Pharmaceutics*, *14*(9), 3164–3177. https://doi.org/10.1021/acs.molpharmaceut.7b00386

Cornmell, R. J., Winder, C. L., Tiddy, G. J. T., Goodacre, R., & Stephens, G. (2008). Accumulation of ionic liquids in Escherichia coli cells. *Green Chemistry*, *10*(8), 836. https://doi.org/10.1039/b807214k

Cox, S. D., & Markham, J. L. (2007). Susceptibility and intrinsic tolerance of *Pseudomonas aeruginosa* to selected plant volatile compounds. *Journal of Applied Microbiology*, *103*(4), 930–936. https://doi.org/10.1111/j.1365-2672.2007.03353.x

Cushnie, T. P. T., & Lamb, A. J. (2011). Recent advances in understanding the antibacterial properties of flavonoids. *International Journal of Antimicrobial Agents*, *38*(2), 99–107. https://doi.org/10.1016/j.ijantimicag.2011.02.014

Cvjetko Bubalo, M., Ćurko, N., Tomašević, M., Kovačević Ganić, K., & Radojčić Redovniković, I. (2016). Green extraction of grape skin phenolics by using deep eutectic solvents. *Food Chemistry*, *200*, 159–166. https://doi.org/10.1016/j.foodchem.2016.01.040

Dai, Y., van Spronsen, J., Witkamp, G.-J., Verpoorte, R., & Choi, Y. H. (2013a). Natural deep eutectic solvents as new potential media for green technology. *Analytica Chimica Acta*, *766*, 61–68. https://doi.org/10.1016/j.aca.2012.12.019

Dai, Y., van Spronsen, J., Witkamp, G.-J., Verpoorte, R., & Choi, Y. H. (2013b). Natural deep eutectic solvents as new potential media for green technology. *Analytica Chimica Acta*, *766*, 61–68. https://doi.org/10.1016/j.aca.2012.12.019

Darvish Damavandi, R., Shidfar, F., Najafi, M., Janani, L., Masoodi, M., Akbari-Fakhrabadi, M., & Dehnad, A. (2021). Effect of *Portulaca Oleracea* (purslane) extract on liver enzymes, lipid profile, and glycemic status in nonalcoholic fatty liver disease: A randomized, double-blind clinical trial. *Phytotherapy Research*, *35*(6), 3145–3156. https://doi.org/10.1002/ptr.6972

Das, A., Pandita, D., Jain, G. K., Agarwal, P., Grewal, A. S., Khar, R. K., & Lather, V. (2021). Role of phytoconstituents in the management of COVID-19. *Chemico-Biological Interactions*, *341*, 109449. https://doi.org/10.1016/j.cbi.2021.109449

Demesa, A. G., Saavala, S., Pöysä, M., & Koiranen, T. (2024). Overview and Toxicity Assessment of Ultrasound-Assisted Extraction of Natural Ingredients from Plants. *Foods*, *13*(19), 3066. https://doi.org/10.3390/foods13193066

Dheyab, A. S., Abu Bakar, M. F., AlOmar, M., Sabran, S. F., Muhamad Hanafi, A. F., & Mohamad, A. (2021). Deep Eutectic Solvents (DESs) as Green Extraction Media of

Beneficial Bioactive Phytochemicals. *Separations*, *8*(10), 176. https://doi.org/10.3390/separations8100176

DIETER, H. H. (n.d.). ACUTE AND CHRONIC TOXICITY OF CHEMICAL WARFARE AGENTS AND WARFARE TOXINS IN DRINKING WATER. In *Management of Intentional and Accidental Water Pollution* (pp. 23–41). Springer Netherlands. https://doi.org/10.1007/1-4020-4800-9_3

Dong, B., An, L., Yang, X., Zhang, X., Zhang, J., Tuerhong, M., Jin, D. Q., Ohizumi, Y., Lee, D., Xu, J., & Guo, Y. (2019). Withanolides from Physalis peruviana showing nitric oxide inhibitory effects and affinities with iNOS. *Bioorganic Chemistry*, *87*, 585–593. https://doi.org/10.1016/j.bioorg.2019.03.051

Duan, L., Tao, H.-W., Hao, X.-J., Gu, Q.-Q., & Zhu, W.-M. (2009). Cytotoxic and Antioxidative Phenolic Compounds from the Traditional Chinese Medicinal Plant, *Myristica fragrans*. *Planta Medica*, *75*(11), 1241–1245. https://doi.org/10.1055/s-0029-1185506

Ebrahimi, R., Sepand, M. R., Seyednejad, S. A., Omidi, A., Akbariani, M., Gholami, M., & Sabzevari, O. (2019). Ellagic acid reduces methotrexate-induced apoptosis and mitochondrial dysfunction via up-regulating Nrf2 expression and inhibiting the IκBα/NFκB in rats. *DARU Journal of Pharmaceutical Sciences*, *27*(2), 721–733. https://doi.org/10.1007/s40199-019-00309-9

EL Moussaoui, A., Jawhari, F. Z., Bourhia, M., Maliki, I., Sounni, F., Mothana, R. A., Bousta, D., & Bari, A. (2020). Withania frutescens : Chemical characterization , analgesic , anti - inflammatory , and healing activities. *Open Chemistry*, *18*, 927–935.

Elhamarnah, Y. A., Nasser, M., Qiblawey, H., Benamor, A., Atilhan, M., & Aparicio, S. (2019). A comprehensive review on the rheological behavior of imidazolium based ionic liquids and natural deep eutectic solvents. *Journal of Molecular Liquids*, *277*, 932–958.

Elkhayat, E. S., Ibrahim, S. R. M., & Aziz, M. A. (2008). Portulene, a new diterpene from *Portulaca oleracea* L. *Journal of Asian Natural Products Research*, *10*(11), 1039–1043. https://doi.org/10.1080/10286020802320590

Elsawy, H., Algefare, A. I., Alfwuaires, M., Khalil, M., Elmenshawy, O. M., Sedky, A., & Abdel-Moneim, A. M. (2020). Naringin alleviates methotrexate-induced liver injury in male albino rats and enhances its antitumor efficacy in HepG2 cells. *Bioscience Reports*, *40*(6). https://doi.org/10.1042/BSR20193686

Erkan, N. (2012). Antioxidant activity and phenolic compounds of fractions from Portulaca oleracea L. *Food Chemistry*, *133*(3), 775–781. https://doi.org/10.1016/j.foodchem.2012.01.091

EUCAST. (2009). *Disk Diffusion Method for Antimicrobial Susceptibility Testing, Version 1.0*.

Ezhilarasan, D. (2021). Hepatotoxic potentials of methotrexate: Understanding the possible toxicological molecular mechanisms. *Toxicology*, *458*, 152840. https://doi.org/10.1016/j.tox.2021.152840

Fabbrocini, G., De Vita, V., Izzo, R., & Monfrecola, G. (2014). The use of skin needling for the delivery of a eutectic mixture of local anesthetics. *Giornale Italiano Di Dermatologia e Venereologia : Organo Ufficiale, Societa Italiana Di Dermatologia e Sifilografia*, *149*(5), 581–585.

Faggian, M., Sut, S., Perissutti, B., Baldan, V., Grabnar, I., & Dall'Acqua, S. (2016). Natural Deep Eutectic Solvents (NADES) as a Tool for Bioavailability Improvement: Pharmacokinetics of Rutin Dissolved in Proline/Glycine after Oral Administration in Rats: Possible Application in Nutraceuticals. *Molecules*, *21*(11), 1531. https://doi.org/10.3390/molecules21111531

Fan, C., Cao, X., Han, T., Pei, H., Hu, G., Wang, W., & Qian, C. (2019). Selective microextraction of polycyclic aromatic hydrocarbons using a hydrophobic deep eutectic solvent composed with an iron oxide-based nanoferrofluid. *Microchimica Acta*, *186*(8), 560. https://doi.org/10.1007/s00604-019-3651-y

Fan, C., Liu, Y., Sebbah, T., & Cao, X. (2021). A Theoretical Study on Terpene-Based Natural Deep Eutectic Solvent: Relationship between Viscosity and Hydrogen-Bonding Interactions. *Global Challenges*, *5*(3). https://doi.org/10.1002/gch2.202000103

Fan, C., Sebbah, T., Liu, Y., & Cao, X. (2021). Terpenoid-capric acid based natural deep eutectic solvent: Insight into the nature of low viscosity. *Cleaner Engineering and Technology*, *3*. https://doi.org/10.1016/j.clet.2021.100116

Federal Register. (1996). *Guidance for Industry : Single Dose Acute Toxicity Testing for Pharmaceuticals*.

Florindo, C., Branco, L. C., & Marrucho, I. M. (2019). Quest for Green-Solvent Design: From Hydrophilic to Hydrophobic (Deep) Eutectic Solvents. *ChemSusChem*, *12*(8), 1549–1559. https://doi.org/10.1002/cssc.201900147

Fuskevåg, O.-M., Kristiansen, C., Lindal, S., & Aarbakke, J. (2000). Maximum tolerated doses of methotrexate and 7-hydroxy-methotrexate in a model of acute toxicity in rats. *Cancer Chemotherapy and Pharmacology*, *46*(1), 69–73. https://doi.org/10.1007/s002800000111

García, D. S., Saturansky, E. I., Poncino, D., Martínez-Artola, Y., Rosenberg, S., Abritta, G., Ascimani-Peña, C., & Cravero, A. (2019). "Hepatic toxicity by methotrexate with weekly single doses associated with folic acid in rheumatoid and psoriatic arthritis. What is its real frequency?" *Annals of Hepatology*, *18*(5), 765–769. https://doi.org/10.1016/j.aohep.2019.01.011

García-Salinas, S., Elizondo-Castillo, H., Arruebo, M., Mendoza, G., & Irusta, S. (2018). Evaluation of the Antimicrobial Activity and Cytotoxicity of Different Components of Natural Origin Present in Essential Oils. *Molecules*, *23*(6), 1399. https://doi.org/10.3390/molecules23061399

Gatea, F., Dumitra Teodor, E., Maria Seciu, A., Nagodă, E., & Lucian Radu, G. (2017). Chemical constituents and bioactive potential of Portulaca pilosa L vs. Portulaca oleracea L. *Medicinal Chemistry Research*, *26*(7), 1516–1527. https://doi.org/10.1007/s00044-017-1862-5

Ghafouri-Fard, S., Shoorei, H., Mohaqiq, M., Tahmasebi, M., Seify, M., & Taheri, M. (2021). Counteracting effects of heavy metals and antioxidants on male fertility. *BioMetals*, *34*, 439–491. https://doi.org/10.1007/s10534-021-00297-x

Gheflati, A., Adelnia, E., & Nadjarzadeh, A. (2019). The clinical effects of purslane (<scp> *Portulaca oleracea* </scp>) seeds on metabolic profiles in patients with nonalcoholic fatty liver disease: A randomized controlled clinical trial. *Phytotherapy Research*, *33*(5), 1501–1509. https://doi.org/10.1002/ptr.6342

Ghisalberti, E. L. (1998). Biological and pharmacological activity of naturally occurring iridoids and secoiridoids. *Phytomedicine*, *5*(2), 147–163. https://doi.org/10.1016/S0944-7113(98)80012-3

Gidado M. J., Gunny, A. A. N., Gopinath, S. C. B., Salleh, N. H. M., Pareek, S., & Balakrishnan, K. (2025). Investigating the Impact of Hydrophobic Deep Eutectic Oil-in-Water Nanoemulsion on Cell Membrane Degradation and Inhibition of C. gloeosporioides in Postharvest Technology. *Food and Bioprocess Technology*, *18*(3), 2314–2324. https://doi.org/10.1007/s11947-024-03587-7

Glee, P. M., Sundstrom, P., & Hazen, K. C. (1995). Expression of surface hydrophobic proteins by Candida albicans in vivo. *Infection and Immunity*, *63*(4), 1373–1379. https://doi.org/10.1128/iai.63.4.1373-1379.1995

Gu, Y., Ting, Z., Qiu, X., Zhang, X., Gan, X., Fang, Y., Xu, X., & Xu, R. (2010). Linalool preferentially induces robust apoptosis of a variety of leukemia cells via upregulating p53

and cyclin-dependent kinase inhibitors. *Toxicology*, *268*(1–2), 19–24. https://doi.org/10.1016/j.tox.2009.11.013

Habibian, M., Sadeghi, G., & Karimi, A. (2020). Phytochemicals and Antioxidant Properties of Solvent Extracts from Purslane (Portulaca oleracea L.): A Preliminary Study. *Food Science and Engineering*, 1–12. https://doi.org/10.37256/fse.11202046

Haddouchi, F., Chaouche, T. M., & Halla, N. (2016). Screening phytochimique, activités antioxydantes et pouvoir hémolytique de quatre plantes sahariennes d'Algérie. *Phytothérapie*. https://doi.org/10.1007/s10298-016-1086-8

Hasan Khudhair, D., Al-Gareeb, A. I., Al-kuraishy, H. M., El-Kadem, A. H., Elekhnawy, E., Negm, W. A., Saber, S., Cavalu, S., Tirla, A., Alotaibi, S. S., & Batiha, G. E.-S. (2022). Combination of Vitamin C and Curcumin Safeguards Against Methotrexate-Induced Acute Liver Injury in Mice by Synergistic Antioxidant Effects. *Frontiers in Medicine*, *9*. https://doi.org/10.3389/fmed.2022.866343

Hayyan, M., Hashim, M. A., Al-Saadi, M. A., Hayyan, A., AlNashef, I. M., & Mirghani, M. E. S. (2013). Assessment of cytotoxicity and toxicity for phosphonium-based deep eutectic solvents. *Chemosphere*, *93*(2), 455–459. https://doi.org/10.1016/j.chemosphere.2013.05.013

Hayyan, M., Looi, C. Y., Hayyan, A., Wong, W. F., & Hashim, M. A. (2015). In Vitro and In Vivo Toxicity Profiling of Ammonium-Based Deep Eutectic Solvents. *PLOS ONE*, *10*(2), e0117934. https://doi.org/10.1371/journal.pone.0117934

Hayyan, M., Mbous, Y. P., Looi, C. Y., Wong, W. F., Hayyan, A., Salleh, Z., & Mohd-Ali, O. (2016). Natural deep eutectic solvents: cytotoxic profile. *SpringerPlus*, *5*(1), 913. https://doi.org/10.1186/s40064-016-2575-9

He, X., Yang, J., Huang, Y., Zhang, Y., Wan, H., & Li, C. (2019). Green and Efficient Ultrasonic-Assisted Extraction of Bioactive Components from Salvia miltiorrhiza by Natural Deep Eutectic Solvents. *Molecules*, *25*(1), 140. https://doi.org/10.3390/molecules25010140

Hobden, C., Teevan, C., Jones, L., & O'Shea, P. (1995). Hydrophobic properties of the cell surface of Candida albicans: a role in aggregation. *Microbiology*, *141*(8), 1875–1881. https://doi.org/10.1099/13500872-141-8-1875

Hong, S.-H., Dinh, L., Abuzar, S., Lee, E., & Hwang, S.-J. (2022). Synthesis of Celecoxib-Eutectic Mixture Particles via Supercritical CO2 Process and Celecoxib Immediate Release Tablet Formulation by Quality by Design Approach. *Pharmaceutics*, *14*(8), 1549. https://doi.org/10.3390/pharmaceutics14081549

Huang, C. B., Alimova, Y., Myers, T. M., & Ebersole, J. L. (2011). Short- and medium-chain fatty acids exhibit antimicrobial activity for oral microorganisms. *Archives of Oral Biology*, *56*(7), 650–654. https://doi.org/10.1016/j.archoralbio.2011.01.011

Humphrey, W., Dalke, A., & Schulten, K. (1996). VMD: Visual molecular dynamics. *Journal of Molecular Graphics*, *14*(1), 33–38. https://doi.org/10.1016/0263-7855(96)00018-5

Iftikhar, A., Akhtar, M. F., Saleem, A., Riaz, A., Zehravi, M., Rahman, M. H., & Ashraf, G. M. (2022). Comparative Potential of Zinc Sulfate, L-Carnitine, Lycopene, and Coenzyme Q10 on Cadmium-Induced Male Infertility. *Int J Endocrinol*. https://doi.org/10.1155/2022/6266613.

International Council for Harmonisation (ICH). (2024). *ICH Q3C (R9) Impurities: Residual Solvents*.

Javed, S., Mangla, B., Sultan, M. H., Almoshari, Y., Sivadasan, D., Alqahtani, S. S., Madkhali, O. A., & Ahsan, W. (2024). Pharmaceutical applications of therapeutic deep eutectic systems (THEDES) in maximising drug delivery. *Heliyon*, *10*(9), e29783. https://doi.org/10.1016/j.heliyon.2024.e29783

Jeliński, T., Przybyłek, M., & Cysewski, P. (2019). Natural Deep Eutectic Solvents as Agents for Improving Solubility, Stability and Delivery of Curcumin. *Pharmaceutical Research*, *36*(8), 116. https://doi.org/10.1007/s11095-019-2643-2

Jesus, A. R., Duarte, A. R. C., & Paiva, A. (2022). Use of natural deep eutectic systems as new cryoprotectant agents in the vitrification of mammalian cells. *Scientific Reports*, *12*(1), 8095. https://doi.org/10.1038/s41598-022-12365-4

Jesus, A. R., Meneses, L., Duarte, A. R. C., & Paiva, A. (2021). Natural deep eutectic systems, an emerging class of cryoprotectant agents. *Cryobiology*, *101*, 95–104. https://doi.org/10.1016/j.cryobiol.2021.05.002

Jiang, K., Liu, L., Liu, X., Zhang, X., & Zhang, S. (2019). Insight into the Relationship between Viscosity and Hydrogen Bond of a Series of Imidazolium Ionic Liquids: A Molecular Dynamics and Density Functional Theory Study. *Industrial & Engineering Chemistry Research*, *58*(40), 18848–18854. https://doi.org/10.1021/acs.iecr.9b02535

Jin, Y., Jung, D., Li, K., Park, K., & Lee, J. (2020). Mixing of menthol-based hydrophobic deep eutectic solvents as a novel method to tune their properties. *Journal of Molecular Liquids*, *301*, 112416. https://doi.org/10.1016/j.molliq.2019.112416

Kamatou, G. P. P., Vermaak, I., Viljoen, A. M., & Lawrence, B. M. (2013). Menthol: A simple monoterpene with remarkable biological properties. *Phytochemistry*, *96*, 15–25. https://doi.org/10.1016/j.phytochem.2013.08.005

Kim, J., Shi, Y., Kwon, C. J., Gao, Y., & Mitragotri, S. (2021). A Deep Eutectic Solvent-Based Approach to Intravenous Formulation. *Advanced Healthcare Materials*, *10*(18). https://doi.org/10.1002/adhm.202100585

Kingston, D. G. I. (2011). Modern Natural Products Drug Discovery and Its Relevance to Biodiversity Conservation. *Journal of Natural Products*, *74*(3), 496–511. https://doi.org/10.1021/np100550t

Klapp, A.-L., Feil, N., & Risius, A. (2022). A Global Analysis of National Dietary Guidelines on Plant-Based Diets and Substitutions for Animal-Based Foods. *Current Developments in Nutrition*, *6*(11), nzac144. https://doi.org/10.1093/cdn/nzac144

Kleszcz, R., Majchrzak-Celińska, A., & Baer-Dubowska, W. (2023). Tannins in cancer prevention and therapy. *British Journal of Pharmacology*. https://doi.org/10.1111/bph.16224

Konrath, E. L., Passos, C. dos S., Klein, L. C., & Henriques, A. T. (2013). Alkaloids as a source of potential anticholinesterase inhibitors for the treatment of Alzheimer's disease. *The Journal of Pharmacy and Pharmacology*, *65*(12), 1701–1725. https://doi.org/10.1111/jphp.12090

Kouamé, T. K., Siaka, S., Kassi, A. B. B., & Soro, Y. (2021). Détermination des teneurs en polyphénols totaux, flavonoïdes totaux et tanins de jeunes feuilles non encore ouvertes de Piliostigma thonningii (Caesalpiniaceae). *International Journal of Biological and Chemical Sciences*, *15*(1), 97–105. https://doi.org/10.4314/ijbcs.v15i1.9

Křížek, T., Bursová, M., Horsley, R., Kuchař, M., Tůma, P., Čabala, R., & Hložek, T. (2018). Menthol-based hydrophobic deep eutectic solvents: Towards greener and efficient extraction of phytocannabinoids. *Journal of Cleaner Production*, *193*, 391–396. https://doi.org/10.1016/j.jclepro.2018.05.080

Kumar, A., Sreedharan, S., Kashyap, A. K., Singh, P., & Ramchiary, N. (2022). A review on bioactive phytochemicals and ethnopharmacological potential of purslane (Portulaca oleracea L.). *Heliyon*, *8*(1), e08669. https://doi.org/10.1016/j.heliyon.2021.e08669

Kumar, N., & Goel, N. (2019). Phenolic acids: Natural versatile molecules with promising therapeutic applications. *Biotechnology Reports*, *24*, e00370. https://doi.org/10.1016/j.btre.2019.e00370

Kyriakoudi, A., Tsiouras, A., & Mourtzinos, I. (2022). Extraction of Lycopene from Tomato Using Hydrophobic Natural Deep Eutectic Solvents Based on Terpenes and Fatty Acids. *Foods*, *11*(17), 2645. https://doi.org/10.3390/foods11172645

Laage, D., & Hynes, J. T. (2008). On the Residence Time for Water in a Solute Hydration Shell: Application to Aqueous Halide Solutions. *The Journal of Physical Chemistry B*, *112*(26), 7697–7701. https://doi.org/10.1021/jp802033r

Lalikoglu, M. (2022). Separation of butyric acid from aqueous media using menthol-based hydrophobic deep eutectic solvent and modeling by response surface methodology. *Biomass Conversion and Biorefinery*, *12*(4), 1331–1341. https://doi.org/10.1007/s13399-021-01711-7

Langman, G., Hall, P. D. L. M., & Todd, G. (2001). Role of non-alcoholic steatohepatitis in methotrexate-induced liver injury. *Journal of Gastroenterology and Hepatology*, *16*(12), 1395–1401. https://doi.org/10.1046/j.1440-1746.2001.02644.x

Lapczynski, A., Letizia, C. S., & Api, A. M. (2008). Addendum to Fragrance material review on linalool. *Food and Chemical Toxicology*, *46*(11), S190–S192. https://doi.org/10.1016/j.fct.2008.06.087

Le Tourneau, C., Lee, J. J., & Siu, L. L. (2009). Dose escalation methods in phase I cancer clinical trials. *Journal of the National Cancer Institute*, *101*(10), 708–720. https://doi.org/10.1093/jnci/djp079

Lee, M.-H., Hong, I., Kim, M., Lee, B.-H., Kim, J.-H., Kang, K.-S., Kim, H.-L., Yoon, B.-I., Chung, H., Kong, G., & Lee, M.-O. (2008). Gene expression profiles of murine fatty liver induced by the administration of methotrexate. *Toxicology*, *249*(1), 75–84. https://doi.org/10.1016/j.tox.2008.04.011

Lemaoui, T., Darwish, A. S., Attoui, A., Abu Hatab, F., Hammoudi, N. E. H., Benguerba, Y., Vega, L. F., & Alnashef, I. M. (2020). Predicting the density and viscosity of hydrophobic eutectic solvents: towards the development of sustainable solvents. *Green Chemistry*, *22*(23), 8511–8530. https://doi.org/10.1039/D0GC03077E

Li, Q., Huang, K. X., Pan, S., Su, C., Bi, J., & Lu, X. (2022). Thymol Disrupts Cell Homeostasis and Inhibits the Growth of Staphylococcus aureus. *Contrast Media & Molecular Imaging*, *2022*, 8743096. https://doi.org/10.1155/2022/8743096

Li, Q., & Verma, I. M. (2002). NF-κB regulation in the immune system. *Nature Reviews Immunology*, *2*(10), 725–734. https://doi.org/10.1038/nri910

Li, S., Culkin, A., Jones, D. S., & Andrews, G. P. (2021). Development of Polycaprolactone-Based metronidazole matrices for intravaginal extended drug delivery using a mechanochemically prepared therapeutic deep eutectic system. *International Journal of Pharmaceutics*, *593*, 120071. https://doi.org/10.1016/j.ijpharm.2020.120071

Li, Y., Pan, Z., Wang, B., Yu, W., Song, S., Feng, H., Zhao, W., & Zhang, J. (2020). Ultrasound-assisted extraction of bioactive alkaloids from *Phellodendri amurensis* cortex using deep eutectic solvent aqueous solutions. *New Journal of Chemistry*, *44*(22), 9172–9178. https://doi.org/10.1039/D0NJ00877J

Liang, Y., Luo, K., Wang, B., Huang, B., Fei, P., & Zhang, G. (2024). Inhibition of polyphenol oxidase for preventing browning in edible mushrooms: A review. *Journal of Food Science*, *89*(11), 6796–6817. https://doi.org/10.1111/1750-3841.17322

Lin, L.-G., Liu, Q.-Y., & Ye, Y. (2014). Naturally Occurring Homoisoflavonoids and Their Pharmacological Activities. *Planta Medica*, *80*(13), 1053–1066. https://doi.org/10.1055/s-0034-1383026

Liu, K., Tan, J.-N., Wei, Y., Li, C., Dou, Y., & Zhang, Z. (2022). Application of choline chloride-based deep eutectic solvents for the extraction of dopamine from purslane (Portulaca oleracea L.). *Results in Chemistry*, *4*, 100299. https://doi.org/10.1016/j.rechem.2022.100299

Liu, M., Lai, Z., Zhu, L., Ding, X., Tong, X., Wang, Z., Bi, Q., & Tan, N. (2021). Novel amorphous solid dispersion based on natural deep eutectic solvent for enhancing delivery of anti-tumor RA-XII by oral administration in rats. *European Journal of Pharmaceutical Sciences*, *166*, 105931. https://doi.org/10.1016/j.ejps.2021.105931

Liu, T., Zhang, L., Joo, D., & Sun, S.-C. (2017). NF-κB signaling in inflammation. *Signal Transduction and Targeted Therapy*, *2*(1), 17023. https://doi.org/10.1038/sigtrans.2017.23

Liu, X.-F., Zheng, C.-G., Shi, H.-G., Tang, G.-S., Wang, W.-Y., Zhou, J., & Dong, L.-W. (2015). Ethanol extract from portulaca oleracea L. attenuated acetaminophen-induced mice liver injury. *American Journal of Translational Research*, *7*(2), 309–318.

Liu, Z., Wu, H., Wei, Z., Wang, X., Shen, P., Wang, S., Wang, A., Chen, W., & Lu, Y. (2016). TRPM8: a potential target for cancer treatment. *Journal of Cancer Research and Clinical Oncology*, *142*(9), 1871–1881. https://doi.org/10.1007/s00432-015-2112-1

Log, T., & Moi, A. L. (2018). Ethanol and Methanol Burn Risks in the Home Environment. *International Journal of Environmental Research and Public Health*, *15*(11), 2379. https://doi.org/10.3390/ijerph15112379

Lomba, L., García, C. B., Ribate, M. P., Giner, B., & Zuriaga, E. (2021). Applications of Deep Eutectic Solvents Related to Health, Synthesis, and Extraction of Natural Based Chemicals. *Applied Sciences*, *11*(21), 10156. https://doi.org/10.3390/app112110156

Lu, J., Zheng, Y., Luo, L., Wu, D., Sun, D., & Feng, Y. (2006). Quercetin reverses d-galactose induced neurotoxicity in mouse brain. *Behavioural Brain Research*, *171*(2), 251–260. https://doi.org/10.1016/j.bbr.2006.03.043

Lu, T., & Chen, F. (2012a). Multiwfn: A multifunctional wavefunction analyzer. *Journal of Computational Chemistry*, *33*(5), 580–592. https://doi.org/10.1002/jcc.22885

Lu, T., & Chen, F. (2012b). Quantitative analysis of molecular surface based on improved Marching Tetrahedra algorithm. *Journal of Molecular Graphics and Modelling*, *38*, 314–323. https://doi.org/10.1016/j.jmgm.2012.07.004

Ma, Y., Liu, M., Tan, T., Yan, A., Guo, L., Jiang, K., Tan, C., & Wan, Y. (2018a). Deep eutectic solvents used as extraction solvent for the determination of flavonoids from *Camellia oleifera* flowers by high-performance liquid chromatography. *Phytochemical Analysis*, *29*(6), 639–648. https://doi.org/10.1002/pca.2777

Ma, Y., Liu, M., Tan, T., Yan, A., Guo, L., Jiang, K., Tan, C., & Wan, Y. (2018b). Deep eutectic solvents used as extraction solvent for the determination of flavonoids from *Camellia oleifera* flowers by high-performance liquid chromatography. *Phytochemical Analysis*, *29*(6), 639–648. https://doi.org/10.1002/pca.2777

Ma, Y., Liu, Y., Su, H., Wang, L., & Zhang, J. (2018). Relationship between hydrogen bond and viscosity for a series of pyridinium ionic liquids: Molecular dynamics and quantum chemistry. *Journal of Molecular Liquids*, *255*, 176–184. https://doi.org/10.1016/j.molliq.2018.01.121

Mączka, W., Wińska, K., & Grabarczyk, M. (2020). One Hundred Faces of Geraniol. *Molecules (Basel, Switzerland)*, *25*(14). https://doi.org/10.3390/molecules25143303

Manurung, R. (2020). PERFORMANCE OF MENTHOL BASED DEEP EUTECTIC SOLVENTS IN THE EXTRACTION OF CAROTENOIDS FROM CRUDE PALM OIL. *International Journal of GEOMATE*, *19*(74), 131–137. https://doi.org/10.21660/2020.74.96998

Marahatha, R., Gyawali, N., Gyawali, K., Tandan, P., Sharma, K., Adhikari, A., & Bhattarai, S. (2021). Pharmacologic activities of phytosteroids in inflammatory diseases : Mechanism of action and therapeutic potentials. *Phytotherapy Research.*, *April*, 1–22. https://doi.org/10.1002/ptr.7138

Marcantonini, G., Bartolini, D., Zatini, L., Costa, S., Passerini, M., Rende, M., Luca, G., Basta, G., Murdolo, G., Calafiore, R., & Galli, F. (2022). Natural Cryoprotective and Cytoprotective Agents in Cryopreservation: A Focus on Melatonin. *Molecules*, *27*(10), 3254. https://doi.org/10.3390/molecules27103254

Marini, H. R., Micali, A., Squadrito, G., Puzzolo, D., Freni, J., Antonuccio, P., & Minutoli, L. (2022). Nutraceuticals: A New Challenge against Cadmium-Induced Testicular Injury. *Nutrients*, *14*(3), 663. https://doi.org/10.3390/nu14030663.

Martínez, G. M., Townley, G. G., & Martínez-Espinosa, R. M. (2022). Controversy on the toxic nature of deep eutectic solvents and their potential contribution to environmental pollution. *Heliyon*, *8*(12), e12567. https://doi.org/10.1016/j.heliyon.2022.e12567

Martínez, L., Andrade, R., Birgin, E. G., & Martínez, J. M. (2009). P <scp>ACKMOL</scp> : A package for building initial configurations for molecular dynamics simulations. *Journal of Computational Chemistry*, *30*(13), 2157–2164. https://doi.org/10.1002/jcc.21224

Martins, M. A. R., Crespo, E. A., Pontes, P. V. A., Silva, L. P., Bülow, M., Maximo, G. J., Batista, E. A. C., Held, C., Pinho, S. P., & Coutinho, J. A. P. (2018). Tunable Hydrophobic Eutectic Solvents Based on Terpenes and Monocarboxylic Acids. *ACS Sustainable Chemistry & Engineering*, *6*(7), 8836–8846. https://doi.org/10.1021/acssuschemeng.8b01203

Martins, M. A. R., Pinho, S. P., & Coutinho, J. A. P. (2019). Insights into the Nature of Eutectic and Deep Eutectic Mixtures. *Journal of Solution Chemistry*, *48*(7), 962–982. https://doi.org/10.1007/s10953-018-0793-1

Masyita, A., Mustika Sari, R., Dwi Astuti, A., Yasir, B., Rahma Rumata, N., Emran, T. Bin, Nainu, F., & Simal-Gandara, J. (2022). Terpenes and terpenoids as main bioactive compounds of essential oils, their roles in human health and potential application as natural food preservatives. *Food Chemistry: X*, *13*, 100217. https://doi.org/10.1016/j.fochx.2022.100217

Melilli, M. G., Pagliaro, A., Bognanni, R., Scandurra, S., & Di Stefano, V. (2020). Antioxidant activity and fatty acids quantification in Sicilian purslane germplasm. *Natural Product Research*, *34*(1), 26–33. https://doi.org/10.1080/14786419.2018.1560291

Meng, Z., Zhao, J., Duan, H., Guan, Y., & Zhao, L. (2018). Green and efficient extraction of four bioactive flavonoids from Pollen Typhae by ultrasound-assisted deep eutectic solvents extraction. *Journal of Pharmaceutical and Biomedical Analysis*, *161*, 246–253. https://doi.org/10.1016/j.jpba.2018.08.048

Middleton, Jr. , M. D. , E. (1996). Biological Properties of Plant Flavonoids: An Overview. *International Journal of Pharmacognosy*, *34*(5), 344–348. https://doi.org/10.1076/phbi.34.5.344.13245

Milkarizi, N., Barghchi, H., Belyani, S., Bahari, H., Rajabzade, F., Ostad, A. N., Goshayeshi, L., Nematy, M., & Askari, V. R. (2024). Effects of Portulaca oleracea (purslane) on liver

function tests, metabolic profile, oxidative stress and inflammatory biomarkers in patients with non-alcoholic fatty liver disease: a randomized, double-blind clinical trial. *Frontiers in Nutrition*, *11*. https://doi.org/10.3389/fnut.2024.1371137

Mir, S. R., & Ali, M. (2016). ChemInform Abstract: Taraxerane-Type Triterpenoids from Portulaca oleracea Linn. Seeds. *ChemInform*, *47*(21). https://doi.org/10.1002/chin.201621219

Mohamed, D. A., Essa, H. A., & Mohamed, R. S. (2019). Purslane and Garden Cress Seeds as Source of Unconventional Edible Oils for Prevention of Hyperlipidemia. *Pakistan Journal of Biological Sciences*, *22*(11), 537–544. https://doi.org/10.3923/pjbs.2019.537.544

Molnar, M., Brahmbhatt, H., Rastija, V., Pavić, V., Komar, M., Karnaš, M., & Babić, J. (2018). Environmentally Friendly Approach to Knoevenagel Condensation of Rhodanine in Choline Chloride: Urea Deep Eutectic Solvent and QSAR Studies on Their Antioxidant Activity. *Molecules*, *23*(8), 1897. https://doi.org/10.3390/molecules23081897

Nadia, J., Shahbaz, K., Ismail, M., & Farid, M. M. (2018). Approach for Polygodial Extraction from *Pseudowintera colorata* (Horopito) Leaves Using Deep Eutectic Solvents. *ACS Sustainable Chemistry & Engineering*, *6*(1), 862–871. https://doi.org/10.1021/acssuschemeng.7b03221

Naghshineh, A., Dadras, A., Ghalandari, B., Riazi, G. H., Modaresi, S. M. S., Afrasiabi, A., & Aslani, M. K. (2015). Safranal as a novel anti-tubulin binding agent with potential use in cancer therapy: An in vitro study. *Chemico-Biological Interactions*, *238*, 151–160. https://doi.org/10.1016/j.cbi.2015.06.023

Nagoor Meeran, M. F., Javed, H., Al Taee, H., Azimullah, S., & Ojha, S. K. (2017). Pharmacological Properties and Molecular Mechanisms of Thymol: Prospects for Its Therapeutic Potential and Pharmaceutical Development. *Frontiers in Pharmacology*, *8*, 380. https://doi.org/10.3389/fphar.2017.00380

Nasri, M., Bedjou, F., Porras, D., & Martínez-Flórez, S. (2017). Antioxidant, anti-inflammatory, and analgesic activities of Citrus reticulata Blanco leaves extracts: An in vivo and in vitro study. *Phytothérapie*. https://doi.org/10.1007/s10298-017-1094-8

Nayaka, H. B., Londonkar, R. L., Umesh, M. K., & Tukappa, A. (2014). Antibacterial Attributes of Apigenin, Isolated from *Portulaca oleracea L. International Journal of Bacteriology*, *2014*, 1–8. https://doi.org/10.1155/2014/175851

Neese, F. (2018). Software update: the ORCA program system, version 4.0. *WIREs Computational Molecular Science*, *8*(1). https://doi.org/10.1002/wcms.1327

Nemzer, B., Al-Taher, F., & Abshiru, N. (2020a). Phytochemical composition and nutritional value of different plant parts in two cultivated and wild purslane (Portulaca oleracea L.) genotypes. *Food Chemistry*, *320*, 126621. https://doi.org/10.1016/j.foodchem.2020.126621

Nemzer, B., Al-Taher, F., & Abshiru, N. (2020b). Phytochemical composition and nutritional value of different plant parts in two cultivated and wild purslane (Portulaca oleracea L.) genotypes. *Food Chemistry*, *320*, 126621. https://doi.org/10.1016/j.foodchem.2020.126621

Oliveira, F. S. N. de, & Duarte, A. R. C. (2021). *A look on target-specificity of eutectic systems based on natural bioactive compounds* (pp. 271–307). https://doi.org/10.1016/bs.abr.2020.09.008

Oliveira, G., Marques, C., de Oliveira, A., de Almeida dos Santos, A., do Amaral, W., Ineu, R. P., Leimann, F. V., Peron, A. P., Igarashi-Mafra, L., & Mafra, M. R. (2021). Extraction of bioactive compounds from Curcuma longa L. using deep eutectic solvents: In vitro and in vivo biological activities. *Innovative Food Science & Emerging Technologies*, *70*, 102697. https://doi.org/10.1016/j.ifset.2021.102697

Oliveira, I., Valentão, P., Lopes, R., Andrade, P. B., Bento, A., & Pereira, J. A. (2009). Phytochemical characterization and radical scavenging activity of Portulaca oleraceae L. leaves and stems. *Microchemical Journal*, *92*(2), 129–134. https://doi.org/10.1016/j.microc.2009.02.006

Paduch, R., Kandefer-Szerszeń, M., Trytek, M., & Fiedurek, J. (2007). Terpenes: substances useful in human healthcare. *Archivum Immunologiae et Therapiae Experimentalis*, *55*(5), 315–327. https://doi.org/10.1007/s00005-007-0039-1

Paiva, A., Craveiro, R., Aroso, I., Martins, M., Reis, R. L., & Duarte, A. R. C. (2014). Natural Deep Eutectic Solvents – Solvents for the 21st Century. *ACS Sustainable Chemistry & Engineering*, *2*(5), 1063–1071. https://doi.org/10.1021/sc500096j

Pandey, A., Belwal, T., Sekar, K. C., Bhatt, I. D., & Rawal, R. S. (2018). Optimization of ultrasonic-assisted extraction (UAE) of phenolics and antioxidant compounds from rhizomes of Rheum moorcroftianum using response surface methodology (RSM). *Industrial Crops and Products*, *119*, 218–225. https://doi.org/10.1016/j.indcrop.2018.04.019

Pandey, A. K., Kumar, P., Singh, P., Tripathi, N. N., & Bajpai, V. K. (2017). Essential Oils: Sources of Antimicrobials and Food Preservatives. *Frontiers in Microbiology*, *7*. https://doi.org/10.3389/fmicb.2016.02161

Pandey, A., & Pandey, S. (2014). Solvatochromic Probe Behavior within Choline Chloride-Based Deep Eutectic Solvents: Effect of Temperature and Water. *The Journal of Physical Chemistry B*, *118*(50), 14652–14661. https://doi.org/10.1021/jp510420h

Park, J., Park, J.-E., Seo, Y.-W., & Han, J.-S. (2019). 5,7-Dimethoxy-3-(2′-hydroxybenzyl)-4-chromanone inhibits α-glucosidase in vitro and alleviates postprandial hyperglycemia in diabetic mice. *European Journal of Pharmacology*, *863*, 172683. https://doi.org/10.1016/j.ejphar.2019.172683

Parthasarathy, M., & Prince, S. E. (2023). Andrographis paniculata (Burm.f.) Nees Alleviates Methotrexate-Induced Hepatotoxicity in Wistar Albino Rats. *Life*, *13*(5), 1173. https://doi.org/10.3390/life13051173

Parveen, F., Madni, A., Torchilin, V. P., Rehman, M., Jamshaid, T., Filipczak, N., Rai, N., Khan, M. M., & Khan, M. I. (2022). Investigation of Eutectic Mixtures of Fatty Acids as a Novel Construct for Temperature-Responsive Drug Delivery. *International Journal of Nanomedicine*, *Volume 17*, 2413–2434. https://doi.org/10.2147/IJN.S359664

Parvizi, F., Yaghmaei, P., Haeri Rohani, S. A., & Mard, S. A. (2020). Hepatoprotective properties of p-coumaric acid in a rat model of ischemia-reperfusion. *Avicenna Journal of Phytomedicine*, *10*(6), 633–640.

Paul, N., Naik, P. K., Ribeiro, B. D., Gooh Pattader, P. S., Marrucho, I. M., & Banerjee, T. (2020). Molecular Dynamics Insights and Water Stability of Hydrophobic Deep Eutectic Solvents Aided Extraction of Nitenpyram from an Aqueous Environment. *The Journal of Physical Chemistry B*, *124*(34), 7405–7420. https://doi.org/10.1021/acs.jpcb.0c03647

Peana, A. T., D'Aquila, P. S., Panin, F., Serra, G., Pippia, P., & Moretti, M. D. L. (2002). Anti-inflammatory activity of linalool and linalyl acetate constituents of essential oils. *Phytomedicine*, *9*(8), 721–726. https://doi.org/10.1078/094471102321621322

Peana, A. T., & Moretti, M. D. L. (2008). Linalool in essential plant oils: pharmacological effects. In *Botanical medicine in clinical practice* (pp. 716–724). CAB International. https://doi.org/10.1079/9781845934132.0716

Pereira, J., Miguel Castro, M., Santos, F., Rita Jesus, A., Paiva, A., Oliveira, F., & Duarte, A. R. C. (2022). Selective terpene based therapeutic deep eutectic systems against colorectal cancer. *European Journal of Pharmaceutics and Biopharmaceutics*, *175*, 13–26. https://doi.org/10.1016/j.ejpb.2022.04.008

Pereira, C. V., Silva, J. M., Rodrigues, L., Reis, R. L., Paiva, A., Duarte, A. R. C., & Matias, A. (2019). Unveil the Anticancer Potential of Limomene Based Therapeutic Deep Eutectic Solvents. *Scientific Reports*, *9*(1), 14926. https://doi.org/10.1038/s41598-019-51472-7

Pérez-Riesgo, E., Gutiérrez, L., Ubierna, D., Acedo, A., Moyer, M., Núñez, L., & Villalobos, C. (2017). Transcriptomic Analysis of Calcium Remodeling in Colorectal Cancer. *International Journal of Molecular Sciences*, *18*(5), 922. https://doi.org/10.3390/ijms18050922

Perkins, S. L., Painter, P., & Colina, C. M. (2014). Experimental and Computational Studies of Choline Chloride-Based Deep Eutectic Solvents. *Journal of Chemical & Engineering Data*, *59*(11), 3652–3662. https://doi.org/10.1021/je500520h

Petropoulos, S. A., Karkanis, A., Fernandes, Â., Barros, L., Ferreira, I. C. F. R., Ntatsi, G., Petrotos, K., Lykas, C., & Khah, E. (2015). Chemical Composition and Yield of Six Genotypes of Common Purslane (Portulaca oleracea L.): An Alternative Source of Omega-3 Fatty Acids. *Plant Foods for Human Nutrition*, *70*(4), 420–426. https://doi.org/10.1007/s11130-015-0511-8

Prezhdo, O., Drogosz, A., Zubkova, V., & Prezhdo, V. (2013). On viscosity of selected normal and associated liquids. *Journal of Molecular Liquids*, *182*, 32–38. https://doi.org/10.1016/j.molliq.2013.03.004

Radošević, K., Čanak, I., Panić, M., Markov, K., Bubalo, M. C., Frece, J., Srček, V. G., & Redovniković, I. R. (2018). Antimicrobial, cytotoxic and antioxidative evaluation of natural deep eutectic solvents. *Environmental Science and Pollution Research*, *25*(14), 14188–14196. https://doi.org/10.1007/s11356-018-1669-z

Ramon, D. J., & Guillena, G. (2020). *Deep Eutectic Solvents: Synthesis, Properties, and Applications* (John Wiley & Sons).

Ribeiro, B. D., Florindo, C., Iff, L. C., Coelho, M. A. Z., & Marrucho, I. M. (2015a). Menthol-based Eutectic Mixtures: Hydrophobic Low Viscosity Solvents. *ACS Sustainable Chemistry & Engineering*, *3*(10), 2469–2477. https://doi.org/10.1021/acssuschemeng.5b00532

Ribeiro, B. D., Florindo, C., Iff, L. C., Coelho, M. A. Z., & Marrucho, I. M. (2015b). Menthol-based Eutectic Mixtures: Hydrophobic Low Viscosity Solvents. *ACS Sustainable Chemistry & Engineering*, *3*(10), 2469–2477. https://doi.org/10.1021/acssuschemeng.5b00532

Rodrigues, L. A., Pereira, C. V., Leonardo, I. C., Fernández, N., Gaspar, F. B., Silva, J. M., Reis, R. L., Duarte, A. R. C., Paiva, A., & Matias, A. A. (2020). Terpene-Based Natural Deep Eutectic Systems as Efficient Solvents To Recover Astaxanthin from Brown Crab Shell Residues. *ACS Sustainable Chemistry & Engineering*, *8*(5), 2246–2259. https://doi.org/10.1021/acssuschemeng.9b06283

Russo, E. B. (2011). Taming THC: potential cannabis synergy and phytocannabinoid-terpenoid entourage effects. *British Journal of Pharmacology*, *163*(7), 1344–1364. https://doi.org/10.1111/j.1476-5381.2011.01238.x

Saha, P., Bose, S., Srivastava, A. K., Chaudhary, A. A., Lall, R., & Prasad, S. (2021). Jeopardy of COVID-19: Rechecking the Perks of Phytotherapeutic Interventions. *Molecules*, *26*(22), 6783. https://doi.org/10.3390/molecules26226783

Samira, K., Mohamed Seif Allah, K., Hadjer, D., & Djellouli, A. (2017). Phenolic compounds and their antioxidant activities in Portulaca oleracea L. related to solvent extraction. *International Journal of Biosciences (IJB)*, *11*(1), 147–155. https://doi.org/10.12692/ijb/11.1.147-155

Santiago-Saenz, Y. O., Hernández-Fuentes, A. D., Monroy-Torres, R., Cariño-Cortés, R., & Jiménez-Alvarado, R. (2018). Physicochemical, nutritional and antioxidant characterization of three vegetables (Amaranthus hybridus L., Chenopodium berlandieri L., Portulaca oleracea L.) as potential sources of phytochemicals and bioactive compounds. *Journal of Food Measurement and Characterization*, *12*(4), 2855–2864. https://doi.org/10.1007/s11694-018-9900-7

Sebbah, T., Yahla, I., Cunha, E., Riazi, A., Amorim, C. G., Rodriguez-Diaz, J. M., & Montenegro, M. C. B. S. M. (2025). Enhanced Extraction and Separation with HPLC-DAD of Phenolic and Flavonoid Antioxidants from Portulaca oleracea L. Leaves Using Tailored Terpenoid-Based NADES: Comparative Assessment of Antiradical and Antimicrobial Activities. *Antioxidants*, *14*(2), 132. https://doi.org/10.3390/antiox14020132

Selamoglu, Z. (2018). Allantoin as Metabolic Compound. *Journal of Traditional Medicine & Clinical Naturopathy*, *07*(01). https://doi.org/10.4172/2573-4555.1000e143

Sherikar, A., Siddique, M. U. M., More, M., Goyal, S. N., Milivojevic, M., Alkahtani, S., Alarifi, S., Hasnain, M. S., & Nayak, A. K. (2021). Preparation and Evaluation of Silymarin-Loaded Solid Eutectic for Enhanced Anti-Inflammatory, Hepatoprotective Effect: *In Vitro – In Vivo* Prospect. *Oxidative Medicine and Cellular Longevity*, *2021*(1). https://doi.org/10.1155/2021/1818538

Shi, Y., Shi, L., Liu, Q., Wang, W., & Liu, Y. (2023). Molecular mechanism and research progress on pharmacology of ferulic acid in liver diseases. *Frontiers in Pharmacology*, *14*. https://doi.org/10.3389/fphar.2023.1207999

Siddaiah, V., Rao, C. V., Venkateswarlu, S., Krishnaraju, A. V., & Subbaraju, G. V. (2006). Synthesis, stereochemical assignments, and biological activities of homoisoflavonoids.

Bioorganic & Medicinal Chemistry, *14*(8), 2545–2551. https://doi.org/10.1016/j.bmc.2005.11.031

Silva dos Santos, J., Gonçalves Cirino, J. P., de Oliveira Carvalho, P., & Ortega, M. M. (2021). The Pharmacological Action of Kaempferol in Central Nervous System Diseases: A Review. *Frontiers in Pharmacology*, *11*. https://doi.org/10.3389/fphar.2020.565700

Silva, E., Oliveira, F., Silva, J. M., Matias, A., Reis, R. L., & Duarte, A. R. C. (2020). Optimal Design of THEDES Based on Perillyl Alcohol and Ibuprofen. *Pharmaceutics*, *12*(11), 1121. https://doi.org/10.3390/pharmaceutics12111121

Silva, E., Oliveira, F., Silva, J. M., Reis, R. L., & Duarte, A. R. C. (2021). Untangling the bioactive properties of therapeutic deep eutectic solvents based on natural terpenes. *Current Research in Chemical Biology*, *1*, 100003. https://doi.org/10.1016/j.crchbi.2021.100003

Silva, J. M., Pereira, C. V., Mano, F., Silva, E., Castro, V. I. B., Sá-Nogueira, I., Reis, R. L., Paiva, A., Matias, A. A., & Duarte, A. R. C. (2019). Therapeutic Role of Deep Eutectic Solvents Based on Menthol and Saturated Fatty Acids on Wound Healing. *ACS Applied Bio Materials*, *2*(10), 4346–4355. https://doi.org/10.1021/acsabm.9b00598

Silva, J. M., Reis, R. L., Paiva, A., & Duarte, A. R. C. (2018a). Design of Functional Therapeutic Deep Eutectic Solvents Based on Choline Chloride and Ascorbic Acid. *ACS Sustainable Chemistry & Engineering*, *6*(8), 10355–10363. https://doi.org/10.1021/acssuschemeng.8b01687

Silva, J. M., Reis, R. L., Paiva, A., & Duarte, A. R. C. (2018b). Design of Functional Therapeutic Deep Eutectic Solvents Based on Choline Chloride and Ascorbic Acid. *ACS Sustainable Chemistry & Engineering*, *6*(8), 10355–10363. https://doi.org/10.1021/acssuschemeng.8b01687

Silva, J. M., Silva, E., Reis, R. L., & Duarte, A. R. C. (2019). A closer look in the antimicrobial properties of deep eutectic solvents based on fatty acids. *Sustainable Chemistry and Pharmacy*, *14*, 100192. https://doi.org/10.1016/j.scp.2019.100192

Silva, R., & Carvalho, I. S. (2014a). *In vitro* Antioxidant Activity, Phenolic Compounds and Protective Effect against DNA Damage Provided by Leaves, Stems and Flowers of *Portulaca oleracea* (Purslane). *Natural Product Communications*, *9*(1). https://doi.org/10.1177/1934578X1400900115

Silva, R., & Carvalho, I. S. (2014b). *In vitro* Antioxidant Activity, Phenolic Compounds and Protective Effect against DNA Damage Provided by Leaves, Stems and Flowers of

Portulaca oleracea (Purslane). *Natural Product Communications*, *9*(1). https://doi.org/10.1177/1934578X1400900115

Silva, Y. P. A., Ferreira, T. A. P. C., Jiao, G., & Brooks, M. S. (2019). Sustainable approach for lycopene extraction from tomato processing by-product using hydrophobic eutectic solvents. *Journal of Food Science and Technology*, *56*(3), 1649–1654. https://doi.org/10.1007/s13197-019-03618-8

Simopoulos, A. P., Norman, H. A., Gillaspy, J. E., & Duke, J. A. (1992). Common purslane: a source of omega-3 fatty acids and antioxidants. *Journal of the American College of Nutrition*, *11*(4), 374–382. https://doi.org/10.1080/07315724.1992.10718240

Su, W., Li, Y., Chang, A. K., Sheng, T., Pei, Y., Li, J., Li, H., Liu, K., Xu, L., Liu, W., Ai, J., Zhang, Z., Wang, Y., Jiang, Z., & Liang, X. (2023). Identification of Novel Alkaloids from *Portulaca oleracea* L. and Characterization of Their Pharmacokinetics and GLP-1 Secretion-Promoting Activity in STC-1 Cells. *Journal of Agricultural and Food Chemistry*, *71*(49), 19804–19816. https://doi.org/10.1021/acs.jafc.3c05191

Talbi, H., Boumaza, A., El-, K., Talbi, J., & Hilali, A. (2015). Evaluation of antioxidant activity and physico-chemical composition of methanolic and aqueous extracts of Nigella sativa L. *Mater. Environ*, *6*(4), 1111–1117.

Tang, X.-H., & Gudas, L. J. (2011). Retinoids, Retinoic Acid Receptors, and Cancer. *Annual Review of Pathology: Mechanisms of Disease*, *6*(1), 345–364. https://doi.org/10.1146/annurev-pathol-011110-130303

Tholl, D. (2015). *Biosynthesis and Biological Functions of Terpenoids in Plants* (pp. 63–106). https://doi.org/10.1007/10_2014_295

Tomé, L. I. N., Baião, V., da Silva, W., & Brett, C. M. A. (2018). Deep eutectic solvents for the production and application of new materials. *Applied Materials Today*, *10*, 30–50. https://doi.org/10.1016/j.apmt.2017.11.005

Tu, Y. (2011). The discovery of artemisinin (qinghaosu) and gifts from Chinese medicine. *Nature Medicine*, *17*(10), 1217–1220. https://doi.org/10.1038/nm.2471

Ulanowska, M., & Olas, B. (2021). Biological Properties and Prospects for the Application of Eugenol-A Review. *International Journal of Molecular Sciences*, *22*(7). https://doi.org/10.3390/ijms22073671

Ullah, H. M. A., Kim, T.-H., Saba, E., Kim, S. D., & Rhee, M. H. (2021). Korean Red Ginseng and *Portulaca oleracea* Extracts Attenuate Lipopolysaccharide-induced Inflammation via Downregulation of Nuclear Factor Kappa-B and the Mitogen-activated Protein Kinase

Signaling Pathway in Macrophage Cell Line RAW 264.7. *Biomedical Science Letters*, *27*(2), 51–58. https://doi.org/10.15616/BSL.2021.27.2.51

USDA (United States Department of Agriculture). (2012). *National Resources Conservation Service* . Plants Database – Plant Profile: Portulaca Oleracea L.

Usta, J., Kreydiyyeh, S., Knio, K., Barnabe, P., Bou-Moughlabay, Y., & Dagher, S. (2009). Linalool decreases HepG2 viability by inhibiting mitochondrial complexes I and II, increasing reactive oxygen species and decreasing ATP and GSH levels. *Chemico-Biological Interactions*, *180*(1), 39–46. https://doi.org/10.1016/j.cbi.2009.02.012

V. Sicari, M. L. R. T. A. M. T. P. (2018). Portulaca oleracea L. (Purslane) extracts display antioxidant and hypoglycaemic effects. *Journal of Applied Botany and Food Quality*, *92*, 39–46.

Vaara, M., & Nurminen, M. (1999). Outer Membrane Permeability Barrier in *Escherichia coli* Mutants That Are Defective in the Late Acyltransferases of Lipid A Biosynthesis. *Antimicrobial Agents and Chemotherapy*, *43*(6), 1459–1462. https://doi.org/10.1128/AAC.43.6.1459

Vaidya, A., & Mitragotri, S. (2020). Ionic liquid-mediated delivery of insulin to buccal mucosa. *Journal of Controlled Release*, *327*, 26–34. https://doi.org/10.1016/j.jconrel.2020.07.037

Van Der Spoel, D., Lindahl, E., Hess, B., Groenhof, G., Mark, A. E., & Berendsen, H. J. C. (2005). GROMACS: Fast, flexible, and free. *Journal of Computational Chemistry*, *26*(16), 1701–1718. https://doi.org/10.1002/jcc.20291

van Osch, D. J. G. P., Zubeir, L. F., van den Bruinhorst, A., Rocha, M. A. A., & Kroon, M. C. (2015). Hydrophobic deep eutectic solvents as water-immiscible extractants. *Green Chemistry*, *17*(9), 4518–4521. https://doi.org/10.1039/C5GC01451D

Viñas-Ospino, A., Panić, M., Bagović, M., Radošević, K., Esteve, M. J., & Radojčić Redovniković, I. (2023). Green approach to extract bioactive compounds from orange peel employing hydrophilic and hydrophobic deep eutectic solvents. *Sustainable Chemistry and Pharmacy*, *31*, 100942. https://doi.org/10.1016/j.scp.2022.100942

Viñas-Ospino, A., Panić, M., Radojčić- Redovniković, I., Blesa, J., & Esteve, M. J. (2023). Using novel hydrophobic deep eutectic solvents to improve a sustainable carotenoid extraction from orange peels. *Food Bioscience*, *53*, 102570. https://doi.org/10.1016/j.fbio.2023.102570

Vincente, A. R., Manganaris, G. A., Ortiz, C. M., Sozzi, G. O., & Crisosto, C. H. (2014). Nutritional Quality of Fruits and Vegetables. In *Postharvest Handling* (pp. 69–122). Elsevier. https://doi.org/10.1016/B978-0-12-408137-6.00005-3

Vishal Chugh, Vigya Mishra, Satya Vart Dwivedi, & K D Sharma. (2019). Purslane (Portulaca oleracea L.): An underutilized wonder plant with potential pharmacological value. *The Pharma Innovation*, *8*(6), 236–246.

Wang, C.-Q., & Yang, G.-Q. (2010). Betacyanins from Portulaca oleracea L. ameliorate cognition deficits and attenuate oxidative damage induced by D-galactose in the brains of senescent mice. *Phytomedicine*, *17*(7), 527–532. https://doi.org/10.1016/j.phymed.2009.09.006

Wang, H., Zhang, L., & Wang, Y. (2017). Isolating and Identifying Organic Acids from Portulaca oleracea and Determining Their Anti-cyanobacterial Activity. *Polish Journal of Environmental Studies*, *26*(1), 441–445. https://doi.org/10.15244/pjoes/64465

Wang, J., Wolf, R. M., Caldwell, J. W., Kollman, P. A., & Case, D. A. (2004). Development and testing of a general amber force field. *Journal of Computational Chemistry*, *25*(9), 1157–1174. https://doi.org/10.1002/jcc.20035

Wang, Y., Cao, S., Yu, K., Yang, F., Yu, X., Zhai, Y., Wu, C., & Xu, Y. (2019). Integrating tacrolimus into eutectic oil-based microemulsion for atopic dermatitis: simultaneously enhancing percutaneous delivery and treatment efficacy with relieving side effects . *International Journal of Nanomedicine*, *Volume 14*, 5849–5863. https://doi.org/10.2147/IJN.S212260

Wang, Y., Wang, X., Wang, X., Song, Y., Wang, X., & Hao, J. (2019). Design and Development of Lidocaine Microemulsions for Transdermal Delivery. *AAPS PharmSciTech*, *20*(2), 63. https://doi.org/10.1208/s12249-018-1263-1

Wei, Z.-F., Wang, X.-Q., Peng, X., Wang, W., Zhao, C.-J., Zu, Y.-G., & Fu, Y.-J. (2015). Fast and green extraction and separation of main bioactive flavonoids from Radix Scutellariae. *Industrial Crops and Products*, *63*, 175–181. https://doi.org/10.1016/j.indcrop.2014.10.013

Weng, L., & Toner, M. (2018). Janus-faced role of water in defining nanostructure of choline chloride/glycerol deep eutectic solvent. *Physical Chemistry Chemical Physics*, *20*(35), 22455–22462. https://doi.org/10.1039/C8CP03882A

Wiener, M. C., & Horanyi, P. S. (2011). How hydrophobic molecules traverse the outer membranes of Gram-negative bacteria. *Proceedings of the National Academy of Sciences*, *108*(27), 10929–10930. https://doi.org/10.1073/pnas.1106927108

Wikene, K. O., Rukke, H. V., Bruzell, E., & Tønnesen, H. H. (2017). Investigation of the antimicrobial effect of natural deep eutectic solvents (NADES) as solvents in antimicrobial

photodynamic therapy. *Journal of Photochemistry and Photobiology B: Biology*, *171*, 27–33. https://doi.org/10.1016/j.jphotobiol.2017.04.030

Wu, J., Xue, X., Fan, G., Gu, Y., Zhou, F., Zheng, Q., Liu, R., Li, Y., Ma, B., Li, S., Huang, G., Ma, L., & Li, X. (2021). Ferulic Acid Ameliorates Hepatic Inflammation and Fibrotic Liver Injury by Inhibiting PTP1B Activity and Subsequent Promoting AMPK Phosphorylation. *Frontiers in Pharmacology*, *12*. https://doi.org/10.3389/fphar.2021.754976

Wu, L., Chen, Z., Li, S., Wang, L., & Zhang, J. (2021). Eco-friendly and high-efficient extraction of natural antioxidants from Polygonum aviculare leaves using tailor-made deep eutectic solvents as extractants. *Separation and Purification Technology*, *262*, 118339. https://doi.org/10.1016/j.seppur.2021.118339

Wu, L., Li, L., Chen, S., Wang, L., & Lin, X. (2020). Deep eutectic solvent-based ultrasonic-assisted extraction of phenolic compounds from Moringa oleifera L. leaves: Optimization, comparison and antioxidant activity. *Separation and Purification Technology*, *247*, 117014. https://doi.org/10.1016/j.seppur.2020.117014

Xia, G.-H., Li, X.-H., & Jiang, Y. (2021). Deep eutectic solvents as green media for flavonoids extraction from the rhizomes of Polygonatum odoratum. *Alexandria Engineering Journal*, *60*(2), 1991–2000. https://doi.org/10.1016/j.aej.2020.12.008

Xia, Z., Qiang, Z., & Dong-Xia, Z. (2011a). Hydrogen Bond Lifetime Definitions and the Relaxation Mechanism in Water Solutions. *Acta Physico-Chimica Sinica*, *27*(11), 2547–2552. https://doi.org/10.3866/PKU.WHXB20111107

Xia, Z., Qiang, Z., & Dong-Xia, Z. (2011b). Hydrogen Bond Lifetime Definitions and the Relaxation Mechanism in Water Solutions. *Acta Physico-Chimica Sinica*, *27*(11), 2547–2552. https://doi.org/10.3866/PKU.WHXB20111107

Xiong, F., Zhang, Y., Li, T., Tang, Y., Song, S.-Y., Zhou, Q., & Wang, Y. (2024). A detailed overview of quercetin: implications for cell death and liver fibrosis mechanisms. *Frontiers in Pharmacology*, *15*. https://doi.org/10.3389/fphar.2024.1389179

Xu, X., Yu, L., & Chen, G. (2006). Determination of flavonoids in Portulaca oleracea L. by capillary electrophoresis with electrochemical detection. *Journal of Pharmaceutical and Biomedical Analysis*, *41*(2), 493–499. https://doi.org/10.1016/j.jpba.2006.01.013

Xu, Z., Cai, Y., Ma, Q., Zhao, Z., Yang, D., & Xu, X. (2021). Optimization of Extraction of Bioactive Compounds from Baphicacanthus cusia Leaves by Hydrophobic Deep Eutectic Solvents. *Molecules*, *26*(6), 1729. https://doi.org/10.3390/molecules26061729

Yang, H., & Dou, Q. P. (2010). Targeting apoptosis pathway with natural terpenoids: implications for treatment of breast and prostate cancer. *Current Drug Targets*, *11*(6), 733–744. https://doi.org/10.2174/138945010791170842

Yang, X., Zhang, W., Ying, X., & Stien, D. (2018). New flavonoids from Portulaca oleracea L. and their activities. *Fitoterapia*, *127*, 257–262. https://doi.org/10.1016/j.fitote.2018.02.032

Yee, N. (2015). Roles of TRPM8 Ion Channels in Cancer: Proliferation, Survival, and Invasion. *Cancers*, *7*(4), 2134–2146. https://doi.org/10.3390/cancers7040882

Yilmaz Öztürk, B., Feyzullazade, N., Dağ, İ., & Şengel, T. (2022). The investigation of in vitro effects of farnesol at different cancer cell lines. *Microscopy Research and Technique*, *85*(8), 2760–2775. https://doi.org/10.1002/jemt.24125

Ysrafil, Y., Sapiun, Z., Slamet, N. S., Mohamad, F., Hartati, H., Damiti, S. A., Alexandra, F. D., Rahman, S., Masyeni, S., Harapan, H., Mamada, S. S., Emran, T. Bin, & Nainu, F. (2023). Anti-inflammatory activities of flavonoid derivates. *ADMET and DMPK*. https://doi.org/10.5599/admet.1918

Yu, L., Cao, L., Chang, Y.-H., Duan, C.-J., Liu, C., Zhao, X.-L., Yue, G.-L., Wang, X.-Q., & Fu, Y.-J. (2021). Enhanced extraction performance of iridoids, phenolic acids from Eucommia ulmoides leaves by tailor-made ternary deep eutectic solvent. *Microchemical Journal*, *161*, 105788. https://doi.org/10.1016/j.microc.2020.105788

Yuan, Z., Lu, X., Lei, F., Sun, H., Jiang, J., Xing, D., & Du, L. (2023). Novel Effect of p-Coumaric Acid on Hepatic Lipolysis: Inhibition of Hepatic Lipid-Droplets. *Molecules*, *28*(12), 4641. https://doi.org/10.3390/molecules28124641

Zeng, G., Xu, P., Huang, D., Liu, L., Zhao, M., Lai, C., & Li, B. (2018). Enhanced antioxidant and antidiabetic properties of natural deep eutectic solvents-prepared Esculetin and its inclusion complex with hydroxypropyl-β-cyclodextrin. . *Journal of Pharmaceutical Sciences*, *107(6)*, 1790-1800.

Zhang, H., Hao, F., Yao, Z., Zhu, J., Jing, X., & Wang, X. (2022). Efficient extraction of flavonoids from Polygonatum sibiricum using a deep eutectic solvent as a green extraction solvent. *Microchemical Journal*, *175*, 107168. https://doi.org/10.1016/j.microc.2021.107168

Zhang, Q., Lin, Z., Zhang, W., Huang, T., Jiang, J., Ren, Y., Zhang, R., Li, W., Zhang, X., & Tu, Q. (2021). Fabrication of green poly(vinyl alcohol) nanofibers using natural deep eutectic solvent for fast-dissolving drug delivery. *RSC Advances*, *11*(2), 1012–1021. https://doi.org/10.1039/D0RA08755F

Zhao, B.-Y., Xu, P., Yang, F.-X., Wu, H., Zong, M.-H., & Lou, W.-Y. (2015). Biocompatible Deep Eutectic Solvents Based on Choline Chloride: Characterization and Application to the Extraction of Rutin from *Sophora japonica*. *ACS Sustainable Chemistry & Engineering*, *3*(11), 2746–2755. https://doi.org/10.1021/acssuschemeng.5b00619

Zhao, C., Ying, Z., Hao, D., Zhang, W., Ying, X., & Yang, G. (2019). Investigating the bioavailabilities of olerciamide A via the rat's hepatic, gastric and intestinal first-pass effect models. *Biopharmaceutics & Drug Disposition*, *40*(3–4), 112–120. https://doi.org/10.1002/bdd.2175

Zhao, C., Zhang, C., He, F., Zhang, W., Leng, A., & Ying, X. (2019). Two new alkaloids from Portulaca oleracea L. and their bioactivities. *Fitoterapia*, *136*, 104166. https://doi.org/10.1016/j.fitote.2019.05.005

Zhao, G., Li, T., Qu, X., Zhang, N., Lu, M., & Wang, J. (2017). Optimization of ultrasound-assisted extraction of indigo and indirubin from Isatis indigotica Fort. and their antioxidant capacities. *Food Science and Biotechnology*, *26*(5), 1313–1323. https://doi.org/10.1007/s10068-017-0112-4

Zhou, L., Liao, T., Liu, W., Zou, L., Liu, C., & Terefe, N. S. (2020). Inhibitory effects of organic acids on polyphenol oxidase: From model systems to food systems. *Critical Reviews in Food Science and Nutrition*, *60*(21), 3594–3621. https://doi.org/10.1080/10408398.2019.1702500

Zhou, Y.-X., Xin, H.-L., Rahman, K., Wang, S.-J., Peng, C., & Zhang, H. (2015a). Portulaca oleracea L.: a review of phytochemistry and pharmacological effects. *BioMed Research International*, *2015*, 925631. https://doi.org/10.1155/2015/925631

Zhou, Y.-X., Xin, H.-L., Rahman, K., Wang, S.-J., Peng, C., & Zhang, H. (2015b). *Portulaca oleracea* L.: A Review of Phytochemistry and Pharmacological Effects. *BioMed Research International*, *2015*, 1–11. https://doi.org/10.1155/2015/925631

Annexes

Annex 1: Calibration curves of gallic acid, quercetin, catechin, and ascorbic acid

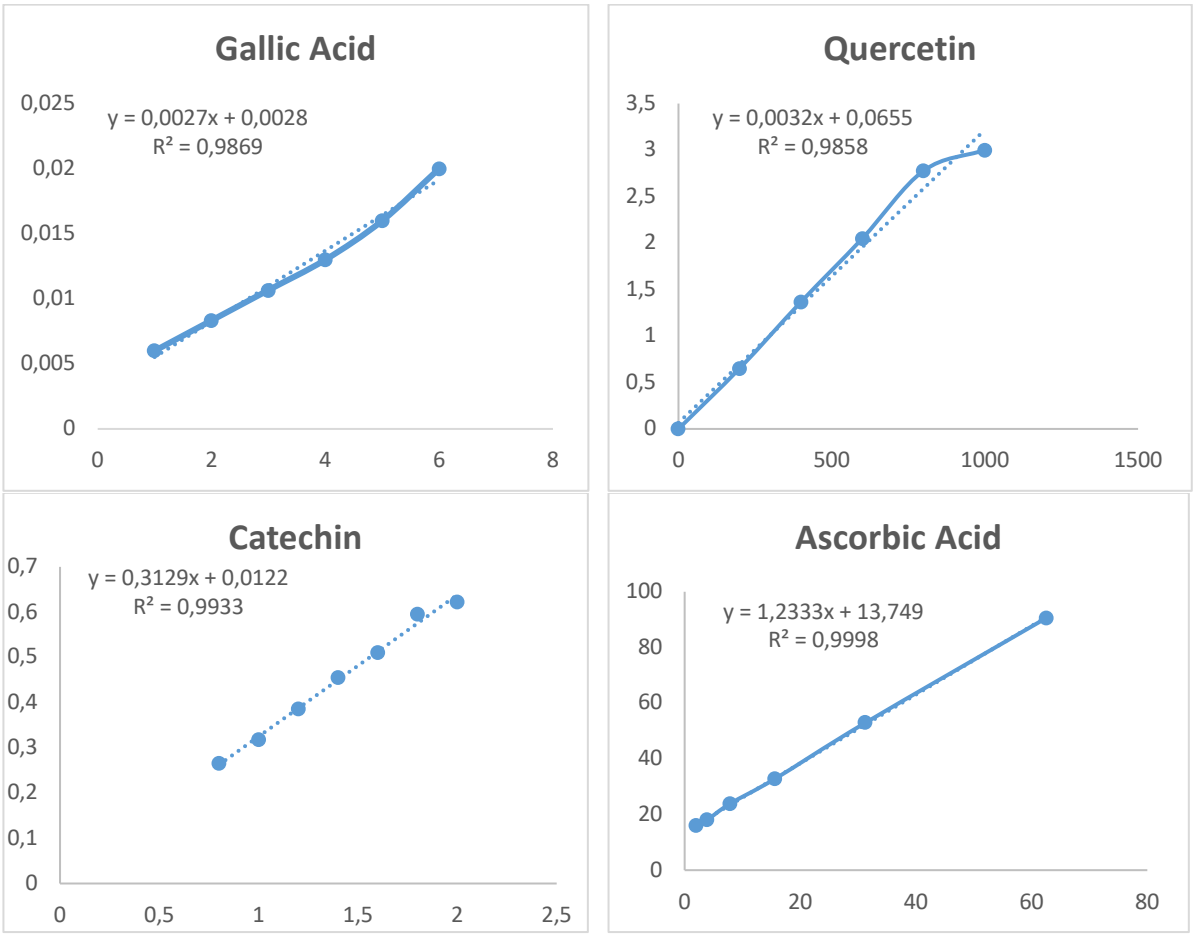

Annex 2: DPPH curves representing all NADESs-POL and the Trolox standard

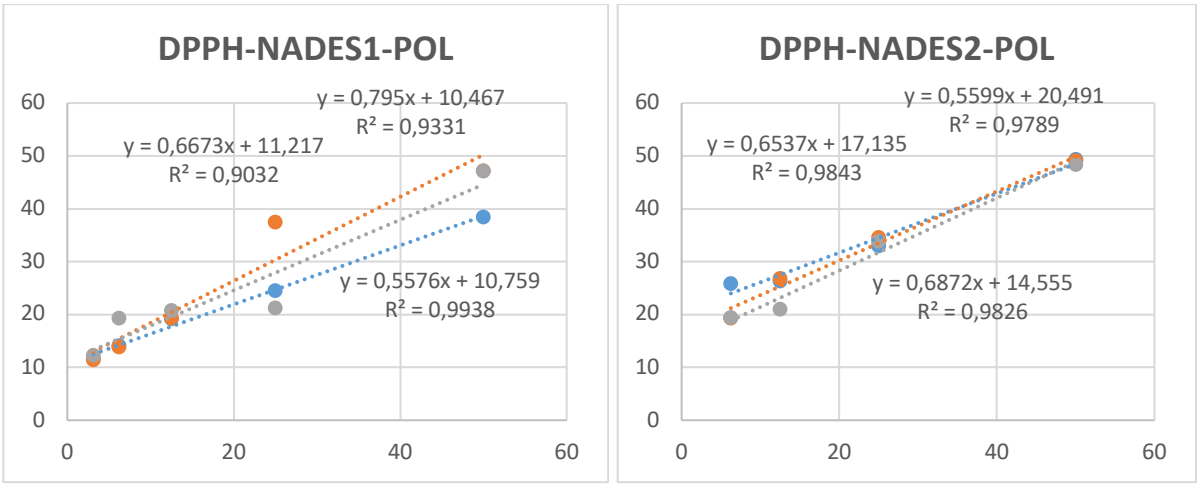

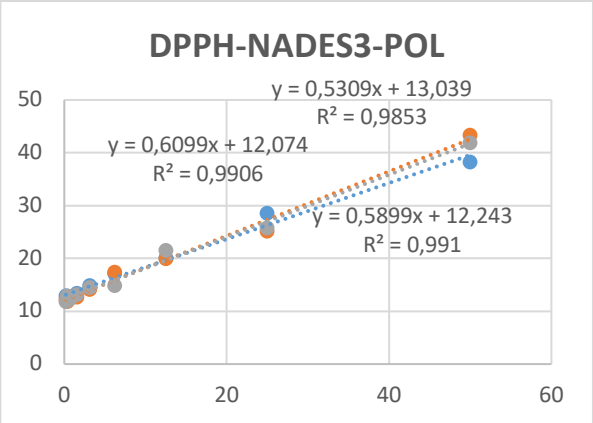
DPPH-NADES3-POL
y = 0,5309x + 13,039
R² = 0,9853
y = 0,6099x + 12,074
R² = 0,9906
y = 0,5899x + 12,243
R² = 0,991

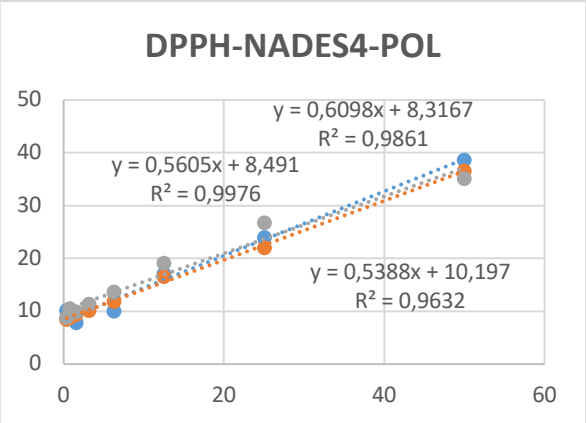
DPPH-NADES4-POL
y = 0,6098x + 8,3167
R² = 0,9861
y = 0,5605x + 8,491
R² = 0,9976
y = 0,5388x + 10,197
R² = 0,9632

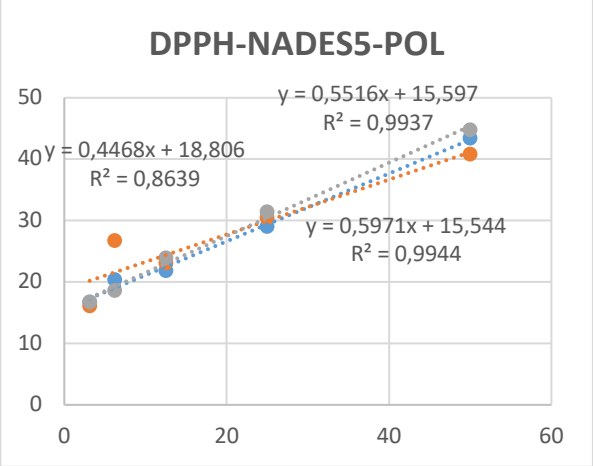
DPPH-NADES5-POL
y = 0,5516x + 15,597
R² = 0,9937
y = 0,4468x + 18,806
R² = 0,8639
y = 0,5971x + 15,544
R² = 0,9944

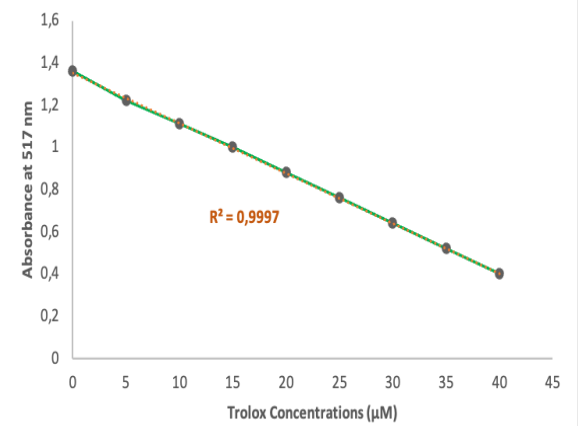
Absorbance at 517 nm
R² = 0,9997
Trolox Concentrations (µM)

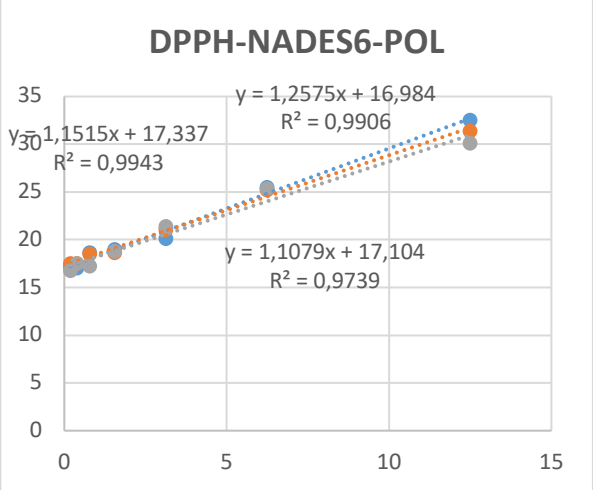
DPPH-NADES6-POL
y = 1,2575x + 16,984
R² = 0,9906
y = 1,1515x + 17,337
R² = 0,9943
y = 1,1079x + 17,104
R² = 0,9739

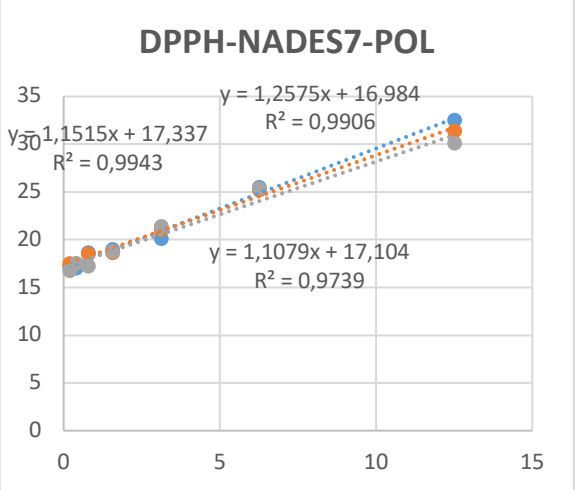
DPPH-NADES7-POL
y = 1,2575x + 16,984
R² = 0,9906
y = 1,1515x + 17,337
R² = 0,9943
y = 1,1079x + 17,104
R² = 0,9739

Annex 3: Fourier transform infrared spectra of menthol/β-citronellol based system. (A) Menthol; (B) β-Citronellol; (C) Corresponding natural deep eutectic solvent. thymol/β-citronellol based system. (D) Thymol; (E) β-Citronellol; (F) Corresponding natural deep eutectic solvent.

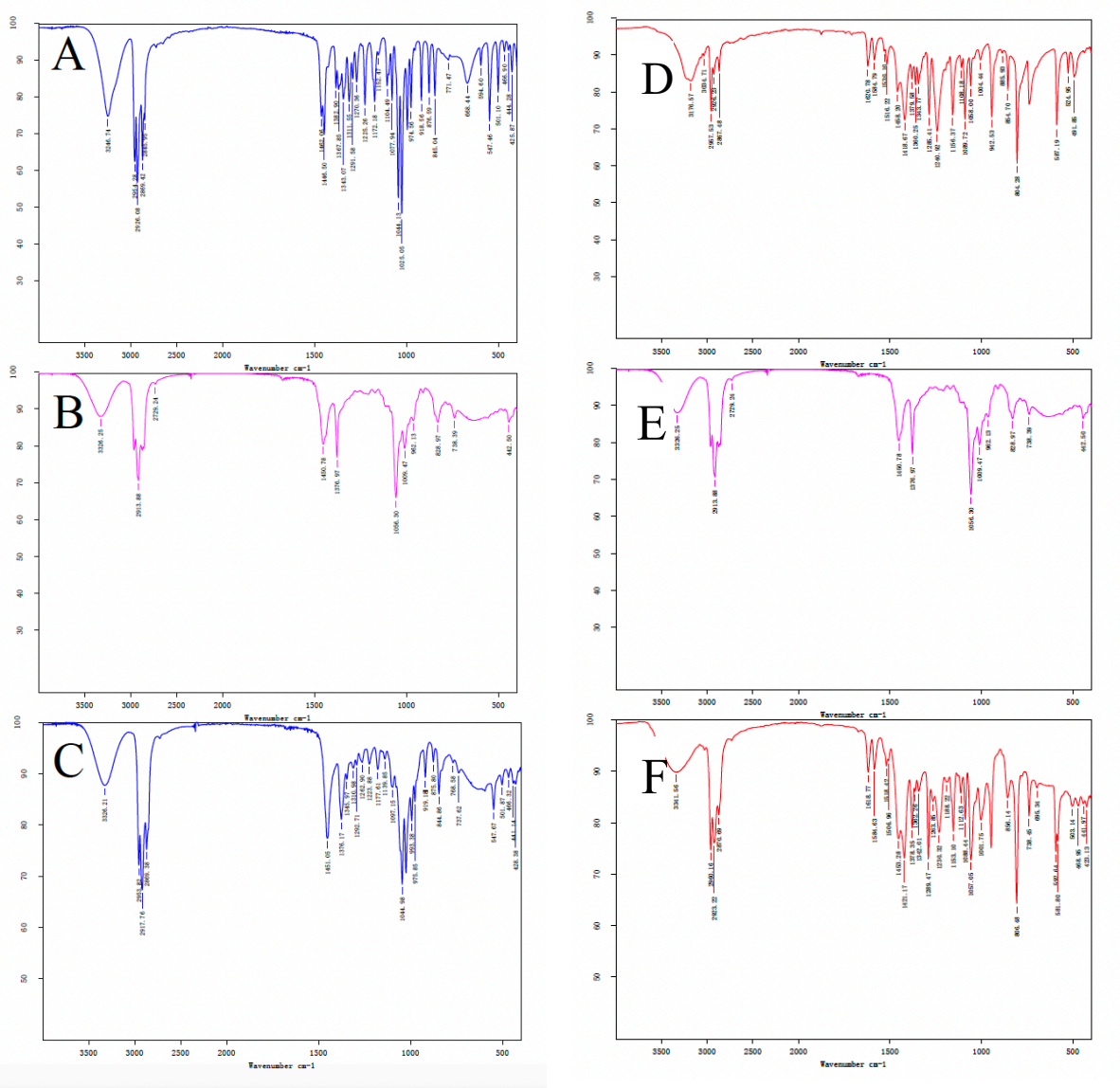

The Fourier transform infrared (FTIR) spectra of two NADESs systems, it can be observed that stronger and broader bands (appeared between 3000 and 3500 cm^{-1}) indicate the presence of intermolecular hydrogen-bond network. On the other hand, in the FTIR spectra of NADESs containing menthol, the hydroxyl band from the menthol is originally located at lower wavenumber values (3246.74 cm^{-1}) and it shifts to the high values (3326.21^{-1}) in the eutectic mixtures. In the FTIR spectra of NADESs containing thymol, the hydroxyl band from the thymol is originally located at lower wavenumber values (3176.57 cm^{-1}) and it shifts to the high

values (3341.56^{-1}) in the eutectic mixtures. The shift of the hydrogen bond was due to the formation of NADESs systems.

Annex 4: HPLC chromatograms obtained from the analysis of selected phenols 1: gallic acid.; 2: caffeic acid.; 3: syringic acid.; 4: coumaric acid.; 5: ferulic acid.; 6: rutin.; 7: quercetin

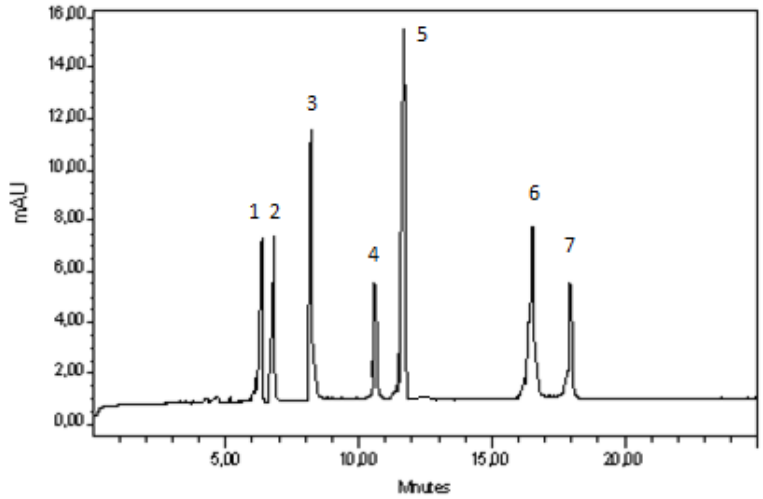

Annex 5: Histograms of AGS cell viability at different treatment concentrations of NADESs and THEDESs (0.075%, 0.10%, and 0.125%)

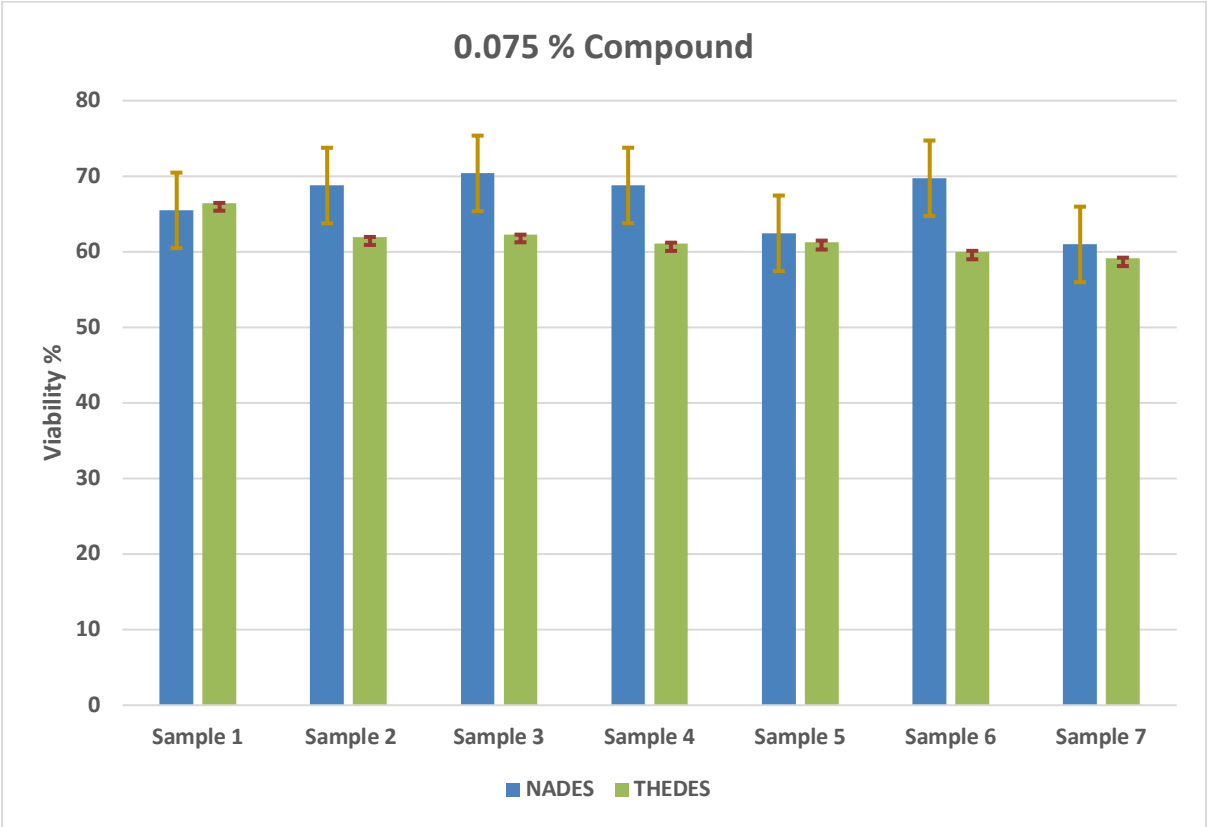

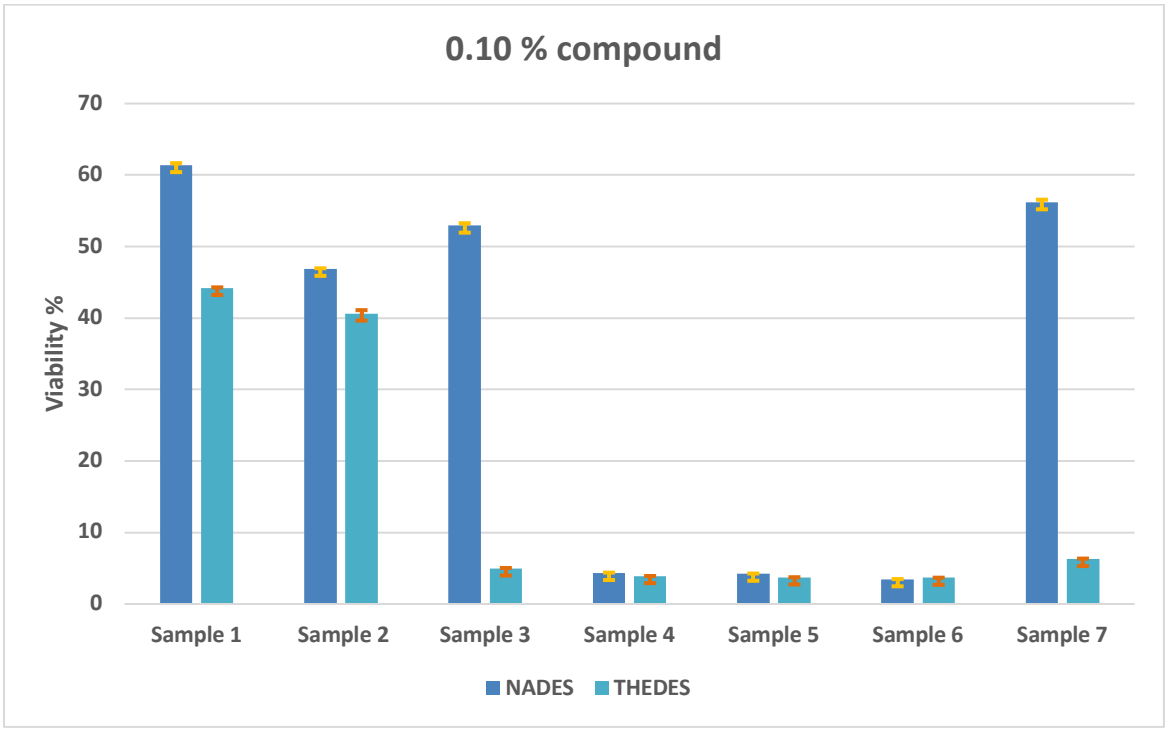
0.10 % compound
Viability %
70
60
50
40
30
20
10
0
Sample 1
Sample 2
Sample 3
Sample 4
Sample 5
Sample 6
Sample 7
NADES
THEDES

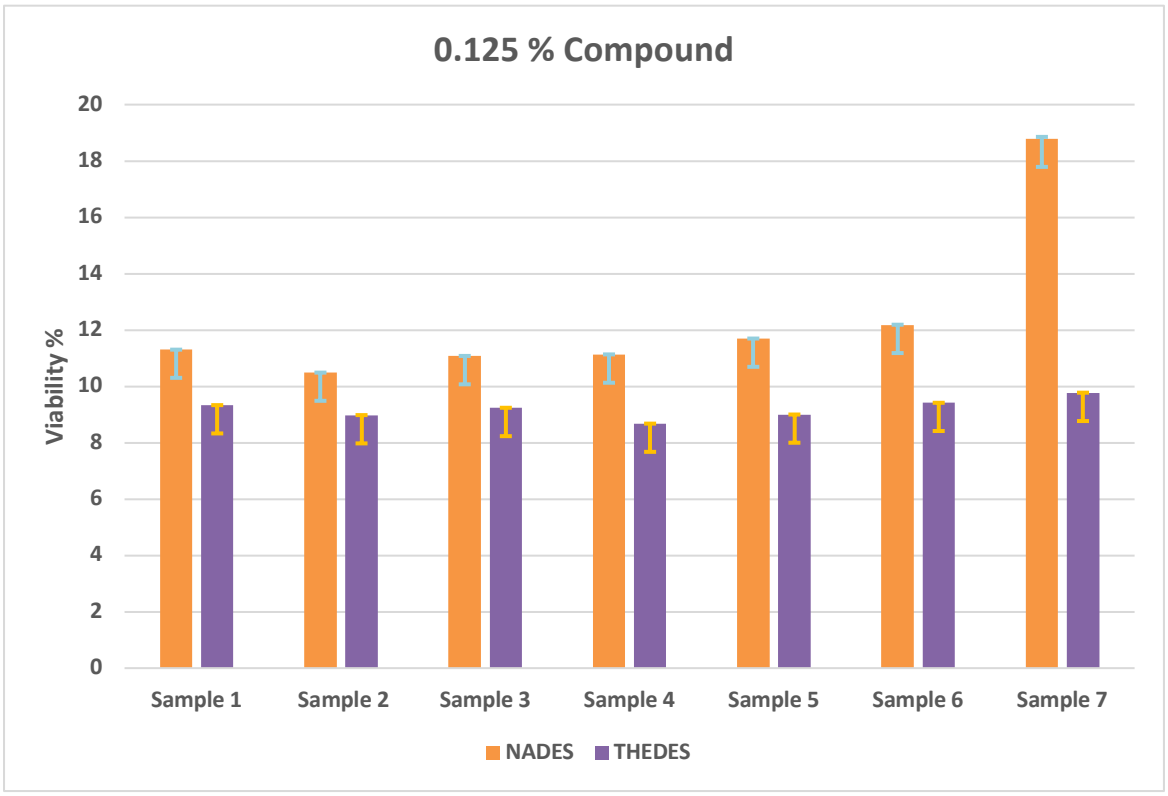
0.125 % Compound
Viability %
20
18
16
14
12
10
8
6
4
2
0
Sample 1
Sample 2
Sample 3
Sample 4
Sample 5
Sample 6
Sample 7
NADES
THEDES